UNIVERSITÀ DEGLI STUDI DI TERAMO

Dipartimento di Scienze degli Alimenti

Tesi in cotutela per il conseguimento del titolo di:

DOTTORE DI RICERCA IN SCIENZE DEGLI ALIMENTI

Settore scientifico-disciplinare:
ING/IND 25 IMPIANTI CHIMICI

UNIVERSITÉ PAUL VERLAINE – METZ

Ecole Doctorale de Lorraine de Chimie et Physique Moléculaires

Thèse en cotutelle pour l'obtention du titre de :

DOCTEUR DE L'UNIVERSITÉ PAUL VERLAINE – METZ

Discipline: CHIMIE
Spécialité: CHIMIE ANALYTIQUE

Produzione di gas di sintesi mediante gassificazione in continuo di biomasse (miscanthus) in apparecchiature a letto fluido e a letto fluido circolante. Caratterizzazione chimica delle frazioni organiche pesanti(tar) prodotte dal processo di gassificazione

*****

Production continue de gaz issus de la gazéification de la biomasse (miscanthus) dans un réacteur à lit fluidisé circulant. Caractérisation chimique des composés organiques lourds produits durant le procédé de gazéification

UNIVERSITÀ ITALO FRANCESE

Area disciplinare :
"Sviluppo sostenibile: energie alternative ed energie rinnovabili"

UNIVERSITÉ FRANCO ITALIENNE

Aire disciplinaire:
"Développement durable: énergies alternatives et énergies renouvelables

Dottoranda – Doctorant *:*
Manuela Di Marcello

Direttore di ricerca :

Prof. Sergio Rapagnà

Directeur de Thèse :
Prof. René Gruber

Co-Encadrement :
Dr. Muriel Matt

Coordinatore responsabile del Dottorato di Ricerca in Scienze degli Alimenti:

Prof.ssa Giovanna Suzzi _____

INDEX

ABBREVIATIONS *7*

CHAPTER 1: INTRODUCTION *9*

1. Biomass valorization for the production of modern energy carriers 10

1.1. Energy from biomass: an overview on the European regulations 10

1.1.1. Role of biomass in reaching the 2020 renewables targets: the case of France and Italy 12

1.2. Biomass sources and main properties 14

1.2.1. Biomass properties 16

1.3. Miscanthus x giganteus: a promising biomass for energy production 19

2. Biomass gasification 22

2.1. Gasification basics 22

2.2. Fluidized bed gasification and gas clean-up technologies 26

2.2.1. Elements of Fluidization state 26

2.2.2. Fluidized bed gasification 28

2.2.3. Gas cleaning treatments 32

2.2.3.1. Particulate removal technologies 34

2.2.3.2. Tars removal technologies 35

3. Characterization of tar produced during biomass gasification 39

3.1. The problematic of sampling 41

3.1.1 Standardization of the sampling protocol: " Biomass gasification - Tar and particles in product gases – Sampling and analysis" (Technical specification UNI CEN/TS 15439:2008) 41

3.1.2 Sampling by adsorption of tar 43

3.2. Choice of Analytical Method suitable for tar determination 44

3.2.1 On-line determination 44

3.2.2 Off line measurement 46

3.2.2.1 Analysis based on separative methods 46

3.2.2.2 Analysis based on spectroscopic Methods 48

References 49

CHAPTER 2: AIM OF THE WORK 58

1. Experimental plan 59

1.1. UNITE – Catalytic biomass gasification experiments 59

1.2. UPV-M – Development of an analytical method for tar measurement 60

2. Aim of the work 60

CHAPTER 3: BIOMASS GASIFICATION 62

1. Introduction 63

2. Experimental 64

2.1. General scheme of the gasification plant 64

2.2. Gasification method 65

2.2.1 Gasification of almond shell using a catalytic filter candle with catalytic layer design 66

2.2.2 Gasification of almond shell using a catalytic filter candle with "fixed bed" design 69

2.2.3 Gasification of almond shell using a catalytic filter candle with "fixed bed" design and 10wt % Fe/olivine 72

2.2.4 Gasification of Miscanthus x giganteus with olivine / 3.9wt % Ni/olivine 73

2.3. Determination of total tar content by Total Organic Carbon analysis 74

3. Results and discussion 75

3.1. Gasification of almond shell using a catalytic filter candle with catalytic layer design 75

3.2. Gasification of almond shell using a catalytic filter candle with "fixed bed" design and 10wt % Fe/olivine 81

3.2.1. Gasification of almond shell using a catalytic filter candle with "fixed bed" design – long-term test 81

3.2.2. Gasification of almond shell using a catalytic filter candle with "fixed bed" design and 10wt % Fe/olivine 89

3.3. Gasification of Miscanthus x giganteus with olivine / 3.9wt % Ni/olivine 94

4. Conclusions 100

References 101

CHAPTER 4: CHARACTERIZATION OF BIOMASS GASIFICATION TARS BY HPLC/UV 103

1. Introduction 104

2. Materials and method 104

2.1. Materials 104

2.2. Method 105

3. Results and discussion 106

3.1. Validation of the method 106

3.2. Characterization of biomass gasification tars 107

3.2.1 Gasification of almond shell using a commercial filter candle 107

3.2.2 Gasification of almond shell using a catalytic filter candle with "fixed bed" design 109

3.2.3 Gasification of almond shell using a catalytic filter candle with "fixed bed" design and 10wt % Fe/olivine 110

3.2.4 Gasification of Miscanthus x giganteus with olivine / 4wt % Ni/olivine 111

3.3. Resume of the most relevant results obtained from tar characterization 112

4. Conclusions 117

References 117

CHAPTER 5: DEVELOPMENT OF ANALYTICAL METHODS FOR TAR DETERMINATION 119

1. Analysis of tar based on UV spectroscopy and planar chromatography 120

1.1 Need for rapid and accurate method for tar analysis 120

1.2 Material and methods 120

1.2.1 Chemicals 120

1.2.2 UV spectroscopy 121

1.2.3 Thin layer chromatography 122

2. Determination of tar content by UV spectroscopy 125

2.1 Introduction 125

2.2 Results and discussion 126

2.2.1 Determination of tar by UV/VIS Spectroscopy - global approach 126

2.2.2 Spectrum mathematical convolution 131

3. Analysis of tar by planar chromatography coupled with a detection by UV and fluorescence 137

3.1 Introduction 137

3.2 Separation of the aromatic families in biomass tar gasification samples 138

3.2.1 Separation on normal and reversed phases 138

3.2.2 Optimization of the separation regarding to solvent sequence elution 141

3.2.3 Separation on NH_2-, and Diol-modified silica plates 145

3.2.4 Interest of reconstituted synthetic tar to optimize resolution on HPTLC plate with concentrating zone 147

3.2.5 Separation on HPLTC RP-18 silica plates with concentrating zone plates 147

3.2.6 Influence of temperature on resolution according aromaticity 149

3.3 Tar quantification by HPTLC/UV 154

4. Conclusions 156

References 157

***GENERAL CONCLUSIONS* 159**

Biomass gasification 160

Tar characterization 162

Further work 163

***ANNEXES* 165**

Annex I: Excel spreadsheet for UV convolution 166

Annex II: Characteristics of the HPTLC plates 169

RÉSUMÉ FRANÇAIS LONG..... 172

COVER PAGE..... 214

ABBREVIATIONS

BFB	Bubbling fluidized bed gasifier
CFB	Circulating fluidized bed gasifier
CFC	Catalytic Filter Candle
CHP	Cogeneration plant, combined heat and power
Daf	dry and ash free basis
d_p	Particle diameter (m)
ECN	Energy Research Center of The Netherlands
EtAc	Ethyl acetate
FC	fixed carbon
FC	Filter Candle
GC/MS	Gas Chromatography with Mass Spectrometry Detection
HPLC	High Performance Chromatography
HPTLC/UV/FL	High Performance Thin Layer Chromatography, detection by UV or Fluorescence
k	numerical factor chosen according to the confidence level desired
kg biomass daf	kg of biomass on dry and ash free basis
LHV	lower heating value
LOD	Limit of Detection
LOQ	Limit of Quantification
m	Slope of the standard calibration curve
MeOH	Methanol
Mtoe	Millions of toe, where toe stands for tonne of oil equivalent. 1 toe is amount of energy released by burning one tonne of crude oil, which corresponds by convention to 42 GJ
MW	Megawatt

n-Hex	n-hexane
Nm^3	Normal Cubic Meter of a gas is the volume of that gas measured under the standard conditions of 0°C, and 1 atmosphere of pressure.
Ni-OL	Ni/olivine
OL	Olivine
MJ/kg daf	MJ of energy produced for kg of biomass daf
MXG	Miscanthus x giganteus
PAH	Polycyclic aromatic Hydrocarbon
Ppmv	ppm in volume
RES	Renewable energy sources
R_f	Retention factor
s_b	Standard deviation of a blank measures
SFS	Synchronous fluorescence spectroscopy
SPA	Solid Phase Adsorption
Syngas	Synthetic gas
TLC	Thin-layer chromatography
TOC	Total Organic Carbon
Tol	Toluene
U_{mf}	Minimum fluidization velocity (m/s)
VM	Volatile matter
wt	Weight
3Cl-3F-eth	Trichlorotrifluoroethane
ρ_f	Density of fluid (kg/m^3)
ρ_p	Density of particle (kg/m^3)

CHAPTER 1: INTRODUCTION

"Energy is key in helping Europe achieve its objectives for growth, jobs and sustainability. High oil prices put the spotlight on Europe's increasing dependency on imported energy. The Union needs to respond strongly to this challenge"

[COM(2005)628 "Biomass Action Plan"]

The present thesis shows the results obtained during the PhD research activity realized in cooperative supervision between the University of Teramo and the University of Metz. The project is financiered by the French-Italian University (Università Italo-Francese / Université Franco-Italienne).

In the present section, the area of investigation of the doctoral thesis is analyzed; the Introduction will provide an overview of fluidized bed biomass gasification as well as the analytical techniques adopted during the research activity for the analysis of tars, which represent the two souls of the present work.

1. Biomass valorization for the production of modern energy carriers

1.1. Energy from biomass: an overview on the European regulations

Renewable energy sources (RES), like biomass, wind and solar energy offer a large unexploited technical potential. The global renewable energy consumption in 1995 was reported to be at about 5%, which make a very modest contribution to the European Union's energy balance.

In order to answer to this gap, in 1997 the European Commission published a White Paper on renewable energy [COM(1997)599]. According to the document, the ambitious targets proposed by the Commission were of doubling the share of renewable energy by 12% by 2010. A key element of the communication was the establishment of a reference legislation, which set indicative 2010 targets for all Member States and required actions to improve the growth, development and access of renewable energy [Directives 2001/77/EC and 2003/30/EC].

In order to implement the RES exploitation, concrete measures were proposed in Action Plans, in which individual actions were clarified and set out by categories. The Biomass Action Plan adopted in 2005 focuses attention on the development of Europe's biomass resources. In 2003 the EU was reported to meet 4% of its energy needs from biomass, and according to the Communication, this value was to be doubled by 2010, while complying with good agricultural practice and sustainable production of biomass. In compliance with the proposed scenario, the overall biomass energy consumption should increase from 20 to 35 Mtoe for electricity, from 48 to 75 Mtoe for heat and from 1 to 19 Mtoe for biofuels production.

As reported in the Plan, several benefits explain the attention focused on the exploitation of biomass-based energy systems. The mains advantages are listed as follows:

- Diversification of Europe's energy supply would provide a decreased share of fossil fuels from 80% to 75% and a reduced reliance on imported energy from 48 to 42%.

- Reduction in greenhouse gas emissions of about 200 million tonnes CO_{2eq} a year;
- Development of new employment and income, mostly in rural areas;
- Potential downward pressure on the oil price as a result of lower demand for oil.

By the way, increasing the use of biomass energy poses several challenges, among which the most relevant is the consideration that energy from biomass is still, generally, more expensive than fossil fuels, even considering the actual oil price at about $80 a barrel; nevertheless, to compete with fossil energy sources an optimal utilization of biomass resources is required. Thus, the key objective is the development of conversion technologies able to raise the energy output and efficiency.

Furthermore, in 2007 the European Council stressed the need to increase energy efficiency: the EU summit endorses a binding target of a 20% share of renewable in overall EU energy consumption by 2020 [7224/1/07 REV1].

With the goal of transforming Europe in a highly energy-efficient, low carbon economy, the European Parliament sealed climate change package "20-20-20" in December 2008. The package "20-20-20" plan overall targets of:

- 20% reduction in EU greenhouse gas emissions below 1990 levels;
- 20% of EU energy consumption to come from renewable resources;
- 20% reduction in primary energy use compared with projected levels, to be achieved by improving energy efficiency.

To achieve the purpose, the EU adopted a new Renewables Directive in April 2009, the 2009/28/EC, which became effective the June 5th, 2009. The Directive amend and repeal the former Directives 2001/77/EC and 2003/30/EC.

The 2009/28/EC sets individual targets for each member state. Also, EU countries were free to decide their own preferred technologies, allowing them to take account of their different potentials. Every nation in the 27-member bloc are bound to increase its share of renewables by 5.5% from 2005 levels, with the remaining increase calculated on the basis of per capita gross domestic product.

In the case of France and Italy, the two countries are required to boost their shares from 10.3% to 23% and from and 5.2% to 17% respectively, by 2020.

In line with the directive mentioned, each member state was obliged to provide a National Renewable Energy Action Plan (NREAPs) by 30 June 2010; the NREAPs offer detailed information on measures that will be taken to reach the proposed target, up to 2020, across three sectors: electricity, heating and cooling, and transport.

1.1.1. Role of biomass in reaching the 2020 renewables targets: the case of France and Italy

The Directive 2009/28/EC stated that it is essential to mobilize new biomass resources and provides a definition by law of the word "biomass": in the article 2, paragraph (e) this is defined as the biodegradable fraction of products, waste and residues from biological origin from agriculture (including vegetal and animal substances), forestry and related industries including fisheries and aquaculture, as well as the biodegradable fraction of industrial and municipal waste.

Table 1. Estimated role of the biomass in reaching the renewable energy target by 2020, for France and Italy

	FR	IT
2020 target (%)	23	17
Expected amount of Energy from RES, corresponding to the 2020 target (Mtoe)	35.6	22.6
Expected amount of energy from biomass (domestic supply) – NREAPs (Mtoe)	21.8	12.9
Energy from biomass (domestic supply) in total renewables (%)	61	57

Due to the extended European renewable energy targets, the demand for biomass feedstock is expected to increase considerably. Especially, woody biomass is supposed to become a globally traded commodity; otherwise waste biomass, which is an under-used resource, could provide a significant contribution to renewable energy targets and reduce the total amount of land filled waste. Biomass will have the decisive role in helping both France and Italy to reach their renewable energy shares by 2020, in fact when compared to the total amount of energy from RES, the expected amount of biomass energy represent about 61% and 57% of the total, respectively (Table 1).

Table 2. Estimated primary energy production from biomass (domestic supply) by 2020, for France and Italy

		Primary energy production (Mtoe)		Primary Energy production (%)	
		FR	IT	FR	IT
Biomass from forestry	Direct supply of wood biomass from forests and other wooded land for energy generation	9.6	4.0	43.9	31.0
	Indirect supply of wood biomass for energy generation	5.7		26.4	
Biomass from agriculture and fisheries	Agricultural crops and fishery products directly provided for energy generation	3.2	1.6	14.7	12.4
	Agricultural by-products/ processed residues and fishery by-products for energy generation	1.0	4.9	4.6	38.0
Biomass from waste	Biodegradable fraction of municipal solid waste including biowaste (biodegradable garden and park waste, food and kitchen waste from households, restaurants, caterers and retail premises, and comparable waste from food processing plants) and landfill gas	1.3	1.8	6.1	14.0
	Biodegradable fraction of industrial waste (including paper, cardboard, pallets)	0.9	0.6	4.1	4.7
	Sewage sludge	0.1		0.2	
	TOTALS	21.8	12.9		

As stated before, the French NREAP has identified biomass as the main source of renewable energy. According to the assessments provided by the French Government, France would raise about 22Mtoe of primary energy production from biomass by 2020; most of it (70%), will be produced thanks to the conversion of biomass from forestry (direct and indirect supply of wood biomass) [Plan d'action national en faveur des énergies renouvelables - Période 2009-2020]. Considering the Italian scenario the amount of primary energy production from biomass is estimated to be at about 13Mtoe by 2020 [Piano di azione nazionale

per le energie rinnovabili dell'Italia]. By the way, in this case the most relevant role between the biomass resources is played by the agricultural by-products and processed residues (Table 2).

Regarding the Italian situation, it should be emphasized that NREAP anticipate a revision of the regulations about the utilization of biomass for energetic purpose.

In fact, the actual definition of biomass in the Italian legislation is quite confused and often contradictory. According to the legislation on renewable energies (D. Lgs. 387/03), the term "biomass" identifies: the biodegradable fraction of products, waste and residues from agriculture (including vegetal and animal matter), forestry and related industries, as well as the biodegradable fraction of industrial and municipal wastes. Environmental legislation (D. Lgs. 152/06), however, provides a more restrictive definition, so are considered "biomass fuels" only the following materials:

- Plant material produced from dedicated crops;
- Plant material produced by mechanical treatment (i.e. pruning) of non-dedicated agricultural crops;
- Plant material produced by forest maintenance;
- Plant material produced by mechanical processing of virgin wood, such as wood chips, not contaminated by pollutants;
- Plant material produced by mechanical processing of agricultural products;
- Exhaust olive residues (oil free) obtained by processing olives residues by chemical extraction.
- Exhaust grape vinasses and their components obtained from winery industry (L. 205/08).

Due to the enactment of the UE Directive 2009/28/EC into a national law, however, it will be considered the possibility of clarify and simplify the regulatory framework for certain wastes, residues and by-products derived from farming, food and forestry, as well as rules for managing non-virgin biomass.

1.2. Biomass sources and main properties

As described in the previous paragraph, the definition biomass is a term that brings together a wealth of extremely heterogeneous materials of biological origin

directly or indirectly produced by photosynthesis. (Figure 1). Thus, biomass resource is available on renewable basis through natural processes, or it can be made available as a byproduct of human activities (i.e. organic wastes) [McKendry, 2002].

In broadest terms biomass is an organic matter, in which the radiant energy of sunlight and the CO_2 are converted into chemical energy, stored in the bonds of molecules at high-energy content, the carbohydrates. When the bonds between adjacent carbon, hydrogen and oxygen in these molecules are broken by digestion, combustion, or decomposition, these substances release their stored, chemical energy. In these terms, biomass could be considered as a sort of natural battery for storing solar energy.

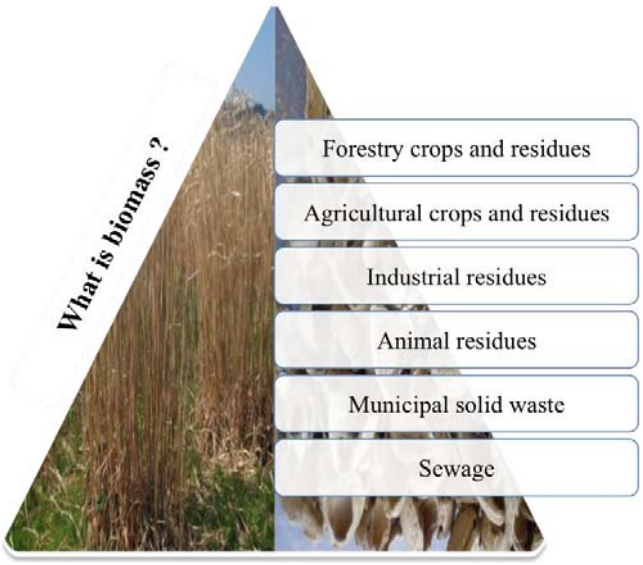

Figure 1: Different biomass sources

The biomass carbon cycle differentiates the carbon in biomass from the one in fossil fuels. Fossil fuels contains carbon that has been out of the atmosphere for million of years. Therefore, when fossil fuels are burned, they put “new” carbon in the atmosphere and the earth, which contribute to the greenhouse effect.

Instead, burning new biomass contributes no carbon dioxide to the atmosphere, because replanting harvested biomass ensures that CO_2 is absorbed and returned for a cycle of new growth (Figure 2) [McKendry, 2002]; if this equilibrium is preserved biomass could be considered as a renewable energy source with almost zero net CO_2 emissions [Gustavsson et al 1995].

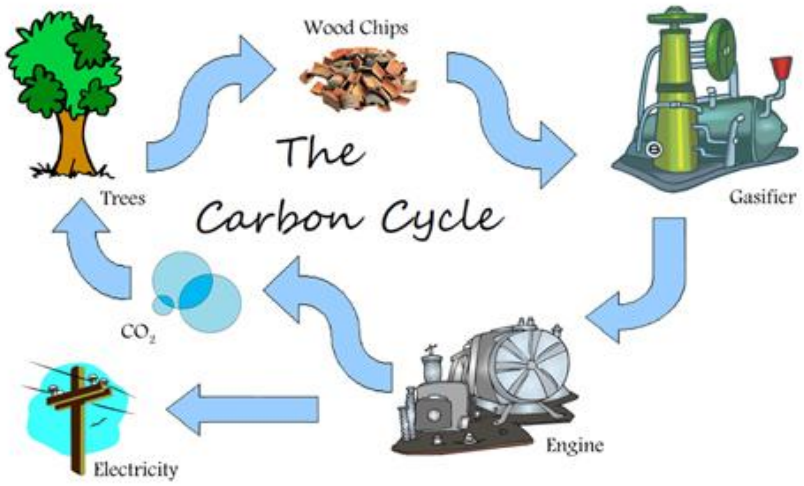

Figure 2: Biomass carbon cycle

Biomass is also an indigenous energy source, available worldwide, that could be converted into electrical/heat energy, transport fuel or chemical feedstock, which in turn may lead to a more secure energy supply.

1.2.1. Biomass properties

In the present paragraph the biomass properties, those that mainly influence the end-use, will be briefly analyzed. The discussion will be focused on woody plants and herbaceous plants/grasses, which represent the majority of the biomass sources available.

Among the different categories (woody/ herbaceous/fruit biomass, blend and mixtures) the most relevant properties that differentiate biomass could be resumed as follows:

- Heating (or calorific) value, which is a measure of the heat released during the combustion of a specific amount of fuel. This value is characteristic for each substance. The calorific value of biomass is an indication of the energy chemically bound in it, so it can be considered as the most important property of a fuel [Erol et al., 2010]. The heating value may be reported on two bases. The higher heating value (HHV, or gross calorific value) is the total energy content released when the fuel is burnt in air and therefore represents the maximum amount of energy potentially recoverable from a given biomass; while the lower heating value (LHV) is

calculated subtracting the latent heat contained in the water vapor from the HHV; the energy required to vaporize the water is not realized as heat. The LHV is the most appropriate value to take into account. When compared with fossil fuels, i.e. coal, biomass has a very reduced LHV, for example the LHV of coal is 30,6 MJ/kg daf, while for a common woody biomass such as poplar this value is barely 18,5 MJ/kg daf (average data reported by the Phyllis Internet Database for biomass and wastes – ECN, the Nederland). The heating value can also be correlated with the carbon concentration, with each 1% increase in carbon elevating the heating value by approximately 0.39 MJ/kg [Jenkins et al., 1998]. So, cellulose has a smaller heating value compare to lignin because of its higher degree of oxidation, in fact a lower energy is contained in C-O and C-H bonds than in C-C bonds; thus comparing perennial grasses and straws with woody biomasses, the firsts show heating value slightly reduced [Sander, 1995; Alauddin et al., 2010]. Yang et al. reported that both particle size and LHV influence the combustion stoichiometry as those parameters impact the burning rate and the mass ration of combustible elements (C, H) to the oxygen, thus higher LHV-biomasses and smaller particle size should be preferable [Bin Yang et al., 2005].

- Moisture content, intrinsic and extrinsic (influenced by the weather conditions). Typically, it ranges from 5% to 35%, depending on the feedstock considered [Pruig-Arnavat et al., 2010]. Based primarily upon the biomass moisture content, the type of biomass selected subsequently dictates the most likely form of energy conversion process. Woody or low moisture content biomasses are the most suitable for thermal conversion technologies, because even if feedstock with high moisture content could be used, they will impact adversely on the conversion process reducing the net calorific value of the fuel, as the evaporation of water is strongly endothermic. The content of moisture together with the percentages of volatile matter, fixed carbon and ash represent the proximate analysis of a given biomass.

- Volatile matter and fixed carbon. The volatile matter (VM) is defined as the portion given off by a material as gas or vapor. This is determined measuring the weight loss at 950°C for 7 min, under controlled conditions, excluding weight of moisture driven off at 105°C. While, the fixed carbon (FC) is the mass remaining after the release of volatiles (excluding moisture and ashes). The VM and FC provide a measure of the ease with which the biomass could be ignited and subsequently gasified or combusted [McKendry, 2002].
- Ashes and trace elements. Due to the intrinsic attributes of a biological matter, the weather conditions, the soil characteristics and the eventual use of fertilizers, the composition of biomass is variable, especially regarding the inorganic constituents. Deviations of several tens of percent from the mean value of each element should be considered common; usually, biomass shows a higher amount of potassium, chlorine, and silicon compared to coal, as well as minor amounts of Ca, Mg, Al, Fe, Na, and S. During combustion or gasification of biomass significant amounts of chlorine and alkali metals are released into the gas phase. They are very harmful in terms of causing fouling and high temperature corrosion [Wei et al., 2005]. 0.2% potassium and 0.1% chlorine are the biomass feedstock target values for power generation; these limits are often largely exceeded in case of straw, making this biomass the less attractive [Sander et al., 1997]. Biomass fuels could be divided into three main groups on the basis of the ash composition: the group 1 is represented from the biomasses with Ca, K rich and Si lean ash, i.e. the woody materials. The biomasses with Si rich and Ca, K lean ash, such as rice husk belongs to group 2 and those with Ca, K and P rich ash belongs to group 3, i.e. sunflower seeds [Hiltunen et al., 2008]. The Si present in the biomass is important because, alkali metals in combination with silica and sulfur - and facilitate by the presence of chlorine - are responsible for slag deposits [Jenkins et al., 1998], which occur via the eutectic melting of SiO_2 with K_2O, trapping chlorides at surfaces and causing corrosion [Thompson at al., 2003]. The eutectic formed, which is low-melting compound, become deposited on

the bed particles, coating them with a sticky ash. Thus, the particles may form large agglomerates, which decrease the mixing of the bed and may result in collapse of the fluidized bed, i.e. defluidization.

- Bulk density. The importance of this parameter is due to the decisive impact on transport and storage costs. The costs of transport, handling and storage for straw are higher than those for wood, so to be competitive straws need to be processed into pellet, with an increase of costs, due to the highest refining degree.

In conclusion, it should be stressed that despite different biomasses may have specific benefits for subsequent processing technologies, the amount of energy potentially available from a given biomass source is the same. What will vary between conversion technologies is the actual amount of energy recovered from the biomass source and the form of that energy [McKendry, 2002]. Because biomass is a relatively dilute energy source compared to concentrated fossil fuels, the key challenge is thus to develop efficient conversion technologies. Gasification is a technically mature thermal conversion process for the production of combustible gases from solid fuels. Synthetic gas (syngas) obtained in this way, appropriately conditioned and upgraded, may be used for electricity generation by means of internal combustion engines, gas turbines, and (in the near future) fuel cells, and also for the production of synthetic bio-fuels [Rapagnà et al., 2010]. A detailed review on gasification technology continued in the paragraph 3.

1.3. Miscanthus x giganteus: a promising biomass for energy production

Miscanthus is a perennial rhizomatous and lignocellulosic C_4 grass that has been recently proposed as one of the most interesting plant for biomass production. C_4 is the metabolic pathway typically followed in the light-independent phase of photosynthesis by tropical plants and plants that live in arid environments, in fact this pathway is designed to efficiently fix CO_2 even at low concentrations, C_4 plants also utilize water in a more efficiently way.

The light-independent reactions of photosynthesis are biochemical reactions that convert carbon dioxide and other compounds into glucose, the fundamental building block in the construction of structural polymers, such as starch and

cellulose. A schema that shows the main difference in the photosynthetic pathways of C_3/C_4 plants is given in figure 3.

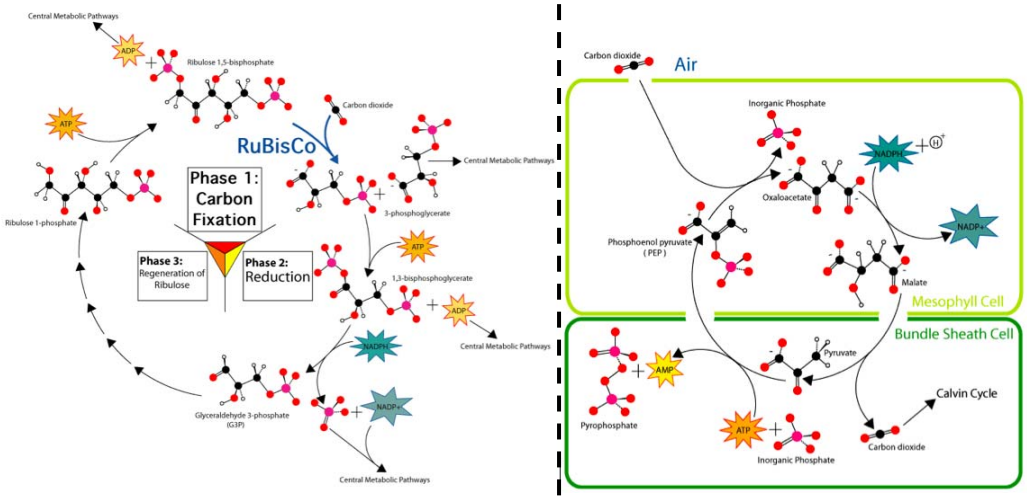

Figure 3: Light-independent reaction of photosynthesis in C_3 (left) and C_4 (right) plants

In the largely diffused C_3 plants, the first step in the light-independent reactions of photosynthesis involves the fixation of CO_2 catalyzed by the enzyme RuBisCO: ribulose-biphophate is carboxilates into two molecules of the three-carbon compound 3-phosphoglycerate. Nevertheless, this enzyme has a dual carboxylase/oxygenase activity, thus an amount of substrate is oxidized; this phenomenon, called photorespiration, increases with temperature and turns into a net loss of carbon and nitrogen from the plant and therefore in a reduced growth.

On the contrary, in C_4 plants the enzyme PEP carboxylase catalyzes the fixation of CO_2 converting the three-carbons phophoenolpyruvate (PEP) into the four-carbon molecule oxalacetate, which gives the "C_4" name to this alternative pathway. The PEP carboxylase has a higher affinity for grabbing carbon dioxide than RuBisCO. This gives C_4 plants a better chance of survival in situation in which the carbon dioxide may be limited.

The genus Miscanthus has its origins in East Asia, but the remarkable adaptability to different environments makes this novel crop suitable for cultivation under a range of European and North American climatic conditions. Field trials have been established throughout Europe from the Mediterranean to southern Scandinavia; most reported trials have used a vigorous sterile clone Miscanthus x giganteus,

(MXG) which has been propagated vegetatively either by rhizome cutting or in vitro culture [Lewadowski et al., 2000]. MXG is used as solid fuel, building materials and for the production of geotextiles and paper pulp;
This particular species maintains high photosynthetic quantum yields and biomass productivity also in cool temperate climates [Naidu et al., 2003]; figure 4 shows a blooming MXG crop in Trier, north-west of Germany.

Figure 4: MXG crop in Trier, Germany

Since 1990, a great number of papers were devoted to the MXG, in different fields: conditions of plantation, culture and harvesting, combustion, valorization in materials like light concrete [Price et al. 2003; Wang et al., 2008; de Jong et al., 2003]. Instead few data are actually available concerning the behavior of MXG in gasification process by using fluidized bed reactor at high temperatures. Anyway this biomass could be successfully used as raw material in gasification process, considering is favorable characteristics. In fact it provides a renewable energy source with almost zero net CO_2 emission since carbon is efficiently fixed. This particular species maintains high photosynthetic quantum yields and biomass productivity also in cool temperate climates [Naidu et al., 2003].
Moreover other advantages, such as high productivity, remarkable adaptability to different environments, low content of mineral and elemental sulphur and the low or no demand of pesticide and fertilizers should be considered. A recent study

carried out in southern Greece on the potential growth and biomass productivity of MXG show how the fertilization within the studied rates did not affect growth and biomass productivity of the crop. By the way it was found a significant effect of plant density, reaching maximum dry biomass yields in excess of 38 ton/ha in the more favorable year 2002, and 28 ton/ha in the warmer and drier year 2001. Such high yield potentials were explained by the particularly great assimilation rates of this crop [Danalatos et al., 2007].

Thanks to its favorable characteristics, MXG could be cultivated on soils not suitable for food crops, thus, MXG do not compete for land, driving up food prices.

The most relevant obstacle in using herbaceous biomasses, such as miscanthus, for heat and electricity generation is their unsuitability compared to wood due to higher silica, potassium and chlorine contents. For heat and electricity application, herbaceous biomass feedstock could begin competitive with fossil fuels, just if they are converted with modern efficient technologies, able to overcome the problems related to the use of higher ash fuels.

2. Biomass gasification

2.1. Gasification basics

Gasification could be defined as a group of processes that converts solid or liquid fuels into a combustible gas with or without contact with a gasification medium [Basu, 2006].

Despite to the different technology used for the recovery of energy from biomass, gasification represents one of the most interesting choices available, due to the fact it is able to convert a large variety of fuels into several valuable products; therefore, biomass gasification can be employed to meet different market needs.

The main advantages of this application are summarized as follows:

- Extensive applicability: through pre-treatment technology, biomass gasification is applicable to deal with all kinds of biomass residues produced in the food processing industry, agriculture, forest industry, etc.
- Scale flexibility: biomass gasifiers could be designed in appropriate scale according to user demands, and eventually scaled-up depending on the

reactor design; the appropriate scale must be decided by local conditions, such as the amount of biomass wastes, demands of energy, etc.

- Economic feasibility: small- and medium-scale biomass gasification plants could utilize biomass residues in small districts, avoiding collection and long distance transportation problems. This enhances the competitiveness of biomass gasification with other energy technologies in the market. From the economic point of view, the keys to make biomass gasification economically feasible are to cut down the investment cost and to extend its application areas [Leung et al., 2004].

Broadly speaking, gasification is as the thermo-chemical conversion of a solid or liquid carbon-based material into a combustible gaseous product by the supply of a gasification agent, which is typically air or steam alone or in mixture, oxygen can also be added in order to increase the heat produced during the gasification. The high temperature and the gasification agent allow the feedstock to be quickly converted into gas by means of different heterogeneous reactions.

The chemistry of biomass gasification is quite complex and formally consists of four stages [Puig-Arnavat et al., 2010]:

1. Drying. In this stage, the moisture content of the biomass is reduced. Typically, the moisture content of biomass ranges from 5% to 35%. Drying occurs at about 100–200°C with a reduction in the moisture content of the biomass of <5%.
2. Devolatilisation (pyrolysis). This is essentially the thermal decomposition of the biomass in the absence of oxygen or air. In this process, the volatile matter in the biomass is reduced. This results in the release of hydrocarbon gases from the biomass, due to which the biomass is reduced to solid charcoal. The hydrocarbon gases can condense at a sufficiently low temperature to generate liquid tars.
3. Oxidation and partial oxidation. This is a reaction between the carbon remaining after pyrolysis and the partially cracked pyrolysis products and oxygen in the air, resulting in formation of CO_2. Hydrogen present in the biomass is also oxidized to generate water. A large amount of heat is released with the oxidation of carbon and hydrogen. If oxygen is present in

substoichiometric quantities, partial oxidation of carbon may occur, resulting in the generation of carbon monoxide.

4. Gasification (reduction). In the absence (or substoichiometric presence) of oxygen, several reduction reactions occur. While, the combustion process oxidizes fuel constituents in an exothermic reaction, the gasification process reduces them to combustible gases in an endothermic reaction.

Processes 1, 2 and 4 absorb heat provided by the exothermic combustion process. The main reactions involved in the coal gasification process are the followings [Puig-Arnavat et al., 2010; Basu, 2006]; it is possible to generalize these reactions even for biomass gasification:

- *Water–gas reaction* is the partial oxidation of carbon by steam added in the gasification medium, as well as the one that could come from water vapor associated with the incoming air, vapor produced from the evaporation of water, and pyrolysis of the solid fuel. Steam reacts with the hot carbon according to the heterogeneous water–gas reaction:

  $C + H_2O_v \leftrightarrow H_2 + CO \qquad \Delta H^0 = +131.4 \text{ kJ/mol} \qquad (1)$

- *Boudouard Reaction.* The carbon dioxide present in the gasifier reacts with char to produce CO according to the following endothermic reaction:

  $CO_2 + C \leftrightarrow 2CO \qquad \Delta H^0 = +172.6 \text{ kJ/mol} \qquad (2)$

- *Shift conversion.* The heating value of hydrogen is higher than that of carbon monoxide. Therefore, steam by carbon monoxide to produce hydrogen is a highly desirable reaction.

  $CO + H_2O_v \leftrightarrow CO_2 + H_2 \qquad \Delta H^0 = -42.0 \text{ kJ/mol} \qquad (3)$

- *Methanation.* Methane could also form in the gasifier through the following overall reaction:

  $C + 2H_2 \leftrightarrow CH_4 \qquad \Delta H^0 = -74.9 \text{ kJ/mol} \qquad (4)$

If the hydrogen production is desired and in the case in which steam is added in the gasification medium, the important reaction to be considered is the *Water Gas Shift Reaction (WGS)*. Conversion of CO by this reaction (3) increases the hydrogen yield as well as getting reducing the CO concentration [Luengnaruemitchai et al, 2003].

As a result of these reactions, a producer gas mainly composed of hydrogen and carbon monoxide is obtained. Carbon dioxide and methane are also present, in addition to inorganic impurities (H_2S, HCl, NH_3, alkali metals), organic impurities (tars) and particulate. The solid residue of the gasification process is the char, which consists of unreacted carbon and the mineral matter (ash) present in the gasifier bed [Rezaiyan et al., 2005].

Regarding the formation of tars, in broad terms, when biomass is heated, its molecular bonds break; the smallest molecules are gases, and the larger molecules are called primary tars. Primary tars, which are always fragments of the original material, can react to become secondary tars by further reactions at the same temperature and tertiary tars, such as phenanthrene and pyrene, at higher temperatures [Milne et al., 1998; Basu, 2006].

Milne et al. classified the tars in four groups according to the reaction regimes:

1. Primary products derived from cellulose, hemicellulose and lignin;
2. Secondary products characterized by phenolics and olefinics structures;
3. Alkyl tertiary products, which are mainly methyl derivatives of aromatic compounds;
4. Condensed tertiary products consisting generally condensed polycyclic aromatic hydrocarbons (PAHs).

Their nature depends on temperature reaction. Table 3 shows the structural modifications as a function of process temperature, going from primary products to aromatic hydrocarbons [Milne et al, 1998]:

Table 3: Evolution of gasification tars as a function of temperature [Milne et al, 1998]

Mixed oxigenates	→	Phenolic ethers	→	Alkyl phenolics	→	Heterociclic ethers	→	PAHs	→	Larger PAHs
400°C		500°C		600°C		700°C		800°C		900°C

The main factors that affect the quality of the producer gas are the gasification medium as well as the operating temperature and pressure. The gasification medium has a decisive impact on the composition of the output tars. Tars from steam gasification contain a higher fraction of phenols and other oxygenates, suggesting interactions between organic compounds in the gas and surface hydroxyl groups produced by dissociative adsorption of water on the oxide

catalyst. In contrast, gasification with air favors the formation of other aromatics and polyaromatics [Torres et al., 2007].

Important influence on the producer gas quality is also exerted by the biomass particle size; an evidence of this consideration is the large amount of papers dedicated on it [Rapagnà et al., 1996; Ryu et al., 2006; Rapagnà et al, 2008; Tinaut et al., 2008].

Small particles have higher burning rates and ignition front speeds, while large particles are thermally thick having slow devolatilisation rate and more distributed heat transfer to the nearby particles [Ryu et al., 2006].

Other aspects affecting the producer gas quality are the reactor heating rate, the residence time and above all the plant configuration [Rezaiyan, et al., 2005].

2.2. Fluidized bed gasification and gas clean-up technologies

2.2.1. Elements of Fluidization state

Broadly speaking, fluidization is a process whereby a bed of solid particles is transformed into something resembling a boiling liquid. This is achieved by pumping a fluid upwards to the bed at a rate that is sufficient to exert a force on the particles that exactly counteracts their weight. In this way, the bed acquires fluid-like properties [Gibilaro, 2001].

Thus, a fluidized bed displays the following characteristics [Basu, 2006]:

- The static pressure at any height is approximately equal to the weight of the bed solids per unit of cross-sectional area above that level;
- An object denser than the bulk density of the bed will sink, while one lighter will float;
- The solids from the bed may be drained like a liquid through an orifice at the bottom or on the side of the container, in similarity to a water jet from a vessel;
- The bed surface maintains a horizontal level, independent of how the bed is tilted. Also, the bed assumes the shape of the vessel;
- Particles are well mixed, and the bed maintains a nearly uniform temperature throughout its body when heated.

Fluidization starts at a point when the bed pressure drop exactly balances the net downward forces (gravity minus buoyancy forces) on the bed packing consequently the solid particles begin to move to the point where they are all suspended in the current.

If the fluid velocity is below the lower limit, the particles are stationary and in direct contact with their neighbors, but when the gas-flow rate through the fixed bed is increased, the pressure drop due to the fluid drag continues to rise until the superficial gas velocity reaches a critical value known as the minimum fluidization velocity, U_{mf}. At the velocity where the fluid drag is equal to a particle's weight less its buoyancy, the fixed bed transforms into an incipiently fluidized bed. In this state the body of solids behaves like a liquid. The U_{mf} value could be experimentally verified or calculated using the Ergun equation [Basu, 2006].

At this point there are two different types of fluidization:

- Homogeneous fluidization, in which a further increase in flow above the minimum fluidization, entails a slight and gradual expansion of the bed;
- Heterogeneous fluidization, in which boiling phenomena occur. Increasing the gas flow rate the fluidization regimes become turbulent and the agitation turns violent.

The behavior of fluidized solid-gas systems depends on the properties of the solid particles, such as the density difference between the particles and the fluidizing medium, $(\rho_p - \rho_f)$, and the mean particle diameter, d_p, as shown by the Geldart's powder classification. This classification system divides powders into four groups, i.e., A, B, C and D. In brief, Group A powders exhibit a non-bubbling fluidization regime (Aeratable – 30-100μm, e.g.. milk powder); Group B powders begin to bubble immediately upon fluidization (Bubbling – 100-1000μm, e.g.. sand); Group C powders are cohesive and do not fluidize in the strict sense (Coesive – 0-30μm, e.g. flour); Group D powders can produce deep spouted beds (Spoutable – >1000μm, e.g. coffee bean).

A bed is at the minimum fluidized condition when the superficial gas velocity is equal to U_{mf}. In this state, there are no bubbles, and only emulsion phase remains. For Group B and D particles, addition of any gas in excess of this goes to the

formation of bubbles, which push their way into the emulsion phase of solids, resulting in bed expansion [Basu, 2006].

In the regimes mentioned (fixed, bubbling and turbulent), solids are generally retained in the bed within a certain height above the grid. Except for some entrainment, there is no large-scale migration of particles with the gas.

The upper limit of fluidization is the terminal velocity, which can be broadly defined as the velocity that is large enough to lift a single particle and carry it out of the fluidized bed. Consider a particle falling freely from rest and accelerating under gravity in an infinite and stationary medium. The buoyancy force and the fluid drag oppose the effect of gravity. The particle accelerates until it reaches an equilibrium velocity called the terminal velocity. The equilibrium condition experienced is equivalent to that of a motionless particle suspended in an upwardly flowing fluid; the particle experiences an upward fluid drag related to the kinetic energy of the fluid and the projected area of the particle.

2.2.2. Fluidized bed gasification

In Figure 5 is reported a simplified outline of the steps involved in the conversion of biomass into energy using gasification. For each step of the process, several technologies could be exploited depending on different aspects, such as for example, the end-use of the producer gas.

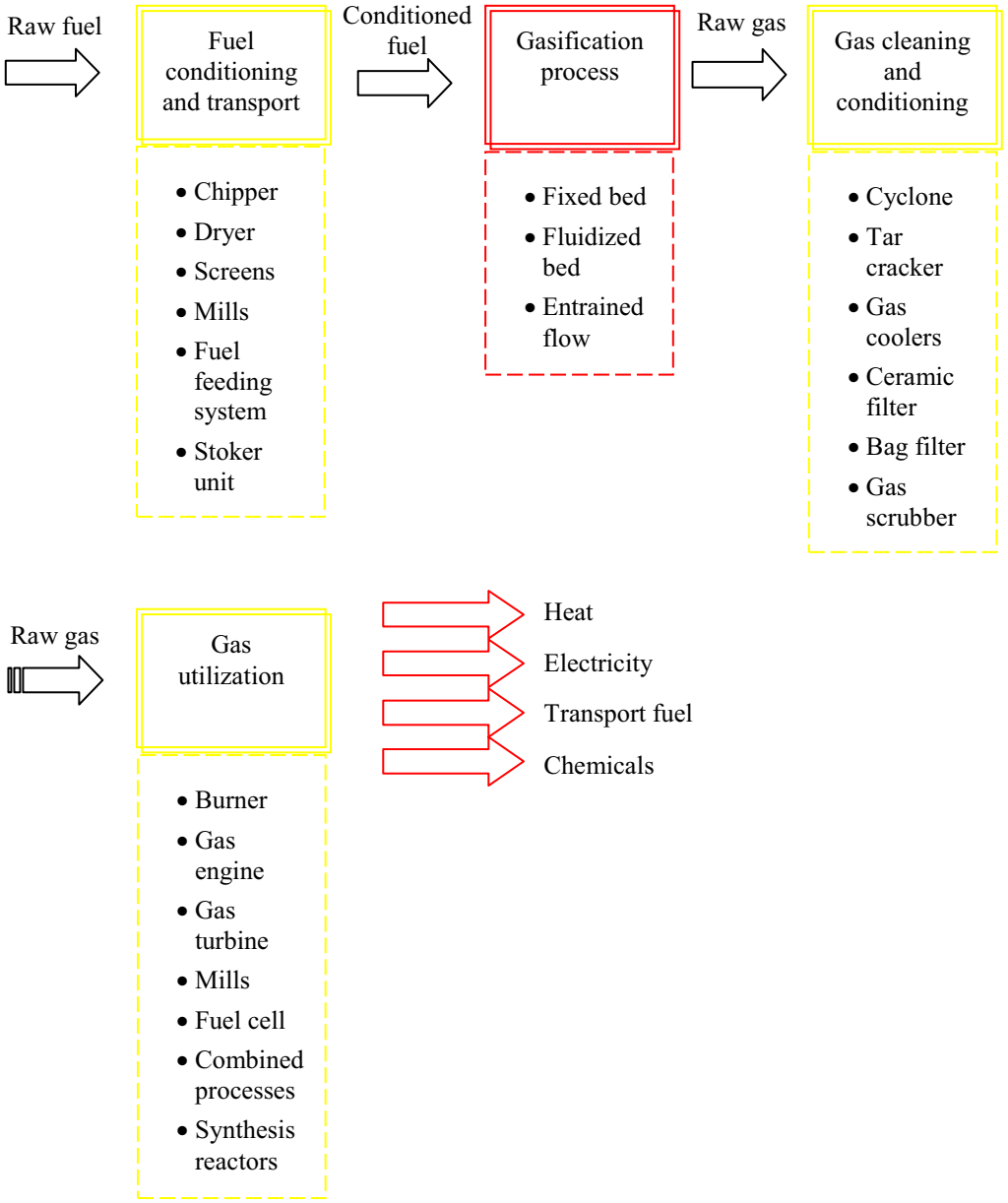

Figure 5: Main steps involved in the production of energy using biomass gasification

Among the different gasification technologies available fluidized bed gasifiers are very attractive, because they take the advantage of the excellent mixing characteristics and high reaction rates of gas-solid mixtures (Figure 6).

Figure 6: Salient features of different design of biomass gasifier [Pruig-Arnavat et al., 2010]

Figure 7 shows a schematic representation of the four processes of drying, pyrolysis, oxidation and gas phase reactions that take place in a fluidized bed gasifier [van Paasen and Kiel, 2004]. When the biomass is introduced into the fluidized bed the high heat and mass transfer characteristic permits the rapid energy conversion at practically isothermal conditions [Natarajan et al., 1997].

Traditionally fixed bed gasifiers are employed for small-scale energy production. In fact, the poor radial heat transfer in fixed beds limits their use to small gasifier, since with large gasifiers maintaining a high enough temperature everywhere in the reactor would lead to hot spot where slagging (formation of molten or partially fused deposits) could occur, especially with biomass feedstock that are more prone to slagging than coal. Fluidized bed gasifiers, instead, provide a uniform temperature and greatly reduce the risk of slagging [Briens et al., 2008].

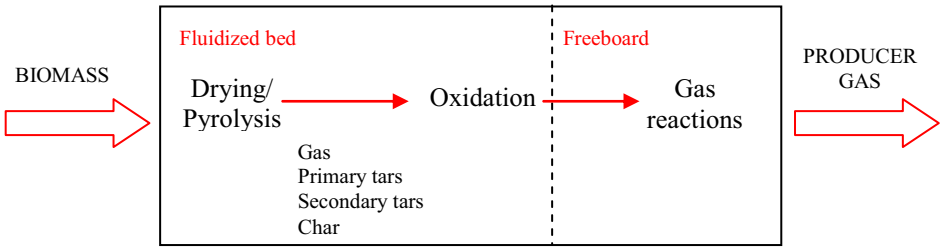

Figure 7: Schema of the gasification stages in a fluidized bed gasifier [van Paasen and Kiel, 2004]

Fluidized bed gasifiers are divided into the following two major types (Figure 8)

- Bubbling fluidized bed gasifier (BFB)
- Circulating fluidized bed gasifiers (CFB)

In fluidized bed gasifiers, biomass particles are feed in the bed of the reactor, where they are fluidized with the bed material and gasified. The bed inventory could be made of inert particles, such as sand, or catalysts particles such as dolomite.

A bubbling fluidized bed cannot achieve high solids conversion, due to the backmixing of solids. The high degree of solid mixing helps gasification, but owing to the intimate mixing of fully gasified fuels with partially gasified, any waste solid stream will contain some partially gasified solids reducing the solid conversion. Particle entrainment from a bubbling bed also contributes to the loss in a gasifier. The other important problem with BFB gasifiers is the slow diffusion

of the oxygen from the bubbles to the emulsion phase, which creates oxidizing conditions in the whole bed decreasing the gasification efficiency. The circulating fluidized bed (CFB) can get around this problem by providing longer solid residence time within its solid circulation loop [Basu, 2006].

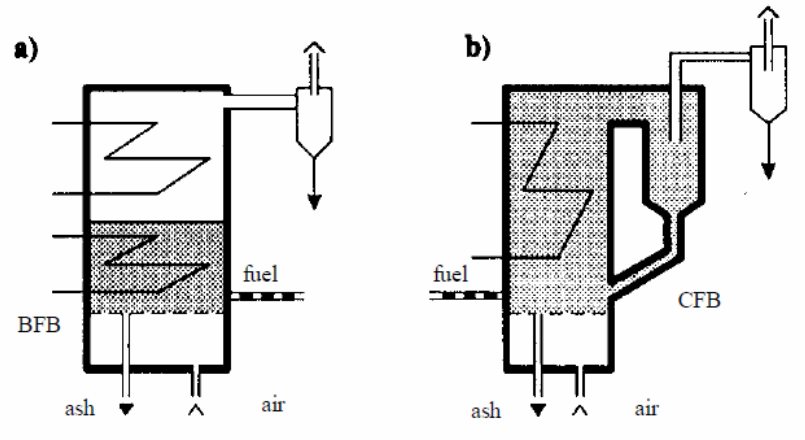

Figure 8: Sketch of a BFB gasifier (**a**) and a CFB gasifier (**b**)

Fluidized bed gasifiers, also, operate at temperatures below the ash melting temperatures (900–1050 °C). As a consequence, the incomplete carbon conversion in a single stage occurs and it is therefore common for the residual char to be either removed and burnt in a separate combustion unit or re-circulated into the gasifier.

In addition, CFB reactors, burning the char in secondary combustor unit provides the heat required for the gasification process, as the heat produced from the combustion is transported by circulating the bed material from the combustion zone to the gasification zone.

2.2.3. Gas cleaning treatments

After the gasification process the raw producer gas may be cleaned and conditioned, in order to reduce is content of impurities; removal requirements vary depending on the end-use of the producer gas.

The main problems to deal with during biomass gasification are enumerated as follows:

- Solid particulate: necessarily originated from the gasification and entrained by the syngas; particulate levels must be reduced below 50

mg/Nm^3 for gas engines and below about 15 mg/Nm^3 for turbines [Rezaiyan et al., 2005], where Nm^3 stands for Normal Cubic Meter of gas. Because the volume of gasses change with temperature or pressure, it is necessary to specify the temperature and pressure the flow rate was measured at: the Nm^3 corresponds to the standard conditions of 0°C, and 1 atmosphere of pressure. The particulate tolerance of fuel cell is about few mg/Nm^3;

- Tar. "Tar is a generic (unspecific) term for entity of all organic compounds present in the gasification product gas excluding gaseous hydrocarbons, C1 through C6" [UNI CEN TS 15439, 2008]. Tar is undesirable because of various problems associated with condensation, formation of tar aerosols and polymerization to form complex structures, which cause problems in the process equipment as well as the engines, and turbines used in the application of the producer gas [Devi et al., 2005], e.g. in the gas quality for successful internal combustion engine operation has been postulated as less than 100 mg/Nm^3 [Hasler et al., 2000]
- Sulphur compounds: generated by the gasification process because of the presence of a limited amount of sulphur in the biomass. H_2S is responsible of chemisorption on Nickel surface in the catalytic gas conditioning systems and in the SOFC (Solid Oxide Fuel Cell);
- Alkali metals: released as chlorides during gasification. As described above, they are responsible of ash softening and melting, thus plugging filter elements and gas passages. They are the major factor of fouling;
- Heavy metals: released during gasification from pollutants in the biomass. They poison the Ni catalyst and/or the anode of the SOFC;
- Hydrogen chloride: fuel bound chlorine in biomass released as HCl during gasification, which is responsible of high temperature corrosion and also facilitate slag deposit;
- NH_3 compounds: fuel bound nitrogen in biomass is principally released into the syngas primarily as ammonia and only a small part as HCN. When combusted NH_3 has the tendency to form NO_x precursors of "acid rains".

Among the problems listed, the discussion will be focused mostly on tar and particulate abatement strategies, which represent the hot topic of the present thesis. Hot gas cleaning is actually a focal point of applied research in the gasification field; this is evident considering the number of papers appearing in the literature [Bridgwater A.V., 2003; Simell et al., 1996; Caballero et al., 2000; van Paasen and Kiel, 2004] and the number of nationally and internationally funded research projects that deal with it in one way or another.

Hot gas conditioning using current or future commercially available catalysts offers the best solution for mitigating biomass gasification tars. Tars are eliminated and methane can be reformed if desired [Dayton et al., 2002].

2.2.3.1. Particulate removal technologies

Traditional particulate removal is carried out by means of cyclonic filters, barrier filters, electrostatic filters and wet scrubber.

Cyclonic filters are a primary mean of removing bulk particulates from gas stream. Cyclones are devices that employ a centrifugal force generated by a spinning air stream to separate particles from a carrier air. Their simple design, low capital cost and nearly maintenance free operation make them ideal for use as pre-cleaners [Kim et al., 2007]. Cyclonic filter are often designed as multiple series; multiple cyclones have overall mass removal efficiencies of 70-90%. However, cyclone collection efficiencies fall off rapidly with particle size. While no accurate statement of collection efficiency can be made without precise details of the cyclone design and fly ash properties, cyclone removal efficiencies will be 90% or greater for 10 μm particles. Experimental results reported by Ji et al. show that the overall collection efficiencies and grade efficiencies increased with the increasing particle concentrations and inlet velocities; most of the particles with the diameter bigger than 10 μm can be removed by cyclone separator [Ji et al., 2009]. Addition of a second multiple cyclones in series with the first will allow for increased removal efficiency. Kim et al. in 2007 developed a novel cyclone train with collection efficiencies of 70% for 1 μm and 97% for 10 μm [Kim et al., 2007].

Cyclone filters also remove condensed tars and alkali material from the gas stream, although the vaporized form of those constituents remain in the gas stream

[Rezaiyan et al., 2005].

Barrier filters, such as ceramic filter candles and bag filters, include a range of porous materials that allow gases to penetrate but prevent the passage of particulates. These filters effectively remove small-diameter particulates in the range of 0.5 to 100 μm. They need to be cleaned periodically passing pulsing clean gas through the filter in the reverse direction of normal gas flow. Tars have the tendency to cling the filter surface and can undergo subsequent carbonization reactions that lead to fouling and plugging.

Hot gas barrier filters provide opportunity to produce a clean fuel gas while retaining the sensible heat of the fuel gas. Ceramic filter candles are suitable for high temperature operation but are fragile and can break from thermal stress during temperature cycling. These filters are also susceptible to reactions with alkali vapors in gasification systems that can lead to decomposition or plugging [Rezaiyan et al., 2005].

In case of electrostatic filters the producer gas flows past high-voltage electrodes that impart an electric charge to particulates. The particulates are then collected as the gas stream passes collector plates of the opposite polarity. Particulates are then removed from the plates by either wet or dry methods. Electrostatic filters are the best suited for large-scale operation [Rezaiyan et al., 2005].

In wet scrubbers, particles are collected by collision with liquid sprays (usually water in case of particulate removal), and the droplets are then captured from the gas stream in a demister. Wet scrubbing requires that the water remain in the liquid phase, so the producer gas must be cooled to below 100°C; this loss of sensible heat may be undesirable. Thus, most gasification systems currently use web scrubbers primarily as a means to efficiently remove tars rather than particulate [Rezaiyan et al., 2005]. In this case the liquid spray is usually diesel fuel.

2.2.3.2. Tars removal technologies

Tar can be removed from the product gas by chemical and physical methods. Chemical methods destroy the tar, converting it to smaller molecules. Physical methods only remove the tar yielding a tar waste stream. Several devices are available for tar conversion and removal. Most removal devices are meant

primarily for particle removal [Basu, 2006].

The most diffused tar removal devices are summarized in Figure 9.

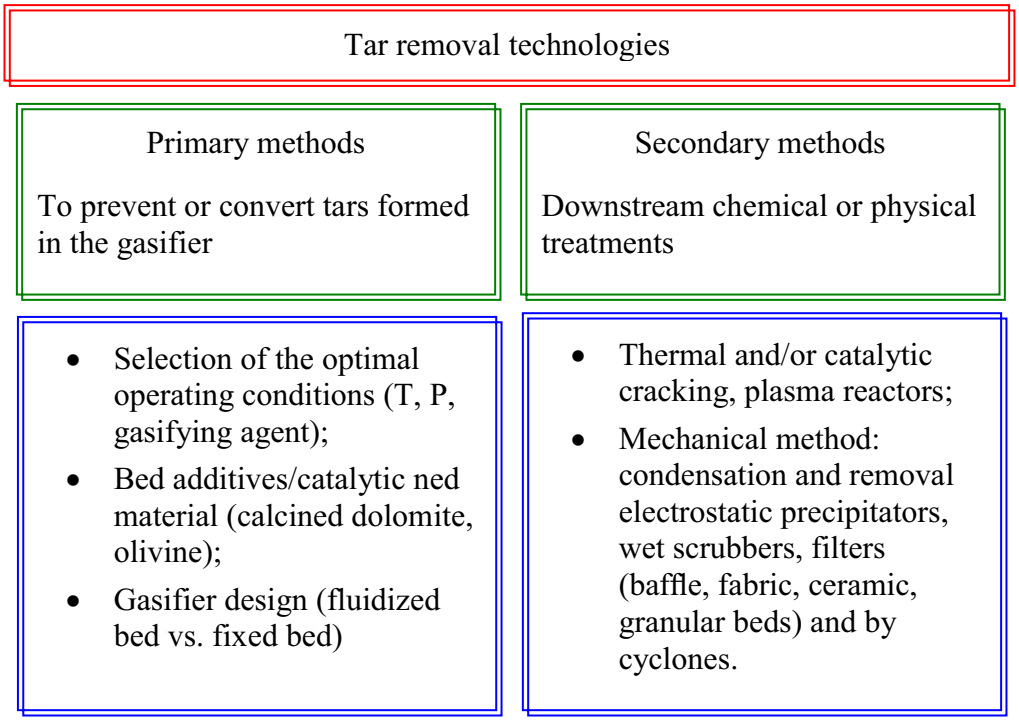

Figure 9: Common devices available for tar conversion and removal

If the gas temperature is maintained above 400°C, the tar does not condense. So, in applications of direct combustion such as cofiring (simultaneous combustion of different fuels in the same boiler, e.g. coal and biomass), one can avoid having to strip the gas of its tar.

Catalytic cracking is preferred to other forms of cleaning as it maintains the heating value of the tar by converting it to other gases [Basu, 2006]. In addition, in case of secondary mechanical methods the gas temperature is reduced to close to ambient, thus the dissipation of the sensible heat results in a loss of energy, if not recovered. This factor penalizes significantly the overall economic performance for "green" electricity generation based on biomass.

Conventional techniques for catalytic tar removal are two step cleaning processes; two different arrangements are possible: in the first case downstream filter equipment is followed by a catalyst unit (for example a fixed bed of catalyst). The inconvenient in this case is that it is necessary to reheat the particles-free gas to

the catalyst operating temperature. In the second case the catalyst unit is placed upstream of the filter unit, but this arrangement could lead to a fast deactivation of the catalyst by particle deposition [Nacked et al., 2007].

Calcined dolomite and nickel-based catalysts are commonly used downstream of the gasifier for catalytic cracking of tar. Their use as catalytic bed materials for tar reduction is another attractive option [Basu, 2006].

The presence of additive in the bed material not only influences the gas composition, but also the heating value of the producer gas. The use of catalytically active materials during biomass gasification changes the producer gas composition and reduces the tar yield. Addition of active bed materials also prevents agglomeration tendencies and subsequent chocking of the bed [Devi et al., 2005].

Several studies were dedicated to evaluation of the activity of olivine – $(Mg,Fe)_2SiO_4$) – and dolomite – $(Ca,Mg)CO_3$ – as bed materials for tar conversion in biomass gasification process. Calcined dolomite is the most widely used nonmetallic primary catalysts for tar conversion; dolomite is a calcium and magnesium carbonate, the surface area and the oxides in its matrix makes it an active catalyst, by the way it is not very robust, and the attritions in fluidized bed gasifier lead to the production of large amount of fines [Dayton, 2002].

Olivine is a natural occurring silicate mineral containing magnesium, iron and silicon, with a higher mechanical strength; Corella et al. reported that olivine generated four to six times less fines than dolomite in the gasification gas [Corella et al., 2004]. It has been recently demonstrated that olivine activity, or more specifically olivine activation, depends on its iron oxides content [Rauch et al., 2006], in fact depending on olivine temperature treatment, iron can be present in the olivine phase, or as iron oxides [Swierczynski et al., 2006].

Rapagnà et al. investigated the catalytic activity of olivine and observed that it has a good performance, comparable to that of calcined dolomite [Rapagnà et al., 2000]. Devi et al. have demonstrated that the addition of 17% of olivine and dolomite to the sand bed improved the conversion of each class of tar. It was also observed that thermal treatment (sand bed only) is only sufficient to remove

heterocyclic tar. The total tar conversions observed were 63% over calcined dolomite and 46% over olivine [Devi et al., 2005].

In 2002, Courson et al. demonstrate that olivine alone does not shows any methane reforming activity; on the contrary Ni/olivine catalyst, obtained by impregnation of natural olivine with a nickel salt solution, exert a methane reforming activity and at the same time enhance the conversion of tars [Courson et al., 2002]. The same synthesis methodology can be applied to other transition metals like cobalt, copper or iron. The production of Fe/olivine is one of the most interesting solution, because this metal does not affect catalyst cost thanks to the lower price of iron compared to nickel and without harm for the environment.

Thanks to nickel dehydrogenation/hydrogenation activity, nickel-based catalysts are very effective in terms of tar removal as well as in decomposition of ammonia and methane, but when they are susceptible of fast deactivation due to sulphur poisoning and carbon deposition [Hepola and Simell, 1997]. Ni-catalysts are also limited by phase transformation, sintering, loss of active components by volatilization or attrition and fouling by deposition of coke and carbonaceous materials [Bangala et al., 1997]

One of the options to protect nickel from deactivation phenomena is to place the catalysts in a secondary unit downstream to a selective guard-bed with calcined dolomite used to decrease the tar content at the inlet of the catalytic bed to a level below 2 g/Nm^3 [Corella et al. 1999]

Unfortunately, the use of gasifier downstream units impacts on the costs; in fact additions to the plant scheme to obtain a tar-free product significantly contribute to the overall investment, especially in small- biomass gasification plants. Small plants involve the use of a compact design in order to decrease the heat loss and to simplify the overall process. Thus, in case of small- and medium plants, the most effective way to obtain a tar-free product is to combine particle filtration and catalytic tar removal in one unit, a catalytic hot gas filter with the specification required to use it in the gasifier unit.

Three systems are currently available to produce a catalytic filter: the usually selected way is the catalytic activation of a porous ceramic hot gas filter element by developing a catalytic coating on the porous support. However this procedure

leaves little freedom in the catalyst layer thickness and is complex to manufacture. Another way is to insert the catalyst in the ceramic grains and binder mixture during common manufacturing of ceramic filter; in this type of catalytic filter, though, the sintering of catalyst could occur. The third way feasible is to integrate a catalyst in a ceramic hot gas filter elements and this way requires a modification of the design by using a porous inner tube to allow the integration of a catalyst particle layer [Nacken et al., 2007].

The combination of particle filtration and catalytic tar removal in one unit, a catalytic hot gas filter have the potential to lead to a valued compact biomass gasifiers, which assures that the hot gas that leaves the reactor is free of solid particles and tar.

3. Characterization of tar produced during biomass gasification

In 1998, Milne et al. reported that analyzing the literature results concerning tar levels, a bewildering array of values was found. Three of many reasons for this have no relation to the gasifiers performance per se, but are a result of:

- the different definitions of "tar" being used;
- the circumstances of the sampling;
- the treatment of the condensed organics before analysis.

There is general agreement about the relative order of magnitude of "tar" production, with fixed-bed updraft gasifiers being the "dirtiest," fixed-bed downdraft the "cleanest," and fluidized beds intermediate. A very crude generalization would place updraft at 100 g/Nm^3, fluid beds at 10 g/Nm^3, and downdraft at 1 g/Nm^3. It is also well established that updraft gasifiers produce mainly primary tars (Figure 5), downdraft gasifiers produce an almost exclusively tertiary tars, and fluid beds produce a mixture of secondary and tertiary tars [Milne et al., 1998].

An important point, independent of the further analytical method applied to tar quantification, is that the sampling is the critical part to obtain a representative and reproducible tar profile during the process. In 2000, Hasler et al. reported the presence a dozen of different sampling methods with various tar definition in use,

and it must be assumed that most of the methods used lead to non-comparable results [Hasler et al., 2000]

During the 1998 EU/IEA/US-DOE meeting on tar measurement protocol, it was agreed by a number of experts to define tar as all organic contaminants with a molecular weight larger than benzene [Maniatis et al., 2000]. Based on their molecular weight is possible to divide tar compounds into five groups as shown in Table 4 [Li and Suzuki, 2009].

Table 4: List of tar compounds that are considered for different tar classes

Tar class	Class name	Property	Representative compouns
1	GC-undetectable	Very heavy tars, cannot detected by GC	Determined by subtraction the GC-detectable tar from the total gravimetric tar
2	Heterocyclic aromatics	Highly water soluble compounds	Pyridine, phenol, cresol, quinoline, isoquinoline, dibenzophenol
3	Light aromatic (1 ring)	Do not pose a problem regarding condensability and solubility	Toluene, ethylbenzene, xylenes, styrene
4	Light PAHs (2-3 rings)	Condense at low temperature even at very low concentration	Indene, naphthalene, methylnaphtalene, biphenyl, acenaphtene, fluorene, phenanthrene, anthracene
5	Heavy PAHs (4-7 rings)	These molecule condense at high temperature at low concentration	Fluoranthene, pyrene, chrysene, perylene, coronene

When the tar vapor pressure exceeds the saturation pressure of the tar, the gas becomes (over) saturated according Raoult's Law. Thermodynamically, this state leads to condensation of the saturated vapor. The tar dewpoint is the temperature at which the real total partial pressure of tar equals the saturation pressure of tar. Thus, when the actual process temperature passes the thermodynamic tar dewpoint, tar can condense out. Hence, in condensation related issues, the tar dewpoint is a powerful parameter to evaluate the performance of gas cleaning systems [Li and Suzuki, 2009].

Heavy tar compounds dominate the tar dewpoint. Class 3 compounds condense at relatively high concentration ($10 g/m^3$), whereas class 5 tars already condense at very low concentration ($0,1 mg/m^3$), when the gas is at atmospheric pressure and ambient temperature [Devi et al., 2005].

3.1. The problematic of sampling

As analytical determination lays on representative sample, sampling is a key step in chemical analysis. The most important issue is to take a representative sample of the material under measurement. The best validated analytical technic could be drastically invalidated introducing large uncertainty with a non-representative sample, especially when the mixture contains volatile compounds and a panel of polar and apolar molecules.

3.1.1 Standardization of the sampling protocol: " Biomass gasification - Tar and particles in product gases – Sampling and analysis" (Technical specification UNI CEN/TS 15439:2008)

The necessity of a feasible comparison between tar values obtained in different gasification plants and by different working unit, has addressed the research to the development of a standard protocol for sampling and analysis of tars.

Thanks to the efforts into the development of the protocol carried out collectively from several research group (EU fifth framework project "Tar Protocol", 2000) [Simell et al., 2000; Knoef et al., 2000; Abatzoglou et al., 2000; Hasler et al., 2000] in 2008 the Technical Specification UNI CEN /TS 15439 was released.

The Technical Specification gives methods for sampling and analysis of tars and particles in order to determine the load of these contaminants in flowing biomass gasification product gases. It is applicable to sampling and analysis of tars and particles in the concentration range typically from 1 mg/Nm^3 to 300 g/Nm^3 (tars) and from 20 mg/Nm^3 to g/Nm^3 (particles) at all relevant sampling point conditions (0°C to 900°C and 0,6 bar to 60 bar) [UNI CEN /TS 15439:2008].

The method is based on the discontinuous extractive sampling of a representative part of a gas stream containing tar, under isokinetic conditions (Figure 10). The sampling train is configured as a heated probe with a heated particle filter to collect solid matter.

Collection of moisture and tar is performed in a series of six impinger bottles, or in specially designed equipment referred to as ''Petersen column'', which consists of a glass column with two washing stages, jacked cooled.

In the series of standard impinger bottles, the first impinger bottle acts as moisture

collector, in which water and tar condensed from the process gas by absorption in 2-propanol.

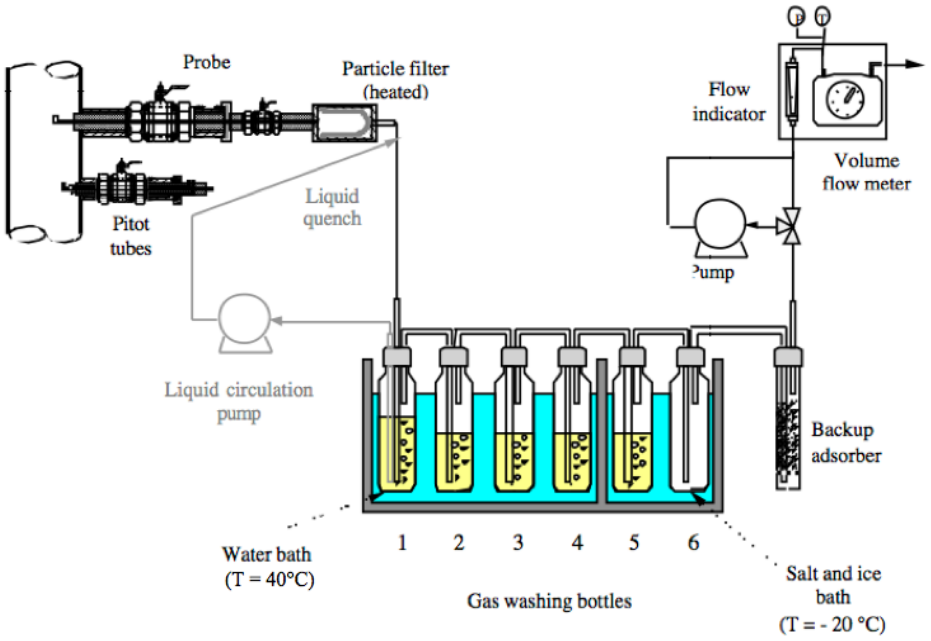

Figure 10: Standard collection system of tars, particulate and moisture

The heat released by gas cooling and condensation is removed by an external water bath. After the moisture collector the gas is passed through a series of four impingers with solvent and one final impinger, which is empty. The temperature of impinger bottles 1, 2, and 4 shall be between 35 °C and 40 °C, the temperature of impinger bottles 3, 5 and 6 shall be between –15 °C and –20 °C (Figure 10).

In figure 11 is reported the schema of the overall post-sampling procedures recommended by the Technical Specification 15439.

Gas chromatograph is the main analysis apparatus; GC should be fitted with a capillary column and a flame ionization detector (GC/FID) or a mass spectrometer (GC/MS). The sampling solution before the analysis shall be stored at a temperature < 5°C, and the analysis shall be performed and completed as soon as possible and within one month of sampling [UNI CEN /TS 15439:2008].

As shown in figure 10, the whole set of procedures are laborious and time consuming. Also, due to the relatively high concentration of tars in the 2-propanol flasks (the order of magnitude is mg/l) a sensible and accurate method like GC/MS is perhaps not the most appropriate technique to consider for the purpose.

Those considerations have led to the investigation of alternative sampling

methods and analytical techniques.

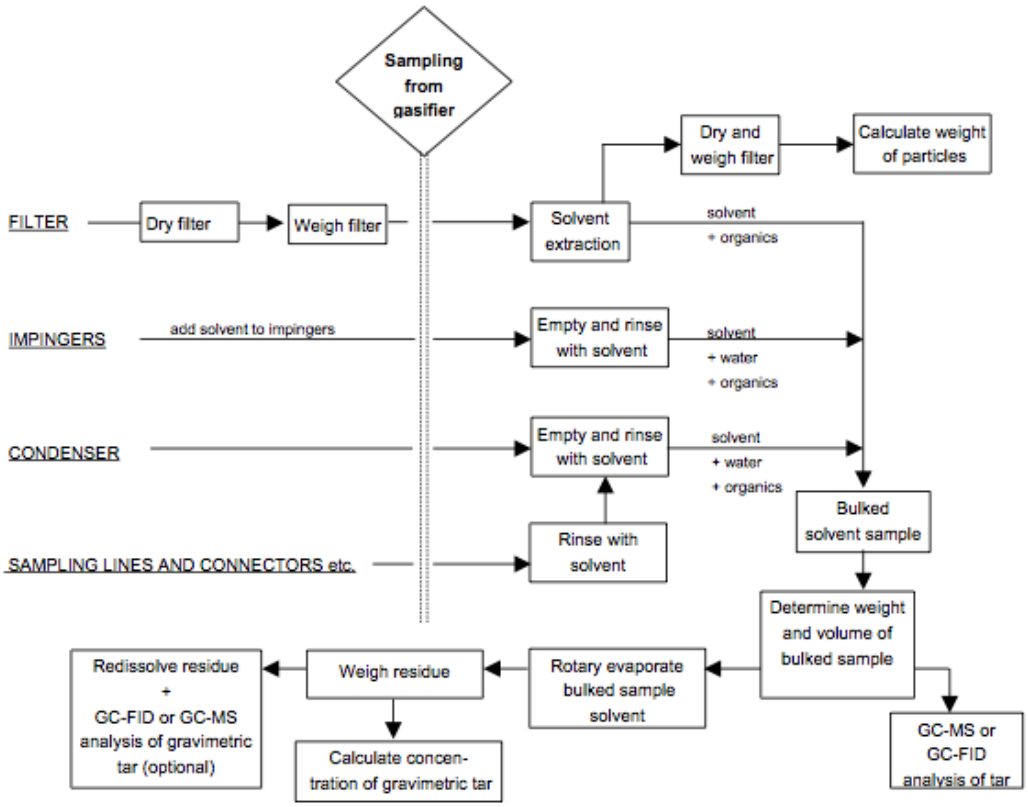

Figure 11: Schema of the overall post-sampling procedures recommended by the Technical Specification 15439

3.1.2 Sampling by adsorption of tar

The main objection to the Technical Specification 15439 concerns the sampling method adopted. Cold-trapping coupled with solvent absorption in impingers involves a long sampling time (about 1 h as a function of tar concentration) and possible sample losses and analytes segregation resulting from aerosol formation. In addition, sample dilution in solvent considerably reduces detection limits and causes disadvantages for gas chromatography separation between solvent and analytes [Dufour et al., 2007].

Since decades several works have been dedicated to the development of an appropriate sampling method for gasification tars [Brage et al. 1997, Xu et al., 2005; Carpenter et al., 2007; Dufour et al., 2007], most of them being using solid phase adsorption (SPA).

Recently, Dufour et al. propose SPA as sampling methods to follow tar

composition in gasification process with a short sampling time. SPA/TD (solid-phase adsorption + thermal desorption) coupled with GC/MS is a more accurate method than impingers especially for light PAHs. Tar sampling time is considerably shortened and limits of detection are increased; by the way, GC/MS analysis of the SPA tubes is about two times longer than for liquid injection due to TD. Another disadvantage of the SPA method is the loss of the sample after TD [Dufour et al., 2007].

A solvent-free tar quantification method is also proposed by Xu et al (2005) as an alternative to the tar protocol and yields results comparable to the evaporative method of the IEA tar protocol. This dry condenser method condenses organic compounds at 105 °C (referred to as "heavy tar") in a disposable tube and a fiberglass mat. By operating above the boiling point of water, the heavy tar is not contaminated with moisture. A gravimetric analysis of the tube and fiberglass mat allows the mass of heavy tar to be determined. Comparisons between the dry condenser methodology and the IEA tar protocol diverged by as much as 50%, with much of the discrepancy attributable to the poor precision of the two methodologies that allows the loss of molecules with high vapor pressure

3.2. Choice of Analytical Method suitable for tar determination

Considering the large panel of analytical tools described in the literature, the choice of a method is generally evicted by the cost effective investment and the limitation of each technic. Where online measurement should be useful to follow immediately the efficiency of the process, only few technics are commercially available.

3.2.1 On-line determination

The detection and quantification of tar could be achieved on-line using spectroscopic properties of aromatic compounds. During the last years several research studies were dedicated to the development of online determination of tars by means of optical methods, such as laser induced systems [Kerellas et al., 2007; Sun et al., 2010].

Aromatic compounds have fluorescent properties, Karellas et al. (2007) proposed to integrate the background observed measuring gas composition by online

Raman spectroscopy: a high fluorescence background is observed and increases with the tar content in the gas flow. However, this signal can be too intense when the tar content and the mass flow of the gas through the measurement cell are very high. In this case, it is not possible to determine in the same time the amount of tars and to define the gas composition,

The other approach [Sun et al., 2010] is based on fluorescence spectroscopy, exciting the tar with a 266 nm laser. The emission spectrum is then recorded with a standard fluorimeter deporting the signal with optical fibers. The measurement was only tested on a synthetic mixture of four standards showing a large variability of fluorescence response factor of each molecule. Moreover, the excitation wavelength disables to detect other molecules. Like the fluorescence signals obey the principle of superposition (according to Beer-Lambert law) the consequence could be complex for the quantification of a larger mixture, like observed in tars.

On the same way, UV spectroscopy could lay to global quantification for tars based on the mathematical treatment of absorbance at chosen wavelength or deconvolution of spectrum [Monakhova et al. (2010)]. The validity of this approach will be developed in this present work as no systems are developed in literature for on-line tar analysis.

Another method described by Moersch et al. (2000) quantifies tar using flame ionization detector (FID). The method is based on the comparison of the total hydrocarbon content of the hot gas and that of the gas with all tars removed. Hot gas from the gasifier is led directly into the set up. However the major obstacles for the application of this principle are due to the use of a filter that traps not only Tar abut also water in gas phase: then the gas flow is modified and also not regular in the FID The addition of this equipment on the plant will the increase technic problems of gas regulation additionally to the cost.

Noteworthy, for many industrial applications, the estimated cost to-benefit ratio is not suitable and such expensive systems cannot be installed for the analysis of the tar composition.

3.2.2 Off line measurement

3.2.2.1 Analysis based on separative methods

As far as the analytical methods are concerned, several options are already available among the technique commonly

used for the determination of PAHs. Because of their negative impact on tar dewpoint and the correlated fouling phenomena, the quantification of GC-undetectable tars (Table 4) has a primary role in tar characterization. The UNI CEN/TS 15439 recommends their evaluation by calculation of gravimetric tars (Figure 11), after an evaporation step in standard condition. The sample weighted is then re-dissolved and analyzed by GC/MS for the determination of GC-detectable tars. However, the evaporation step could result in a loss of volatile tars from the sample.

On the contrary, high performance liquid chromatography (HPLC) allows the quantification of individual light hydrocarbons as well as heavy hydrocarbons with a molecular mass higher than coronene (6-aromatic rings, class 5) [van Paasen and Kiel, 2004], without evaporative steps.

Applications of HPLC, coupled with UV and/or fluorescence detector, in the field of PAHs analysis in different matrices are well documented [Palmentier et al., 1989; Bazylak et al., 1990; Kayaly-Sayadi et al., 2000, Zhang et al., 2007]. Liquid chromatography is widely used in petroleum chemistry, being most important for determination of thermally unstable and non-volatile compounds [Berezkin et al., 2007]. Thus this robust analytical tool could be successfully employed in tar characterization.

Recently, Zhang et al. developed an interesting method for the identification and quantitative determination of PAHs in heavy products derived from coal and petroleum with HPLC. After the separation of PAHs by a high-resolution column, identification was made through four methods: (1) the relative retention time (RRT) method, (2) the stop-flow-UV scanning method, (3) the method of fluorescence characteristic index and (4) the method of UV characteristic index.

Size exclusion Chromatography was also adapted to tar analysis in biomass fixed bed gasification [Phuphuakrat et al. (2010)] to follow the molecular mass tar

distribution varying air supply. To follow the evolution of the compounds, the analysis were completed by GC-FID quantification.

Besides the need for a thorough characterization of the samples, there is also a need to develop analytical methods (online and/or offline) capable to provide data on the total tar content in a rapid and efficient way. Better yet, if this quantitative measurement can be supported by a rapid screening assay, able to provide qualitative information on the nature of the compounds present in the sample.

Concerning the conventional chromatographic methods, thin-layer chromatography (TLC) frequently becomes an optimal method for resolving some important problems. As compared to the column version, this technique is characterized by the simplicity of its experimental operations, a simple preparatory routine for running a series of determinations (the sample preparation step for the subsequent run is frequently unnecessary, since the plate with a sorbent layer is disposable) and a low cost [Berezkin, 2007]. Planar chromatography (TLC) coupled with UV and fluorescent densitometry, also is particularly well adapted to complex systems and takes the advantage of simultaneous development of standards and samples, and the possibility of scanning the same sample under different conditions [Matt et al., 2003].

Also, HPTLC (high performance thin-layer chromatography) is carried out using automatic sample application that will help to improve the chromatographic separation as well as validate the quantitative analytical approach.

Several publications concern the use of this technique in separation and group type analysis of heavy petroleum fractions refined to various degrees, including natural base oils and coal tar pitch [Herod and Kandiyoti, 1995; Sharma et al., 1998; Lazaro et al., 1999; Kamiński et al., 2003; Matt et al., 2003; Li et al., 2004].

Hydrocarbon group type analysis (HGTA) is able to determine four classes of compounds: (1) saturated compounds; (2) aromatic compounds, including hydrocarbons with one, two, three r more aromatic rings, sometimes further divided into subgroups based on the number of aromatic rings; (3) resins and (4) asphaltenes [Kamiński et al., 2003]. No applications of HPTLC in biomass gasification tars have been investigated.

3.2.2.2 Analysis based on spectroscopic Methods

Between the optical methods, fluorescence measurements and in particular synchronous fluorescence (SFS) would appear to be techniques worth considering, thanks to the strong fluorescence emission of aromatic compounds. A number of studies on qualitative and quantitative analysis of polycyclic aromatic hydrocarbons in different media using these techniques have been reported in the literature [Schwarz et al., 1976; Vo-Dihn, 1978; Lázaro et al., 2000; Patra et al., 2001; Sharma et al., 2007]. In conventional fluorescence applications an emission spectrum is obtained by scanning the emission wavelengths at a fixed excitation level. Otherwise, a synchronous fluorescence scan consists of a record of the spectrum where both monochromators are scanning, keeping a constant appropriate (delta lambda, $\Delta\lambda$) between excitation and emission wavelengths. That results in a narrowing of spectral bands, simplification of emission spectra and contraction of spectral range [Patra et al., 2002].

On the other hand, traditional and inexpensive UV spectroscopy also has the potential to be successfully applied in qualitative and quantitative PAHs analysis [Vogt et al., 2000]; In fact, absorbance at different wavelengths of UV light is a function of the different aromatic cluster sizes in the sample molecules and changes in the relative intensities of absorbance of the fractions indicate structural changes with changing molecular size. At higher wavelengths (450 and 350 nm), absorbance by larger aromatic clusters predominates, whereas at 280 and 300 nm, more information about the smaller aromatic clusters and low molecular mass can be obtained [Lazaro et al., 2001]. However few applications have been reported in the field of tar detection [Li et al., 1994].

A complete analysis of tar from sewage sludge in a spouted bed reactor was based on chromatographic (GC-FID; GC-MS, SEC), spectroscopic (synchronous UV Fluorescence) associated to thermal gravimetric methods (to follow the boiling point distributions of tar) [Adegoroye et al. 2004]. These tools were useful to follow the evolution of tar changing the temperature of the process, as the increasing of gasification temperature will be followed by a decrease of global molecular weight of tar, without complete conversion of heavy PAHs; the authors

observed also alkyl or heteroatom substituents as the temperature of formation increased.

References

Abatzoglou N., Barker N., Hasler P., Knoef H. (2000) The development of a draft protocol for the sampling and analysis of particulate and organic contaminants in the gas from small biomass gasifiers. Biomass and Bioenergy 18:5-17

Adegoroye A., Paterson N., Li1 X., Morgan T., Herod A.A., Dugwell, D.R., Kandiyoti. R. (2004) The characterisation of tars produced during the gasification of sewage sludge in a spouted bed reactor, Fuel 83 :1949–1960

Alauddin Z.A.B.Z., Lahijani P., Mohammadi M., Mohamed A.R. (2010) Gasification of lignocellulosic biomass in fluidized beds for renewable energy development: A review. Renewable and Sustainable Energy Reviews, 14:2852–2862

Bangala D.N., Abatzoglou N., Martin J.P., Chornet J.P. (1997) Catalytic gas conditioning: application to biomass and waste gasification. Industrial & Engineering Chemistry Research. 36:4184-4192

Basu, P. (2006) Combustion and gasification in fluidized beds, Taylor & Francis Group, LLC (USA)

Bazylak G. and Maslowska J. (1990) HPLC determination of PAHs in mineral oil used as dispersing agents for herbicides. Fresenius' Journal of Analitycal Chemistry, 336(3):205-209

Berezkin V.G. (2007) On the application of thin-layer chromatography in petroleum chemistry. Petroleum Chemistry 47:415-420

Bin Yang Y., Ryu C., Khora A., Yatesb N.E., Sharifia V.N., Swithenbank J. (2005) Effect of fuel properties on biomass combustion. Part II. Modelling approach—identification of the controlling factors. Fuel 84, 2116–2130

Brage C., Yu Q., Chen G., Sjöström K. (1997) Use of amino phase adsorbent for biomass tar sampling and separation. Fuel, 76(2):137-142

Bridgwater A. V. (2003) Renewable fuels and chemicals by thermal processing of biomass. Chemical Engineering Journal, 91:87–102.

Briens C., Piskorz J., Berruti F. (2008) Biomass valorization for fuel and chemical production – A review. International Journal of Chemical Reactor Engineering. Vol. 6, Review R2

Caballero M.A., Corella J., Aznar M.P., Gil J. (2000) Biomass gasification with air in fluidized bed. Hot gas clean-up with selected commercial and full-size nickel-based catalysts. Industrial & Engineering Chemistry Research, 39:1143–1154

Carpenter D.L., Deutch S.P, French R.J. (2007) Quantitative Measurement of Biomass Gasifier Tars Using a Molecular-Beam Mass Spectrometer: Comparison with Traditional Impinger Sampling. Energy Fuels, 21(5):3036–3043

COM(1997)599 "Energy for the future: renewable sources of energy" White Paper for a Community Strategy and Action Plan http://europa.eu/documents/comm/white_papers/pdf/com97_599_en.pdf

Corella, J., Orio, A., and Toledo, J. M. (1999) Biomass gasification with air in a fluidized bed: exhaustive tar elimination with commercial steam reforming catalysts, Energy and Fuels, 13(3):702-709

Corella J., Toledo J.M., Padilla R. (2004) Olivine or Dolomite as In-Bed Additive in Biomass Gasification with Air in a Fluidized Bed: Which Is Better?. Energy and fuels, 18:713-720

Courson C., Undron L., Świerczyńsky, Petit C., Kiennemann A. (2002) Hydrogen production from biomass gasification on Nickel Catalysts. Tests for dry reforming of methane. Catalysis Today 76:75-86

Danalatos N.G., Archontoulis S.V., Mitsios I. (2007) Potential growth and biomass productivity of Miscanthus×giganteus as affected by plant density and N-fertilization in central Greece. Biomass and Bioenergy, 31(2-3):145-152

Dayton D. (2002) A Review of the Literature on Catalytic Biomass Tar Destruction. Milestone Completion Report - NREL/TP-510-32815 http://www.fnr-server.de/ftp/pdf/btl/1126857146_ga_teer.pdf

Decreto Legislativo 29 dicembre 2003, n. 387 "Attuazione della direttiva 2001/77/CE relativa alla promozione dell'energia elettrica prodotta da fonti energetiche rinnovabili nel mercato interno dell'elettricità" http://www.camera.it/parlam/leggi/deleghe/testi/03387dl.htm

Decreto Legislativo 3 aprile 2006, n. 152 "Norme in materia ambientale" http://www.camera.it/parlam/leggi/deleghe/06152dl.htm

de Jong W., Pironand A., Wójtowicz M.A. (2003). Pyrolysis of Miscanthus Giganteus and wood pellets: TG-FTIR analysis and reaction kinetics. Fuel, Volume 82 (9), 1139-1147

Devi L., Ptasinski K., Janssen F.J.J.G., van Paasen S.V.B., Bergman P.C.A., Kiel J.H.A (2005) Catalytic decomposition of biomass tars: use of dolomite and untreated olivine. Renewable Energy, 30:565-587

DIRECTIVE 2001/77/EC OF THE EUROPEAN PARLIAMENT AND OF THE COUNCIL of 27 September 2001on the promotion of electricity produced from renewable http://eur-lex.europa.eu/LexUriServ/LexUriServ.do?uri=OJ:L:2001:283:0033:0033:EN:PDF

DIRECTIVE 2003/30/EC OF THE EUROPEAN PARLIAMENT AND OF THE COUNCIL of 8 May 2003 on the promotion of the use of biofuels or other renewable fuels for transport http://eur-lex.europa.eu/LexUriServ/LexUriServ.do?uri=OJ:L:2003:123:0042:0046:EN:PDF

DIRECTIVE 2009/28/EC OF THE EUROPEAN PARLIAMENT AND OF THE COUNCIL of 23 April 2009 on the promotion of the use of energy from renewable sources and amending and subsequently repealing Directives 2001/77/EC and 2003/30/EC http://eur-lex.europa.eu/LexUriServ/LexUriServ.do?uri=OJ:L:2009:140:0016:0062:en:PDF

Erol M., Haykiri-Acma H., Küçükbayraka S.(2010) Calorific value estimation of biomass from their proximate analyses data. Renewable Energy, 35(1):170-173

Gibilaro, L. G. (2001) Fluidization-Dynamics, Butterworth Heinemann, Oxford (UK)

Gustavsson L., Börjesson P., Johansson B., Svenningsson P. (1995) Reducing CO2 emissions substituting biomass for fossil fuels. Energy, 20(11):1097-1113

Hasler P., Nussbaumer T. (2000) Sampling and analysis of particles and tars from biomass gasifiers. Biomass and Bioenergy, 18:61-66

Hepola J., Simell P. (1997) Sulphur poisoning of nickel-based hot gas cleaning catalysts in synthetic gasification gas II. Chemisorption of hydrogen sulphide. Applied Catalysis B: Environmental 14:305-321

Herod A.A, Kandiyoti R. (1995) Fractionation by planar chromatography of coal tar pitch for charcterisation by size-exclusion chromatography, UV fluorescence and direct-probe mass spectrometry. Journal of Chromatography A, 708:143-160

Hiltunen M., Barišić V., Coda Zabetta E. (2008) Combustion of different types of biomass in CFC boilers. 16th European Biomass Conference, Proceedings of the 16th EU BC&E, ISBN 978-88-89407-58-1

Jenkins B.M., Baxter M.M., Miles T.R. Jr., Miles T.R. (1998) Combustion properties of biomass. Fuel Processing Technology, 54(1-3):17-46

Ji Z., Xiong Z., Wu X., Chen H., Wu H. (2009) Experimental investigations on a cyclone separator performance at an extremely low particle concentration. Powder Technology 191:254-259

Kamiński M., Gudebska J., Górecki T., Kartanowicz R.. (2003) Optimized conditions for hydrocarbon group type analysis of base oils by thin-layer chromatography-flame ionisation detection. Journal of Chromatography A, 991:255-266

Karellas S., Karl J. (2007) Analysis of the product gas from biomass gasification by means of laser spectroscopy Optics and Lasers in Engineering. 45(9):935-946

Kayali-Sayadi M.N., Rubio-Barroso S., Díaz- Díaz C.A, Polo-Díez L.M. (2000) Rapid determination of PAHs in soil samples by HPLC with fluorimetric detection following sonication extraction. Fresenius' Journal of Analitycal Chemistry, 368(7):697-701

Kim G.N., Choi W.K., Jung C.H. (2007) The development and performance evaluation of a cyclone train for the tar removal of contaminated hot particulate in hot cell. Separation and Purification Technology, 55:313-320

Knoef H., Koele H.J. (2000) Survey of tar measurement protocols. Biomass and Bioenergy 18:55-9

Lazaro M.J., Domin M., Herod A.A., Kandiyoti R. (1999) Fractionation of a wood tar pitch by planar chromatography for the characterisation of large molecular mass materials. Journal of Chromatography A, 840:107-115

Lazaro M.J., Moliner R., Suelves I., Herod A.A., Kandiyoti R. (2001) Characterisation of tars from the co-pyrolysis of waste lubricating oils with coal. Fuel, 80:179-194

Lázaro E., San Andrés M.P., Vera S. (2000) Determination of five polycyclic aromaric hydrocarbons in aqueous micellar media by fluorescence at room temperature. Analytica Chimica Acta, 413:159-166

Legge 30 dicembre 2008, n. 205 "Conversione in legge, con modificazioni, del decreto-legge 3 novembre 2008, n. 171, recante misure urgenti per il rilancio competitivo del settore agroalimentare" www.parlamento.it/parlam/leggi/08205l.htm

Leung D.Y.C., Yin X.L., Wu C.Z. (2004) A review on the development and commercialization of biomass gasification technologies in China Renewable and Sustainable Energy Reviews, 8(6):565-580

Lewandowski I., Clifton-Brown J.C., Scurlock J.M.O, Huisman W., Miscanthus: European experience with a novel energy crop. Biomass and Bioenergy, 19(4):209-227

Li W., Morgan T.J., Herod A.A, Kandiyoti R. (2004) Thin-layer chromatography of pitch and a petroleum vacuum residue. Relation between mobility and molecular size shown by size-exclusion chromatography. Journal of Chromatography A, 1024:227-243

Li C., Suzuki K. (2009) Tar property, analysis, reforming mechanism and model for biomass gasification – An overview. Renewable & Sustainable Energy Reviews 13:594-604

Luengnaruemitchai A., Osuwan S., Gulari E. (2003) Comparative studies of low-temperature water–gas shift reaction over Pt/CeO_2, Au/CeO_2, and Au/Fe_2O_3 catalysts. Catalysis Communications 4(5):215-221

Matt M., Galvez E.M., Cebolla L.V., Membrado L., Bacaud R., Pessayre S. (2003) Improved separation and quantitative determination of hydrocarbon types in gas oil by normal phase high-performance TLC with UV and fluorescence scanning densitometry. Journal of Separation Science, 26:1665-1674

McKendry P. (2002) Energy production from biomass (part 1): overview of biomass, Bioresource Technology 83:37-46

Maniatis K. and Beenackers A.A.C.M. (2000) Tar Protocols. IEA Bioenergy Gasification Task, Biomass and Bioenergy 18(1):1-4

Milne T.A., Evans R.J., Abatzoglou N. (1998) Biomass gasifier "Tars": their nature, formation and conversion, NREL/TP-570-25357

Moersch O., Spliethoff H., Hein K.R.G. (2000) Tar quantification with a new online analyzing method Biomass and Bioenergy 18 : 79±86

Monakhova Y., Astakhov S. Kraskov A., Mushtakova S., (2010) Independent components in spectroscopic analysis of complex mixtures, Chemometrics and Intelligent Laboratory Systems 103 : 108–115

Natarajan E., Nordin A., Rao A.N. (1998) Overview of combustion and gasification of rice husk in fluidized bed reactors Biomass and Bioenergy, 14(5-6):533-546

Nacken M., Ma L., Engelen K., Heidenreich S., Baron G.V. (2007) Development of a tar reforming catalyst for integration in a ceramic filter element and use in hot gas cleaning. Industrial and Engineering Chemistry Research 46:1945–1951.

Naidu L.S., Moose S.P., Al-Shoaibi A.K., Raines C.A. Long S.P. (2003) Cold Tolerance of C4 photosynthesis in Miscanthus x giganteus: Adaptation in Amounts and Sequence of C4 Photosynthetic Enzymes. Plant Physiology 132:1688-1697

Palmentier J.P.F., Britten A.J., Charbonneau G.M., Karasek F.M. (1989) Determination of polycyclic aromatic hydrocarbons in lubricating oil base stocks using high-performance liquid chromatography and gas chromatography—mass spectrometry. Journal of Chromatography A, 469:241-251

Patra D., Mishra A.K. (2001) Investigation on simultaneous analysis of multicomponent polycyclic aromatic hydrocarbon mixtures in water samples: a simple synchronous fluorimetric method. Talanta, 55:143-153

Phuphuakrat T., Nipattummakul N., Namioka T., Kerdsuwan S. Yoshikawa K., (2010) Characterization of tar content in the syngas produced in a downdraft type fixed bed gasification system from dried sewage sludge Fuel 89 : 2278–2284

Piano di azione nazionale per le energie rinnovabili dell'Italia (conforme alla direttiva 2009/28/CE e alla decisione della Commissione del 30 giugno 2009) http://www.sviluppoeconomico.gov.it/pdf_upload/documenti/PAN_Energie_rinnovabili.pdf

Plan d'action national en faveur des énergies renouvelables Période 2009-2020 En application de l'article 4 de la directive 2009/28/CE de l'Union europeenne http://www.developpement-durable.gouv.fr/IMG/pdf/0825_plan_d_action_national_ENRversion_finale.pdf

Price L., Bullard M., Lyons H., Anthony S. Nixon P. (2004). Identifying the yield potential of Miscanthus x giganteus: an assessment of the spatial and temporal variability of M. x giganteus biomass productivity across England and Wales. Biomass and Bioenergy, 26 (1), 3-13

Puig-Arnavat M., Bruno J.C., Coronas A. (2010) Review and analysis of biomass gasification models. Renewable and Sustainable Energy Reviews, 14:2841-2851

Rapagnà S. and Latif A. (1996) Steam gasification of almond shells in a fluidized bed reactor: the influence of temperature and particle size on product yield and distribution. Biomass and Bioenergy, 12(4):281-288

Rapagnà S., Jand N., Kiennemann A., Foscolo P.U. (2000) Steam-gasification of biomass in a fluidised-bed of olivine particles. Biomass & Bioenergy, 19:187-197.

Rapagnà S., Mazziotti di Celso G. (2008) Devolatilization of Wood Particles in a Hot fluidized Bed: Product Yields and Conversion Rate. Biomass and Bioenergy 32:1123-1129.

Rapagnà S., Gallucci K., Di Marcello M., Matt M., Nacken M., Heidenreich S., Foscolo P.U. (2010) Gas Cleaning, Gas Conditioning and Tar Abatement by means of a Catalytic Filter Candle in a Biomass Fluidized-Bed Gasifier. Bioresource Technology, 101(18):7134-41

Rauch R., Pfeifer C., Bosch K., Hofbauer H., Świerczyński D., Courson C., Kiennemann A. (2006) Comparison of different olivines for biomass steam gasification. Science in thermal and chemical biomass conversion, Ed. by A.V. Bridgwater and D.G.B Boocock CPL Press

Rezaiyan J., and Cheremisinoff N.P. (2005) Gasification technologies: a primer for engineers and scientists. CRC Press, Taylor and Francis Group (USA)

Ryu, C., Yang Y.B., Khor A., Yates N.E., Sharifi V.N., Swithenbank J. (2006). Effect of fuel properties on biomass combustion: Part I. Experiments – fuel type, equivalence ratio and particle size. Fuel, 85(7-8): 1039-1046.

Sander B. (1997) Properties of Danish biofuels and the requirements for power production. Biomass and Bioenergy, 12(3):177-183

Schwarz F.P., Wasik S.P. (1976) Fluorescence measurements of benzene, naphthalene, anthracene, pyrene, fluoranthene and benzo[e]pyrene in water. Analytical Chemistry. 48(3)524-528

Sharma B.K., Sarowha S.L.S., Bhagat S.D., Tiwari R.K., Gupta S.K., Venkataramani P.S. (1998) Hydrocarbon group type analysis of petroleum heavy fractions using the TLC-FID technique. Journal of Analytical Chemistry, 360:539-544

Sharma H., Jain V.K., Khan Z.H. (2007) Identification of polycyclic aromatic hydrocarbons (PAHs) in suspended particulate matter by synchronous fluorescence spectroscopic technique, Spectrochimica Acta Part A, 68:43-49

Simell P., Kurkela E. Stahlberg P. Hepola J. (1996) Catalytic hot gas cleaning of gasification gas. Catalysis Today, 27:55-62

Simell P., Ståhlberg P., Kurkela E., Albrecht J., Deutsch S., Sjöström K. (2000) Provisional protocol for the sampling and analysis of tar and particulates in the gas from large-scale biomass gasifiers. Biomass and Bioenergy 18:19-38

Sun R., Zobel N., Neubauer Y., Cardenas Chavez C., Behrendt F. (2010) Analysis of gas-phase polycyclic aromatic hydrocarbon mixtures by laser-induced fluorescence. Optics and Lasers in Engineering, 48(12):1231-1237

Świerczyński D., Courson C., Bedel L., Kiennemann A, Vilminot S. (2006) Oxidation reduction behavior of iron-bearing olivines $(Fe_xMg_{1-x})_2SiO_4$ used as catalysts for biomass gasification. Chemistry of Materials, 18:897-905.

Thompson D.N., Shaw P.G., Lacey J.A. (2003) Post-harvest processing methods for reduction of silica and alkali metals in wheat straw. Applied Biochemistry and Biotechnology, 105(1-3):205-218

Tinaut F.V., Melgara A., Pérez J., Horrillo A. (2008) Effect of biomass particle size and air superficial velocity on the gasification process in a downdraft fixed bed gasifier. An experimental and modelling study. Fuel Processing Technology, 89(11):1076-1089

Torres W., Pansare S.S., Goodwin J.G. Jr. (2007) Hot Gas Removal of Tars, Ammonia, and Hydrogen Sulfide from Biomass Gasification Gas Catalysis Reviews, 49(4):407-456

UNI CEN/TS 15439 "Biomass gasification - Tar and particles in product gases - Sampling and analysis", European Committee for Standardization, 2008

Van Paasen S.V.B., Kiel J.H.A. (2004) Tar formation in a fluidized bed gasifier: Impact of fuel properties and operating conditions. ECN-C-04-013 Report, 1-58.

Vogt F., Tacke M., Jakusch M., Mizaikoff B. (2000) A UV spectroscopic method for monitoring aromatic hydrocarbons dissolved in water. Analytica Chimica Acta, 422(2):187-198

Vo-Dinh T. (1978) Multicomponent Analysis by Synchronous Luminescence Spectrometry", Analytical Chemistry. 50(3), 396-401

Wang D., Portis A.R. Jr, Moose S.P., Long S.P. (2008). Cool C4 photosynthesis: pyruvate Pi dikinase expression and activity corresponds to the exceptional cold tolerance of carbon assimilation in Miscanthus x giganteus. Plant Physiology, 148(1):557-567

Wei X., Schnell U., Hein K.R.G. (2005) Behaviour of gaseous chlorine and alkali metals during biomass thermal utilization. Fuel, 84(7-8):841-848

Xu M., Brown R.C., Norton G., Smeenk J. (2005) Comparison of a Solvent-Free Tar Quantification Method to the International Energy Agency's Tar Measurement Protocol. Energy Fuels, 19(6):2509-2513

Zhang C., Zhang X., Yang J., Liu Z.. (2007) Analysis of polynuclear aromatic hydrocarbons in heavy products derived from coal and petroleum by high performance liquid chromatography. Journal of Chromatography A, 1167:171-177

CHAPTER 2: AIM OF THE WORK

1. Experimental plan

1.1. UNITE – Catalytic biomass gasification experiments

A bench-scale biomass gasification plant operating at atmospheric pressure is utilized in this work, to check an innovative, catalytic hot gas cleaning system for the efficient conversion of tars and particulate abatement: the innovation concerns the fact that those two processes are carried out in-situ, in one- single step. Thus, several catalysts and gasifier arrangements were tested.

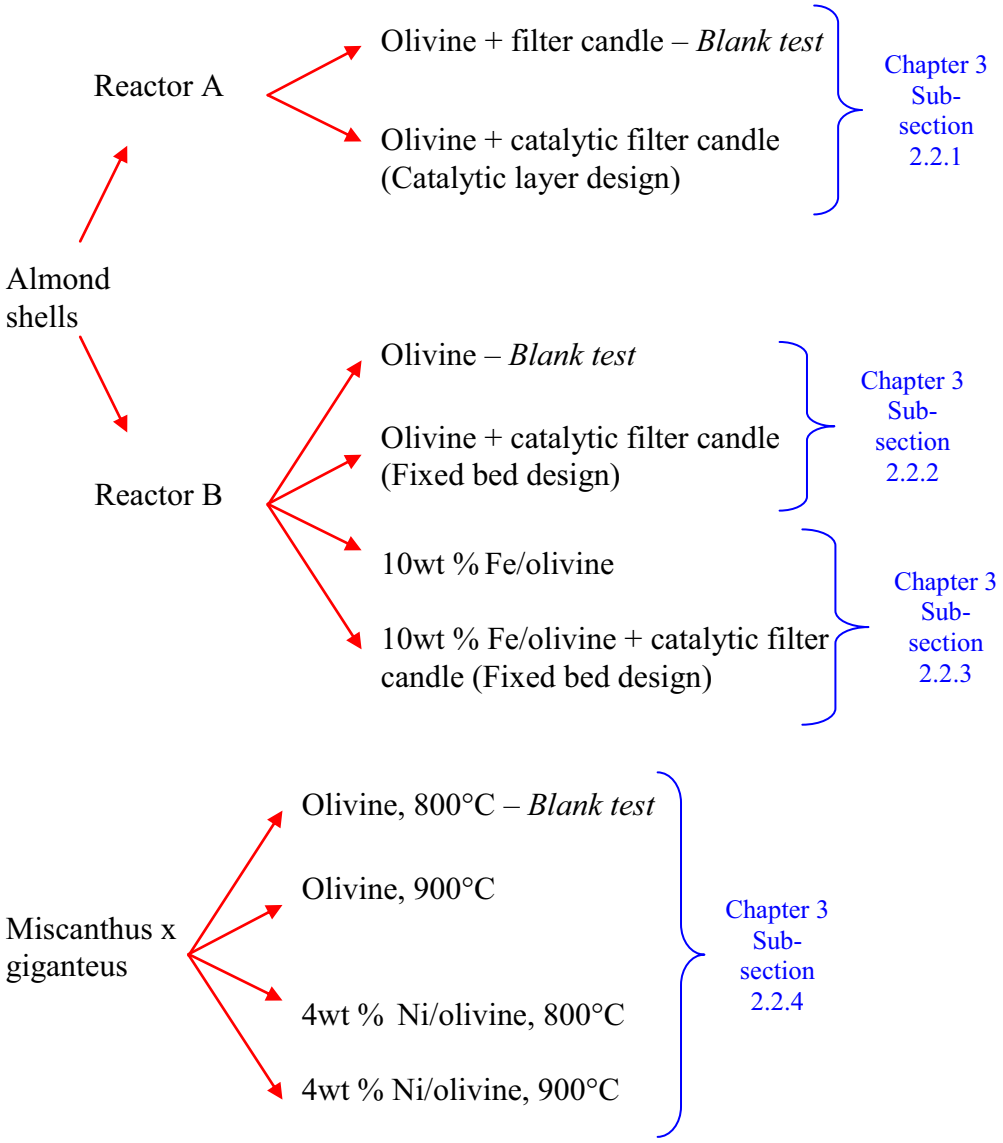

Figure 1: Set of experiments carried out in the University of Teramo

Here is reported a simplified schema of the gasification experiments carried out in the "Energy & Environment" laboratory of the University of Teramo (Figure 1). A detailed description of the condition adopted in each test will be provided in Chapter 3, section 2 "Experimental".

1.2. UPV-M – Development of an analytical method for tar measurement

At the end of each gasification test, samples recovered according to technical specification UNI CEN/TS 15439 and stored in proper condition, were characterized by HPLC/UV in the LCME of the University of Metz.

The results obtained were also used as reference data in studies concerning the development of an original screening test, able to give quali-quantitative information concerning the aromatic components in a fast and cost-effective way (Figure 2).

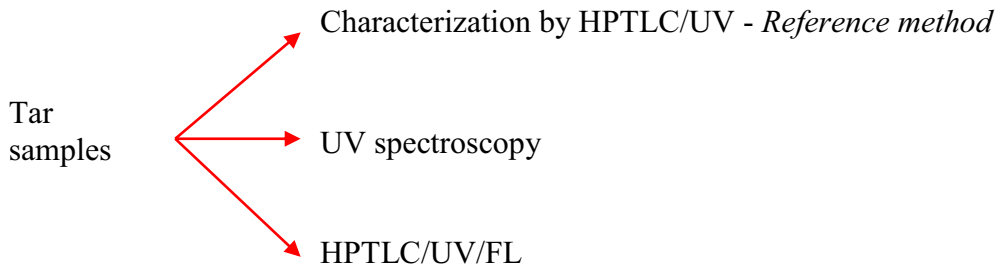

Figure 2: Set of analytical method investigated during the permanence in the University of Metz

2. Aim of the work

As described above several gasification tests have been carried out to check the gas purity resulting from the combined effect of different gas conditioning and cleaning actions developed in this project using as biomass:

- Crushed almond shells
- Miscanthus x giganteus pellets

The aims of the three years- research project could be summarized as follows:

- Evaluation of in-bed catalytic additives (olivine, Ni-olivine, Fe-olivine) and secondary catalysts (commercial filter candles catalytically active) for tar and particulate abatement at real gasification conditions;
- Evaluation of the overall process performances via determination of:

    - Instantaneous gas yield and composition, tar content, carbon conversion, pressure drop across the filter candle, etc.
    - Mass balances. The values have been utilized to verify the compatibility and reliability of measured data.
    - Influence of operating parameters.
- Chemical characterization of tars produced during the gasification process;
- Development of an original analytical method for tar measurements based on UV spectroscopy and HPLTC/UV/FL.

CHAPTER 3: BIOMASS GASIFICATION

*The main part of the gasification experiments presented in this Thesis were carried out under the European Project Unique, in collaboration with the University of L'Aquila (*http://www.uniqueproject.eu/*). The project funded by the Seventh Framework Programme for Research and Technological Development involves ten European partner (research centres, universities and industry), and it is devoted to the development of a compact version of a gasifier by integrating the fluidized bed steam gasification of biomass and the hot gas cleaning and conditioning system into one reactor vessel, placing a bundle of catalytic ceramic candles in the gasifier freeboard; furthermore, by using a catalytically active mineral substance for primary tar reforming and by optimising the addition of sorbents into the bed for removal of detrimental trace elements. This arrangement will guarantee the conversion of tar, elimination of trace elements and an efficient abatement of the particulate, delivering high purity syngas, suitable to assure a high share of power generation even in small- to medium-scale (few MW) CHP and power plants, and to increase the overall economic revenue.*

1. Introduction

The great potential of biomass as a renewable and CO_2 neutral feedstock for energy production is now universally recognized. Gasification is a technically mature thermal conversion process for the production of combustible gases from solid fuels. Syngas obtained in this way, appropriately conditioned and upgraded, may be used for electricity generation by means of internal combustion engines, gas turbines, and (in the near future) fuel cells, and also for the production of synthetic bio-fuels. Industrial plant simplification and intensification could play an important role in biomass applications in general and in particular in increasing the feasibility of gasification processes.

Biomass steam gasification as a source of hydrogen and other valuable gases provides a convenient energy vector for a wide range of applications. The use of steam as a gasification agent gives rise to an increase in fuel gas product yield as a result of reductions in both tar and char brought about by the steam reforming processes [Rapagnà et al. 2000].

During the present work, two different biomasses were used: crushed and sieved almond shells and Miscanthus x giganteus straw pellets. However in presence of catalytic filters in the freeboard of the gasifier, the diameter of the tube to deliver the biomass inside the gasifier it is not able to handle MXG pellets. For this reason, almond shells particles having about 1.0 mm of diameter have been used for most of the runs. Also, considering that MXG has a substantially higher content of ash and chlorine when compared to almond shells, during project execution it was preferred to work with crushed almond shells in the majority of the experiments. Anyway, interesting data concerning MXG gasification have been reported in the present work.

The experimental tests of biomass steam gasification described in this thesis were carried out using promising in-bed additives for primary tar abatement, such as Ni/olivine and Fe/olivine and a catalytically activated segment of a full industrial size filter candle. This innovative device was placed in the freeboard of a bench scale fluidized bed gasifier and operated over an extended period of time.

The activity of the catalysts was determined as a function of time in order to evaluate its performance under real gasification conditions. The gas product composition was monitored during each run and tar samples collected at the end of a run were analyzed as described in the sections below and in Chapters 4 and 5.

2. Experimental

2.1. General scheme of the gasification plant

Figure 1 shows a sketch of the bench-scale gasification plant used during the experiments. This is mainly composed of a bubbling fluidized bed gasifier with an internal diameter of 0.10 m, externally heated by means of a 6 kW electric furnace.

The biomass is provided from the top of the reactor by a continuous biomass screw-feeder. The gasification medium is a mixture of steam and nitrogen; steam is generated from liquid water fed, by means of a peristaltic dosing pump, to a cylindrical, stainless steel evaporator arranged in a 2.4 kW electric furnace.

During the experiments carried out using a lower steam flow rate, nitrogen was also supplied from the top of the reactor, to avoid any obstruction of the biomass-feeding probe.

A cyclone and a ceramic filter are used to assure the particulate removal; nevertheless these equipment become redundant in case of the utilization of catalytic/non catalytic filter candle in the gasifier freeboard.

Tar is removed thanks to a gas cooling section; three condensers in series are utilized to separate condensable components: the first, made of stainless steel, is cooled with tap water; the remaining two, made of glass, are cooled with refrigerated diethylene glycol. The condensable fraction (water + tar) is thus recovered in three Erlenmeyer flasks and available for further analysis.

Online gas analyzers for the volume composition measurement of H_2, CO, CO_2, CH_4, NH_3 and H_2S, are fed at cold gas rate of 1.5 l/min and outputted to a PC where the experimental data are stored as a function of time.

The gas analyzers used are the following:

- Continuous ABB gas analyzer series AO2000:
    - URAS 14 (Infrared Photometer) for CO, CO_2 and CH_4

- LIMAS 11UV (UV photometer) for H_2S
- CALDOS 17 (thermal conductivity - Silicon sensor) for H_2

- Continuous SIEMENS gas analyzer ULTRAMAT 6 (Infrared Photometer) for NH_3

Temperature in various plant locations is measured by means of four thermocouples; measurement devices for the continuous monitoring of flow rate and pressure drops are also present.

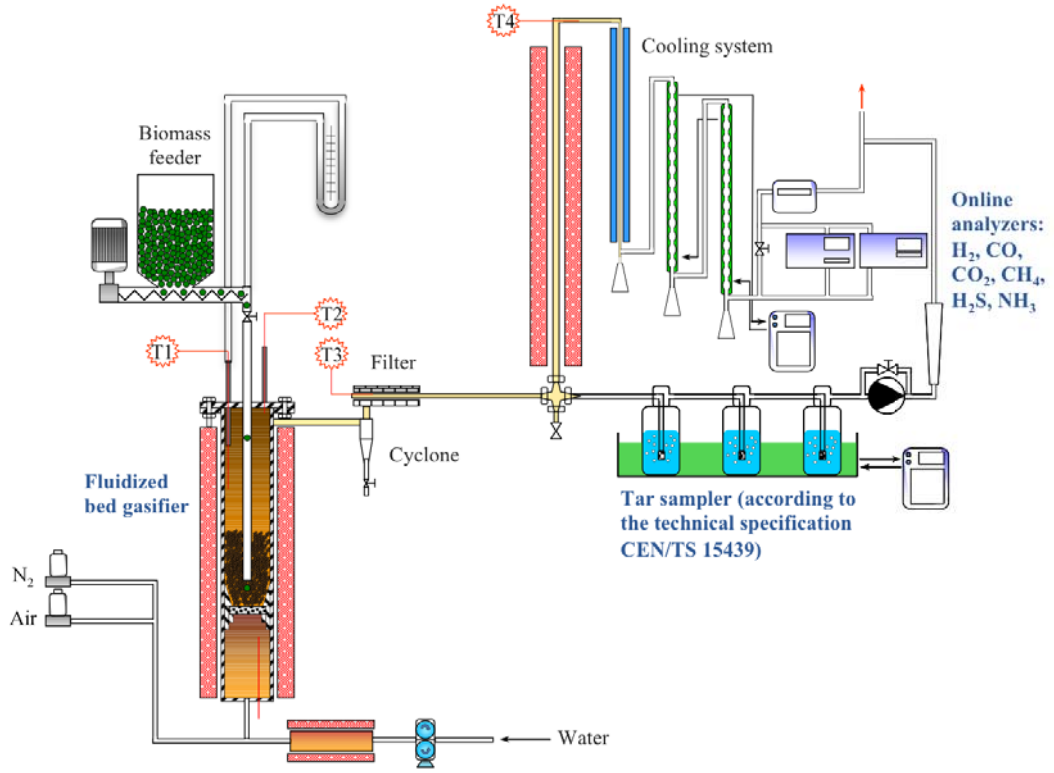

Figure 1: Sketch of the entire biomass gasification plant

2.2. Gasification method

For each experimental tests, the bed is first fluidized with air and heated to the chosen operating temperature; the fluidizing gas is then switched to a nitrogen/steam mixture and after stabilization of the system (1-2 minutes) the biomass feeding starts. Nitrogen is supplied to help a smooth feeding of biomass particles and to stabilize the flow.

Biomass feeding rate is kept constant during the test, to avoid changes in the gas-production rate inside the reactor, and the consequently pressure fluctuations that would disturb the whole system.

At the end of each test period, the quantity of char produced by gasification is determined by the analysis of CO_2 and CO in the exit gas, burning under air stream the whole carbonaceous residue trapped into the gasifier.

Different bed inventories and also catalysts and biomasses have been used during the work. All the arrangements, as well as the biomass characteristics, will be extensively explained in the following sub-section.

2.2.1 Gasification of almond shell using a catalytic filter candle with catalytic layer design

Gasification of almond shells was realized using natural olivine bed inventory.

- Crushed and sieved almond shells had a Sauter diameter of 1039 μm;
- 3 kg of olivine particles with Sauter diameter of 306 μm and density of 2500 kg/m^3 were used.

In Table 1 is reported the proximate and ultimate analysis of almond shells. The analysis was performed by Research Center ENEA Trisaia (Italy).

Table 1: Almond shell proximate and ultimate analysis

Composition of the dry matter, %wt/wt$_{dry}$ [a]		Proximate analysis, %wt/wt		Elemental composition %wt/wt$_{dry}$	
Cellulose	36	Dry matter	92.3	C	48.9
Hemicellulose	29	Ash	1.2	H	6.2
Lignin	29	Volatile	71.7	N	0.18
		Fixed Carbon	19.5	O*	43.5
				Cl	0.029
				S	0.026

[a]Avarage data obtained using the Phyllis, database for biomass and waste [http://www.ecn.nl/phyllis/]

[b] %O = 100-(%C + %H + %N + %Cl + %ash)

In this case, the gasifier has been properly modified to house a catalytic/non catalytic filter candle in the reactor freeboard, as showed in figure 2. The catalytic/non catalytic ceramic candles were both provided by PALL Filtersystems GmbH (Germany).

The catalytic activation of the ceramic filter involved a first impregnation step in which a standard hot gas filter element (of outer diameter 60 mm, inner-diameter 40 mm) was impregnated with a fine-wet milled suspension of a MgO-Al_2O_3 precursor; in a second impregnation step the support-coated filter element was

impregnated with a concentrated nickel nitrate hexahydrate solution by incipient wetness, to achieve a NiO loading of 60 wt % with respect to the $MgO\text{-}Al_2O_3$ support after drying and final sintering at 900°C. Due to the catalytic activation strategy used, this kind of catalytically activated filter candle is defined of "catalytic layer design" [Nacken et al., 2009].

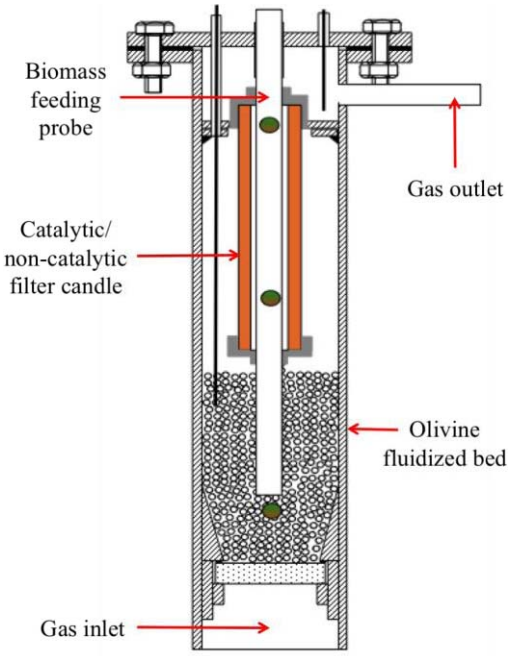

Figure 2: Sketch of the gasifier properly modified to house a catalytic/non catalytic filter candle in the reactor freeboard – Reactor A

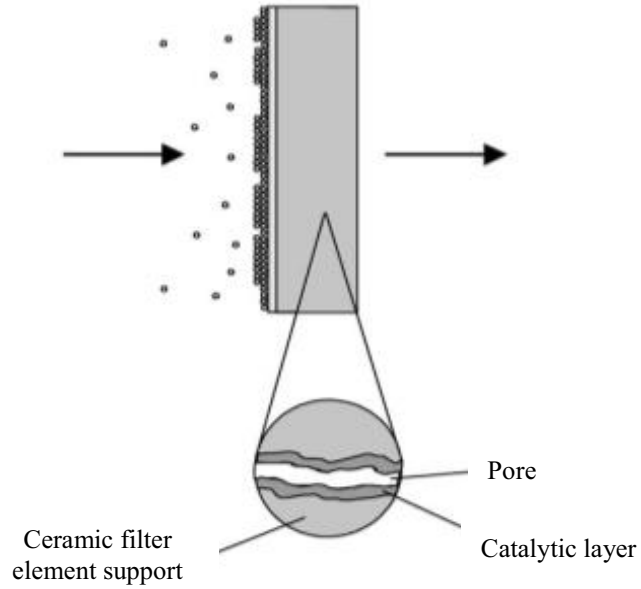

Figure 3: Structure of the catalytic filter candle with catalytic layer design [Nacken et al., 2009]

Figure 4: Pictures of the catalytic/non catalytic filter candle showing the dimension and the blockage system in the reactor A- freeboard.

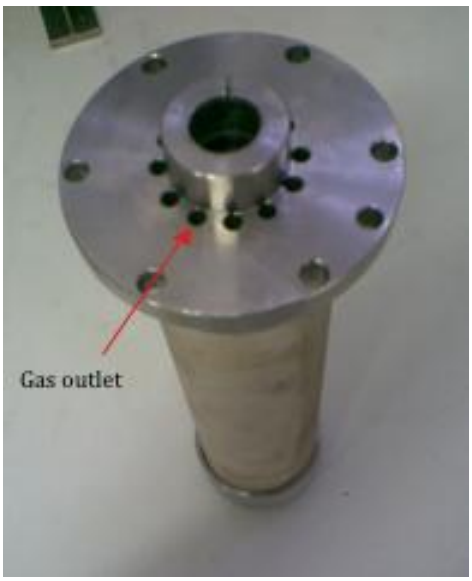

Figure 5: Pictures of the catalytic/non catalytic filter candle with the upper flange of the blockage system in the reactor A- freeboard.

As shown in Figures 2 and 4, the catalytic/non catalytic filter candle is blocked on the biomass-feeding probe, using two stainless steel flanges. The upper flange presents a series of holes, which permit the gas passing through the filter to find

the way out (Figure 5).

The operating conditions for each test carried out during this set of gasification experiments are reported in table 2.

Nitrogen is supplied to help a smooth feeding of biomass particles, to stabilize the flow and to adjust the face filtration velocity close to its nominal value (fixed by PALL Filtersystems GmbH to be of the order of 90 m/h). During test 1-VI no nitrogen is supplied in order to obtain the greatest possible concentration of reactants in the gasifier bed, and in contact with the Ni catalyst in the filtration candle.

Table 2: Operating gasification conditions: OL = olivine; FC = Filter Candle; CFC = Catalytic Filter Candle (N250107001)

Gasification test	1-I	1-II	1-III	1-IV	1-V	1-VI
Duration, min	60	60	120	60	60	30
Bed temperature, °C	720-803	829	840	832	831	831
Biomass flow rate, g/min	8.0	8.0	8.0	8.0	8.0	10.0
N_2 flow rate, l/min	14.0	16.5	16.5	16.5	6.0	0
Steam feeding rate, g/min	6.6	6.6	6.7	7.2	7.8	13.3
Bed material	OL	OL	OL	OL	OL	OL
Filter candle	FC	FC	CFC	CFC	CFC	CFC

2.2.2 Gasification of almond shell using a catalytic filter candle with "fixed bed" design

During this set of experiments the reforming activity of an innovative catalytic ceramic candles was evaluated during a long-term test (22h).

- The biomass feedstock consisted of crushed and sieved almond shells with an average particle size of 1054 μm (biomass composition is reported in Table 1);
- The fluidized bed inventory was made of 3 kg of olivine (d = 306 μm, ρ = 2500 kg/m^3)

The new candle prototype involves a porous inner tube allowing the integration of catalyst grains as fixed bed inside the ceramic filter candle (Figure 6). The advantage of such catalyst integration is the higher flexibility it provides for potential applications.

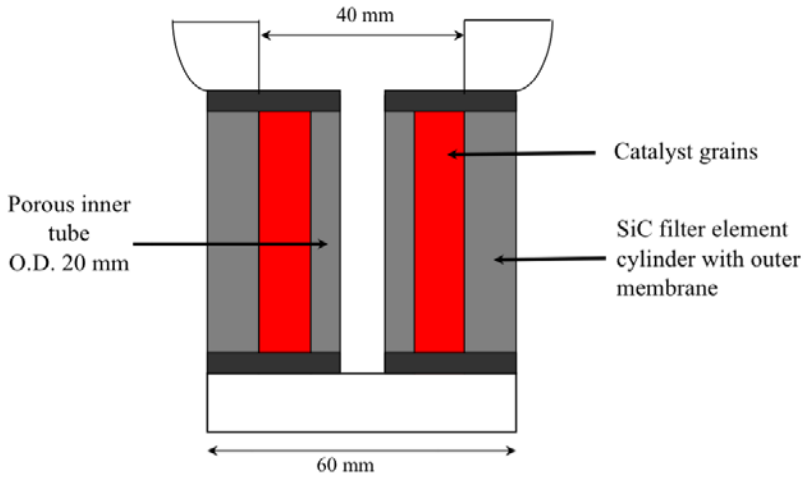

Figure 6: Sketch of the new candle prototype (J041108.1) integrating a fixed bed of catalyst grains

Figure 7: Assembly sequence of the candle in the gasifier

The Ni catalyst used in the present application was filled into the hollow-cylindrical space of a thermo-shock resistant silicon carbide (SiC) based hot gas

filter element of 60 mm outer diameter and 40 mm inner diameter and a porous inner tube of 20 mm outer diameter. The Ni catalyst was manufactured by incipient wetness impregnation of MgO grains of the size range 0.1 - 0.3 mm by using a nickel nitrate hexahydrate solution to adjust a NiO loading of 6wt% [Nacken et al. 2007].

To facilitate the operation of extraction and replacement of the candle inside the reactor a new shape was developed. In this case, just the head of the candle, which is slightly larger compared to the candle body (Figure 7), is blocked inside the gasifier freeboard. Thus, a new reactor was built to allow housing of the new filter element of about 400 mm length into the freeboard. A sketch of the new gasifier is given in Figure 8.

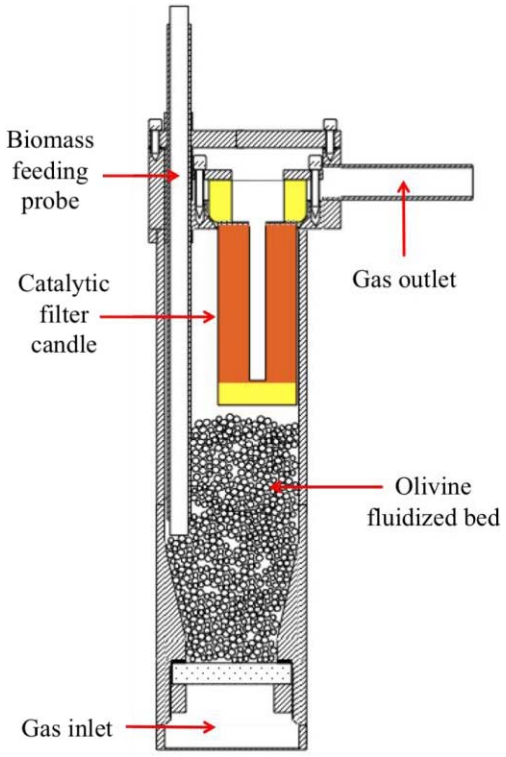

Figure 8: Sketch of the gasifier properly designed to house the new filter element into the freeboard (the catalytic section is highlighted in orange) – Reactor B

The long-term test (22 hours) was performed with intermediate stops to allow system monitoring and char burning to avoid its accumulation in the bed inventory.

All the operating gasification conditions for this set of experiments are reported in table 3. Nitrogen permits to adjust the face filtration velocity close to its nominal value, fixed by PALL Filtersystems GmbH to be of the order of 60 m/h.

Table 3: Operating gasification conditions. OL = Olivine; CFC = Catalytic Filter Candle (J041108.1)

Gasification test	2-I	2-II	2-III	2-IV	2-V	2-VI	2-VII	2-VIII	2-IX	2-X
Duration, min	60	90	56	120	120	160	120	180	240	230
Bed temperature, °C	808	815	808	814	813	814	813	813	811	808
Biomass flow rate, g/min	8.0	9.0	9.0	6.0	6.0	4.5	5.5	6.0	6.0	6.0
Nitrogen flow rate, l/min	11.2	12.0	12.0	11.2	12.0	9.0	6.0	5.0	5.0	5.4
Steam feeding rate, g/min	8.5	8.4	9.0	6.6	6.3	3.8	6.2	6.2	6.0	6.0
Bed material	OL	OL	OL	OL	OL	OL	OL	OL	OL	OL
Filter candle	-	CFC	CFC	CFC	CFC	CFC	CFC	CFC	CFC	CFC

2.2.3 Gasification of almond shell using a catalytic filter candle with "fixed bed" design and 10wt % Fe/olivine

A test campaign with simultaneous utilization of the catalytic filter candle in the freeboard and Fe/olivine catalyst in the fluidized bed of the gasifier has been carried out, concerning continuous steam gasification of biomass.

- Crushed and sieved almond shells had an average particle size of 1054 μm (biomass composition is reported in Table 1);

The fluidized bed inventory was made of:

- 3 kg of 10wt % Fe-olivine particles (d = 393 μm, ρ = 2500 kg/m^3; the particle density was measured by comparison with a bulk of olivine particles having the same volume, assuming similar bulk void fraction).

The operating conditions are reported in table 4.

Table 4: Operating gasification conditions. Fe/OL = 10wt %Fe/olivine; CFC = Catalytic Filter Candle (J041108.1)

Gasification test	3-I	3-II	3-III	3-IV	3-V
Duration, min	154	80	120	120	150
Bed temperature, °C	828	821	820	814	812
Biomass flow rate, g/min	5.0	5.0	5.7	5.0	5.6
Nitrogen flow rate, l/min	11.2	11.2	6.0	11.2	6.0
Steam feeding rate, g/min	6.0	6.0	6.0	6.0	5.0
Bed material	Fe/OL	Fe/OL	Fe/OL	Fe/OL	Fe/OL
Filter candle	-	-	-	CFC	CFC

Fe/olivine catalyst was prepared and characterized from the team of the ECPM-LMSPC, University of Strasbourg (France). The main step in the catalysts production consists of impregnation of natural olivine with an aqueous solution of iron nitrate ($Fe(NO_3)_3 \cdot 9H_2O$), in an appropriate concentration to assure an iron content of 10wt% [Rapagnà et al., in press].

The 10wt % Fe/olivine was tested in real gasification condition using the fluidized bed gasifier with the B design (Figure 8).

2.2.4 Gasification of Miscanthus x giganteus with olivine / 3.9wt % Ni/olivine

The aims of this test campaign were to verify the potential of Miscanthus x giganteus as biomass for gasification, as well as the suitability of Ni/olivine in real fluidization dynamics. No filter candles, either catalytic, were placed inside the gasifier during this set of tests.

Each experiment of MXG steam gasification was carried out at two different temperatures (800°C and 900°C) in order to evaluate its effect on the gasification products.

- MXG was provided by MBR (Germany); after the harvest, miscanthus is stored in straw form but it cannot be used because of its high size dispersion. Therefore, a pelletization step must be performed. Thus, pellet of 6 mm of diameter were used in our tests (Figure 9). The proximate and ultimate analyses are reported in Table 5: the analyses of the MXG harvested straw were realized by the ICPHW of Zabrze (Poland);
- The fluidized bed inventory was alternatively made of 3 kg of olivine ($d_{average}$ = 306 μm, $\rho_{particle}$ = 2500 kg/m^3) or 3 kg of Ni/olivine ($d_{average}$ = 480 μm, $\rho_{particle}$ = 2500 kg/m^3).

Figure 9: MXG pellet (6 mm of diameter)

Table 5: MXG proximate and ultimate analysis

Composition of the dry matter, %wt/wtdry		Proximate analysis, %wt/wt		Elemental composition %wt/wt_{dry}	
Cellulose	43	Dry matter	90.6	C	48.67
Hemicellulose	27	Ash	2.8	H	5.45
Lignin	24	Volatile	80.2	N	0.45
				O*	42.50
				Cl	0.23
				S	0.04

*%O = 100-(%C + %H + %N + %Cl + %ash)

The catalyst was provided by the ECPM-LMSPC, University of Strasbourg. It was prepared by wet impregnation of natural olivine with a solution of nickel nitrate hexahydrate to obtain a nickel content of 3.9 wt %. After water evaporation, the 3.9 wt % Ni/olivine was dried overnight and then calcined [Świerczynski et al., 2006].

All the operating gasification conditions for MXG test campaign are reported in table 6.

Table 6: Operating gasification conditions. OL = Olivine; Ni-OL = Ni-olivine

Gasification test	4-I	4-II	4-III	4-IV
Duration, min	60	60	120	60
Bed temperature, °C	798	899	799	901
Biomass flow rate, g/min	8.0	8.0	8.0	8.0
Nitrogen flow rate, l/min	17.0	17.0	17.2	17.0
Steam feeding rate, g/min	8.2	8.2	8.2	8.4
Bed material	OL	OL	Ni/OL	Ni/OL
Filter candle	-	-	-	-

2.3. Determination of total tar content by Total Organic Carbon analysis

At the end of each gasification run, the condensate fraction recovered in the Erlenmeyer flasks (Figure 1) was weighted and a representative amount of each sample was filtered using a 0.45 μm pore size filter, and eventually diluted with high purity distilled water. The total organic carbon (TOC) content was measured by injecting the sample, using an automatic microlitre syringe, into a Shimadzu TOC-VCPN Total Organic Carbon Analyzer operating at the catalytic combustion oxidation temperature of 680°C. The total tar content was then calculated from the

TOC value, assuming naphthalene as the key component representative of the tar fraction. All the data concerning the tar content in the present chapter will be based on this analytical method.

Nevertheless, considering the limitations of this technique in tar analysis, such as the fact that the majority of tars are not water-miscible, the UNI CEN/TS 15439 sampling method was introduced, and the tar fraction was properly characterized using HPLC/UV.

The HPLC/UV method, as well as, the results obtained and the comparison with TOC results will be extensively discussed in Chapter 4.

3. Results and discussion

3.1. Gasification of almond shell using a catalytic filter candle with catalytic layer design

The performance of a catalytically activated filter candle with catalytic layer design developed by PALL GmbH (Figure 3) were evaluated and compared with the results obtained by means of a segment of a commercial ceramic hot gas filter. The filtration device was integrated in the reactor vessel leading to hot gas filtration and eventually tar abatement in one-single step.

The syngas quality was monitored in terms of gas composition, H_2S, NH_3 and tar content as function of the operating time of the fluidized bed gasifier. Mass balances have been utilized to verify the compatibility and reliability of measured data. The influence of operating parameters has been explored.

The pressure drop across vs. fluid velocity across the filter candle was also measured, either at room temperature up to gasification temperature (up to 870°C), to reveal possible gas leakages and to assess the suitability of the whole system for high temperature gasification experiments (Figure 10).

No granular material was introduced in the reactor, to keep clean the filter surface. In each test, the air flow rate has been measured by means of a mass flow controller (MKS Type 1500 Series, flow range 0 – 50 l/min), and kept constant for about ten minutes. The steady state pressure drop across the filter has been recorded by means of two pressure probes inserted in the reactor through its head, with the tips placed in the regions inside and outside the candle, respectively. The

data points at high temperature show a relatively larger pressure drop than the corresponding value at room temperature: the combined increase of gas viscosity and reduction of gas density with temperature may be responsible for this experimental behavior.

It is necessary to point out that the candle is made of two layers in series, and the frictional loss related to the very thin mullite layer could be assumed as a concentrated source of pressure drop quantifiable in terms of kinetic heads. It could well be the controlling resistance.

It is worth mentioning that, when the reactor has been brought down to room temperature, tests have been repeated with cold air and the results were very much the same as those obtained previously Additional details on the measurement of the differential pressure of the integrated catalytic filter element are reported in a recent publication [Rapagnà et al., 2009].

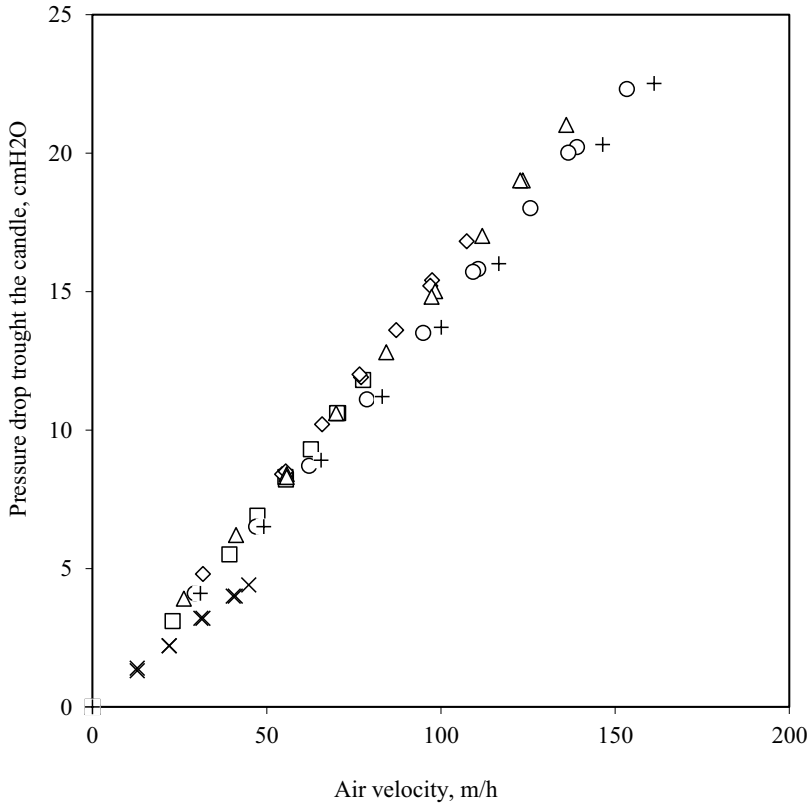

Figure 10:. Air pressure drop through the non-catalytic ceramic candle as a function of the external air superficial velocity and reactor temperatures. (x) 19 °C, (□) 263 °C, (◊) 465 °C, (Δ) 680 °C, (○) 805 °C, (+) 870 °C.

In Figure 11 is reported the syngas composition as a function of gasification time. During test 1-I, the operating temperature was increased progressively with operation time by changing the set point of the electric furnace. A strict correlation between the operative bed temperature and the gas composition and the gas yields was found; this relation is well documented in literature [Rapagnà et al. 1997; Turn et al., 1998]: Turn et al. reported that for fluidized bed biomass gasification increasing the reactor temperature from 750°C to 950°C hydrogen concentration incremented from 31% to 45% based on dry inert-free gas.

In our experiment, increasing the operative temperature from 720°C to 800°C resulted in a increment of hydrogen production from 35% to about 45%, dry and N_2 free basis. On the contrary, methane and carbon monoxide slightly reduce, while carbon dioxide remains fairly constant (Figure 10).

The higher gas phase H_2 concentration and the slightly augmented gas yields can be attributed to increased steam and carbon dioxide gasification reactions rates brought about by higher reactor temperatures [Turn et al., 1998].

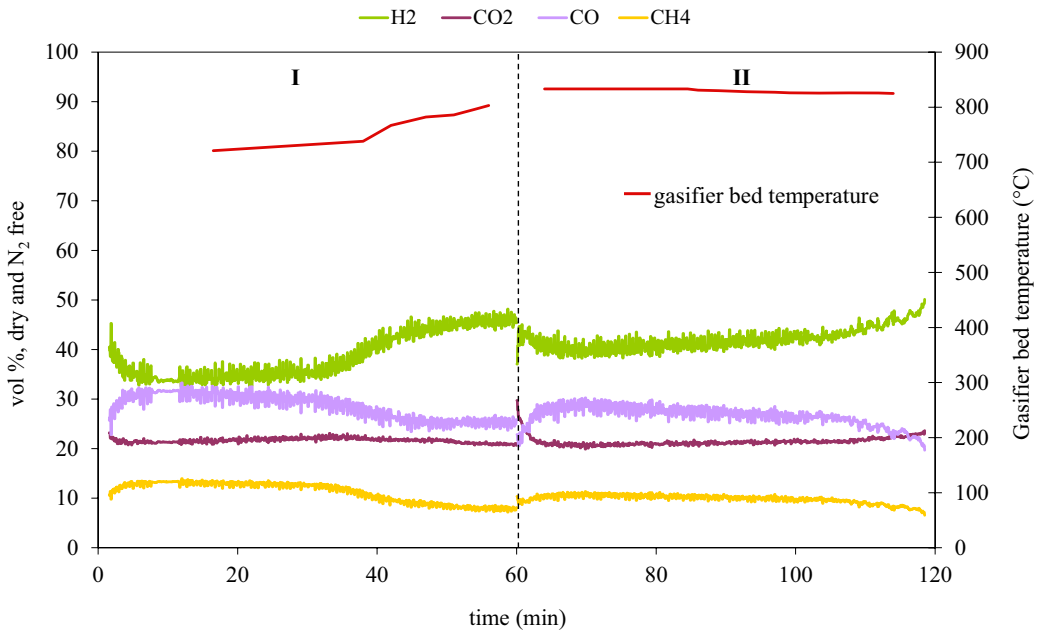

Figure 11: Syngas composition as a function of gasification time. Tests 1-I and 1-II: Steam gasification of almond shell with olivine bed inventory + commercial filter candle

The relatively high tar yield found at the end of this test (6.09 g/Nm^3 dry gas yield on average) can be attributed to the low temperature of the bed during the first

half of test; this explanation is supported by the result of test 1-II, for which the measured tar content was considerably lower. During this test, at a uniform temperature of 829°C was provided, leading to a rather constant hydrogen production of about 44% in the dry and N_2 free producer gas (Figure 11).

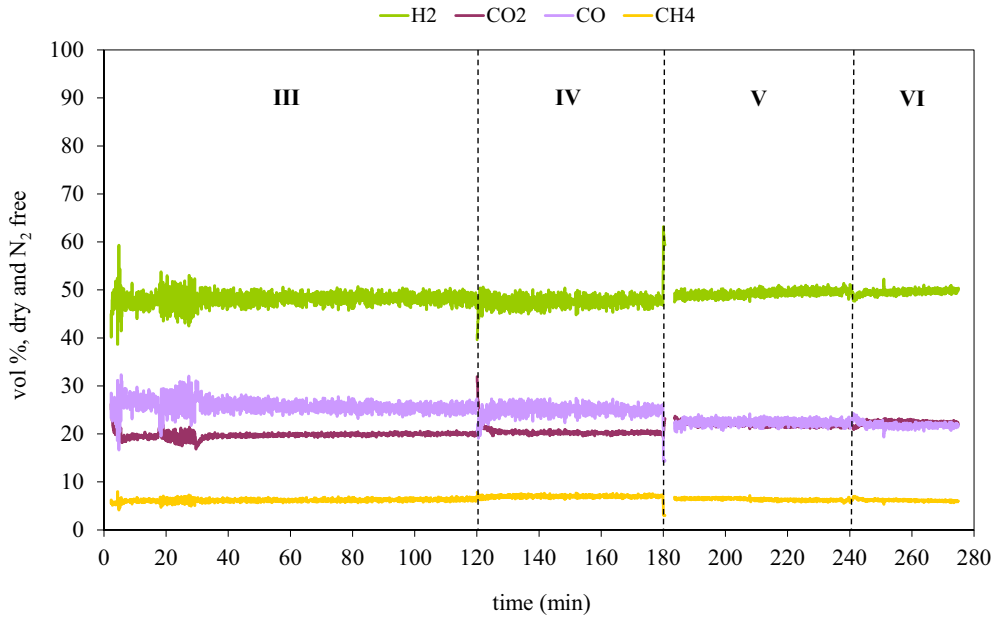

Figure 12: Syngas composition as a function of gasification time. Tests 1-III-VI: Steam gasification of almond shell with olivine bed inventory + catalytically activated filter candle with "catalytic layer" design

Table 7: Results of almond shells steam gasification tests with a commercial filter candle (1-I and 1-II) and with a catalytic filter candle of "catalytic layer" design (1-III – 1-VI) housed in the gasifier freeboard.

	1-I	**1-II**	**1-III**	**1-IV**	**1-V**	**1-VI**
Duration of test (min)	60	60	120	60	60	30
Gasifier bed temperature (°C)	720-803	829	840	832	831	831
Gasifier outlet temperature (°C)	675-715	750	791	780	801	801
Steam/biomass dry	0.89	0.89	0.91	0.97	1.06	1.44
Water conversion %	16	19	37	27	39	35
Gas yield (Nm^3 dry/kg daf)	**0.9-1.1**	**1.30-1.40**	**1.60**	**1.60**	**1.55**	**1.80**
Tar content (g/Nm^3 dry)	**6.03**	**1.90**	**0.72**	**n.a.**	**0.70**	**0.92**
Char residue (g/kg daf)	97	71	82	70	55*	
Carbon conversion %	79	85	89	85	88	
H_2 (vol% dry gas, N_2 free)	**35-47**	**44**	**48**	**48**	**49**	**50**
CO_2 (vol% dry gas, N_2 free)	**22**	**21**	**20**	**21**	**22**	**23**
CO (vol% dry gas, N_2 free)	**32-26**	**26**	**26**	**25**	**23**	**21**
CH_4 (vol% dry gas, N_2 free)	**13-8**	**10**	**6**	**6**	**6**	**6**
Filtration velocity (m/h)	85	106	145	110	77	64

*The total amount of char residue is relative to tests V and VI

A significant improvement of all the relevant performance indicators resulted from the use of the catalytic filter candle as reported in Figure 12 and in Table 7 (tests 1-III-VI).

Tests V and VI were carried out consecutively; thus the combustion of char deposited in the reactor was carried at the end of the latter test so that the quantity reported in Table 7 refers cumulatively to both tests: for mass balance calculation purposes the char residue in each test is assumed proportional to the duration of test.

In test V and VI, the N_2 flow rate was reduced to 6 l/min and zero respectively, and at the same time the steam feed rate was increased, in order to assure bubbling fluidization conditions in the bed. This results in a promotion of the WGS reaction, thus the CO reduces and H_2 concentration by volume in the dry and N_2 free output gas increase; the higher water partial pressure in the reactor also leads to a rise in char gasification resulting in higher gas yield.

The presence of H_2S and NH_3 in the producer gas were also monitored. For the biomass feedstock used in these experiments H_2S concentration remains always well below the concentration used for the activity studies of the catalytic filter candle. Nacken et al. experienced the completely conversion of naphthalene at 900°C in the presence of 100 ppmv of H_2S, when the innovative cylindrical catalyst particle layer based catalytic filter element was tested. Decreasing the temperature at 850°C and 800°C a naphthalene conversion of 90% and 50% respectively was achieved [Nacken et al., 2007; Nacken et al., 2009].

The maximum value detected in our experiments was about 20 ppmv, which corresponds to a level of about 100 ppmv in dry and N_2 free producer gas. This value cuts by half for the last two tests (1-V and 1-VI) reaching 50 ppmv on dry and N_2 free basis.

Concerning the ammonia concentration, when the filter candle is used, its content range from 4500 ppmv (test 1-I at lower temperature) to a minimum of 2000 ppmv. However, the use of the Ni-based filter candle leads to a reduction in the NH_3 concentration in the product gas reduces from 1500 to 500 ppmv for the test 1-VI (Figure 13). At the same time an increased H_2 concentration is reported, as described above.

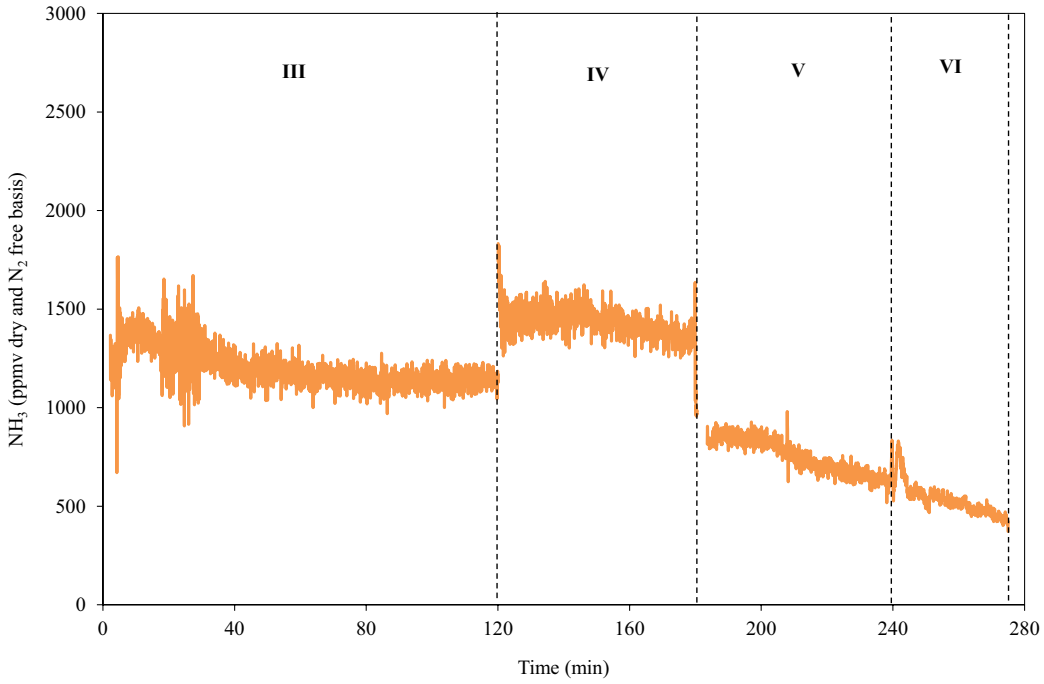

Figure 13: NH_3 in the syngas as a function of gasification time. Tests 1-III – 1-VI: Steam gasification with the catalytically activated filter candle with "catalytic layer" design

A resume of the most significant results obtained during this set of experiments is reported in Table 8. The percentage variations between the results without/with the catalytic filter are calculated using test 1-II as reference tests.

Table 8: Percentage variation of the main gasification indicators. 1-II: percentage variation calculated with respect to test 1-I. 1-III – 1-VI: percentage variation with respect to test 1-II

	1-II	1-III	1-IV	1-V	1-VI
Steam/biomass ratio	***0.9***	***0.9***	***1.0***	***1.1***	***1.4***
Gas yield, %	+35	+19	+19	+15	+33
Tar content in the producer gas, %	-68	-62	n.a.	-63	-52
Tar content per kg biomass daf, %	-57	-55	n.a.	-58	-35
H_2 yield, %	+44	+31	+29	+28	+53
CH_4 yield, %	+18	-23	-21	-23	-17

As shown in Table 8, the innovative concept of integrating a catalytic hot gas filter in the gasifier freeboard leads to a simultaneous increase of the gas yield and hydrogen concentration, by significantly reducing the tar content of the raw syngas; at the same time, it also allows efficient particle separation, so that the final result is a hot and clean fuel gas made available right at the exit of the gasifier reactor.

Nevertheless, as stated in the "Experimental" section the catalytic activated filter candle is blocked on the biomass-feeding probe. This plant configuration entails quite hard-working operations to lock/unlock the filter on the probe and also the dilatation of the metal due to the high gasification temperature could involve an unwanted pressure able to break the relatively fragile ceramic structure (Figure 14). Thus, in order to avoid this problem a new catalytic filter shape was designed in collaboration with PALL GmbH.

Figure 14: The main problem experienced in our experiments was the breakage of the ceramic candle (picture on the right)

3.2. Gasification of almond shell using a catalytic filter candle with "fixed bed" design and 10wt % Fe/olivine

3.2.1. Gasification of almond shell using a catalytic filter candle with "fixed bed" design – long-term test

Measurements with (tests 2-II – 2-X) and without (test 2-1) the new catalytically active filter candle integrated in the gasifier were performed; tests with the filter candle were carried out consecutively in order to evaluate the catalyst performance as a function of time. Altogether, the catalytic filter candle has been tested for a total of 22 hours in gasification conditions with a plain olivine bed inventory. No damages to the candle and its fittings were found at the trial end.

The new "fixed bed" design catalytic filter candle was chosen thanks to the proven higher catalytic performances. In fact, Nacken et al., found a complete naphthalene conversion at 800°C in presence of 100 ppmv H_2S at a typical superficial velocity of 72 m/h; this result is explained with the integrated higher and better accessible Ni catalyst amount for tar reforming in "fixed bed" design [Nacken et al., 2010].

Table 9: Results of steam gasification of almond shells with olivine bed inventory (2-I) and with a catalytic filter candle of "fixed bed" design (test 2-II – 2-X) housed in the gasifier freeboard.

	2-I	**2-II**	**2-III**	**2-IV**	**2-V**	**2-VI**	**2-VII**	**2-VIII**	**2-IX**	**2-X**
Duration of test (min)	*60*	90	56	120	120	160	120	180	240	230
Gasifier bed temperature (°C)	*808*	815	808	814	813	814	813	813	811	808
Gasifier outlet temperature (°C)	*738*	816	816	825	815	818	822	812	809	819
Steam/biomass dry	*1.06*	0.94	1.00	1.10	1.06	0.85	1.13	1.03	1.00	0.99
Water conversion %	*16*	34	24	21	35	40	36	37	41	42
Gas yield (Nm^3 dry/kg daf)	***1.00***	**1.65**	**1.54**	**1.49**	**1.62**	**1.60**	**1.68**	**1.77**	**1.77**	**1.79**
Tar content (g/Nm^3 dry)	***3.67***	**0.91**	**0.95**	**0.79**	**0.55**	**0.71**	**0.75**	**0.81**	**0.85**	**0.75**
Char residue (g/kg daf)	*94*	68	107	70	68	78	66	48	36	41
Carbon conversion %	*80*	86	78	85	86	84	86	90	92	91
H_2 (vol% dry gas, N_2 free)	***39***	**50**	**52**	**55**	**56**	**52**	**54**	**53**	**53**	**53**
CO_2 (vol% dry gas, N_2 free)	***26***	**23**	**23**	**22**	**21**	**19**	**22**	**20**	**20**	**20**
CO (vol% dry gas, N_2 free)	***24***	**21**	**22**	**20**	**20**	**23**	**19**	**22**	**22**	**22**
CH_4 (vol% dry gas, N_2 free)	***10***	**5**	**4**	**4**	**4**	**5**	**5**	**5**	**5**	**5**
Filtration velocity (m/h)	-	102	95	81	79	63	61	62	61	62

The gasification indicators take into account during each tests have been compared with the data measured for the reference test, which consisted of almonds shells steam gasification with a bed of natural olivine (test 2-I).

The significant parameters for each test, such as gas yield, tar and char content, composition of the purified syngas, are given in Table 9. In all experiments, the steam/biomass mass ratio was kept quite constant, and close to 1.

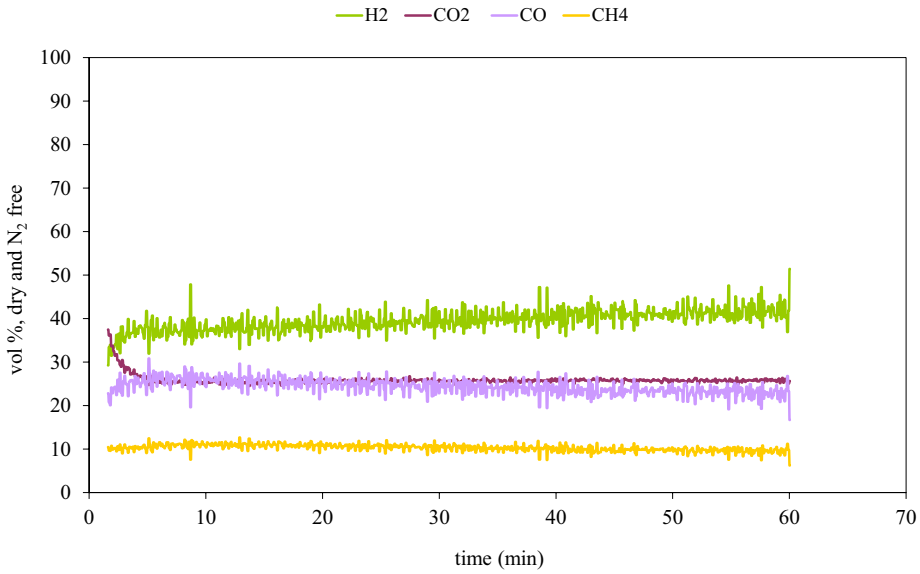

Figure 15: Syngas composition as a function of gasification time. Test 2-I: Steam gasification of almond shells with olivine bed inventory

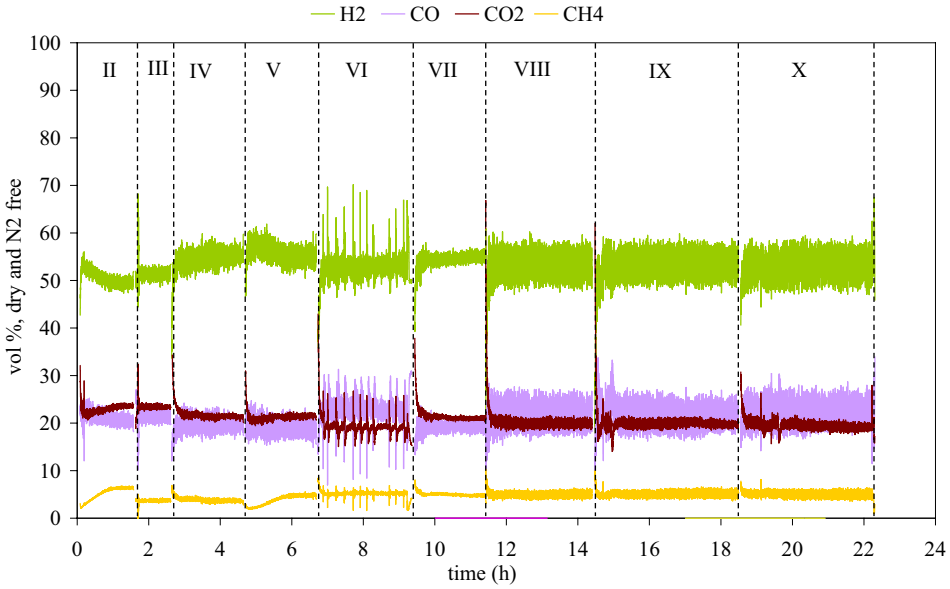

Figure 16: Syngas composition as a function of gasification time. Test 2-II – 2-X: Steam gasification of almond shells with olivine bed inventory and a catalytically active filter candle with "fixed bed" design inserted in the gasifier freeboard

Comparing data obtained using the catalytic filter candle, with the results of test 2-I (without any gas cleaning element inserted in the gasifier), allows to notice a substantial improvement of all the representative gasification parameters. This

observation is valid in general for the entire test campaign carried out, even if slight fluctuations in the results could be observed among tests.

The syngas composition expressed as the percentage by volume of H_2, CO, CO_2 and CH_4, for the reference test and for the long-term test are reported in Figure 15 and 16, respectively.

During the first 90 minutes of gasification in the presence of the catalytic candle (test 2-II) a strong reduction in methane and tar content (measured by TOC analysis) was observed , when compared with test 2-I, these values decreasing by 49% and 75%, respectively. This clearly results in an increase in gas yield and hydrogen content (Table 9).

As shown in Figure 16 there is a progressive increase in H_2 concentration during the first five hours, stabilizing in time to reach about 53% on a dry and N_2 free basis (tests 2-VIII – 2-X).

The largest concentration of H_2 was observed for tests 2-IV and 2-V, with a percentage by volume of around 55% and with a consequential low concentration of methane. In comparison with test I, the CH_4 content decreases from 10.3% to 3.8%.

The experimental tests also show an interesting evolution in gas yield and the tar content. For test V for example the gas yield obtained, 1.62 Nm^3 dry/kg daf, is mainly caused by increased reforming of tar brought about by the catalyst, which shows a maximum in its activity. Tar content in fact decreases from 0.79 to 0.55 g/Nm^3. Increasing the gasification time beyond 6 hours (tests 2-VI – 2-X) shows a growing trend followed by stabilization with regard to both the methane and tar content in the product gas when compared with the previous results, suggesting that a minor decrease of the number of active sites has occurred resulting in a slightly lower but stable activity. At the same time the gas yield increases due to an increased char conversion.

In order to resume the improvement obtained using the catalytic filter candle with “fixed bed” design, the main gasification parameters have been reported as percentage variation with respect to the blank test (Table 10). The average values weighted by gasification time are also given in Table 10: these show the catalytic filter to have given rise to an average increase in gas yield of 69%, of hydrogen

yield by 130% and correspondingly, methane and tar content in the gas are seen to have been reduced by 20% and 79%, respectively, and tar production by 64%.

Table 10: Percentage variation of the main gasification indicators with respect to test 2-I

	2-II	2-III	2-IV	2-V	2-VI	2-VII	2-VIII	2-IX	2-X	*Average*
Gas yield, %	+66	+54	+49	+62	+61	+68	+77	+77	+79	*+69*
Tar content in the producer gas, %	-75	-74	-78	-85	-81	-79	-78	-77	-80	*-79*
Tar content per kg biomass daf, %	-56	-60	-68	-76	-69	-65	-61	-59	-64	*-64*
H_2 yield, %	+113	+103	+107	+130	+115	+132	+141	+140	+143	*+130*
CH_4 yield, %	-16	-47	-44	-40	-18	-18	-13	-11	-12	*-20*

In addition, the ammonia and hydrogen sulfide concentration in the producer gas was monitored. NH_3 was found to have been reduced by an order of magnitude, from 1000 ppmv (on dry and N_2-free basis) in the blank test to an average value of 100 ppmv with the catalytic candle – providing further confirmation of the activity of the NH_3 reforming catalyst brought about by nickel (Figure 17); considering the H_2S, in all the experiments its concentration remained below that found to be of negligible significance in the preliminary activity studies of the catalytic filter [Nacken et al., 2010]. For the black test its value was about 100 ppmv on dry and N_2-free basis, according to the measurement made for the test 1-II in which a commercial filter candle, with no catalytic activity, was used. Nevertheless, its concentration generally decrease when the Ni-catalyst is adopted.

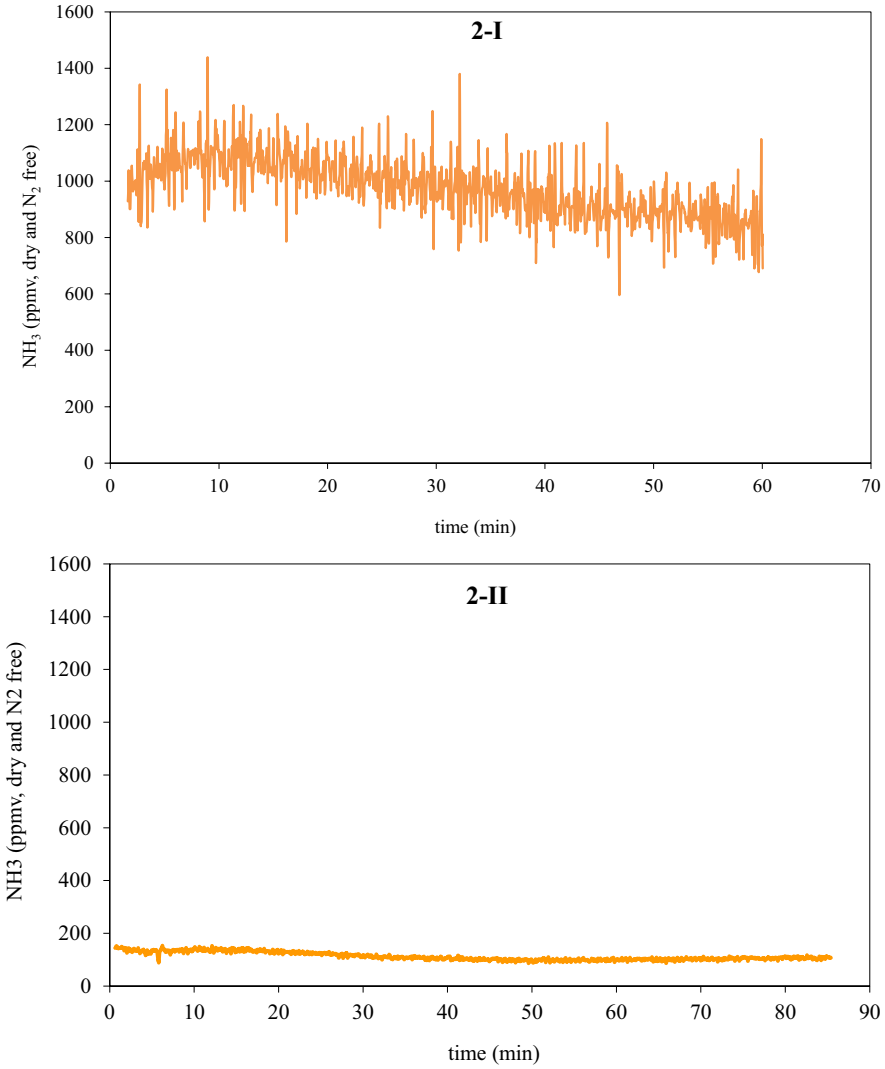

Figure 17: NH_3 concentration in the syngas as a function of gasification time during the blank test (2-I) or with the catalytic filter candle with "fixed bed" design (2-II)

To conclude the investigation on the behavior of the catalytic filter candle with "fixed bed" design in fluidized bed gasification, a test campaign was dedicated to measure the pressure drop across the filter, at various temperature steps either on the empty system (with no powder in it) (Figure 18) and, as a function of time, during some of the gasification experiments (Figure 19).

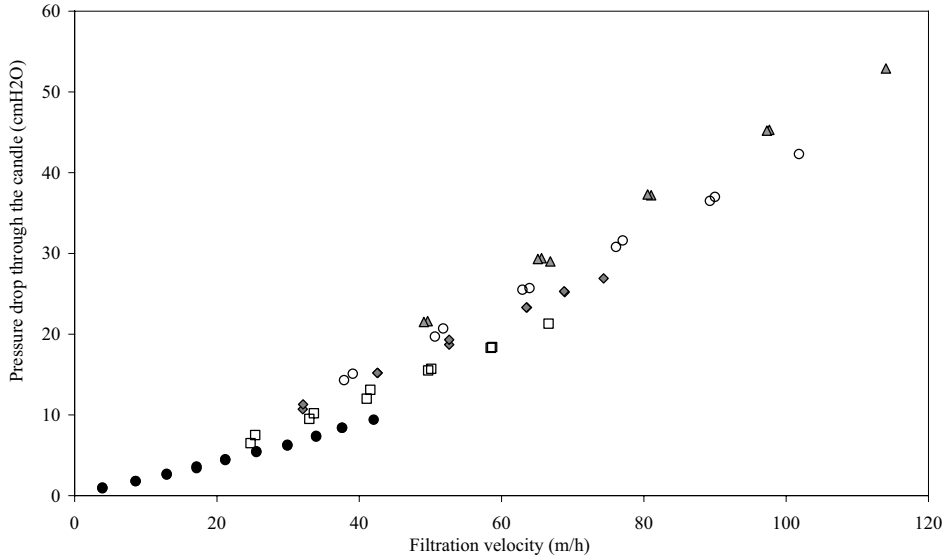

Figure 18: Pressure drop across the catalytic filter candle with the reactor empty of particles; temperature levels:(●) 20 °C, (□) 300 °C, (◆450 °C, (○) 600 °C, (▲800 °C

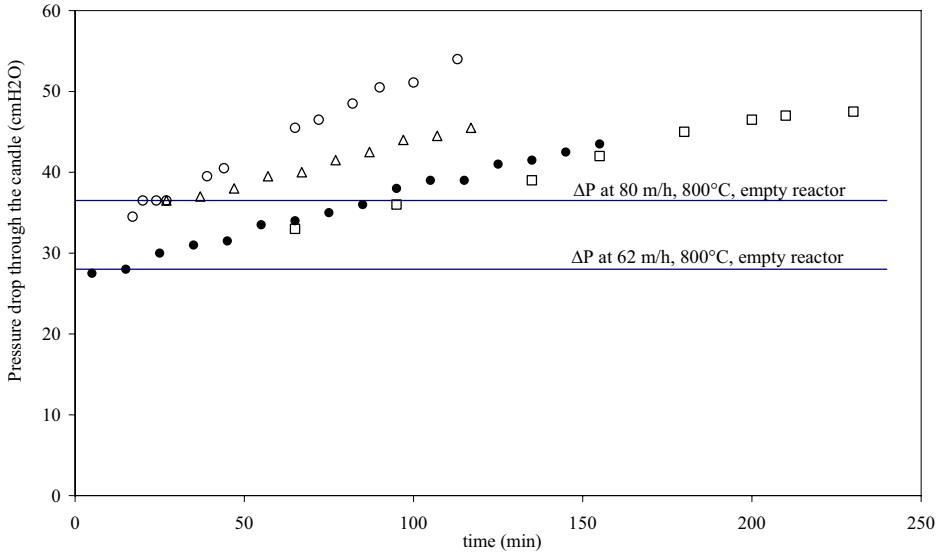

Figure 19: Pressure drop across the catalytic filter candle, as a function of time on test; average filtration velocity: (○) 81 m/h - test 2-IV, (Δ) 79 m/h - test 2-V, (●) 63 m/h - test 2-VI, (□) 62 m/h- test 2-X

From Figure 18 it is evident that the behavior of the catalytic filter candle containing a fixed bed of catalyst particles is similar to that reported for catalytic layer design; this is due to the presence in both filters of a very thin outer mullite membrane where most of the resistance to gas flow is located.

Figure 19 shows that for each gasification run the initial pressure drop is comparable to that measured, under similar temperature and face velocity

conditions, with the system empty of powder. As time progresses, the pressure drop increases almost linearly with time, with a gradient reflecting the growing thickness of the particle layer that deposits on the filter.

When the candle has been extracted from the reactor at the end of the test campaign, it has been found that patches of a fine particle layer (diameter less than 45 μm) were still adhering to the outer filtration surface (Figure 20); however, considering that after each gasification run the char accumulated in the bed is burnt in a current of air, this presumably leads to the breaking up of the sticky particle layer built up during the previous gasification step.

Figure 20: Catalytic ceramic candle before and after the whole gasification test of 22 hours

The growing fraction of fines in the bed as time progresses does not lead to a substantial change in the pressure drop trend, indicating that the fines fraction always remain below reasonable limits. Additional information concerning the pressure drop across the filter element are reported in literature [Rapagnà et al., 2010].

3.2.2. Gasification of almond shell using a catalytic filter candle with "fixed bed" design and 10wt % Fe/olivine

Fe/olivine catalyst with a relative high metal content (10wt%) has been tested as catalytic bed inventory for primary reforming of tar in the real fluidized bed gasification condition.

Also, tests with the simultaneous use of 10wt % Fe/olivine and the catalytically activate filter candle have been carried out in order to to check the gas purity resulting from combining effect of cleaning and conditioning of the syngas. The results obtained have been compared with the blank tests (2-I), which allows the assessment of 10wt% Fe/olivine catalyst performance against olivine and the evaluation of the combined effect Fe/olivine plus Ni-candle.

Table 11: Results of steam gasification of almond shells with 10wt% Fe/olivine bed inventory (3-I, 3-II and 3-III) and with 10wt% Fe/olivine + catalytic filter candle with "fixed bed" design (3-IV and 3-V)

	2-I	**3-I**	**3-II**	**3-III**	**3-IV**	**3-V**
Duration of test (min)	*60*	154	80	120	120	150
Gasifier bed temperature (ºC)	*808*	828	821	820	814	812
Gasifier outlet temperature (°C)	*738*	818	724	717	829	720
Steam/biomass dry	*1.06*	1.3	1.3	1.14	1.3	1.02
Water conversion %	*16*	20	19	25	29	37
Gas yield (Nm^3 dry/kg daf)	***1.00***	**1.37**	**1.42**	**1.41**	**1.75**	**1.69**
Tar content (g/Nm^3 dry)	***3.67***	**1.18**	**1.67**	**n.a.**	**0.30**	**n.a.**
Char residue (g/kg daf)	*94*	125	101	115	126	121
Carbon conversion %	*80*	74	79	77	74	75
H_2 (vol% dry gas, N_2 free)	***39***	**53**	**53**	**52**	**56**	**54**
CO_2 (vol% dry gas, N_2 free)	***26***	**28**	**27**	**26**	**22**	**21**
CO (vol% dry gas, N_2 free)	***24***	**13**	**15**	**16**	**17**	**20**
CH_4 (vol% dry gas, N_2 free)	***10***	**6**	**6**	**6**	**4**	**5**
Filtration velocity (m/h)	-	-	-	-	77	60

The significant results of all gasification runs, such as temperature, gas yield, water conversion, tar content in the syngas downstream of the catalytic filter element, char residue, carbon conversion, as well as the composition of the cleaned syngas are given in Table 11. Clearly, an increased gas yield and hydrogen content is noticeable as a result of the utilization of Fe/olivine instead of olivine. Thus, even without any candle in freeboard, a significant improvement of all the representative gasification parameters could be observed. This observation

is valid in general for the entire test campaign carried out with Fe/olivine; slightly different operating conditions (3-I, 3-II, 3-III) do not show significant changes in the results. The high gas yield indicates that iron is a good catalyst to reform tars, and the high hydrogen content is mainly due to the positive effect of Fe on the water gas shift reaction conversion: rather the results obtained can be considered a confirmation of the good activity of the new catalyst.

In Figures 21, the product gas composition obtained using the Fe/olivine bed inventory, is expressed as the percentage by volume of H_2, CO, CO_2 and CH_4 in dry, nitrogen free gas, as a function of gasification time.

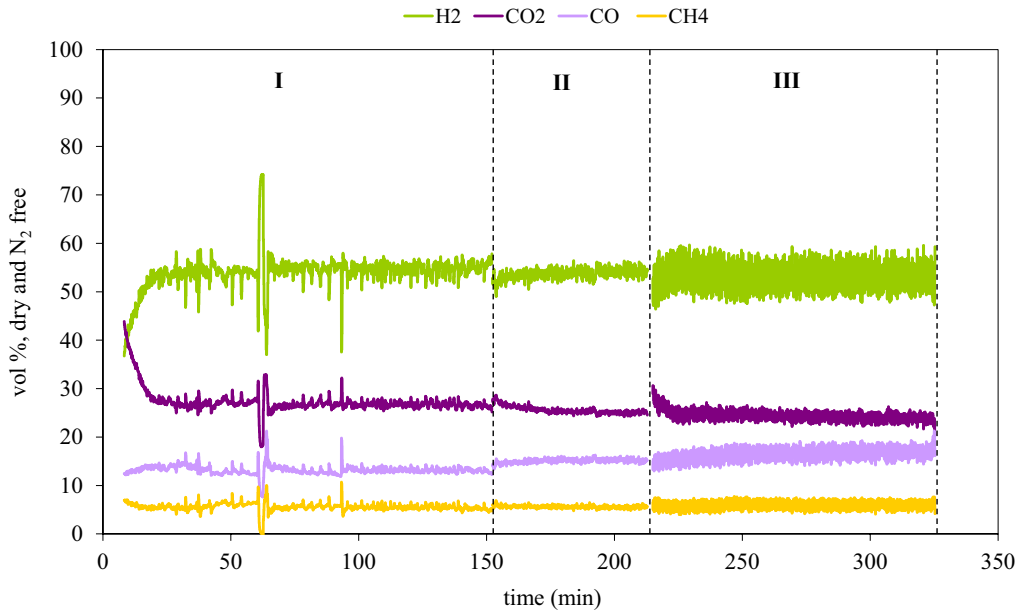

Figure 21: Syngas composition as a function of gasification time. Test 3-I, 3-II and 3-III: steam gasification of almond shells with 10wt % Fe/olivine bed inventory

As shown in Figure 21, an almost constant value is kept for H_2 concentration in tests 3-I, 3-II and 3-III, equal to about 53% by volume (dry, N_2 free gas), resulting in an weighted average enhancement in the H_2 yield of 88% in comparison to test 2-I.

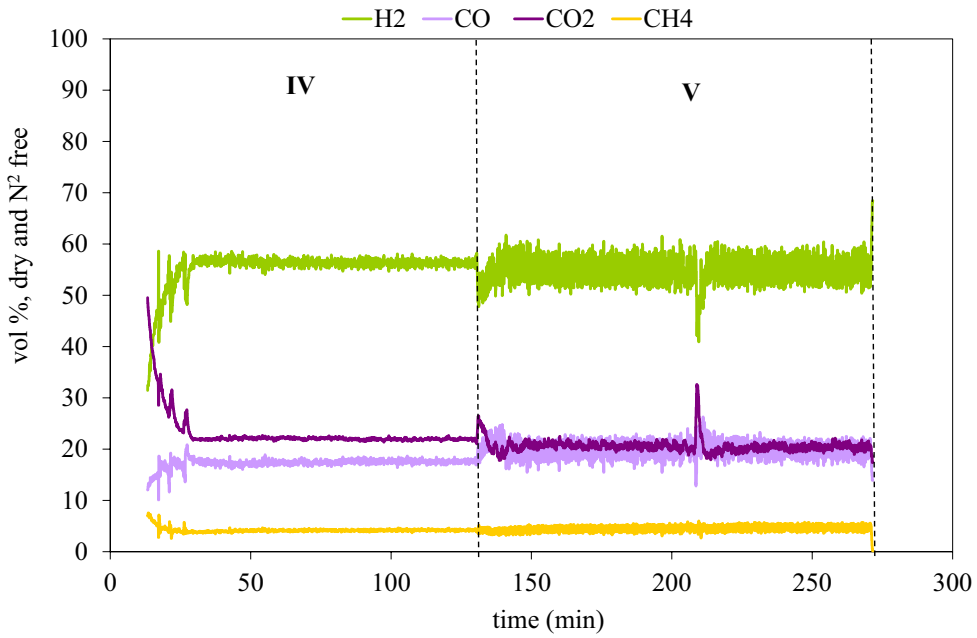

Figure 22: Syngas composition as a function of gasification time. Test 3-IV and 3-V: steam gasification of almond shells with 10wt % Fe/olivine bed inventory + catalytic filter candle with "fixed bed" design

Using 10wt% Fe/olivine combined with the catalytic filter candle inserted in the freeboard a further substantial improvement of all representative parameters was observed, as shown by results reported in Table 11 and in Figure 22.

A resume of the most important results achieved is reported in table 12, where the percentage variations for each test (as well as the weighted average) are calculated with respect to test 2-I (blank test).

Table 12: Percentage variation of the main gasification indicators with respect to test 2-I

	3-I	3-II	3-III	*Average*	3-IV	3-V	*Average*
Gas yield, %	+37	+42	+41	*+39*	+75	69	*+72*
Tar content in the producer gas, %	-68	-54	-	*-63*	-92	-	*-92*
Tar content per kg biomass daf, %	-56	-35	-	*-49*	-86	-	*-86*
H_2 yield, %	+86	+93	+88	*+88*	+151	+134	*+142*
CH_4 yield, %	-18	-15	-15	*-16*	-30	-16	*-22*

The comparison of data obtained using 10wt % Fe/olivine combined with the catalytic filter candle (tests 3-IV and 3-V) with the results of the blank test, allows to reach the best results by far. In fact, the highest concentration of H_2 is observed for tests 3-IV and 3-V, with a percentage increase of about 41% (average between the two tests) in comparison to the blank test (test 2-I), which corresponds to an

increased H_2 yield by 142% (Table 12). As a consequence and at the same time, a low concentration of methane is reported: in comparison with test 2-I, the CH_4 content in the dry, N_2 free syngas decreases from 10% to 4-5%.

For test 3-IV the high gas yield obtained, 1.75 Nm^3 dry/kg daf, is mainly attributable to increased reforming of tar brought about by the catalysts, which show the maximum synergic effect. Tar content measured by TOC is 0.30 g/Nm^3 dry (N_2 free basis) in test 3-IV, which is the lowest level reached in the whole test campaign. No noticeable improvements have been achieved in test 3-V, performed at higher concentration of reactants conditions.

It is, also, necessary to stress that in addition to the gasification/combustion time, the Fe/olivine particles were fluidized with air also during the heating up process, starting from room temperature up to the gasification temperature. It is then possible to consider that before performing test 3-IV, the Fe/olivine particles have been fluidized for more than 20 hours. This is a quite important indication that the active iron sites are still present on the surface of the olivine particles, and they are not lost due to attrition phenomena.

Table 13: Percentage variation of the main gasification indicators with respect to test 2-I for the different catalysts used

	CFC "fixed bed"design	10wt% Fe/olivine	10wt% Fe/olivine+ CFC "fixed bed" design
Gas yield, %	+69	+39	+72
Tar content in the producer gas, %	-79	-63	-92
Tar content per kg biomass daf, %	-64	-49	-86
H_2 yield, %	+130	+88	+142
CH_4 yield, %	-20	-16	-22

The percentage variations of the most significant parameters for the different catalysts examined in this section are reported in table 13. Each values corresponds to the weighted average of the variations with respect to the blank test 2-I. As described above, Table 13 clearly highlight the significant improvement obtained using the combined effect of 10wt% Fe/olivine with the catalytic filter candle inserted in the gasifier freeboard: especially the tar content in the producer gas decrease significantly, from -79% for the Ni-based filter

element to -92% obtained when the catalytic filter is combined with the effect of primary catalysts.

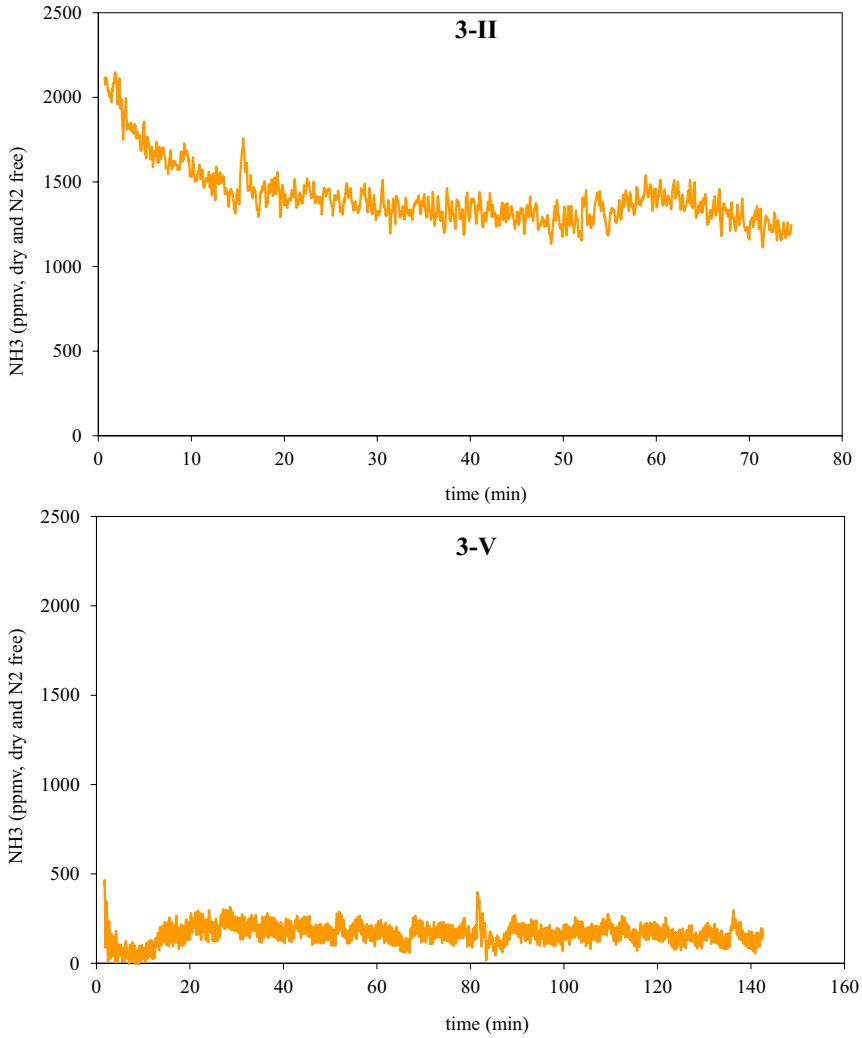

Figure 23: NH_3 concentration in the syngas from 10wt % Fe/olivine (3-II) and 10wt % Fe/olivine + catalytic filter candle (3-V) as a function of gasification time

As far as the ammonia concentration in the syngas is concerned, in the "Fe/olivine tests", its content is of the order of 2000 ppmv (dry and N_2 free): this higher value, when compared with gasification using plain olivine bed material, could be due to the increased iron concentration in Fe/olivine, in fact, Fe is a catalyst commonly used in ammonia synthesis. By the way, NH_3 content decreases to 200 ppmv (on dry and N_2-free basis) when the effect of the candle overlaps; An example of the reduction in the ammonia content obtained with 10wt% Fe/olivine plus the catalytic filter (test 3-V), when compared to a test carried out with 10wt % Fe/olivine (test 3-II) is given in Figure 23.

The presence of H_2S in the product gas has been also monitored. In all experiments, with the biomass used as a feedstock, its concentration remains below the concentration used for the preliminary activity studies of the catalytic filter candle (100 ppmv), indicating that the H_2S deactivation resulting from the poisoning of the catalytic layer only occurs to a negligible extent.

To conclude, pressure drop measurements through the filter candle fixed in the reactor freeboard have been performed during gasification runs 3-IV and 3-V, as a function of time. The results obtained are reported in Figure 24 and compared with some previous results .

The relatively higher pressure drop in test IV at 77 m/h filtration velocity should be related to the remarkable production of fine particles by 10wt % Fe/olivine. On the other hand, the agreement found between pressure drop data recorded in test 3-V (at 60 m/h) and in the previous test at the same filtration velocity, suggest that no additional formation of fine particles occurred.

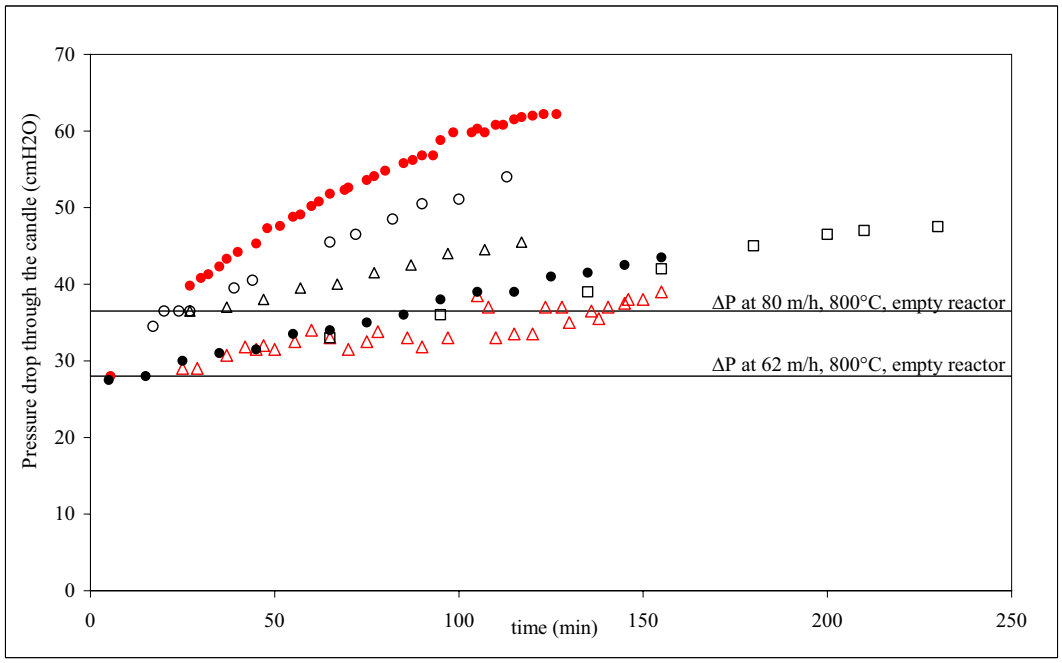

Figure 24: Pressure drop across the catalytic filter candle, as a function of time; filtration velocity: (○) 81 m/h, (Δ) 79 m/h, (●) 63 m/h, (□) 62 m/h (previous tests); (●) 77m/h – test 3-IV, (Δ) 60 m/h – test 3-V.

3.3. Gasification of Miscanthus x giganteus with olivine / 3.9wt % Ni/olivine

Part of this doctorate research activity was dedicated to the evaluation of MXG as

a new biomass feedstock for gasification: in fact, despite to the advantages of this energetic crop, just few data are present in literature on this subject [Khelfa et al., 2009; de Jong et al.,1999; Smolinski et al., 2010].

MXG gasification was carried out using plain olivine or 3.9wt % Ni/olivine bed inventories at two different temperature 800 and 900°C. The delta of 100°C was chosen in order to evaluate the influence of this parameter on the process.

The experiments give also important information concerning the behavior of Ni/olivine as primary catalyst for in-bed tar and ammonia reforming. The most important results obtained as well as the percentage variation of the main gasification indicators are reported in Tables 14 and 15, respectively. The percentage variations have been calculated with respect to the reference test 4-I, steam gasification of MXG with olivine bed inventory at 800°C.

Table 14: Results of MXG steam gasification tests with olivine bed inventory (test 4-I and 4-II) and Ni-olivine bed inventory (tests 4-III – 4-IV) at different operating temperatures

	4-I	**4-II**	**4-III**	**4-IV**
Duration of test (min)	60	60	120	60
Gasifier bed temperature (ºC)	798	899	799	901
Gasifier outlet temperature (°C)	752	841	786	897
Steam/biomass dry	1.10	1.10	1.10	1.10
Water conversion %	11	29	31	28
Gas yield (Nm3 dry/kg daf)	**1.00**	**1.54**	**1.70**	**1.64**
Tar content (g/Nm3 dry)	**2.87**	**1.25**	**0.41**	**n.a.**
Char residue (g/kg daf)	97	51	97	n.a.
Carbon conversion %	79	89	81	n.a.
H2 (vol% dry gas. N2 free)	**37**	**45**	**50**	**50**
CO2 (vol% dry gas. N2 free)	**25**	**23**	**24**	**24**
CO (vol% dry gas. N2 free)	**24**	**22**	**19**	**19**
CH4 (vol% dry gas. N2 free)	**14**	**10**	**7**	**7**

Table 15: Percentage variation of the main gasification indicators with respect to test 2-I for the different catalysts used

	4-II	4-III	4-IV
Gas yield, %	+54	+70	+64
Tar content in the producer gas, %	-56	-86	-
Tar content per kg biomass daf, %	-33	-76	-
H2 yield, %	+90	+131	+122
CH4 yield, %	+8	-16	-16

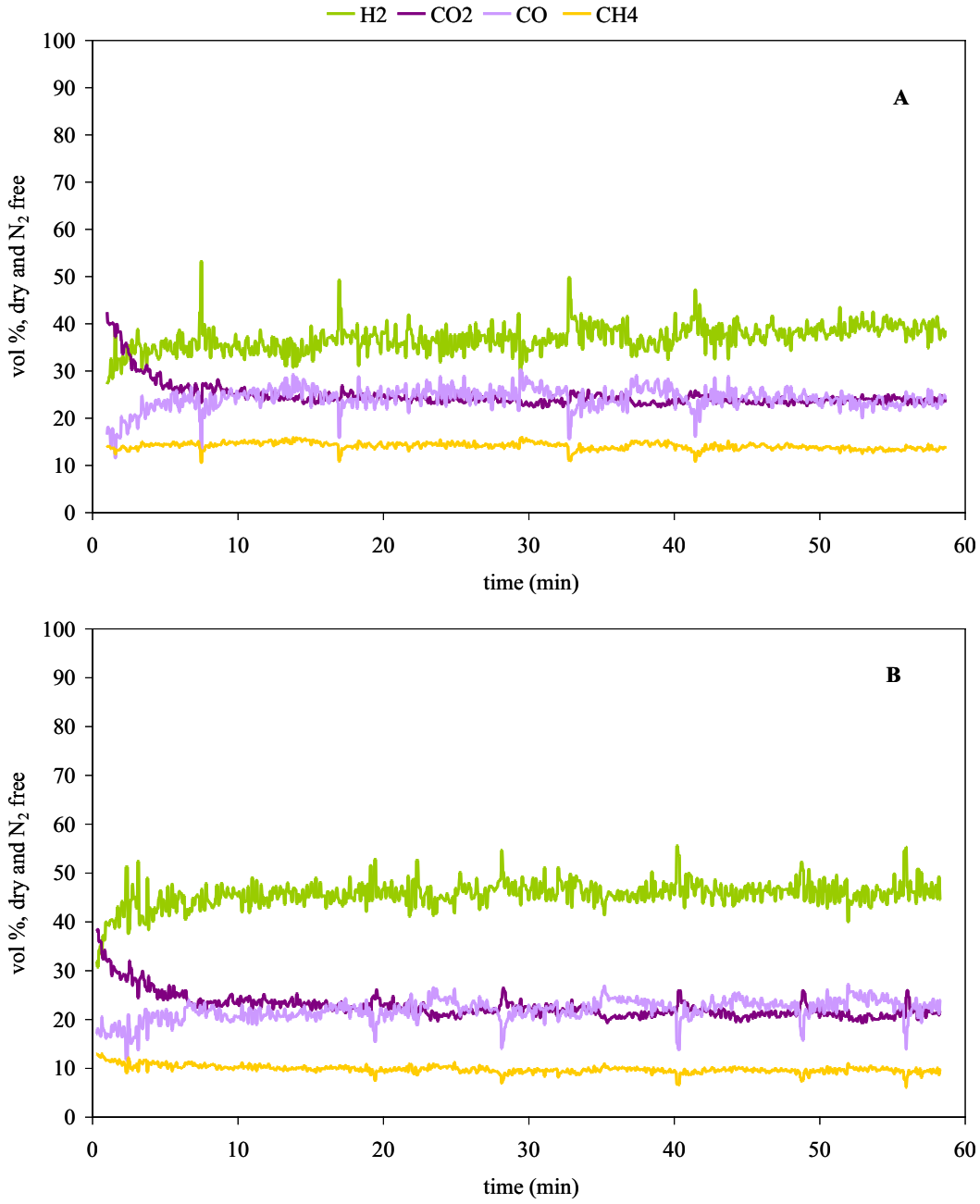

Figure 25: Syngas composition as a function of gasification time: MXG steam gasification at 800°C (**A**) and 900°C (**B**) with olivine bed inventory

As shown in Tables 14 and 15, increasing the temperature, a significant raise of gas yield was reported (54 %), thanks to a simultaneously decreasing of tar and especially char content, in fact per Nm^3dry/kg daf of syngas produced they reduce by 34 % and 19 %.

The syngas composition obtained by MXG steam gasification at 800°C and 900°C with olivine bed inventory is reported in Figure 25; the H_2 percentage by volume

in the dry and N_2 free gas increase from 37% to 45% when the higher temperature is adopted, which correspond to an augmented hydrogen yield of 90 %. In the case of the experimental runs carried out using the Ni-based in-bed catalyst, as expected, a promotion of tar-reforming reactions is reported, leading to an augmented hydrogen formation, increasing the gas yields and lowering the hydrocarbons content (tar + methane) in the product gas (tests 4-III and 4-IV).

The nickel impregnation of natural olivine leads to an improved catalytic efficiency at 800°C, however no significant upgrading could be reported when the operative temperature is set to 900°C (Figure 26).

In case of test 4-III (Ni/olivine at 800°C), an increased gas and hydrogen yields of 70 % and 131 %, respectively, were measured when compared with the result obtained by using only olivine particles at the same operative temperature (test 4-I). As a consequence, tar content in the producer gas drastically diminishes by 86% (Table 15).

During the catalytic gasification test performed at temperature higher that that utilized in industrial application (900°C), a slightly decrease of the catalyst activity was observed in terms of gas yield and water conversion, as reported in the experimental data (Table 14). This result suggests that the catalyst it is not suitable to be utilized at temperature higher than that utilized in the industrial gasifiers (800 – 850°C). Temperature higher than 850°C are also not recommended due to the formation of high molecular weight tars that impact adversely on their dewpoint [van Paasen et al., 2004]. By the way, the Ni/olivine catalyst tested in this work has been utilized in a circulating bed reactor for a long-term test at 838°C [Pfeifer et al., 2006], showing a constant catalytic activity

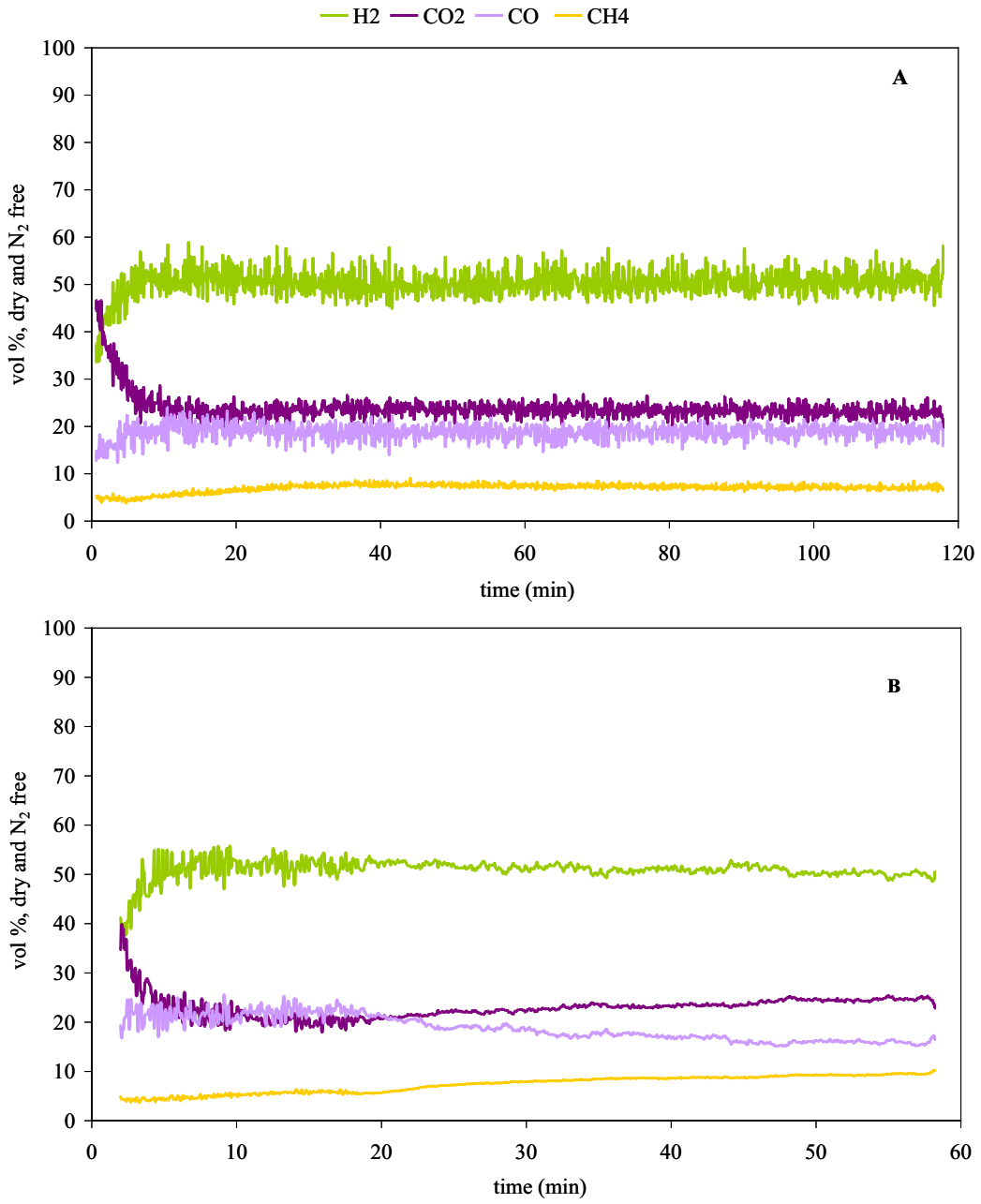

Figure 26: Syngas composition as a function of gasification time: MXG steam gasification at 800°C (**A**) and 900°C (**B**) with 3.9wt % Ni/olivine bed inventory

The efficiency in NH_3 reforming of the Ni-based catalyst was also monitored. Comparing the results obtained during test 4-I, with those reported with almond shells gasification at similar operating conditions (test 2-I), an higher ammonia content was found in case of miscanthus gasification: this could be attributed to the higher nitrogen content in MXG compared to almond shells, which are 0.45% wt/wt dry and 0.18 % wt/wt dry, respectively.

The ammonia concentration in the product gas from gasification with olivine, is almost half in the case of gasification run at the highest temperature (900°C); nevertheless, its contend drastically decrease when the 4wt% Ni/olivine by a factor 5 (Figure 27), which is a further demonstration of the good catalytic activity exerted from the 3.9 wt% Ni/olivine.

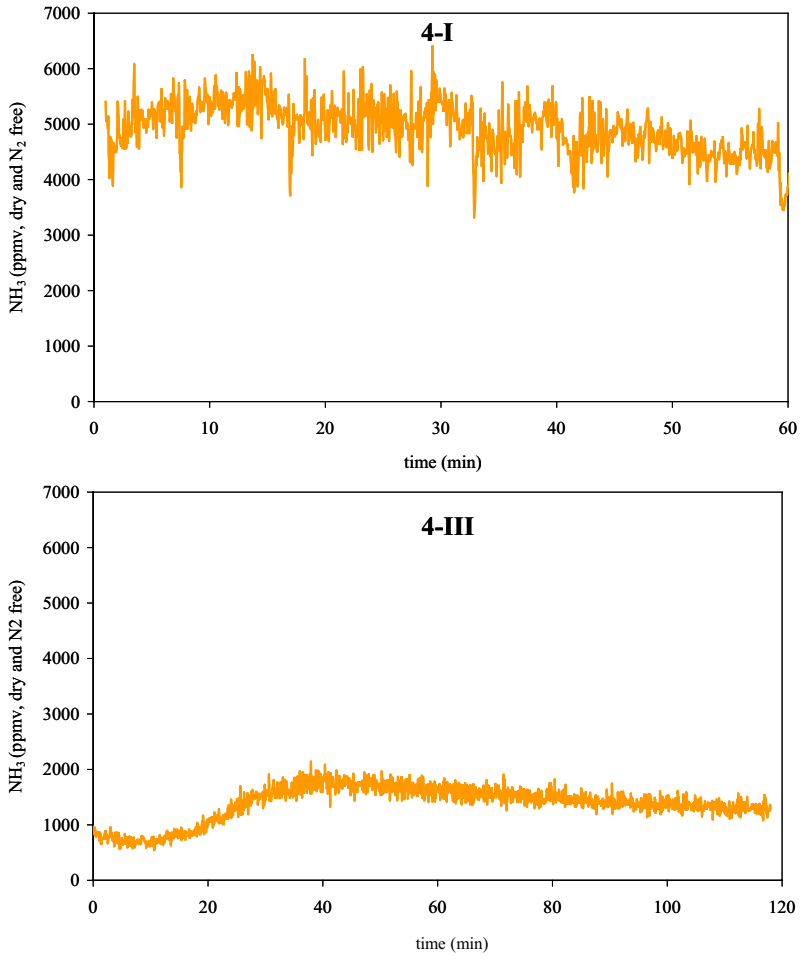

Figure 27: Ammonia concentration as a function of gasification time for test 4-I (800°C – olivine) and test 4-III (800°C – 4wt % Ni/olivine)

It is possible to compare the results obtained for test 2-I, Almond shell gasification with olivine bed inventory at 800°C (test 2-I) with those reported for test 4-I, considering the similarity of the operating gasification conditions. Besides the two different biomasses used, no significant differences could be measured, except a slight variability concerning tar content. These data confirm that the gasification output are primarily influenced by the operating condition adopted for the same reactor design.

In conclusion, it is remarkable that when Miscanthus x giganteus straw pellets were tested at temperature higher than 850°C, no bed defluidization was observed, confirming that this biomass could be successfully employed in fluidized bed gasification process.

4. Conclusions

During the present work crushed and sieved almond shells and Miscanthus x giganteus pellets have been uses as biomass feedstock: when similar gasification operating condition have been adopted, no significant differences in the syngas composition as well as in the gas yields are observed.

For MXG gasification, increasing the gasifier bed temperature up to 900°C, a significant promotion of gas yield was reported thanks to the enhanced tar and char gasification. By the way, the most interesting results were obtained at lower temperature (800°C) using the Ni-based in-bed catalyst. In this conditions, 3.9wt % Ni/olivine leads to an augmented hydrogen formation, increasing the gas yields (+70%) and lowering the hydrocarbons content (tar + methane) in the product gas.

The innovative concept of integrating a catalytic hot gas filter in the fluidized bed gasifier freeboard was also tested. The encouraging results show a simultaneous increase of the gas yield and hydrogen concentration, by significantly reducing the tar content of the raw syngas; two kind of catalytic filter were investigated:

- Catalytic filter candle with “catalytic layer” design;
- Catalytic filter candle with “fixed bed” design;

Thanks to the integrated higher and better accessible Ni catalyst amount for tar reforming in “fixed bed” candles, the latter design was preferred; this promising technology permits to achieve an increased gas yield and hydrogen content, by a substantial reduction of tar content in the raw syngas and enhanced conversion of char that cannot be elutriated from the gasifier.

The catalytic filter candle with “fixed bed” design leads to a decrease tar content in the producer gas by 79% and consequently an increase in the gas yield by 69% and in its hydrogen concentration, rendering the biomass product gas amenable for fuel cell applications. While, the “catalytic layer” design allows, in the optimum conditions, a relatively limited improvement in gas yield by 33%.

At the same time, the catalytic filter allows efficient particle separation, so that the final result is a hot and clean fuel gas made available right at the exit of the gasifier reactor. When applied to gasification systems of small to medium scale, this would determine a remarkable power plant simplification and intensification, combined with the potential of much higher conversion efficiency of biomass energy to electric power.

When the gasification time is increased up to 22 h, the catalytic performance of the filter element remains stable, even if a slight reduction concerning the methane and tar conversion was observed.

Additional test were carried out in order to evaluate the performances of 10% Fe/olivine catalyst in real gasification condition. The iron-based catalyst has been chosen for reactivity due to its strong metal-support interactions and significant amount of metallic iron available after reduction. Also Fe/olivine appears as a very interesting in-bed primary catalyst, for both economic and environmental reasons: iron does not affect the catalyst cost due to its lower price in comparison to nickel. Moreover, the fines particles separated from the product gas, can be easily disposal due to the absence of carcinogenic metals such as nickel compounds.

Although, higher ammonia production and lower carbon conversion have been observed in presence of 10wt% Fe/olivine bed inventory, the performance of the catalyst is not compromised: the tar reforming extent obtained by means of 10% Fe/olive catalyst is on average of 63%; methane is also partially converted (16%); as a result, an increase is obtained in the gas yield (about 39%) and the hydrogen concentration in the dry gas (N_2 free basis) raises 53%.

Further improvements have been obtained by the combination of Fe/olivine and the catalytic filter system, resulting in highest catalytic reforming activity (92% of tar abatement, +72% of gas yield). A slight additional reduction of methane (22%) and simultaneous higher water conversion have been observed.

References

de Jong W., Andries J., Hein K.R.G. (1999) Coal/biomass co-gasification in a pressurised fluidised bed reactor. Renewable Energy, 16(1-4):1110-1113

Khelfa A., Sharypov V., Finqueneisel G., Weber J.V. (2009) Catalytic pyrolysis and gasification of Miscanthus Giganteus: Haematite (Fe2O3) a versatile catalyst. Journal of Analytical and Applied Pyrolysis, 84(1):84-88

Nacken M., Ma L., Engelen K., Heidenreich S., Baron G.V. (2007) Development of a tar reforming catalyst for integration in a ceramic filter element and use in hot gas cleaning. Industrial and Engineering Chemistry Research, 46:1945–1951.

Nacken M., Ma L., Heidenreich S., Baron G. V. (2009) Performance of a catalytically activated ceramic hot gas filter for catalytic tar removal from biomass gasification gas. Applied Catalysis B: Environmental, 88:292-298.

Nacken M., Ma L., Heidenreich S., Baron G.V. (2010) Catalytic activity in naphthalene reforming of two types of catalytic filters for hot gas cleaning of biomass-derived syngas. Industrial and Engineering Chemistry Research 49(12):5536–5542

Pfeifer C., Rauch R., Hofbauer H., Świerczyński D., Courson C., Kiennemann A. (2006) Hydrogen-rich Gas Production with a Ni-catalyst in a Dual Fluidized Bed Biomass Gasifier, Science in Thermal and Chemical Biomass Conversion, A.V. Bridgwater and D.G.B. Boocock (Eds.), CPL Press, 1:677-690

Phyllis, database for biomass and waste http://www.ecn.nl/phyllis/

Rapagnà S., Latif A. (1996) Steam gasification of almond shells in a fluidised bed reactor: the influence of temperature and particle size on the product yield and distribution Biomass and Bioenergy, 12:281-288

Rapagnà S., Gallucci K., Di Marcello M., Foscolo P.U., Nacken M., Heidenreich S. (2009) In Situ Catalytic Ceramic Candle Filtration for Tar Reforming and Particulate Abatement in a Fluidized-Bed Biomass Gasifier. Energy & Fuels, 23:3804-3809

Rapagnà S., Virginie M., Gallucci K., Courson C., Di Marcello M., Kiennemann A., Foscolo P.U. Fe/olivine catalyst for biomass steam gasification: preparation, characterization and testing at ral process condition. Catalysis Today. *In press*

Smoliński A., Stańczyk K., Howaniec N. (2010) Steam gasification of selected energy crops in a fixed bed reactor, 35(2):397-404

Świerczynski D., Courson C., Bedel L., Kiennemann A., Guille J. (2006) Characterization of Ni-Fe/MgO/Olivine catalyst for fluidized bed steam gasification of biomass. Chemistry of Materials, 18:4025-4032

Van Paasen S.V.B., Kiel J.H.A. (2004) Tar formation in a fluidized bed gasifier: Impact of fuel properties and operating conditions. ECN-C-04-013 Report, 1-58.

CHAPTER 4: CHARACTERIZATION OF BIOMASS GASIFICATION TARS BY HPLC/UV

1. Introduction

Quantitative measurement of tar in the syngas stream is important to assess the effectiveness of cleanup and conditioning processes and verify the suitability of the cleaned syngas for its intended downstream use (e.g. catalytic conversion to liquid fuels, hydrogen recovery, or electricity production). The characterization of tars is, also, key step in the evaluation of the performances of catalytic biomass gasification. In fact, it is therefore believed that the problems related to tar, e.g. fouling, is fundamentally not concerned with the tar quantity, but is with its properties and composition. The condensation behavior of tar is an integral effect of all tar components that are present in the syngas.

In order to obtain a representative set of all the organic compounds present in tar fraction, the standard method for tar and particles sampling in the producer gas, has been introduced in the gasification plant, according to technical specification UNI CEN/TS 15439. This method is based on the discontinuous extractive sampling under isokinetic conditions of a representative part of the gas stream containing tar at the exit of the reactor (Chapter 1, Section 3.1). The sampling train is configured as a heated probe and the volatile tars are trapped in heated or chilled impinger bottles containing a known quantity of 2-propanol.

HPLC/UV is the technique that has been chosen to characterize the tars in the samples collected according to UNI CEN/TS 15439.

In the following sections, the method as well as the most significant results obtained will be analyzed and discussed.

2. Materials and method

2.1. Materials

The aromatic hydrocarbons used: phenol (Ph-OH), toluene (Tol), styrene (Styr) indene (Ind), naphthalene (Nap), biphenyl (Bph), diphenyl ether (DphE), fluorene (Fle), phenanthrene (Phe), anthracene (Ant), fluoranthene (Fla) and pyrene (Pyr) were provided from Acros Organics (Geel, Belgium).

Stock standard solutions of 1 mg/ml in dichloromethane (HPLC gradient grade from Fisher Scientific, Loughborough, Leicestershire, UK) were prepared and

used for further dilutions in 2-propanol (HPLC gradient grade from Fisher Scientific, Loughborough, Leicestershire, UK). Phenol mother solution at 1 mg/ml was prepared directly in 2-propanol.

The methanol used as mobile phase in HPLC/UV analysis was provided from Fisher Scientific (Loughborough, Leicestershire, UK) as well.

2.2. Method

Tar samples were recovered according the UNI CEN/TS 15439 and properly stored at 4°C before the measurement. It should be stressed that the heated particle filter described in the UNI CEN/TS 15439 to collect and quantify solid matter is not currently installed in our plant.

20µl of each sample were injected in a HPLC apparatus (Hitachi "Elite LaChrom" L-2130). The system was equipped with an UV detector (Hitachi UV-detector L2400) set at 254 nm, which corresponds to the absorbance of the aromatic ring. If necessary, samples were diluted in 2-propanol before the analysis, but the majority of them were analyzed without any preparatory step.

The column for the chromatographic separation of the tar fraction was a reversed phase C18, 150 x 4.6 mm (Alltech “Apollo C18 5 µm”), protected with a guard column.

A gradient elution was realized using methanol/water, at a flow rate of 1 ml/min. The gradient chosen is reported in table 1.

Table 1: Gradient elution

Time, min	% Methanol	% Water
0	45	55
5	45	55
21	75	25
28	75	25
32	85	15
40	85	15
42	100	0
48	100	0

3. Results and discussion

3.1. Validation of the method

Twelve molecules have been identified using the above-described method. The identified compounds were confirmed by GC/MS analysis, and they are in qualitatively agreement with the data found in the literature [Devi et al., 2005].

The quantification was realized using external calibration; thus for each compound, calibration curves were constructed using at least six levels of concentration which covered the concentration ranges expected in the various samples. Each point of the calibration curves was repeated at least three times.

The main parameters of the standards calibration curves such as the minimum and maximum concentration injected (C_{min} and C_{max}), the number of measurement for the calibration set (n), the linear equations constants as well as the retention time (t_r) of each molecule are reported in Table 2.

Table 2: Parameter of the standard calibration curves for tars quantification

	t_r (min)	C_{min} (mg/l)	C_{max} (mg/l)	n	Slope	y-intercept	R^2	LOD (mg/l)	LOQ (mg/l)
Ph-OH	5.5	5.33	1065.00	18	91.46	-154.12	0.996	3.14	6.55
Tol	18.1	14.00	2300.00	26	35.30	65.89	0.999	1.95	6.51
Styr	19.8	0.89	53.10	6	1622.93	-54.72	0.998	0.17	0.49
Ind	20.4	1.02	108.00	12	1114.22	1770.06	0.997	0.33	1.12
Nap	21.6	1.00	200.00	18	394.07	1575.17	0.991	0.06	0.22
Bph	22.3	0.21	41.20	16	2059.28	-535.52	0.990	0.28	0.32
DphE	27.9	1.36	150.00	13	337.4	1496.5	0.992	0.23	0.77
Fle	30.4	0.32	39.38	15	2903.10	-2431.60	0.998	0.86	0.93
Phe	31.9	0.11	16.50	16	4230.02	1431.75	0.995	0.03	0.10
Ant	33.5	0.05	5.50	18	8214.59	1174.03	0.992	0.01	0.03
Fla	36.2	0.42	39.75	13	1698.96	-823.01	0.999	0.53	0.77
Pyr	37.3	0.30	29.70	13	1318.98	-40.16	0.997	0.06	0.14

The limit of detection (LOD) and the limit of quantification (LOQ) were also calculated according to the equations (1) and (2) [Skoog et al., 2005]; the results obtained are illustrated in Table 2.

$$LOD = \frac{k \cdot s_b}{m} \qquad k = 3 \qquad (1)$$

$$LOQ = \frac{k \cdot s_b}{m} \qquad k = 10 \qquad (2)$$

Those two values are very important in quantitative analysis; in fact the limit of detection (LOD) represents the concentration of analyte that produces a signal significantly different from that of the blank, i.e., the concentration corresponding to the minimum significant signal. Thus, could be assumed as the value at which the analysis is just feasible. When a signal is greater than the LOD we can say that the analyte is present in the sample, but to establish the limit beyond which it is legitimate to perform quantitative measurements is necessary to define the limit of quantification (LOQ), which measure the concentration at which quantitative results can be reported with a high degree of confidence level.

It can be seen from these results that the limits are low enough to determine tar compounds in the biomass gasification samples.

Calibration curves allow us to obtain the concentration of tar in the impinger bottles, i.e. the mg/l of tar in 2-propanol.

Knowing the volume of solvent (ml) and the volume of gas passed into the bottles (Nm^3 dry), the concentration of tars in the syngas can be easily calculated and expressed in mg/Nm^3 dry.

Those quantitative results obtained by means of HPLC/UV have been used as reference value for further analytical investigations.

3.2. Characterization of biomass gasification tars

3.2.1 Gasification of almond shell using a commercial filter candle

Figure 1 reports the tar content in the syngas downstream of the commercial filter candle provided by PALL GmbH (tests 1-I and 1-II). The data regarding the test carried out with the catalytic filter candle with fixed layer design are not available.

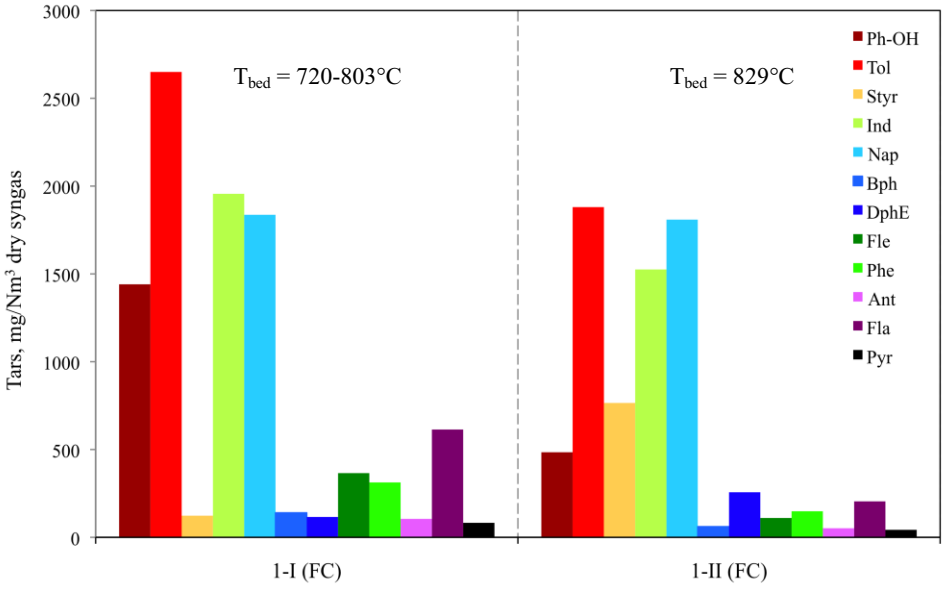

Figure1: Tar distribution in the syngas downstream of the filter candle

As is to be expected, the main compounds turn out to be the low molecular weight hydrocarbons, such as toluene, naphthalene, indene, styrene and phenol; the data obtained in Test 1-I confirm the important correlation between temperature and the quality of the producer gas: increasing the fluidized bed temperature from 720 to 830°C gives rise to a decrease in the tar content, which goes from 9.7 to 7.3 g/Nm^3 dry syngas.

With the exception of styrene and diphenyl ether, which exhibit an anomalous behavior, and naphthalene that is known to be quite refractory to thermal cracking, all compounds show a significant decrease of their concentration.

When the concentration of tar for kg biomass daf is concerned, increasing the bed temperature the three- and four-rings aromatics (class 4 and class 5 in Table 4, Chapter 1) decrease with an average percentage of 40%.

Those compounds are very important when the dewpoint is considered. The tar dewpoints of exit gas from test 1-I and 1-II were determined using the on-line calculation tool developed by ECN. As stated in the Introduction chapter the model is based on ideal gas law. The calculation is done using Raoult's law and the vapour pressure data of individual tar compounds [http://www.thersites.nl/completemodel.aspx].

For test 1-I the calculated tar dewpoint is 124.3°C; this value slightly reduce to a value of 109.3°C for test 1-II according with the light reduction observed in tar concentration.

3.2.2 *Gasification of almond shell using a catalytic filter candle with "fixed bed" design*

The reforming activity of the innovative catalytic ceramic candles with fixed bed design was evaluated during a long-term test (22h). The results concerning the tars distribution in the syngas are reported in Fig. 2. The main compounds are toluene and naphthalene. These light aromatics are present in high concentration in test I (no catalytic candle, blank test); as observed, they drastically decrease when the catalytic filter candle is used, due to the good tar reforming activity promoted by the nickel catalyst. The same behavior is observed for the heavier aromatics (class 4 and 5).

The results of the HPLC/UV analytical determinations confirm completely the evidence of catalyst activity arising from the gas composition discussed above. With regard to the entire tar production trend throughout the 22 hours on test, a strong decrease of the aromatics concentration is observed during the first hours (tests II-IV).

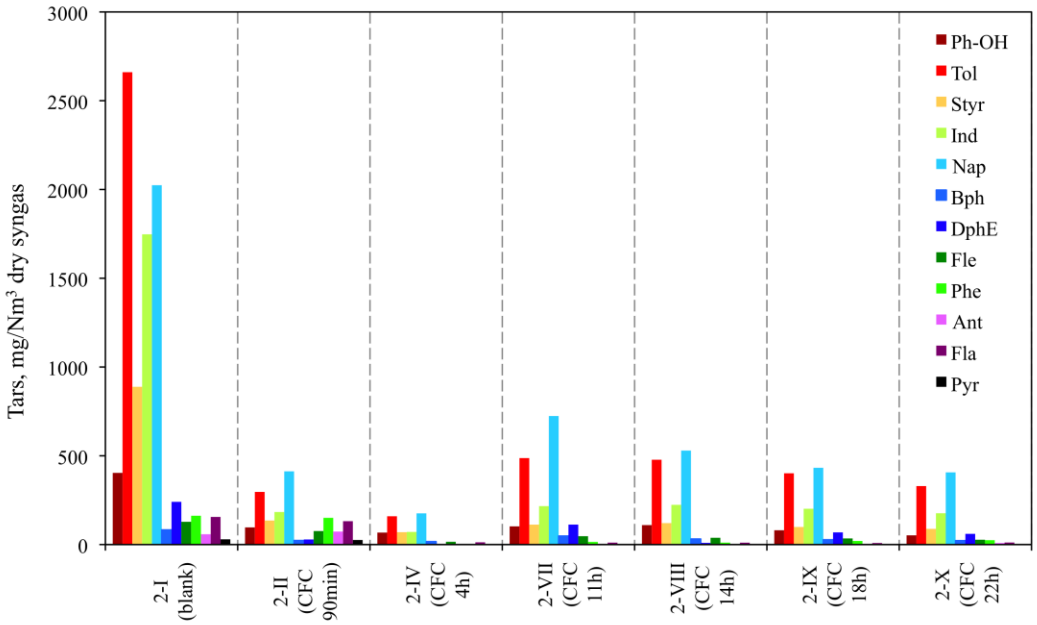

Figure 2: Tar distribution in the syngas downstream of the catalytic filter candle (CFC) with fixed bed design during the long-term test of 22h (2-II – 2-X) and from the blank test (plain olivine)

In test IV about 90% of toluene and naphthalene in the producer gas are reformed. For greater total gasification times (tests VII – X) a slightly larger concentration of aromatics is observed: for test X, toluene and naphthalene decrease by 78% and

64% respectively from the values obtained in the blank test I (with no catalytic candle). Gas yield and water conversion data, reported in Tables 9 – Chapter 3, suggest that in the later tests the experimental conditions may have given rise to a somewhat lower availability of steam thereby preventing further tar reforming [Rapagnà et al., 2010]. The total tar content nevertheless still remains very low, its value corresponds to 1.2 g/Nm^3 dry syngas, against 8.6 g/Nm^3 dry found in the blank test. This confirms the constant performance of the catalyst during time.

3.2.3 Gasification of almond shell using a catalytic filter candle with "fixed bed" design and 10wt % Fe/olivine

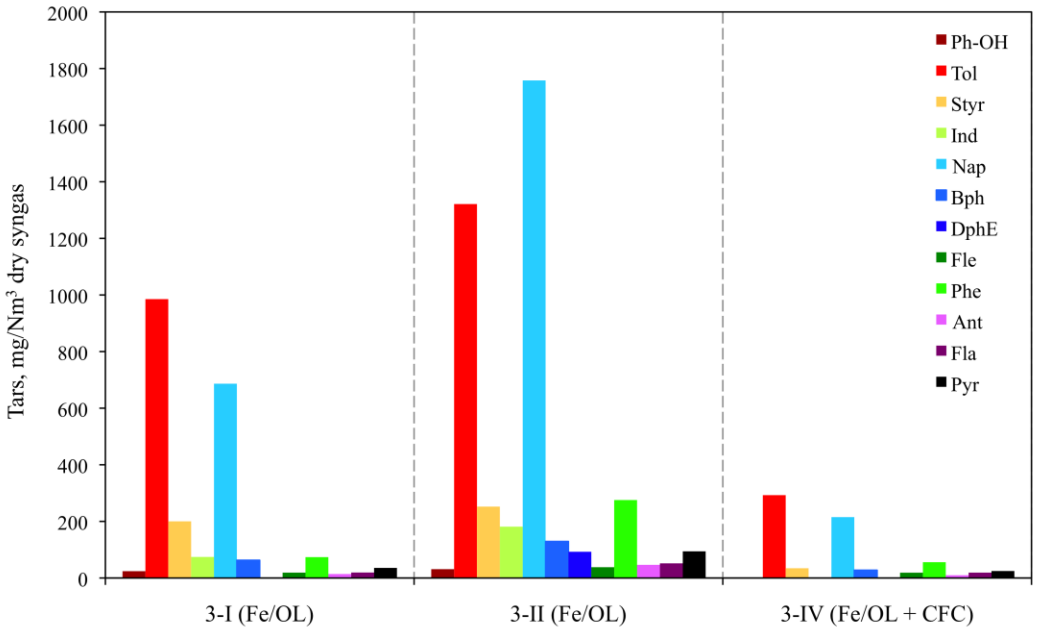

Figure 3: Tar distribution in the syngas from gasification with 10wt % Fe/olivine (3-I and 3-II) and with 10wt % Fe/olivine plus the CFC with fixed bed design (3-IV)

The performance of 10wt % Fe/olivine for tar conversion in real gasification is reported in Figure 3.

The results obtained with 10wt % Fe/olivine shows how the catalyst is active on tar conversion: the iron impregnation of natural olivine results in a promotion of reforming activity, which leads to a decreased tar concentration. For test 3-I the tar content in the producer gas is 2.2 g/Nm^3 dry, resulting in a decrease by 74% when compared to the test performed with plain olivine particles (2-I). During test 3-II a decrease by 50% was measured; this difference may be explained

considering the slight divergence observed for the gasifier outlet temperatures, which are 818°C and 724°C, respectively. Nevertheless, it should be consider that the sampling method is pretty elaborate, thus could affect considerably the results obtained and the different tar concentration can largely reflects the problematic of sampling of the tar protocol.

As expected, light aromatics such as toluene, indene and naphthalene represent the primary molecules of tar fraction. It is also to stress that HPLC/UV analyses of samples obtained from Fe/olivine gasification tests show a content of higher molecular weight hydrocarbons generally very low when compared to the test with plain olivine (Figure 2): their concentration for kg biomass daf decreases by 40%.

When the effect of 10wt % Fe/olivine is combined with the ones of the catalytic filter candle with fixed bed design (test 3-IV) a strong decrease of both low and high molecular weight tars is observed, and a final concentration of 0.7 g/Nm^3 dry was measured, which corresponds to le lowest value reported.

3.2.4 Gasification of Miscanthus x giganteus with olivine / 4wt % Ni/olivine

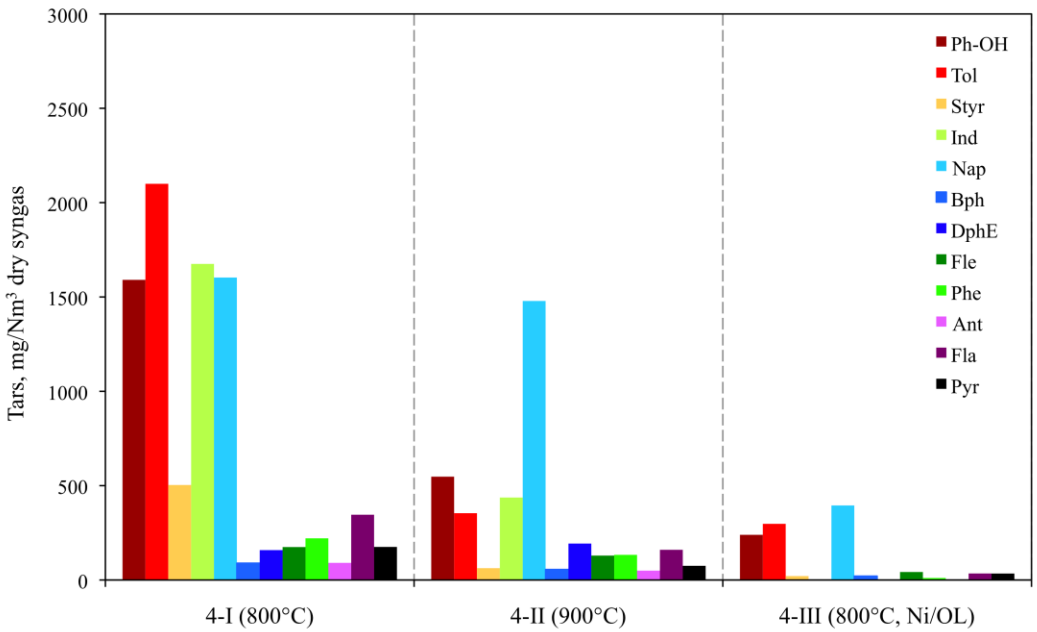

Figure 4: Tar distribution in the syngas from gasification with olivine at 800°C (4-I), 900°C (4-II) and with 4wt % Ni/olivine (4-III)

Tar characterization of the samples recovered during MXG gasification experiments is reported in Figure. The results confirm what observed above.

The main molecules are the light aromatics. At 900°C a significant reduction of the aromatic molecules is observed, except for naphthalene, due to the stability of this molecule to thermal cracking treatments. On the opposite, when the nickel catalyst is used (4-III) a relevant decrease of all aromatics is reported, which turns into a tar concentration of 1.1 g/Nm^3 dry: the tar production per kg biomass daf decrease by 80%, when compared to test 4-I.

Even if, no long-term test has been performed, as stated above, the Ni/olivine catalyst tested in this work has been previously utilized in a CFB reactor, at temperature of 838°C for 30 hours, showing a constant catalytic activity and a good behavior in fluidization regime [Pfeifer et al., 2006].

3.3. Resume of the most relevant results obtained from tar characterization

Figure 5 represents the cumulative data of tar composition related to the different test campaigns. For the tests carried out with 10wt % Fe/olivine and the long-term test with the catalytic filter candle (fixed bed design), the specific concentration of each compound in the fuel gas has been determined on averaging the corresponding value over the duration of test.

The results will be confronted with the blank test 2-I, in which crushed almond shells were gasified using a fluidized bed of plain olivine (Table 3).

Table 3: Tar content form the different test campaign and percentage variation with respect to test 2-1 (steam gasification of almond shell with plain olivine)

Gasification test	Tar content g/Nm^3 dry	Tar content in the producer gas, %	Tar content per kg biomass daf, %
2-I	***8.6***		
4-I	8.7	+2	+2
1-II	7.3	-14	15
4-II	3.7	-57	-36
3-I,II	3.2	-62	-48
4-III	1.1	-87	-78
2-II,IV,VII-X	1.4	-84	-73
3-IV	0.7	-92	-86

From the qualitative point of view, no significant difference in the tar composition could be reported, even when different biomass are used: as described above in all the experiments, the main compounds turn out to be the low molecular weight hydrocarbons, such as toluene, styrene, indene and naphthalene. The higher

phenol content reported in case of MXG gasification, when compared with almond shells, could be considered the only exception.

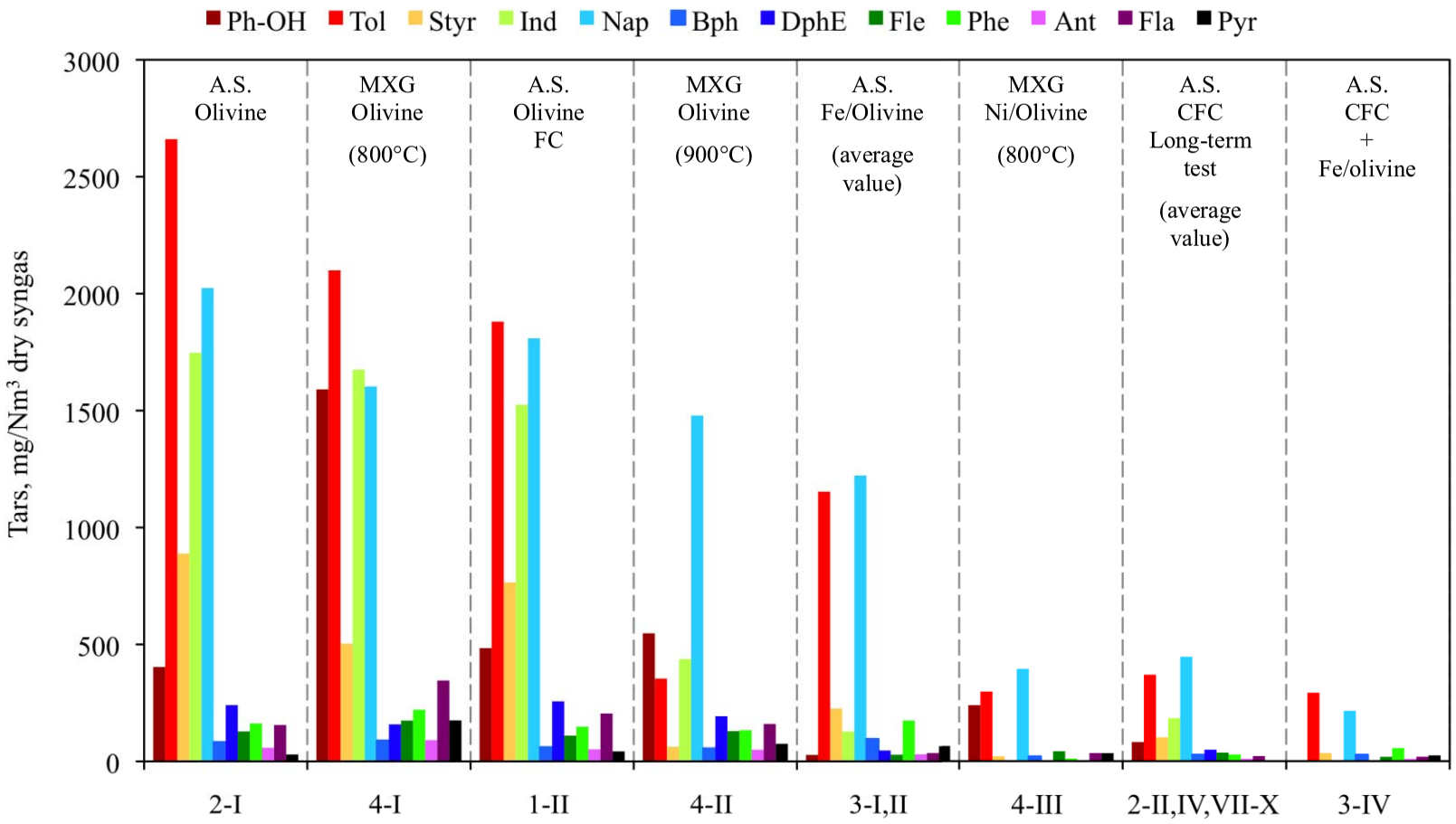

Figure 5: Tar distribution in the syngas from gasification tests performed (A.S. = almond shells)

Furthermore, on quantitative base, MXG and almond shells show the same tar concentration when analogous conditions are adopted: for tests 2-I (steam gasification of almond shells at 808°C) the tar content measured is 8.6 g/Nm^3 dry, while for test 4-I (steam gasification of MXG at 800°C) is 8.7 g/Nm^3 dry (Table 2).

During tests realized using a Ni-based catalyst (4-III; 2-II,IV,VII-X) a considerable reduction of all tars in the producer gas has been observed thanks to the well-established tar reforming activity promoted by this metal.

By the way, during tests conducted with 10wt % Fe/olivine particles in the fluidized bed (tests 3-I,II), tar level remains well below that measured in the reference test. With Fe/olivine, naphthalene in the producer gas, which is considered quite refractory to cracking/reforming reactions, decrease by 40%. This evidence confirms that the iron impregnation of natural olivine leads to a promotion of reforming activity and a corresponding decrease of tar concentration.

The experimental results for test with 10wt % Fe/olivine and Ni-candle, confirm the maximum synergic effect already reported: in fact, the simultaneous use of Fe/olivine and the catalytically active filter candle leads to a drastic abatement of tars in the producer gas. Light molecules as well as heavy compounds are reformed, resulting in a tar reduction in the syngas of 92% in comparison with test 2-I.

Figure 6 show the correlation between the calculated tar dewpoint and the tar content. Devi et al. reported that increasing the gasification temperature from 800°C to 900°C with an olivine bed inventory results in a slight decrease in the dewpoint from 172°C to 150°C [Devi et al., 2005]. Similar data were measured in case of MXG gasification at 800°C and 900°C (4-I; 4-II); for the second test a decrease by 10°C was measured, turning into a dewpoint of 109.5°C.

Test 4-I shows the upper tar dewpoint (120.6°C); in fact, tar recovered during this experiment have the higher level of heavy fractions (Figure 5).

Despite of the strong reduction in total tar concentration observed for the latter test (3-IV) a limited impact on the tar dewpoint is reported: its value decreases from 106.6°C, calculated for the reference test, to 89.7°C.

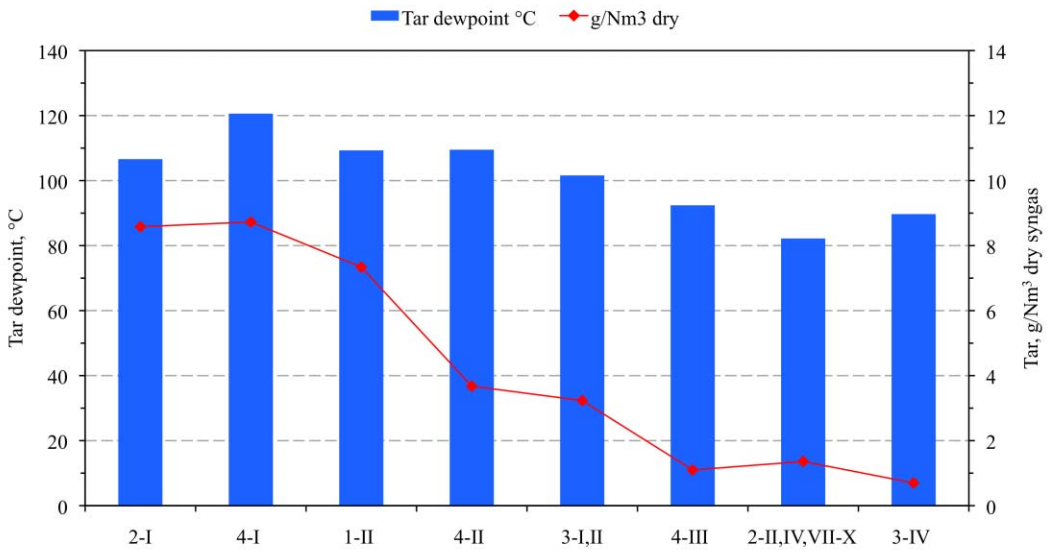

Figure 5: Correlation between the tar concentration and its dewpoint calculated for the different test campaign performed

By the way, heavy tar compounds dominate the tar dewpoint. According to van Paasen et al. class 5 tars (≥ 4 aromatic rings) already condense at low concentration (0.1 mg/Nm^3) when the gas is at atmospheric pressure and at ambient temperature. Thus, it should be stressed that no molecules heavier than pyrene were identified and quantified in our study, so the tar dewpoint in Figure 6 can be an underestimate.

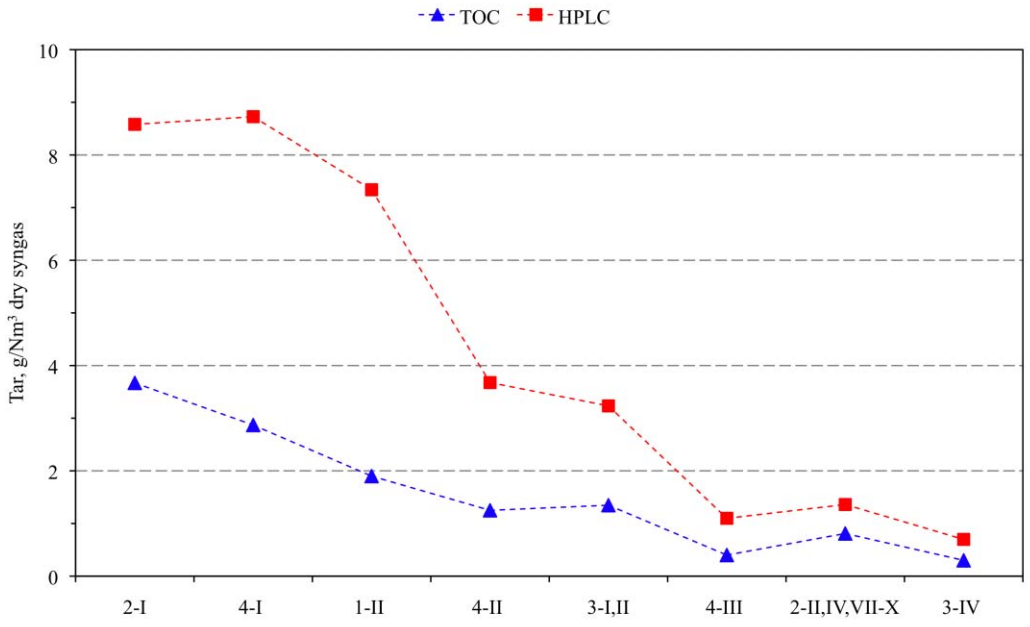

Figure 6: Correlation between the tar concentration measured by TOC and HPLC/UV analysis for the different test campaign performed

As discussed above, tar concentration data have been measured by TOC analysis of the condensate fraction and by HPLC/UV of the samples obtained according to UNI CEN/TS 15439. The evolution of tar concentrations obtained by both analytical methods follows the same trend with a fairly good agreement between the tar content ratios obtained among tests at different experimental conditions. Nevertheless, a variation in the absolute values of tar content detected by both methods has been recorded, as expected, considering the substantial differences between the analytical techniques applied in this study, and also in the nature of the analyzed samples (Figure 6).

Moreover, the variation observed is relevant in case of higher tar content, suggesting that in this range of concentration the cooling system allows to recovery only a part of the tars; on the contrary when the tar content decrease around 1 g/Nm^3 dry the two techniques show a very good agreement.

4. Conclusions

Tar characterization of the samples recovered according to the UNI CEN/TS 15439 was carried out by HPLC/UV. This valid technique has shown that no significant difference in the tar composition could be reported when different biomass were used; MXG could be confirmed as a good biomass feedstock candidate for syngas production.

Also, tar analysis confirms the good results obtained during this study. The iron impregnation of natural olivine leads to a significant improvement in gas quality: the tar content in the producer gas decrease more than 60%. Thus, Fe/olivine appears as a very interesting in-bed primary catalyst. Nevertheless, the innovative concept of integrating a catalytic hot gas filter Ni-based in the freeboard of a fluidized bed gasifier results in greatly reduction of tar content. When its action is combined with the 10wt % Fe/olivine as bed material a minimum tar content of 0.7 g/Nm^3 dry is reported.

References

Devi L.. Ptasinski K.J.. Janssen F.J.J.G.. van Paasen S.V.B. Bergman P.C.A.. Kiel J.H.A. (2005) Catalytic decomposition of biomass tars: use of dolomite and untreated olivine. Renewable Energy. 30:565–587

Li C.. Suzuki K. (2009) Tar property. analysis. reforming mechanism and model for biomass gasification – An overview. Renewable & Sustainable Energy Reviews 13:594-604

Pfeifer C., Rauch R., Hofbauer H., Świerczyński D., Courson C., Kiennemann A. (2006) Hydrogen-rich Gas Production with a Ni-catalyst in a Dual Fluidized Bed Biomass Gasifier, Science in Thermal and Chemical Biomass Conversion, A.V. Bridgwater and D.G.B. Boocock (Eds.), CPL Press, 1:677-690

Rapagnà S., Gallucci K., Di Marcello M., Matt M., Nacken M., Heidenreich S., Foscolo P.U. (2010) Gas Cleaning, Gas Conditioning and Tar Abatement by means of a Catalytic Filter Candle in a Biomass Fluidized-Bed Gasifier. Bioresource Technology, 101(18):7134-41

Skoog D.A., West D.M., Holler F.J., Crouch S.R. (2005) Fondamenti di Chimica Analitica – II Edizione. EdiSES s.r.l., Napoli (Italia)

van Paasen S.V.B., Kiel J.H.A. (2004) Tar formation in a fluidized bed gasifier: Impact of fuel properties and operating conditions. ECN-C-04-013 Report, 1-58.

http://www.thersites.nl/ "Thersites: website for tar dewpoint calculations"; December 2003

CHAPTER 5: DEVELOPMENT OF ANALYTICAL METHODS FOR TAR DETERMINATION

1. Analysis of tar based on UV spectroscopy and planar chromatography

1.1 Need for rapid and accurate method for tar analysis

The analysis of tar lays on time-consuming cost-effective methods (liquid or gas chromatography), the potentiality of other traditional techniques will be evaluated on the base that they can be easily encountered in a laboratory (UV spectroscopy) or offer new potentiality with recent apparatus development (planar chromatography). As described in the bibliographic chapter, each analytical technique presents partial defect leaving place to new approach developed here: the potentiality of UV spectroscopy for tar analysis could contribute to the development on new on-line determination. The approach of the work is then based on a total analysis of tar without separation step

Moreover, planar chromatography showed interesting potential for PAHs analysis and can be an alternative to other chromatographic systems.

Noteworthy that all these methods are generally robust and give accurate results to quantify mixtures of compounds, however few results have been shown in the field of tar analysis.

1.2 Material and methods

1.2.1 Chemicals

Phenol (Ph-OH), toluene (Tol), styrene (Styr) indene (Ind), naphthalene (Nap), biphenyl (Bph), diphenyl ether (DphE), fluorene (Fle), phenanthrene (Phe), anthracene (Ant), fluoranthene (Fla) and pyrene (Pyr) were provided from Acros Organics (Geel, Belgium).

All the solvent used in the work were provided by Fisher Scientific (Loughborough, Leicestershire, UK):

- Dicloromethane;
- 2-propanol;
- n-hexane (n-Hex) – dielectric constant = 1.9;
- Toluene (Tol) – dielectric constant = 2.4;

- Methanol (MeOH) – dielectric constant = 32.7;
- Acetonitrile;
- Diethyl ether;
- Trichlorotrifluoroethane (3Cl-3F-eth) – dielectric constant = 2.4;
- Ethyl acetate (EtAc) – dielectric constant = 6.0.

1.2.2 UV spectroscopy

Stock standard solutions (1 mg/ml) in dichloromethane (HPLC gradient grade from Fisher Scientific, Loughborough, Leicestershire, UK) were prepared for all PAFs and used for further dilutions in 2-propanol (HPLC gradient grade from Fisher Scientific, Loughborough, Leicestershire, UK). Phenol mother solution at 1 mg/ml was prepared directly in 2-propanol.

The UV/VIS spectra of the tar samples recovered according to the technical specification UNI CEN/TS 15439:2008, as well as those of the standard tar compounds, were recorded in a UV/VIS Spectrometer (UV4000 TECHCOMP) equipped with deuterium and tungsten lamps, at the wavelength range of 200-500 nm. Measurements were performed using a standard 1 cm x 1 cm quartz cell, using 2-propanol as reference cell.

All the samples available were used in this study, including those in which the tar concentration was adversely affected because of problem experienced during the sampling procedure (the results of these samples were not shown in Chapter 4).

In addition to the samples obtained from the gasification tests carried out in the laboratory of the University of Teramo, 12 samples were obtained from the "Instituto de Carboquimica" (CSIC, Zaragoza, Spain) and 3 from the Research Center ENEA Trisaia (Italy).

The samples and the standard solutions were diluted in 2-propanol in adapted concentration to obtain absorbances below 1.5 AU in the 235-300 nm region.

The resulted spectra were imported as data files in Excel to allow the mathematical data treatment using the solver function. An example of sheet is given in Annexe I. The parameters of the solver were set as follows:

- All the concentration are ≥ 0
- indene $\leq$ toluene

- naphthalene ≥1
- fluoranthene ≥1
- The maximal absorbance value of reconstituted spectrum ≤ the maximal absorbance value of measured spectrum over the all wavelength range 200-230 nm

1.2.3 Thin layer chromatography

The stationary phases tested in the present work are the followings:

- HPTLC Nano-SIL 20 glass plates 10x10 cm (Macherey-Nagel GmbH & Co. KG, Düren Germany);
- HPTLC Silica gel 60 glass plates 20x10 cm (Merck KGaA, Darmstadt, Germany);
- HPTLC Silica gel 60 NH_2 glass plates 20x10 cm (Merck KGaA, Darmstadt, Germany);
- HPTLC Silica gel 60 DIOL F_{254}s glass plates 10x10 cm (Merck KGaA, Darmstadt, Germany);
- Pre-coated glass plates RP-18, F_{254} for Nano TLC 10x10 cm (Macherey-Nagel GmbH & Co. KG, Düren Germany);
- HPTLC glass plates RP-18 W 20x10 cm (Merck KGaA, Darmstadt, Germany);
- HPTLC Silica gel 60 RP-18 with concentrating zone (20 x 2.5 cm) 20x10 glass plates (Merck KGaA, Darmstadt, Germany).

The plates 20x10 cm were cut at 10x10 cm by means of SmartCUT plate cutter from CAMAG (Muttenz, Switzerland). Additional information concerning the plates used are reported in the "Annex II: Characteristics of the HPTLC plates".

Before the measurements, each plate used was pre-washed with acetonitrile and air-dried at room temperature.

The equipment used for the HPTLC measurements were all provided from CAMAG (Muttenz, Switzerland). The schema of the analysis is reported in Figure 1 and consists of:

- semi-automatic sample application for qualitative and quantitative analyses performed by a Linomat 5 autosampler. The instrument is

suitable for medium sample throughput, and take the advantage of automatic sample application as narrow bands using the spray-on technique. Changing of sample (cleaning, filling and replacing the microsyringe) is performed manually.

- Developing in horizontal chamber 10x10 cm (Figure 2), which minimize the amount of solvent to be used: 2 ml of solvent were used for each migration step;
- Air-drying step of the developed plate at room temperature;
- Scanning of the HPTLC plate carried out by Camag TLC Scanner 3 (Slit length = 3 mm; slit width = 0.3mm) in UV/VIS absorption and/or Fluorescence spectroscopy. Data were registered using WinCAT software version 1.3.4 incorporating track optimization position.

Semi-automatic autosampler | *Horizontal developing chamber (10x10 cm)* | *TLC plates scanner: UV/VIS and Fluorescence* | *Data analysis software*

Figure 1: Schema of the instrument used for HPTLC/UV/FL tar analyses

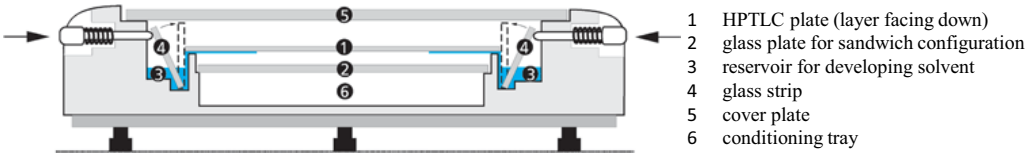

Figure 2: Sketch of the CAMAG Horizontal developing chamber

After the insertion of the plate in the chamber, and before each the developing start, the chamber was saturated with mobile phase vapor for 2 minutes.

Samples recovered in 2-propanol according to the technical specification UNI CEN/TS 15439:2008 were used in this study; to achieve the best separation of the

hydrocarbons families, different combinations of HPTLC plates and solvents have been tested, as reported in Table 1. Data regarding the quantity of the standard and the volume of the analyzed samples spotted on the plates are also provided in this section (Table 1).

Table 1: Condition of the most significant test carried out in HPTLC/UV/FL

	Stationary phase	Mobile phase	mm*	Sample	µl	Standard	µl	µg
(a)	Pre-coated plate RP-18, F_{254} for nano TLC	n-Hex	90	1-I 1-IV 2-I 2-IV	10 10 10 10	Bph Phe Fla Pyr Ant	5.0 2.0 2.0 0.5 2.0	5.0 2.0 2.0 0.5 5.0
(b)	HPTLC Nano-SIL 20 glass plate	n-Hex	90	1-I 1-II 2-I	10 10 10	Phe Fla Pyr Ant Fle DBA Bph	2.0 2.0 2.0 0.5 5.0 2.0 5.0	2.0 2.0 2.0 0.5 5.0 2.0 5.0
(c)	Pre-coated plate RP-18, F_{254} for nano TLC	MeOH n-Hex:Tol 90/10 v/v n-Hex	30 50 90	1-I 1-II 2-I	10 10 10	Bph Phe Fla Pyr Ant DBA Fle	5.0 2.0 2.0 2.0 0.5 2.0 5.0	5.0 2.0 2.0 2.0 0.5 2.0 5.0
(d)	HPTLC Nano-SIL 20 glass plate	MeOH n-Hex:Tol 90/20 v/v n-Hex	30 50 90	4-I 4-II 4-III 2-I Std mix	10 10 10 10 10	Pyr Fla Phe Ant Nap	1.0 1.0 1.0 0.5 5.0	1.0 1.0 1.0 0.5 5.0
(e)	HPTLC Nano-SIL 20 glass plate	MeOH 3Cl-3F-eth n-Hex	20 50 90	2-I 2-VIII 3-I 3-IV 4-I	20 20 20 20 20	Bph Phe Pyr Chrys DBA	4.0 1.0 1.0 0.7 1.0	5.6 2.0 2.2 1.0 1.0
(f)	HPTLC Silica gel DIOL F_{254}s plate	MeOH n-Hex	30 90	2-IX 3-I 3-IV 4-I	20 20 20 20	Bph Phe Pyr Chrys DBA	5.0 4.0 4.0 2.0 2.0	5.0 2.0 2.0 1.0 1.0
(g)	HPTLC Silica gel 60 NH_2 plate	MeOH n-Hex	30 90	2-IX 3-I 3-IV 4-I	20 20 20 20	Bph Phe Pyr Chrys DBA	5.0 4.0 4.0 2.0 2.0	5.0 2.0 2.0 1.0 1.0
(h)	HPTLC Silica gel 60 NH_2 plate	MeOH n-Hex	30 90	4-I 3-II Std mix (2-I) Std mix (2-I)	20 20 20 40	Bph Phe Pyr Chrys DBA	5.0 4.0 4.0 2.0 2.0	5.0 2.0 2.0 1.0 1.0

				Std mix (2-I)	60			
(i)	HPTLC RP-18 Silica gel 60 with concentrating zone	EtAc:n-Hex 50/50 v/v n-Hex	30 90	Std mix (2-I) Std mix (3-II) 3-I 3-II 3-III	20 20 20 20	Phe Pyr Chrys DBA	4.0 4.0 2.0 2.0	0.5 0.5 0.5 0.5
(j)	HPTLC RP-18 Silica gel 60 with concentrating zone	EtAc:n-Hex 50/50 v/v n-Hex	30 90	Std mix (3-II) 3-II 3-III ENEA 2 ENEA 3	10 10 10 2 2	Phe Pyr Chrys DBA	4.0 4.0 2.0 2.0	0.5 0.5 0.5 0.5

*the migration distance is measured from the beginning of the plate

2. Determination of tar content by UV spectroscopy

2.1 Introduction

The application of UV spectroscopy for semi-quantitative tar analysis was investigated; the technique was chosen thanks to the capability to follow tars evolution after a simple dilution, in a fast and cost-effective ways.

The application of spectra deconvolution was also investigated. Mathematical data treatment, especially deconvolution approach for multicomponent mixture analysis has shown an interest in UV spectroscopy.

The interest of computing the UV spectrum is well described in a general review [Monakhova et al., 2010], and several application have been already explored; for example, Tourand et al. quantified PAHs in contaminated soils after solvent extraction by mathematical data treatment: registering the UV spectrum of the extract, its shape and intensity could be rebuilt combining the spectra of standards. Due to the limitation of the computing, only 6 compounds were used as references [Touraud et al., 1998].

Recently the deconvolution development was validated at low UV wavelengths (between 200 and 250 nm) to follow the quality of wastewater regarding mineral effluent [Tsoumanis et al., 2010]. Noteworthy, that the deconvolution was also used on HPLC analysis, in order to improve the quantification step on non-resolved chromatographic peaks using Diode array detector [Gaganis et al., 2003].

The deconvolution is generally focused to seek a solution to a “black mixture” problem, by resorting to an abstract mixture model through the superposition of unknown components with no assumptions about their molecular structure or type of spectra.

The chemometrics methods pioneered in spectral analysis by Lawton and Sylvestre [Lawton and Sylvestre, 1971] are targeted at making quantitative predictions about the concentrations and pure component spectra; in opposition to deconvolution, this approach will be called as “convolution” in the present work.

2.2 Results and discussion

2.2.1 Determination of tar by UV/VIS Spectroscopy - global approach

The choice of UV/VIS spectroscopy as analytical tool could be a useful technique as this instrumentation can be encountered easily in chemical laboratories. Other global quantitative methods (like TOC) are also limited to water samples criticized to the restriction of the “tar protocol”. A rapid off-line evaluation or eventually on-line semi-quantitative analysis at a single wavelength should be an interesting tool to follow the process regarding to tar dew point.

As aromatic compounds could form clusters in solution that will influence the absorbance of the mixture (depending on the molecules and the concentration) and considering also the limitation of absorbance scale for the linearity of the Beer lambert’s law, it is necessary to ensure a reliable absorbance that should be a strict linear response depending on the dilution.

In Figure 3A are reported the spectra of the sample 3-III (gasification of almond shells with 10wt % Fe/olivine bed material) obtained at different dilution level from 1:10 up to 1:40.

Because of the complexity of tar samples, few qualitative information concerning tar composition could be obtained using this approach; nevertheless, when the absorbance recorded at several wavelengths, in the range of 220-300 nm was correlated with the dilution factor applied, a linear correlation was found for all the measured wavelengths, except in the case of 220 nm. This could be feasibly explained considering that in every dilution step investigated, at 220 nm the

absorbance value largely exceed 1.5 AU, which is considered the upper limit to work with (Figure 3B).

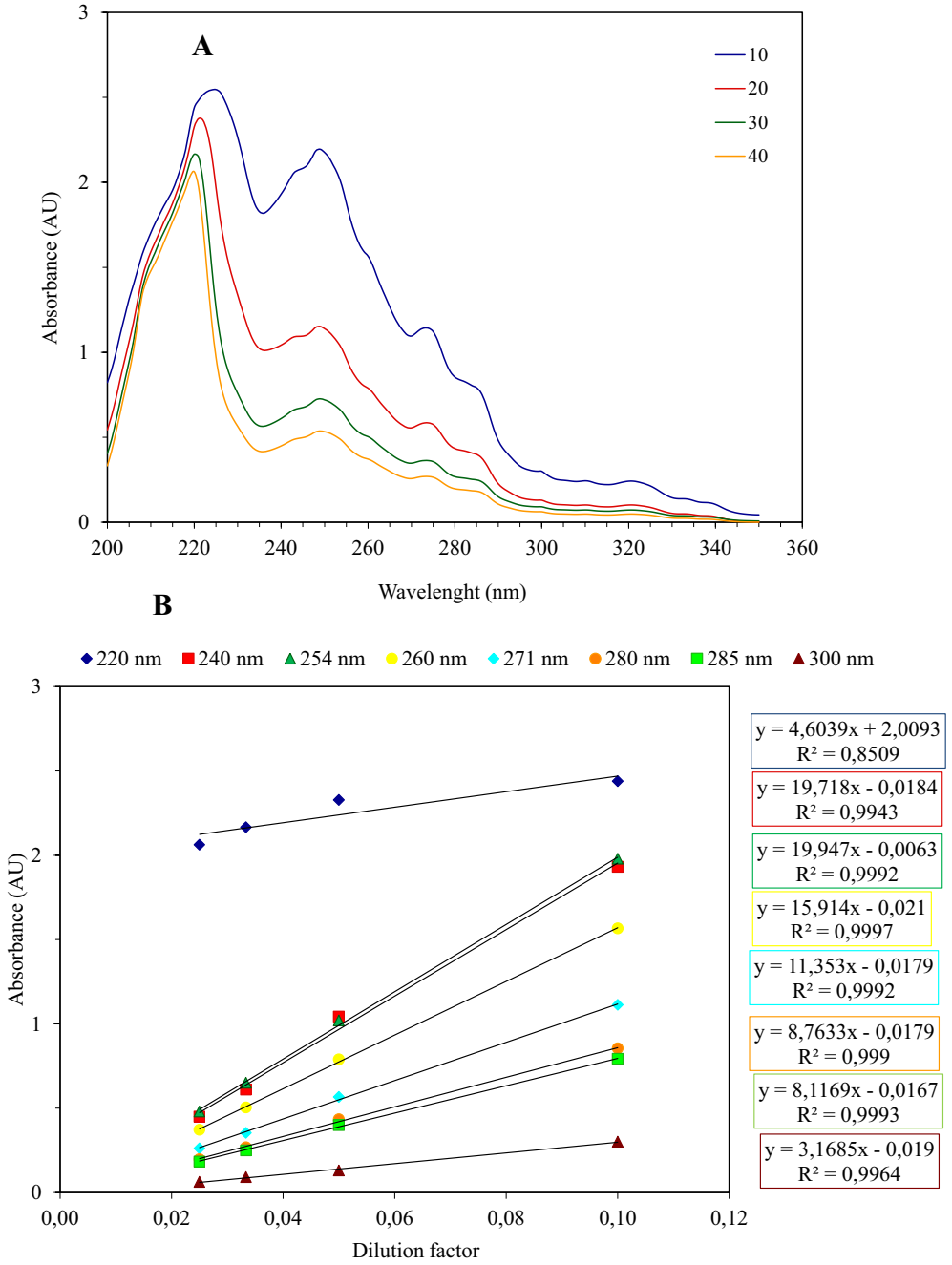

Figure 3: Absorbance spectrum of sample 3-III at different dilution level (1:10, 1:20, 1:30, 1:40) (A). Correlation between the dilution factor and the absorbance at different wavelength (B)

Thus, the spectra of all the samples were recorded, and the value of absorbances at different wavelength were examined to determine the tar content; it is important to

stress that concerning the absorbance peaks no significant differences regarding to the origin of the sample (our work, CSIC samples, ENEA samples) were found in the spectra registered: all the spectra were similar, showing the same shape. The only exception was a tar sample provided from Research Center ENEA Trisaia (Figure 9), which consisted of tar produced during updraft gasification of almond shells and therefore, it was not taken into account during the work. All the other samples analyzed came from fluidized bed gasifiers (CFB in case of CSIC) of different size and design.

To evaluate the choice of a single wavelength absorbance to obtain tar concentration, absorbance of a gasification sample was taken as reference (A_r) knowing its tar concentration (HPLC data). Then, the concentration of each sample was calculated by means of a proportion and for one selected sample, the concentration was calculated as follows:

$$C_s = \frac{C_r \cdot A_s}{A_r}$$

Where C_r and A_r are the concentration by HPLC/UV and the absorbance of the "reference sample" at a fixed wavelength, A_s is the absorbance measured for the sample "s" at the same wavelength, and C_s is its (hypothetically) unknown concentration.

An example of the results obtained is reported in Figure 4. In this case the reference sample used was that recovered from the gasification test 4-I (gasification of Miscanthus x giganteus at 800°C, with olivine bed).

As reported in Figure 4, a very good agreement between the chromatographic and the spectroscopic technique was found. The analysis of the linear regression shows that the slope is close to 1, consequently the UV spectra does not overestimate the total concentration of PAHs

For the five wavelength (254 nm, 260 nm, 271 nm, 280 nm and 285 nm) tested the results were similar, confirming that this is the optimal range of wavelength to take into account for the determination of tar content. The only two samples which show an effect of the wavelength chosen on the calculated concentration are the highest two in Figure 2B, which come from ENEA plant.

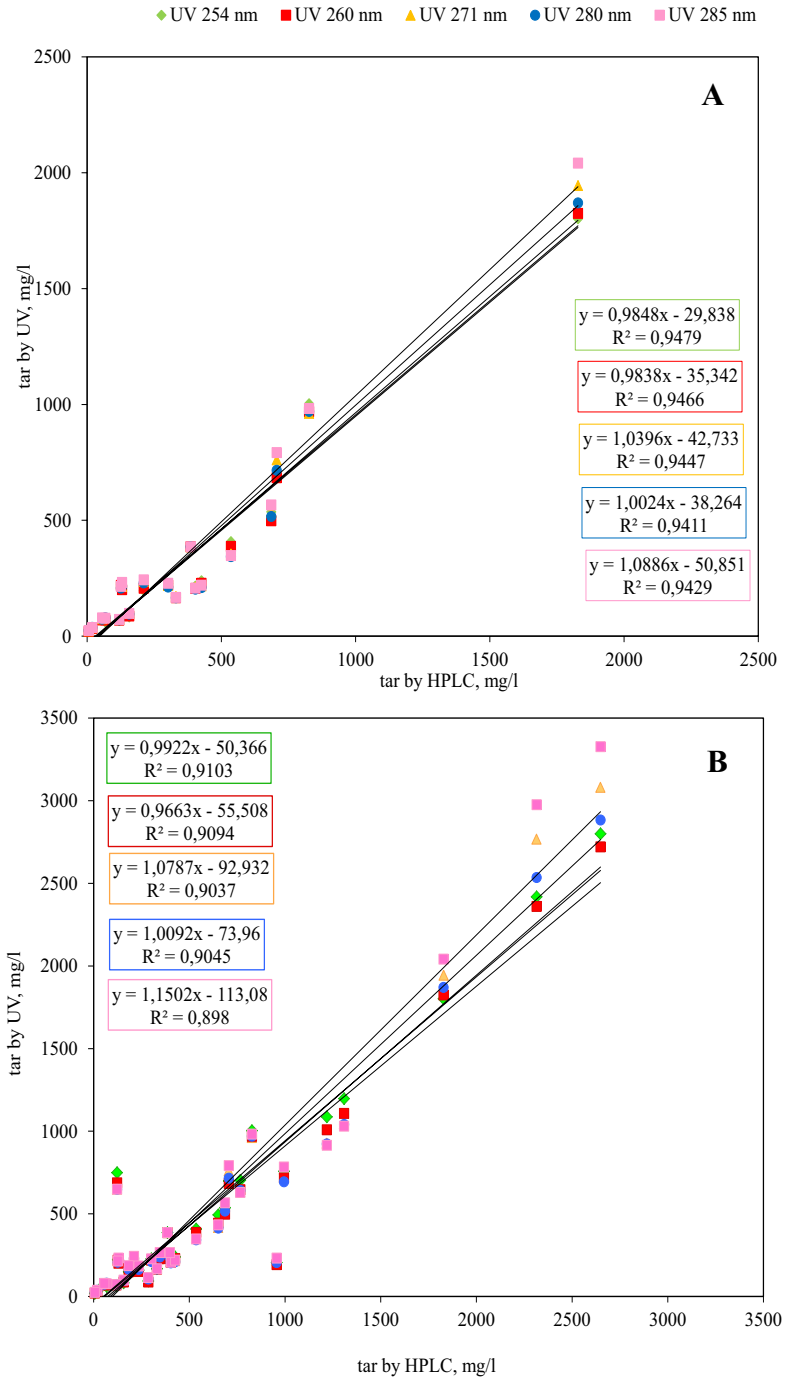

Figure 4: Correlation between the tar content measured by HPLC/UV and the one obtained by UV spectroscopy for Teramo gasification plant (A) and for 3 gasification plants – Teramo, CSIC, ENEA (B)

From the data shown (Figure 4), the best results were observed at 280 nm. A detail of the correlation obtained at this wavelength is reported in Figure 5. Inside 33 samples measured, just 2 were rejected (the points highlighted in red), because

in those cases the UV method was greatly overestimate/underestimate the tar content; actually, no explanation can be given for these samples.

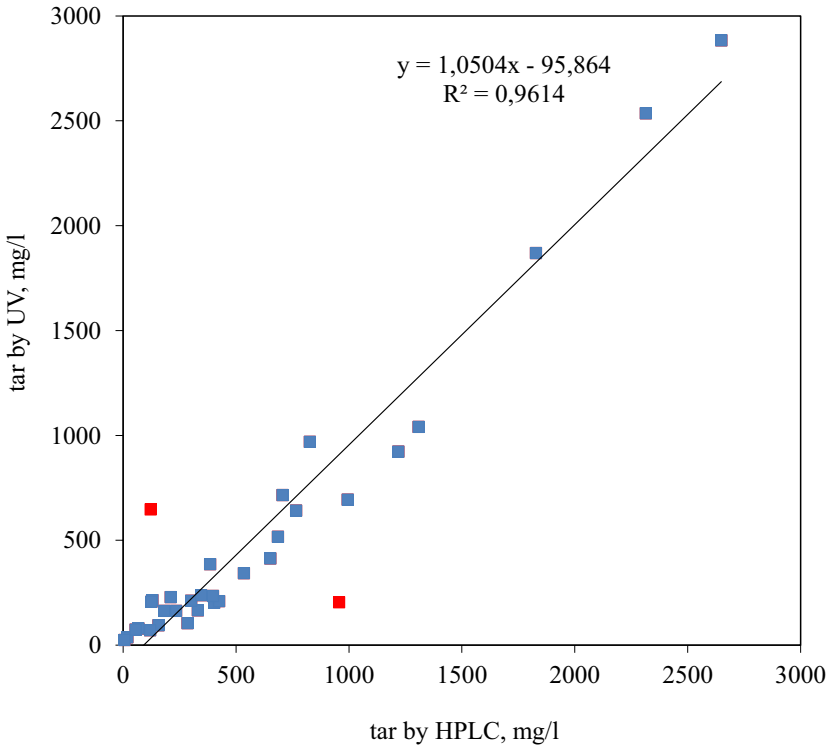

Figure 5: Correlation between the tar content measured by HPLC/UV and the one obtained by UV spectroscopy at A = 280 nm, for 3 gasification plants – Teramo, CSIC, ENEA

In addition to the evaluation of the impact of different wavelengths on the calculated tar content, all the samples available were tested as "reference sample", in order to check the effect of their nature on the results.

In the majority of the cases the data were absolutely comparable, and the slope of the linear regression was about 1. Nevertheless, it was observed that in the experiments in which the tar concentration in 2-propanol is very low, the tar content calculated by UV spectroscopy could be underestimate, an example of it, is given in Figure 6, where the "reference sample" is the test 3-IV (10wt % Fe/olivine + catalytic filter candle with "fixed bed" design). The tar content in 2-propanol for this test is 56 mg/l, against the 386 mg/l measured for test 4-I.

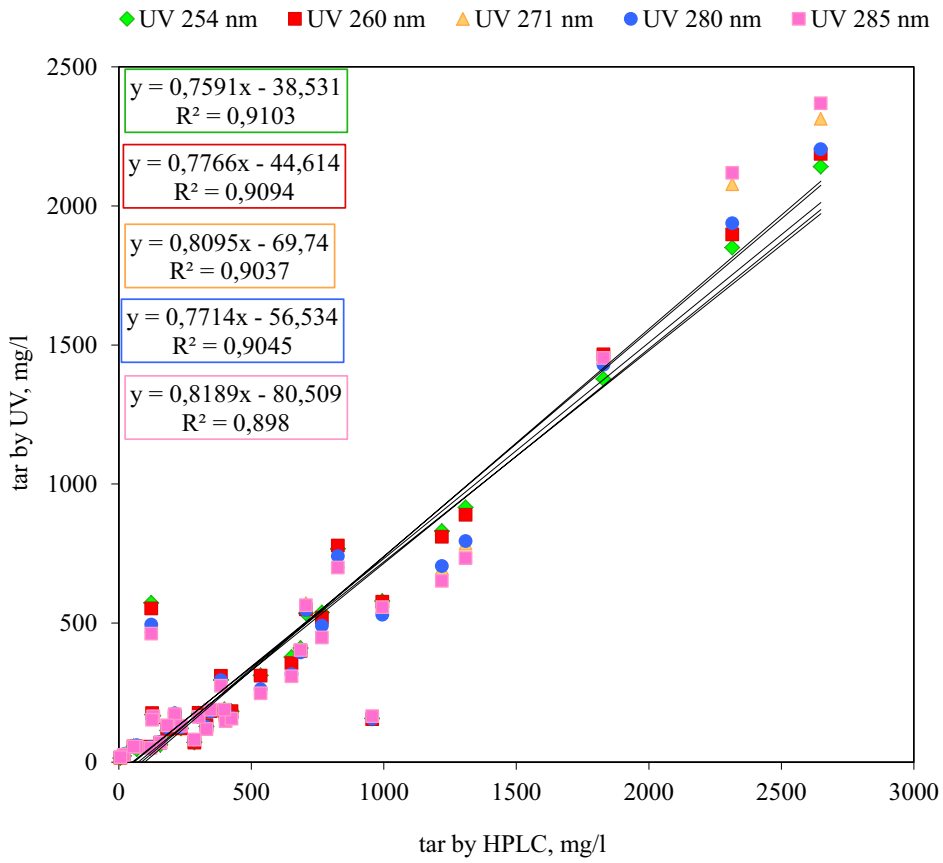

Figure 6: Correlation between the tar content measured by HPLC/UV and the one obtained by UV spectroscopy for 3 gasification plants – Teramo, CSIC, ENEA

2.2.2 Spectrum mathematical convolution

Thanks to the fruitful results obtained, it was decided to evaluate the application of mathematical data treatment for the determination of tar content in 2-propanol solutions obtained during tar sampling and containing the identified PAHs.

The exploitation of UV spectra is based on a multicomponent approach with the use of a convolution method. Any spectrum can be considered as a weighted sum of spectra of absorbing species in the linearity range of the Beer–Lambert's law. A classical least-squares algorithm is used for the calculation of spectra contribution with the study of the associated quadratic error (value and distribution). In practice, it can be assumed that the UV spectrum of an unknown sample can be depicted by using a linear combination of a small number of defined reference spectra related to either specific compounds of known mixtures

The total concentration of PAHs can be estimated as the product of the spectrum contribution coefficient by the corresponding concentrations. On the Figure 7, all the spectra of standards are presented in the concentration range they were recorded individually. In addition, the signal obtained for a real sample (experiment 1-III, orange-dotted line) diluted 100 times, is shown to display the general shape of the spectrum.

As it can be observed, the combination of standards can give the sample spectrum, adapting the reliable concentration as the additive Beer-Lambert's law allows it.

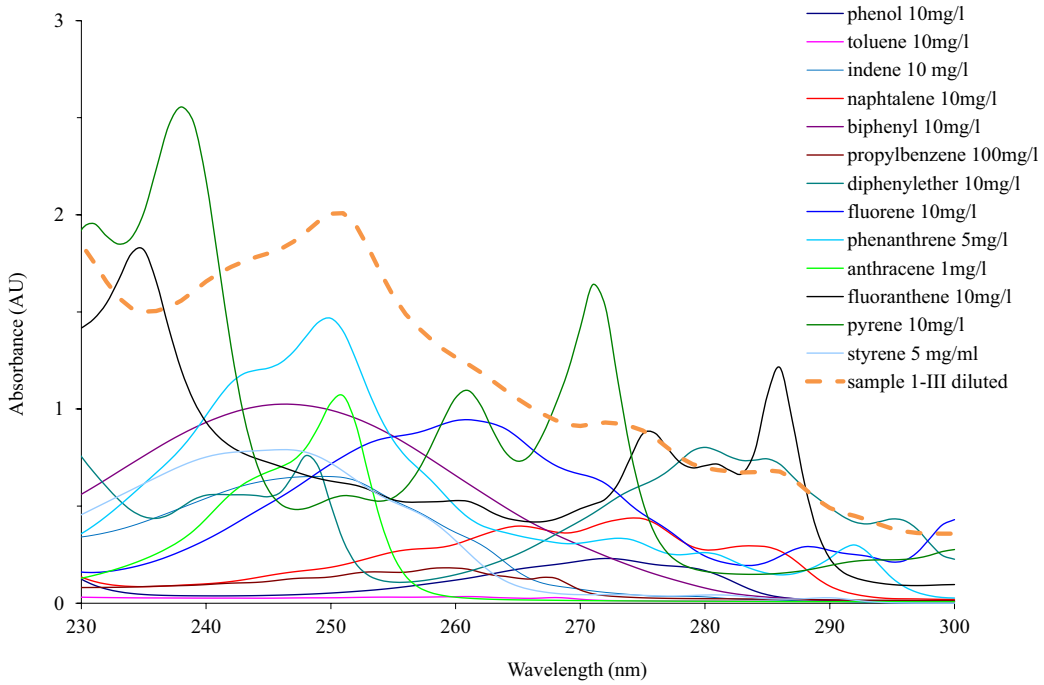

Figure 7: Spectrum of each standard of PAHs used in the convolution UV Tar spectrum

In practice, it can be assumed that the UV spectrum S_u of an unknown sample can be built by using a linear combination of a small number of defined reference spectra S_r related to either specific compounds :

$$S_u = \sum_{i=1}^{p} \alpha_i \, . \, S_{ri} \pm e$$

where αi and e are, respectively, the coefficient of the i^{th} reference spectrum and the restitution error.

The total quadratic error E_t is computed as follows:

$$E_t = \sum_{i=1}^{q} e(\lambda_i)^2$$

where *e* is the error value at the wavelength λ, defined as the difference between measured and restituted absorbances. The value and distribution of this quadratic criterion is useful to check the choice of the reference spectra and to minimize the error value.

Calculations were performed with Excel® using the solver function as described in Excel for Chemists [Billo, 2001]. As expected, the best fitted curves were obtained resolving the convolution in the range 236 – 300 nm because of the no specific absorption of aromatic molecules at lowest wavelength (200 – 235 nm). Moreover, as the tars are defined as the aromatic hydrocarbons higher than benzene and the main absorbance region of this compound is below 220 nm (Figure 8), the convolution in the range 236-300 nm allows a good approximation of tar content over 220 nm without interferences.

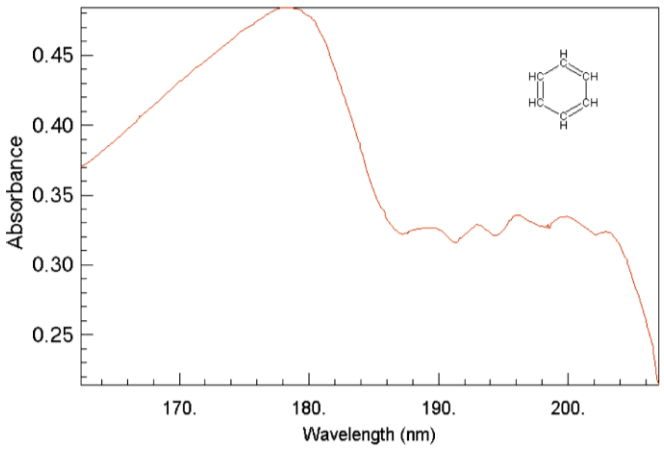

Figure 8: UV spectrum of benzene (NIST chemistry webbook: http://webbook.nist.gov/)

Figure 9 shows the comparison between the modeling and measured spectra. As the composition of the tar was established with chromatographic analysis (GC/MS and HPLC), the aromaticity of the compounds is between 1 and 4 rings with a variable condensed structure. However the molecules present in higher concentration will impose largely the UV absorbance below 300 nm, regarding to their molar absorption coefficient ε.

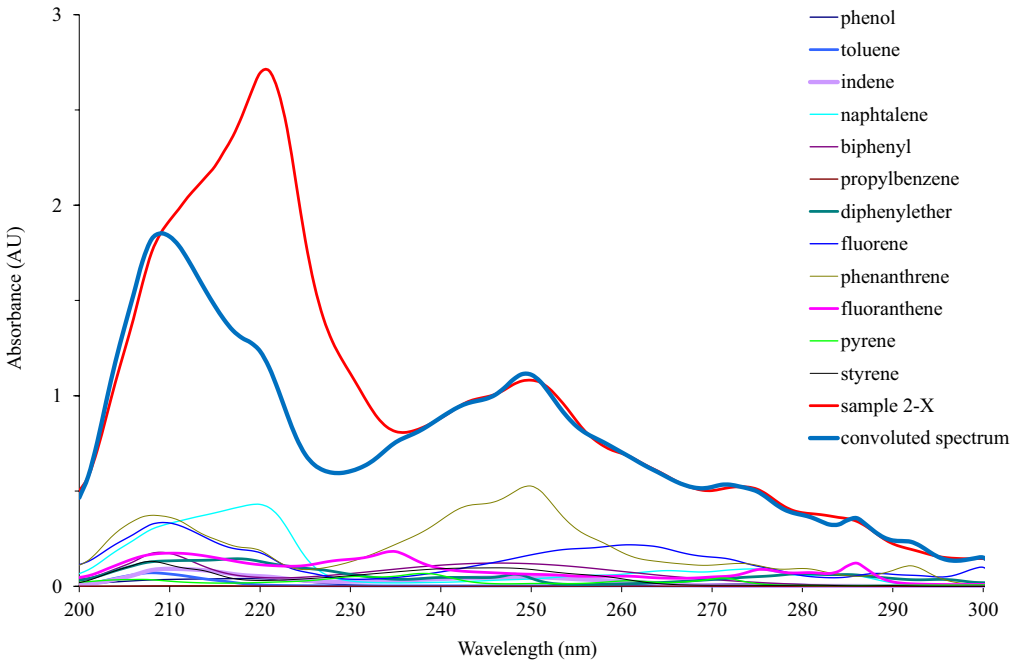

Figure 9: Example of the result of convolution of 12 standards for Tar UV spectrum restitution

The resulting evaluation of tar concentration on the gasification experiments shows a good agreement between UV convolution and the quantification obtained with the reference method, HPLC (Figure 10A).

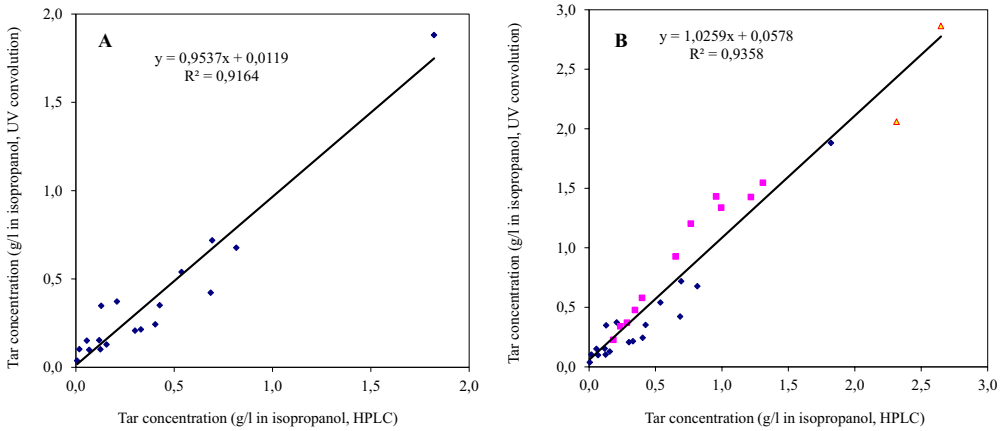

Figure 10: (**A**) study on the correlation for Teramo gasification plant (**B**) correlation combining 3 plants of gasification (Teramo ◆, Zaragoza ■, ENEA ▲)

The analysis of the regression is particularly interesting, as the slope is near 1 and the intercept is closed to 0: the convolution of UV spectra does not overestimate the total concentration of PAHs. The correlation coefficient of the linear regression allows to conclude on the relationship of the two methods. The analysis

of variance of the regression gives a significant value of F (>200). The hypothesis H_0 of the independence of the values x and y is rejected. Then we can conclude on a relationship between results determined by HPLC and those calculated by convolution.

In order to test the feasibility to apply convolution on Tar samples issued from other plants, but on the same gasification principle i.e. fluidized bed (Figure 10B) 12 samples were obtained from the "Instituto de Carboquimica" (CSIC, Zaragoza – Spain) and 3 from the Research Center ENEA Trisaia (Italy). The first sample of ENEA was not integrated in the correlation because of its origin: it was obtained on a fixed bed updraft gasifier and the UV spectrum was different (Figure 11), reflecting another distribution of tar. This was confirmed by HPLC analysis.

The results of regression confirm the correlation, as the linear regression equation and coefficient of correlation of the whole set of points are closed to those obtained only on Teramo samples (Figure 8A).

To be more significant, this work should be completed by other samples coming from several gasification plants. In any case, the UV profile gives good information on the PAHs distribution, and a changing in the spectrum should disabled the use of convolution with the set of aromatic standards.

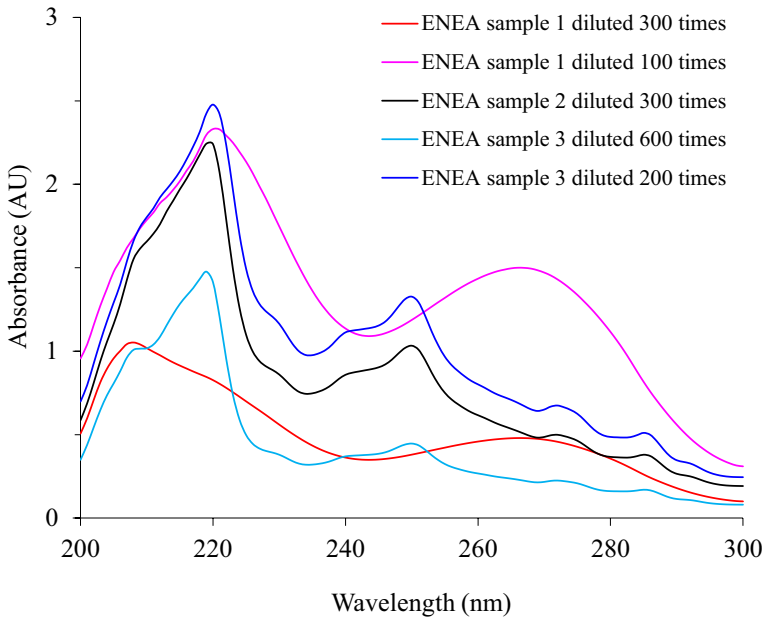

Figure 11: UV spectra of the samples coming from ENEA after dilution

As the global concentration of PAHs can be determined by spectrum convolution, the only restriction of the mathematical treatment lays on the worst individual correlation for the concentration of each aromatic molecule. An example of this is given in Table 2. The reason that could explain this limitation is linked to the fact that several spectrum of isolated compounds are partially, until completely overlapped (phenanthrene and anthracene, indene and biphenyl, naphthalene and fluorene …) so the contribution of each molecule cannot be distinguished with a good agreement. This study must be completed to check if less representative standard could be used to obtain a similar correlation, taking in account their zone of absorbance.

Table 2: Comparison of the concentration obtained by HPLC and UV deconvolution for each aromatic compound on the sample 2-I

Standard	HPLC determination (mg/l)	UV convolution (mg/l)
phenol	0.42	0.15
toluene	2.77	1.04
styrene	0.92	1.25
indene	1.84	0.96
naphthalene	2.11	1.00
biphenyl	0.09	1.14
DPE	0.25	0.73
fluorene	0.13	1.44
phenanthrene	0.17	0.01
anthracene	0.06	0.08
fluoranthene	0.16	0.96
pyrene	0.03	0.22
Total (diluted solution))	8.95	8.99
Total in isopropanol	537.2	539.5

However, even considering the limitation encountered during the work, UV spectroscopy appears as interesting option to adopt in order to provide a quantification of the tar fraction in gasification sample in a rapid and cost-effective way. Moreover the technique present the interesting prospective to be used as an on-line control method for gasification experiments, thanks to utilization of on-line UV intensity display module.

3. Analysis of tar by planar chromatography coupled with a detection by UV and fluorescence

3.1 Introduction

Chemical analyses have advances to identify extremely low concentrations of chemicals or toxicological substances of great potential hazard. In parallel with the technological advancements, the cost of analysis has increased dramatically. Therefore, economic efficiency can only be achieved by the application of adequate equipment and the well-calculated use of time and materials [Reimers et al., 2001]. Generally chromatographic methods are used to quantify PAHs, thanks to their selectivity and sensitivity. In this field, thin-layer chromatography (TLC) is a "blast from the past" technique thanks to the substantial progress made with automation and its suitability for a wide range of different uses. The TLC provides a very sensitive and flexible method for routine measurements and it has the capabilities for quick and reliable analyses of mixture of various substances. In comparison to HPLC and GC analyses. Larger number of samples can be examined at the same time and all the sample is studied even at the deposit point where irreversible adsorption could be observed on chromatographic column.

Moreover, TLC can be used as screening method for a quick overview of the composition of a contaminant.

TLC is a chromatography technique performed on a sheet of glass, plastic, or aluminum foil, which is coated with a thin layer of adsorbent material known as the stationary phase; after the sample has been applied on the plate, a solvent or solvent mixture (known as the mobile phase) is drawn up the plate via capillary action. Because different analytes ascend the TLC plate at different rates, separation is achieved.

TLC offers a greater variety of stationary phases than any other kind of chromatography to provide the required selectivity for a particular separation, including e.g. inorganic, organic, mechanical impregnated, polar and non-polar chemically bonded phase. Commercial precoated normal phase TLC and HPTLC (high performance thin-layer chromatography) plates containing silica gel, an organic binder, and a fluorescent indicator are most often used. Nevertheless,

reports of the use of bonded RP-18 (C-18) and diol, CN, and NH_2 layers are steadily increasing [Sherma et al., 2010].

Mobile phases are usually chosen after guided trial and error testing of reported solvent mixtures with appropriate strengths and optimum selectivities relative to the layer and the mixture to be separated [Sherma et al., 2010]; mobile phase controls selectivity determining relative retention and resolution.

Coupling the TLC/HPTLC with UV and fluorescence densitometry as detector offers the possibility of peak scanning. Furthermore, scanning of the complete sample allows the adsorption problems traditionally associated with column chromatographic methods to be avoided. An additional vantage is the simultaneous development of standards and samples, and the possibility of scanning the same sample under different conditions [Matt et al., 2003].

3.2 Separation of the aromatic families in biomass tar gasification samples

The main goal of this work was to develop an analytical method for tar characterization: the separation of tar molecules according their aromaticity (i.e. number of aromatic rings) by HPTLC could provide important information about the high molecular weight hydrocarbons (> 3 aromatic rings) in tar samples, which represent one of the major problems to deal with in biomass gasification.

HPTLC has the capability to separate even very heavy aromatics, without the drawback of column chromatography. Hence, it appears as a rapid and affordable technique for qualitative or quantitative analysis of biomass gasification tars. The most important results obtained in this field will be discussed in the present section.

3.2.1 Separation on normal and reversed phases

Preliminary studies were realized comparing the separation on normal and reversed stationary phase: thin layer chromatography offers less theoretical plates than liquid or gas chromatography, however the polarity of stationary phase could enhance the separation, The results obtained on Nano-SIL 20 plate and HPTLC RP-18 F_{254} plate for nano-TLC are shown in Figure 12 A. Standard and samples

were spotted at 15 mm in a 4mm length narrow band. The sample/standard used as well as their volume are reported in Table 1 (a) and (b)

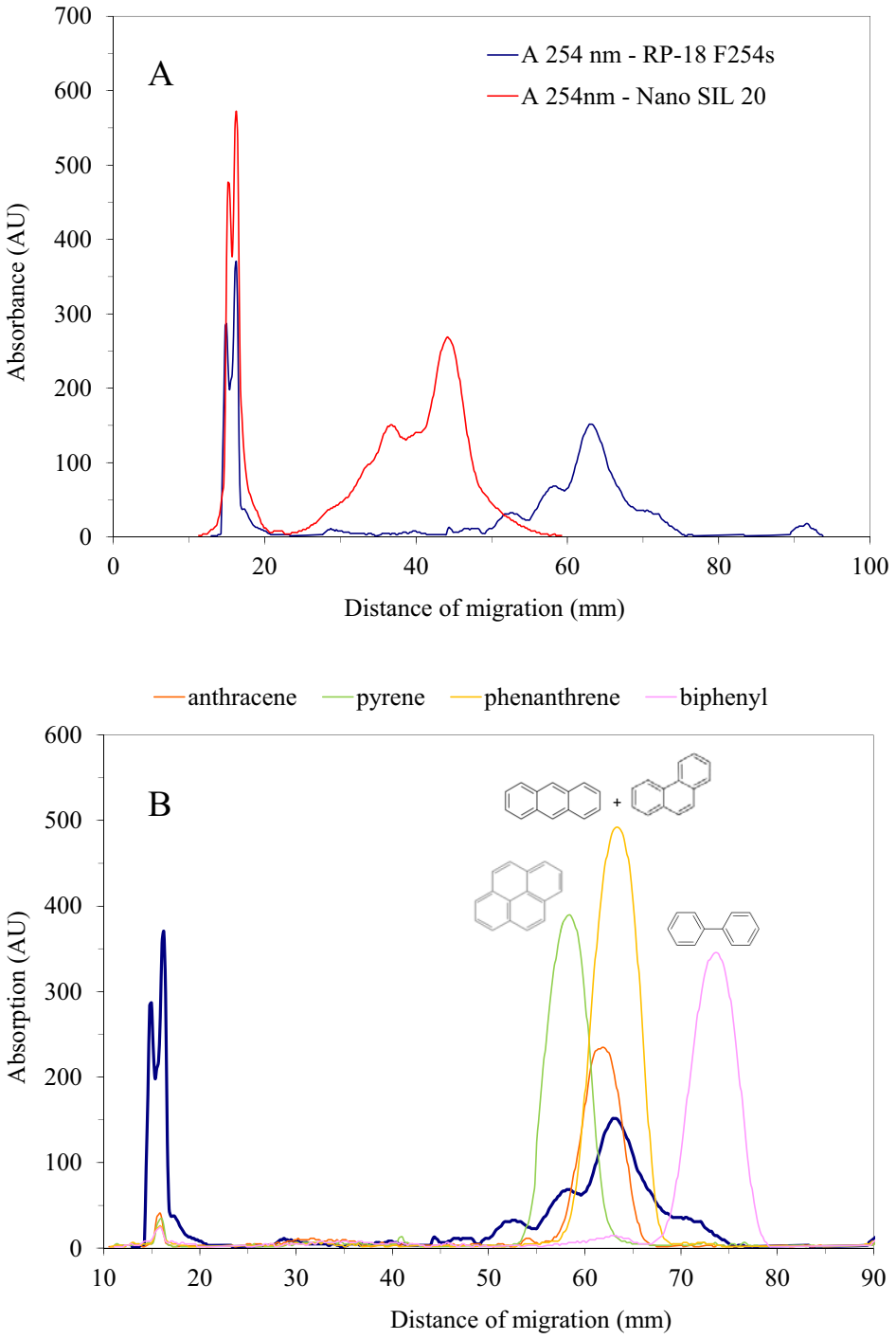

Figure 12: (**A**) Chromatogram of sample 2-I (steam gasification of almond shell with olivine bed inventory) of the HPLTC Nano-SIL 20 plate and of the RP-18 F_{254} plate for nano-TLC. (**B**) Chromatogram of sample 2-I and selected standards on RP-18 F_{254} plate for nano-TLC ; migration with n-hexane over 90 mm

The migration step was performed with n-hexane, until the solvent front reaches 90 mm of distance from the beginning of the plate, placed in the horizontal chamber described in material part. An example of the migration observed is reported in Figure 12, the chromatogram of sample 2-I is shown. The use of horizontal chamber limits the sample tracks broadening and merging. In fact, the common method of development in thin-layer chromatography employs capillary forces to transport the mobile phase through the layer. These weak forces arise from the decrease in free energy of the solvent as it enters the porous structure of the layer. For fine particle layers capillary forces are unable to generate sufficient flow to minimize the main sources of zone broadening [Poole, 2003], especially in case of traditional development in vertical tank, where the gravity adversely impact on the solvent migration.

As expected reverse phase C18 plates has a higher capability to separate PAHs when compared to normal silica gel plates. In fact, those plates are based on silica gel 60 modified with aliphatic hydrocarbons. The hydrocarbon chain length in combination with the degree of modification strongly affects retention of the molecules on the plate.

The retention factor, $R_{f,}$ is defined as the distance traveled by the compound divided by the distance traveled by the solvent.

Thus the larger an R_f of a compound, the larger the distance it travels on the TLC plate. The R_f found for biphenyl, phenanthrene, anthracene and pyrene standards on RP-18 plate were 0.82, 0.71, 0.69 and 0.65 respectively.

Nonetheless, RP-18 F_{254}s could not be scanned in fluorescence mode, because of the fluorescent indicator present on this kind of plate, which interferes with the PAHs signal.

In figure 13 are reported the chromatograms of the sample 2-I, obtained in detection by UV at different wavelengths: clearly the peaks in the chromatograms change according to the absorbance of the molecule. The presence of molecules that absorb at 366 nm means that heavy aromatics are detected in the sample. In fact, the ultraviolet absorption bands of PAHs is related to molecular structural features: when additional rings are fused in the benzene structure, its characteristic

bands shift to longer wavelength, depending on where the new aromatic ring is fused [Harvey, 1991].

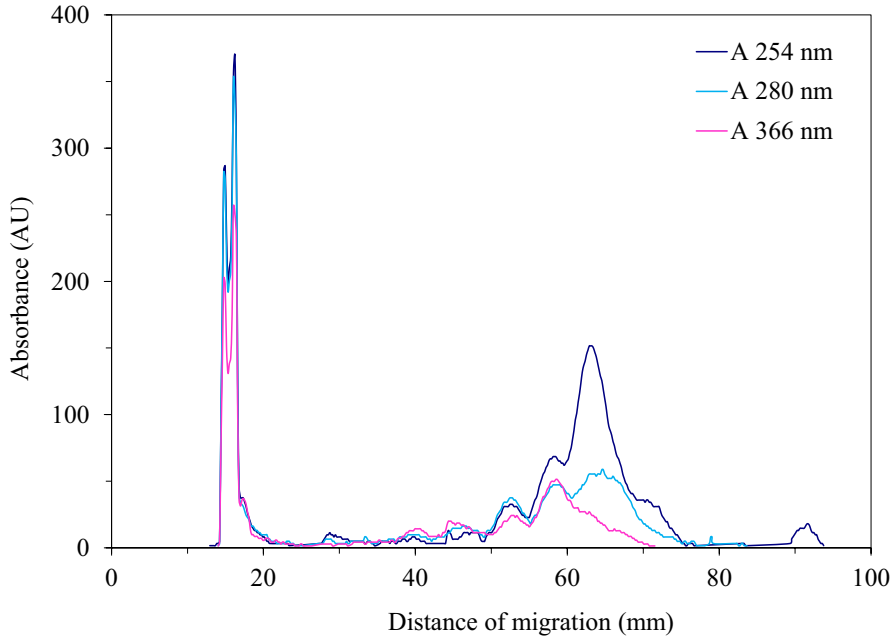

Figure 13: Chromatograms of sample 2-I (olivine) on RP-18 F_{254} plate for nano-TLC at different UV wavelength.

It is important to observe that for both the plates (Nano-SIL 20 and RP-18), when only n-hexane is used as phase mobile, a relevant peak is present in the spot position: these compounds that do not migrate with the solvent could be polar compounds, even of low molecular weight.

3.2.2 Optimization of the separation regarding to solvent sequence elution

In order to validate the polarity dependence of non-eluted peak, more polar solvent was used in the first step of elution. Thus, a three-stage elution with a decreasing polarity was tested (Table 1 – c): MeOH (30 mm), n-hexane:toluene 90:10 (50 mm) and n-hexane (90 mm) profile are reported in Figure 14. Even if it was possible to confirm the presence of polar compounds not identified by HPLC/UV, that move when methanol is used, no additional separation was achieved.

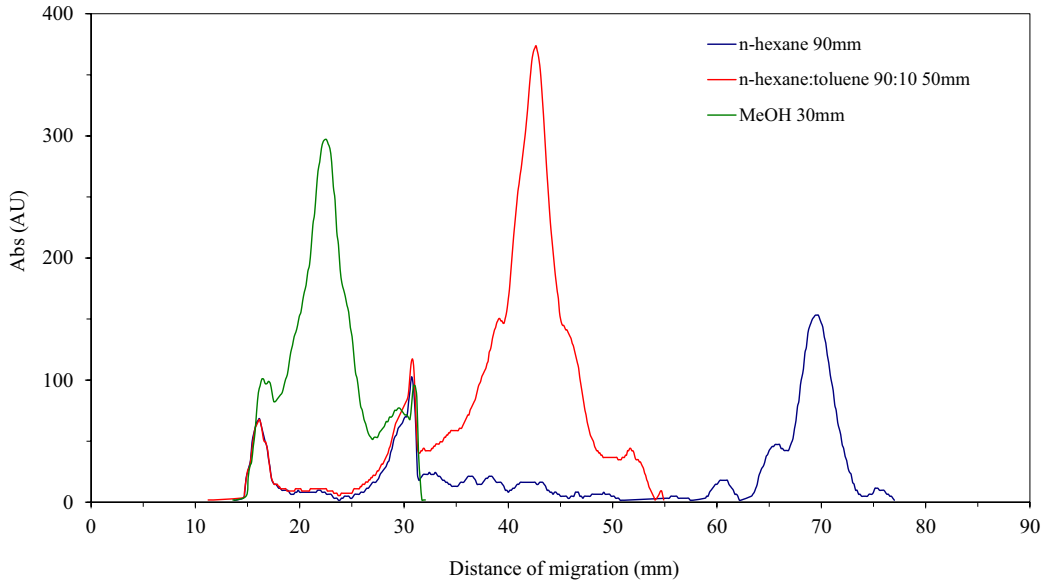

Figure 14: Chromatograms of sample 2-I (olivine) on RP-18 F_{254} plate for nano-TLC recorded at A = 254 nm after each steps of a three-stage elution with 1st MeOH over 30 mm,2nd n-Hex:Tol (90/10 V/V) over 50 mm and 3rd n-Hex over 90 mm

A similar gradient elution, with a slight modification in the second stage (n-hexane:toluene 90:20, 50 mm) was tested on the Nano-SIL 20 plate (Table 1 – d). Figure 15 shows the differences in the chromatograms of sample from tests 2-I (steam gasification of almond shell at about 800°C) and 4-I (steam gasification of MXG at 800°C).

HPTLC chromatogram shows compounds that differentiate the MXG tar from the almond shells tar. At 34 mm an unidentified peak is detected (Figure 15A). A peak at 32 mm is also detected. This peak, which is also present with a minor intensity in the chromatogram of sample 2-I, emits when excited at a fluorescence wavelength of 254 nm – emission measured over 400 nm (Figure 15B), which clearly corresponds to an aromatic compound of molecular weight higher than dibenzanthracene, which elute at 48 mm. In addition, fluorescence gives a better definition of the peaks thanks to an increased sensitivity.

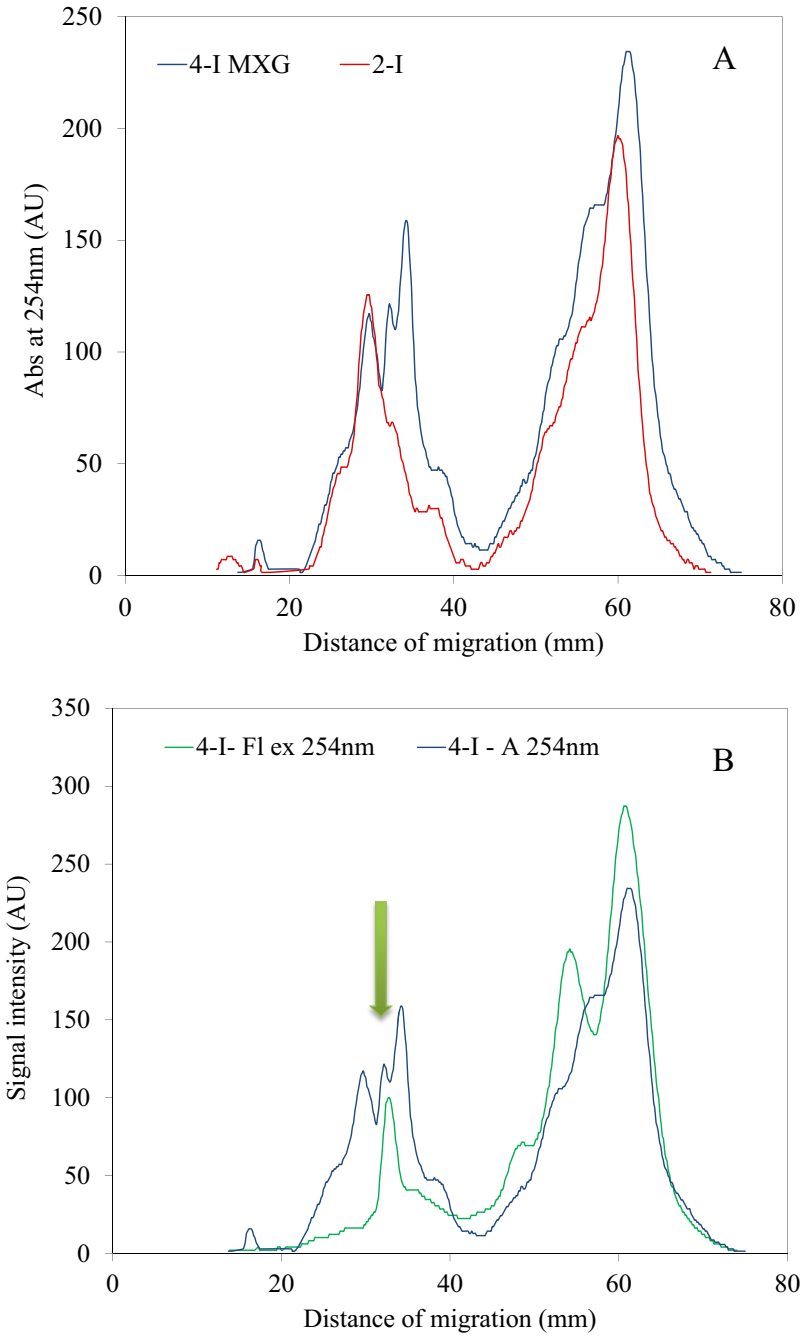

Figure 15: (**A**) Chromatograms of samples 2-I (almond shells, olivine, ≈ 800°C) and 4-I (MXG, olivine, 800°C) on HPLTC Nano-SIL 20 plate recorded at A = 254 nm.
(**B**) Chromatograms of sample 4-I on HPLTC Nano-SIL 20 plate in fluorescence and absorption mode.

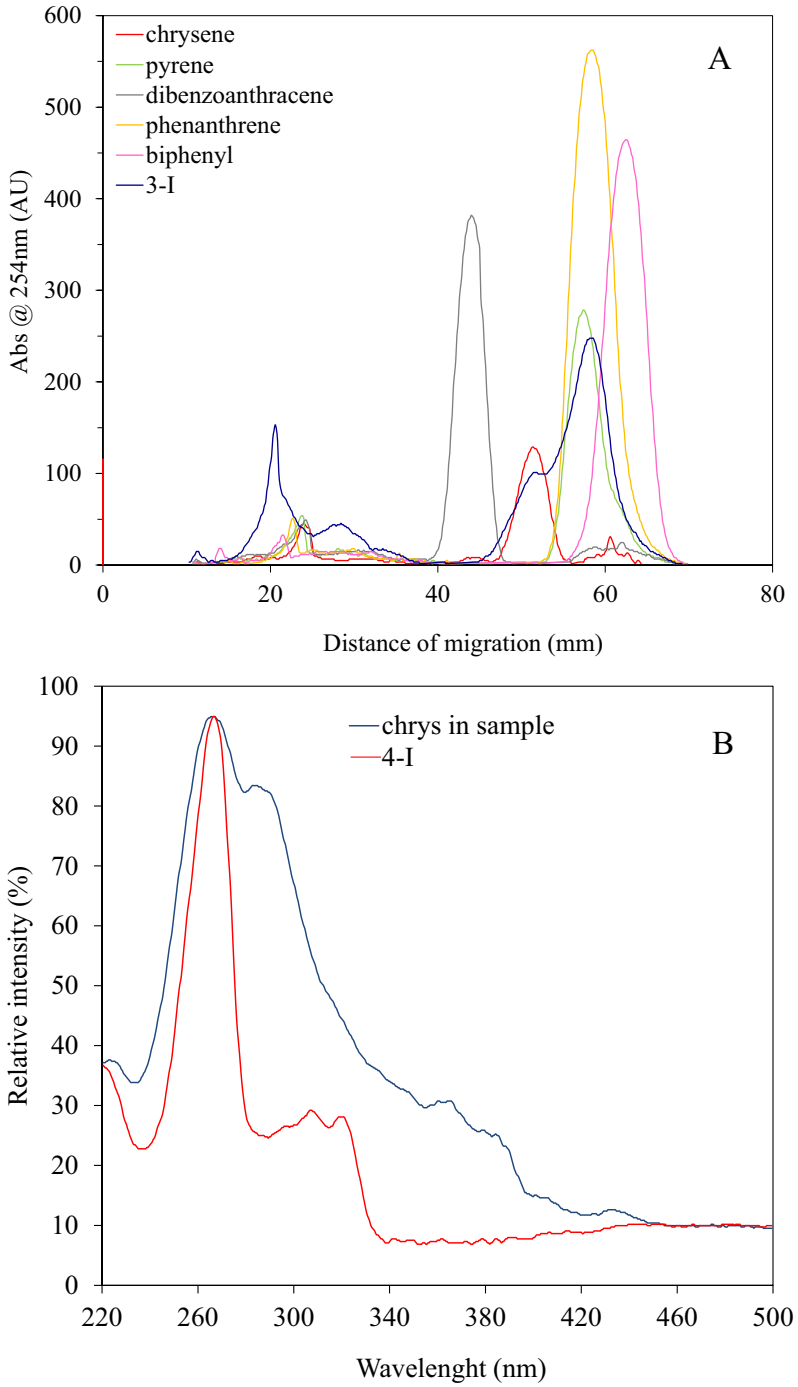

Figure 16: (**A**) Chromatograms of sample 3-I (Fe/olivine) and five selected standards on HPTLC Nano-SIL plate recorded at A = 254 nm with 3-Cl-3Fl-Eth in the second step of migration. (**B**) UV spectra of pure chrysene and the corresponding peak in the sample 4-I, eluted on the same plate (Table 1 – e).

In order to increase the separation of the known aromatic molecules into families according to the number of aromatic rings other mobile as well as stationary phases were tested. Hence, a further effort was the investigation of

trichlorotrifluoro ethane (3-Cl-3Fl-Eth), as well as diethyl ether in the second step of elution.

In both cases the results were not interesting. The use of 3-Cl-3Fl-Eth does not exert benefic effects on the separation as shown in Figure 16A: all the known molecules in sample 3-I (steam gasification of almond shells with olivine bed inventory) merge in the last peak of the chromatogram. The small and bad-resolved peak that elute at about 50 mm corresponds to the chrysene. The identification of this molecule in the sample was obtained thanks to HPTLC method, comparing the UV spectra of the unknown peak with the standard (Figure 16B). Moreover, the use of 3-Cl-3Fl-Eth and diethyl ether has been rapidly shelved, because the new solvents present the disadvantage of bad migration on the plates tested (Nano SIL 20, RP-18).

Considering the results of this tests, a new mobile phase was introduced as first step in a two-stage migration: ethyl acetate was chosen thanks to its higher polarity (dielectric constant = 6.0) and used diluted 50/50 v/v with n-Hexane in order to have a first step with intermediate polarity, but more polar that the 3Cl-3F-eth or the n-Hex/Tol mix (the results concerning the use of this mobile phase sequence will be shown in Sub-section 3.2.5).

3.2.3 Separation on NH_2-, and Diol-modified silica plates

NH_2-, and Diol-modified silica sorbents are less polar then the classical silica phases, therefore they are well suited to separate hydrophilic or charged substances. The amino modified silica NH_2 plates provide weak basic ion exchange characteristics, with special selectivity for charged compounds.

This kind of plates have an intermediate polarity between the conventional silica gel and the C18 plates, thus their effect in separation of complex mixtures of hydrocarbons, such as fluidized bed biomass tars, was investigated.

The samples/standards applied on the plates were eluted by means of a two-stage migration with methanol (30 mm) and then n-Hex (90 mm). An example of the results obtained is reported in Figure 17.

Diol-modified plates are not suitable for the purpose of this research activity; on the contrary, the NH_2-modified plates seems to be more interesting, as in a two-stages elution gives a resolution comparable to that observed in RP-18 plates

(Figure 18). R_f values of the standards investigated are: biphenyl 0.7, phenanthrene 0.61, pyrene 0.58, chrysene 0.48 and dibenzoanthracene 0.43.

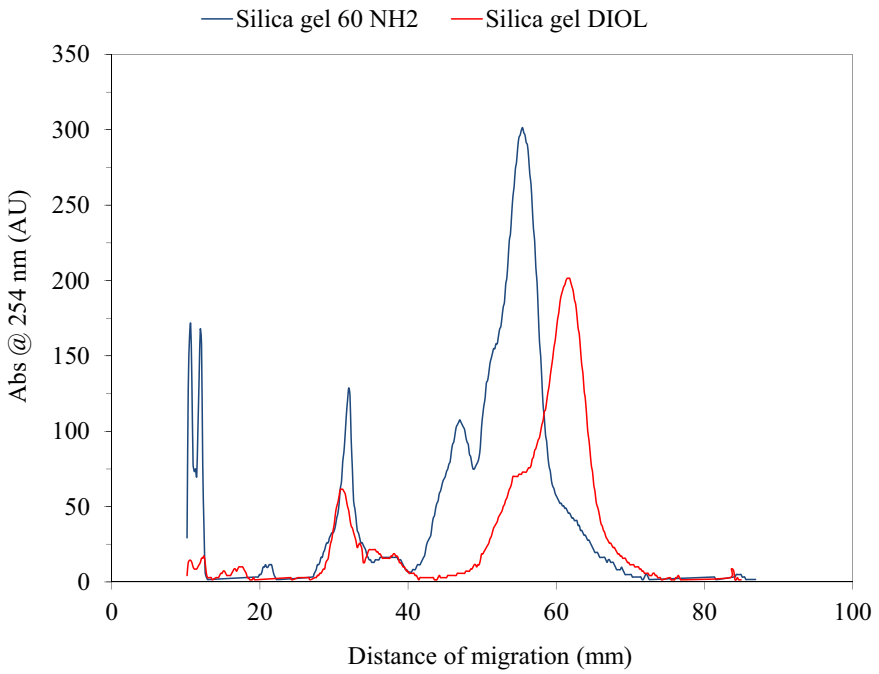

Figure 17: Chromatograms of sample 3-I (Fe/olivine) on HPLTC Silica gel DIOL F_{254}s and HPLTC Silica gel 60 NH_2 plates with a two-stage elution (1) MeOH, (2) n-Hex (Table 1 – f,g)

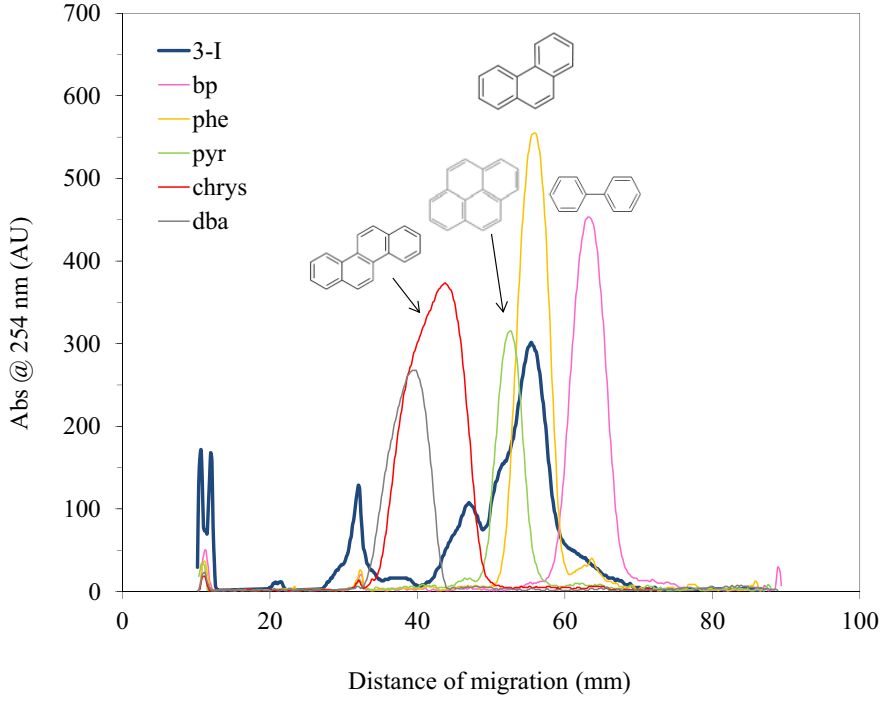

Figure 18: Chromatograms of sample 3-I (Fe/olivine) and five selected standards on HPLTC Silica gel 60 NH_2 plate recorded at A = 254 nm

3.2.4 Interest of reconstituted synthetic tar to optimize resolution on HPTLC plate with concentrating zone

To understand the samples migration and evaluate the capability of HPTLC to quantify tar content in the biomass gasification samples, synthetic tar solutions were prepared mixing PAHs standards according to the concentration measured by HPLC/UV for samples 2-I (olivine) and 3-II (Fe/olivine). In addition, chrysene (4-rings) and dibenzoanthracene (5-rings) were added in synthetic tar solution. The synthetic tar analyzed on HPTLC plates (figure 19) shows a signal intensity proportional to the amount of synthetic sample "std mix 2-I" spotted (chromatographic conditions in Table 1 – h). It can be assumed that this response will be a benefit for quantitative measurements.

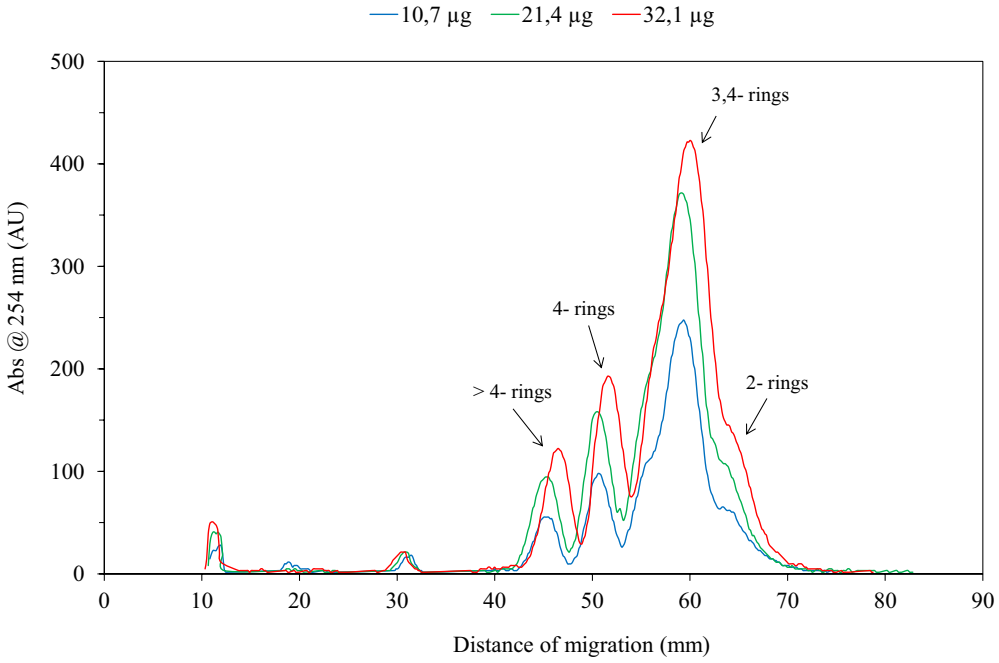

Figure 19: HPTLC UV response with increasing amount of standard mixture Chromatograms of std mix 2-I applied in growing amount, HPLTC Silica gel 60 NH_2 plate

3.2.5 Separation on HPLTC RP-18 silica plates with concentrating zone plates

HPLTC RP-18 silica plates with concentrating zone were also tested. Concentrating zone plates allow for easy application of large volumes of diluted samples offering:

- Highly facilitated sample loading

- Better resolution due to uniform sharp bands
- Includes a purification, sample preparation step

Merck's concentrating zone plates are based on different adsorption properties of two silica sorbents: a large pore concentrating sorbent where the samples are applied, and a selective separation layer for the separation. Independent of shape, size or position of the spots the sample always concentrates within minutes as narrow band at the interface of the two adsorbents where the separation starts. The RP-18 silica plates with concentrating zone are especially suited for the high-resolution separation of polycyclic aromatic hydrocarbons (PAH) [Merck ChromBook 2008/09].

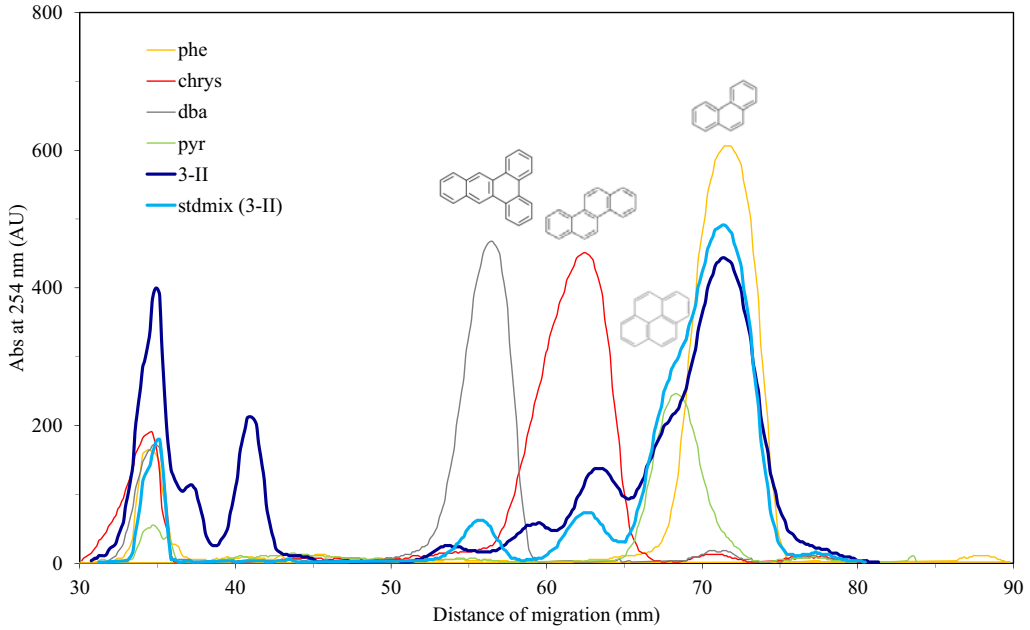

Figure 20: Chromatograms of sample 3-II (Fe/olivine), of the synthetic tar mix "std mix" 3-II, and four selected standards on HPLTC Silica gel 60 RP-18 with concentrating zone plate recorded at λ = 254 nm (Table 1 – i)

Thus, samples and standards were spotted on the concentrating zone of the RP-18 plate, and the migration step was carried out using ethyl acetate/n-hexane (50/50 v/v) over 35 mm and n-hexane since the solvent reaches 90 mm of distance (Table 1 – i). Preliminary results obtained with this new stationary phase/mobile phase combination is reported in Figure 20: a slight separation between 3-aromatic and the condensed 4-aromatic pyrene is observed. Furthermore, the separation of the

main non-resolved peak and the peak corresponding to linear 4-aromatics structures, such as chrysene, is increased.

3.2.6 Influence of temperature on resolution according aromaticity

Separations by planar chromatography are normally carried out at room temperature. However, since decades the effect of temperature on TLC analysis was investigated [Abbott et al., 1964; Issaq et al., 1979; Reimers et al., 2001]. In certain cases it may be necessary to develop the plate at lower or higher temperatures than room temperature (20°C) in order to achieve a separation.

It has been shown that lower temperatures affect the separation of compounds by TLC. Abbott et al. studied the effect of temperature (+40 °C to -20°C) on development times and R_f values of 12 chlorinated pesticides. They found that the migration rates of all compounds studied were temperature dependent. Separation was least effective at -20°C. Abbott et al. also observed that development of the plates at low temperatures was not only faster but also that more compact spots were obtained, which resulted in better resolution [Abbott et al., 1964].

Recently, Reimers et al. described the semi-quantitative determination of a mixture of heavy PAHs in soil samples on reverse phase plate using n-hexane, n-hexane/methyl tert-butyl ether 8/2 v/v, acetonitrile/dichloromethane/water 9/1/1 v/v/v at – 20°C [Reimers et al., 2001].

Thus, three tests were carried out using the same conditions of Figure 20 (conditions in Table 1 –i and j), but at – 23°C, placing the developing chamber as well as the solvents used in the freezer at least half an hour before the analysis. The data measured show that when the "cold-chain" is well adopted a significant increased separation is achieved. The results are shown in Figure 21. The R_f measured in this experiments were in good agreement during two tests, in which the "cold chain" was respected. The R_f of the standard used at -23 °C, as well as the data obtained at room temperature are reported in Table 3

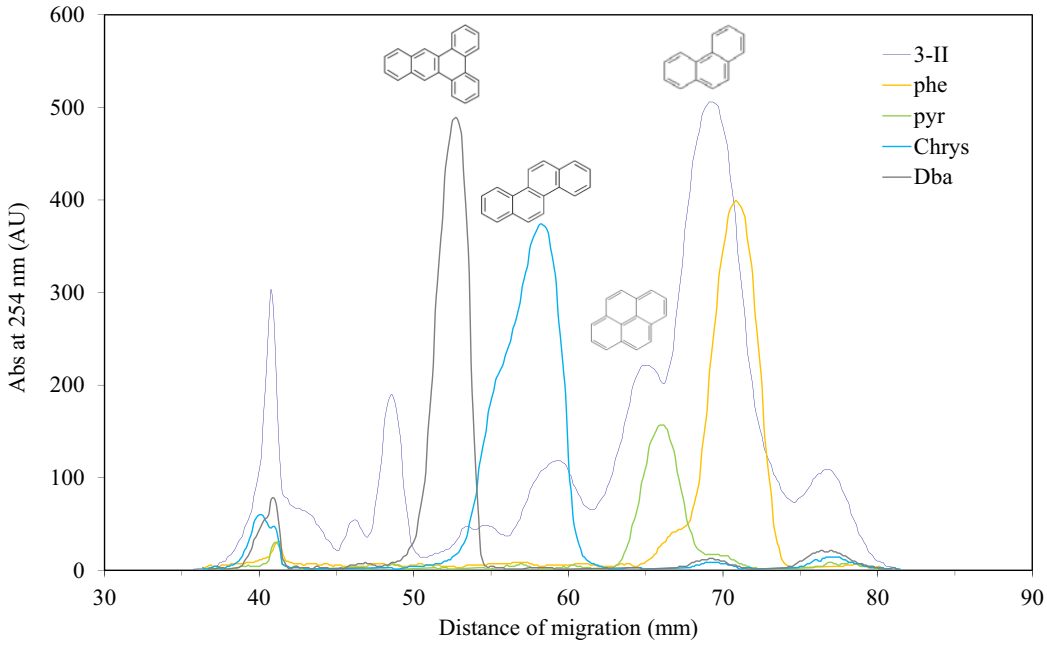

Figure 21: Chromatograms of sample 3-II (Fe/olivine) and four selected standards on HPLTC Silica gel 60 RP-18 with concentrating zone plate (migration at -23°C), recorded at λ= 254 nm (table 1 –j)

Table 3: Retention factor measured for the HPTLC RP-18 Silica gel 60 plate when the migration step was carried out at room temperature of at -23 °C.

	Rf at 20°C	**Rf at -23 °C**
Stationary phase	*HPTLC RP-18 Silica gel 60 with concentrating zone*	*HPTLC RP-18 Silica gel 60 with concentrating zone*
Mobile phase	*EtAc:n-Hex 50/50 v/v (35mm) n-Hex (90mm)*	*EtAc:n-Hex 50/50 v/v (35mm) n-Hex (90mm)*
Phe	0.79	0.79
Pyr	0.76	0.73
Chrys	0.69	0.64
DBA	0.62	0.58

In Figure 22, is reported the comparison between the chromatograms of different samples eluted on the HPTLC RP-18 Silica gel 60 with concentrating zone with the mobile phase reported in table 3, at -23°C . It should be stressed that during this analyses it was no more possible to use MXG gasification tar as well as older almond shells tar samples, due to their ageing. As expected, no significant differences were found between sample 3-II and the sample 2 provided from Research Center ENEA Trisaia, as both these samples are the results of almond shells gasification by means of Fe/olivine catalyst. The major difference is represented by their concentration in the 2-propanol solution, which is clearly higher for the ENEA tar sample, especially considering that the volume of the

sample spotted on the plate was 5 times less than the volume of Fe/olivine sample from Teramo gasifier.

The sample 3-IV (gasification of almond shells with Fe/olivine + catalytically activated filter candle with "fixed bed" design) shows a very low concentration of heavy aromatics, as further demonstration of the goodness of this catalytic process.

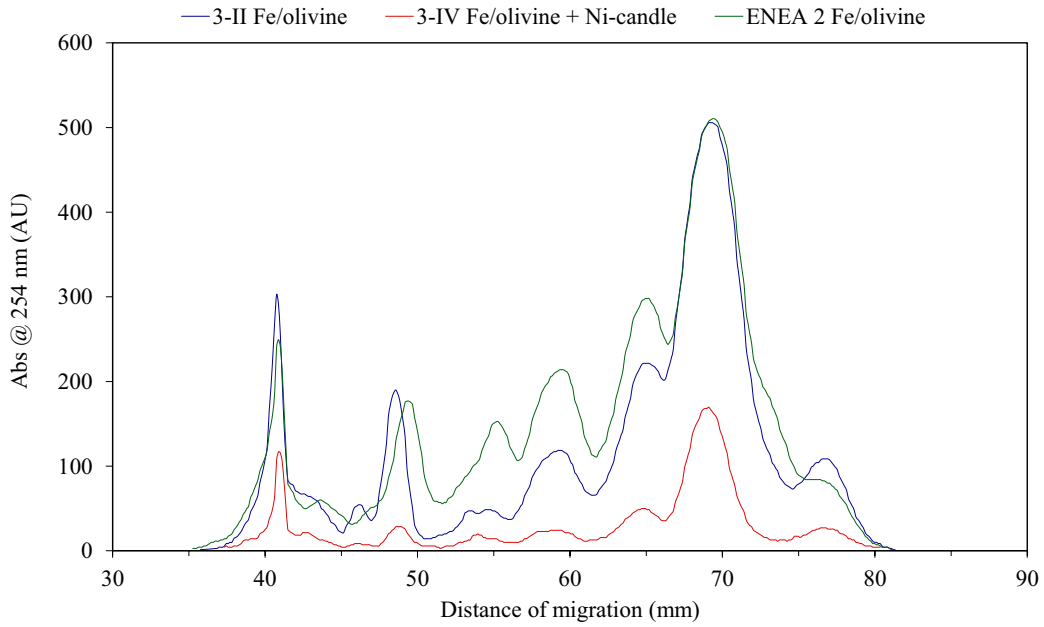

Figure 22: Chromatograms of sample 3-II (Fe/olivine), 3-IV (Fe/olivine + Ni-candle) and sample 2 from ENEA on HPLTC Silica gel 60 RP-18 with concentrating zone plate (migration at -23°C), recorded at λ = 254 nm (table 1 –j)

In order to get additional information concerning the unknown peaks (Figure 22), the plate was detected at different wavelength in UV absorption and Fluorescence emission mode. The most relevant results are showed in Figure 23.

In Figure 23A is reported the comparison between the detection at 254 nm and 283 nm (which corresponds to the maximum absorption band of DBA) for sample 3-II (Fe/olivine): increasing the wavelength then just the high molecular weight HAPs will absorb. Comparing the data measured for the real sample with those recorded for the synthetic tar sample, it was possible to confirm that the dibenzoanthracene is not present in gasification tars.

The unknown peak B at about 48 mm in Figure 23A and at about 42 mm in Figure 20 do not absorb at 283 nm. Also this peak has no fluorescence emission when exited at 254 nm or 283 nm.

The spectrum of the B peak was recorded, and a maximum was observed at 260 nm, suggesting that this molecule(s) could be light aromatic polar compound. By Unfortunately, as the RP-18 plate with concentrating zone interferes in the spectrum at wavelength upper than 300 nm, it was not possible to have additional detailed information.

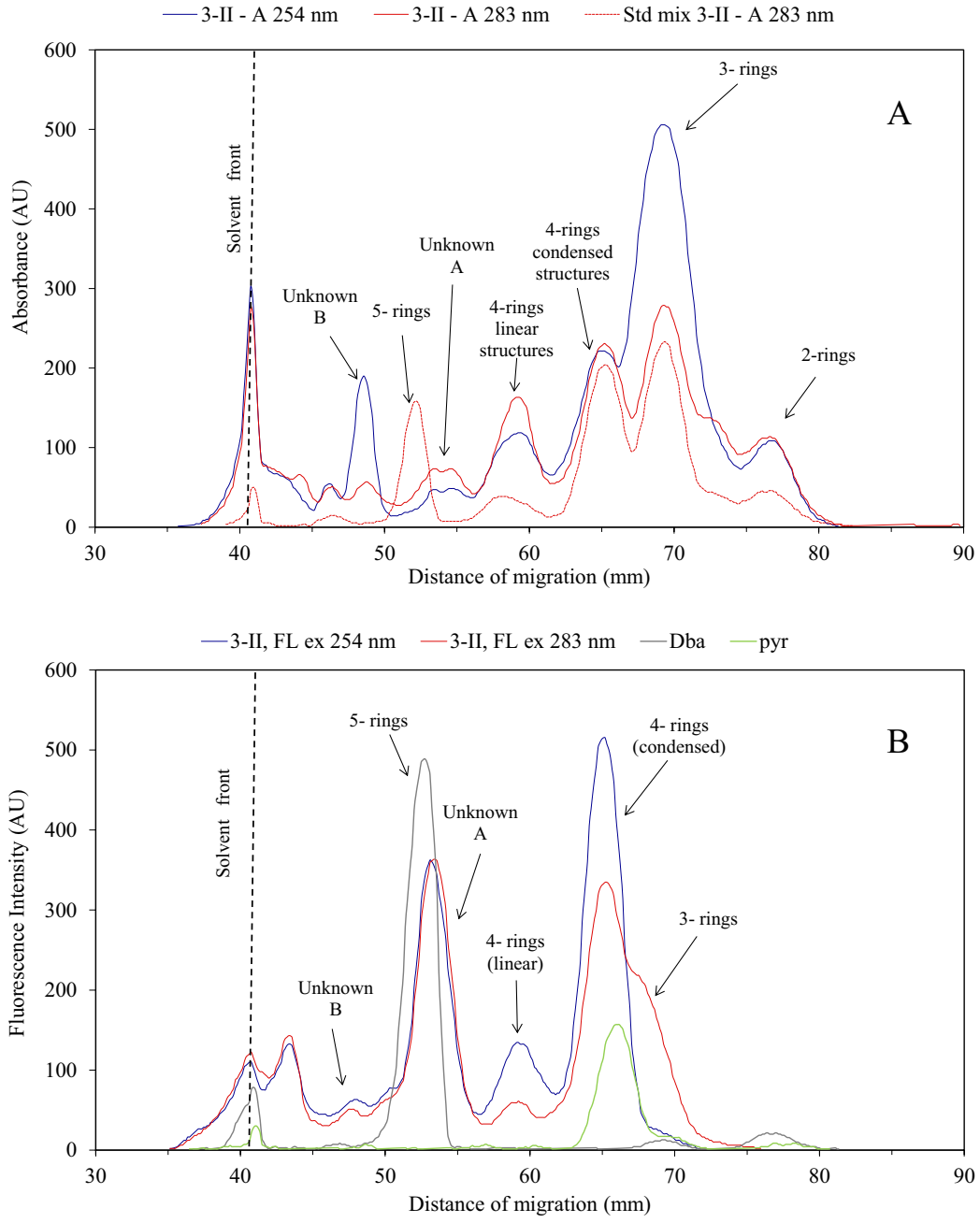

Figure 23: Chromatograms of sample 3-II (Fe/olivine), and the synthetic sample 3-II on HPLTC Silica gel 60 RP-18 with concentrating zone plate (migration at -23°C), recorded at different wavelengths in absorption and fluorescence mode (table 1 –j)

The unknown A peak seems to be a heavy aromatic molecule(s) presents in a small concentration in the investigated sample, with a chemical structure similar to that of dibenzoanthracene. When excited both at 254 nm and 283 nm the compound strongly emits (Figure 23B). The spectrum of this peak was measured, but due to the very low concentration and the strong interference of the plate at absorbance higher than 300 nm, no useful information was obtained.

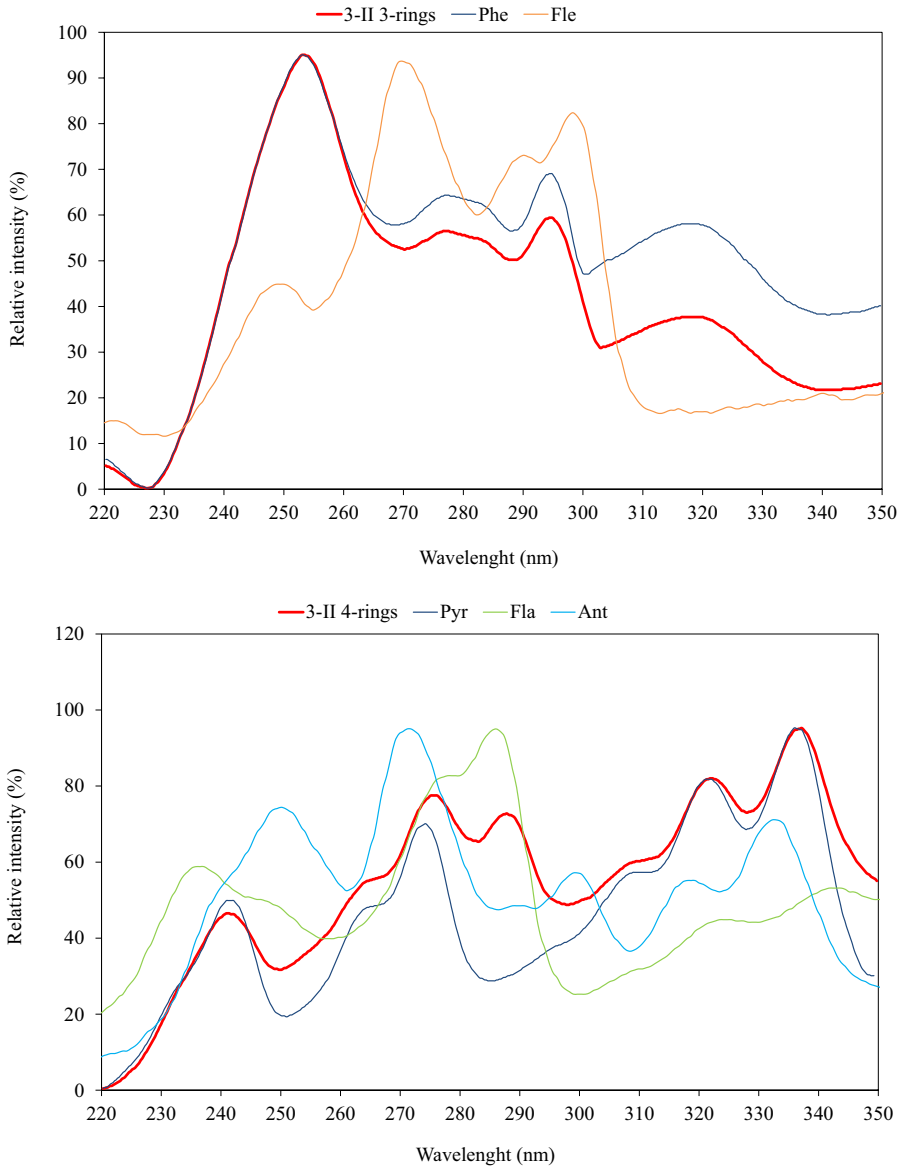

Figure 24: Absorption spectra of identified peaks in sample 3-II (Fe/olivine), on HPLTC Silica gel 60 RP-18 with concentrating zone plate (migration at -23°C)

The spectra of the identified peaks are reported in figure 24, and compared with standards spectra obtained on the same condition: the peak observed at the distance

of migration of 70 mm (figure 23A) shows a good similarity with phenanthrene () spectrum when fluorene () is well distinguishable. Concerning the peak migrated at 65 mm (same figure), the spectrum obtained corresponds to a combination of pyrene () and fluoranthene () as anthracene () shows a different spectrum with specific absorption bands.

The combined use of optimal separation coupled with densitometry analysis can led to the observation that HPTLC/UV/FL could be successfully used in qualitative analysis of tar sample. Further investigations could also be concluding for quantitative analysis according the number of rings.

3.3 Tar quantification by HPTLC/UV

For HPTLC quantitative Tar determination, the migration was performed on a RP-18 W plate but merging the PAHs in a single large peak that contained the identified aromatic molecules (2-, 3- and 4- rings aromatics). The area of the peak was proportional to the amount spotted, according results observed in figure 19. As stated previously, it was observed that increasing the amount of synthetic sample “std mix 2-I” applied on the plate, an augmented signal intensity was measured (Figure 19).

Thus, a tar quantification method based on HPTLC/UV was investigated. The data were analyzed comparing with HPLC/UV results. The well characterized sample 3-II (Fe/olivine) was used in calibration procedure using the standard addition method.

Tar sample was diluted in an appropriate volume of 2 ml (1/8 v/v, 1/10 v/v, 1/15 v/v, 1/20 v/v) to validate the sensitivity of the method regarding to the tar concentration. Thus a known concentration of total aromatics (synthetic standard mixture based on sample 3-II) was added to the diluted samples; the addition volumes were small (ranging from 10 µl to 40 µl) in order to simplify the dilution step and neglect the volume added.

The samples were then spotted on a HPTLC RP-18 W and eluted with ethyl acetate/n-hexane 50/50 over 40 mm and n-hexane until 90 mm from the beginning of the plate. The detection was performed scanning the plate in UV at 254 nm.

The four standard addition curves were obtained recording the amount of added standard (µg applied on the HPTLC plate) vs. the area of the identified peak. The curves are reported in figure 25. Each point was repeated at least four times. The best results (based on standard deviation of peak area) were obtained for the highest dilution of original sample (figure 25d), however the slope of the linear regression responds also well with the dilution, so the intercept of the x-axis can give the quantity of tar in the sample.

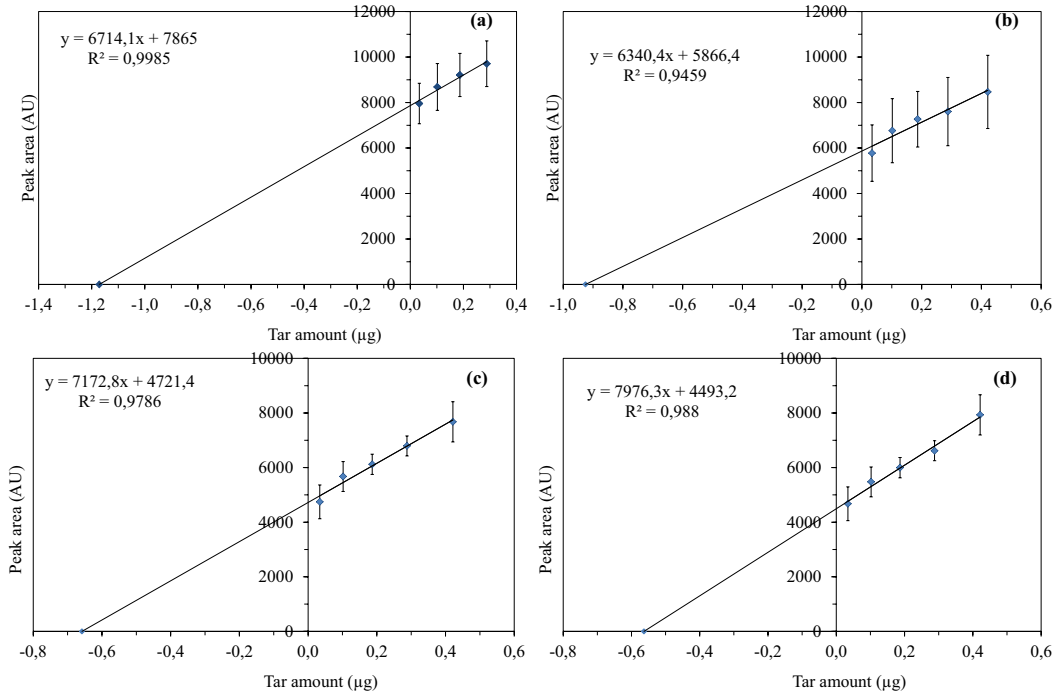

Figure 25: Calibration curves obtained by standard addition method for different amount of sample 3-II (Fe/olivine). Sample 3-II was diluted 1/8 v/v (**a**), 1/10 v/v (**b**), 1/15 v/v (**c**) and 1/20 v/v (**d**) and then added with a growing amount of standard mix.

The amount of tar in sample 3-II measured by HPTLC/UV thanks to the standard addition method and the amount of tar quantified by HPLC/UV has been correlated in Figure 26. The two techniques demonstrate a good agreement (R^2 = 0.991), the slope of the linear regression curve is near 1.20: it would seem that HPTLC method overestimates the tar in the samples. This difference can also be attributed to a better agreement of tar composition as HPTLC allows a complete cartography of the sample where HPLC quantifies the eluted detectable peaks.

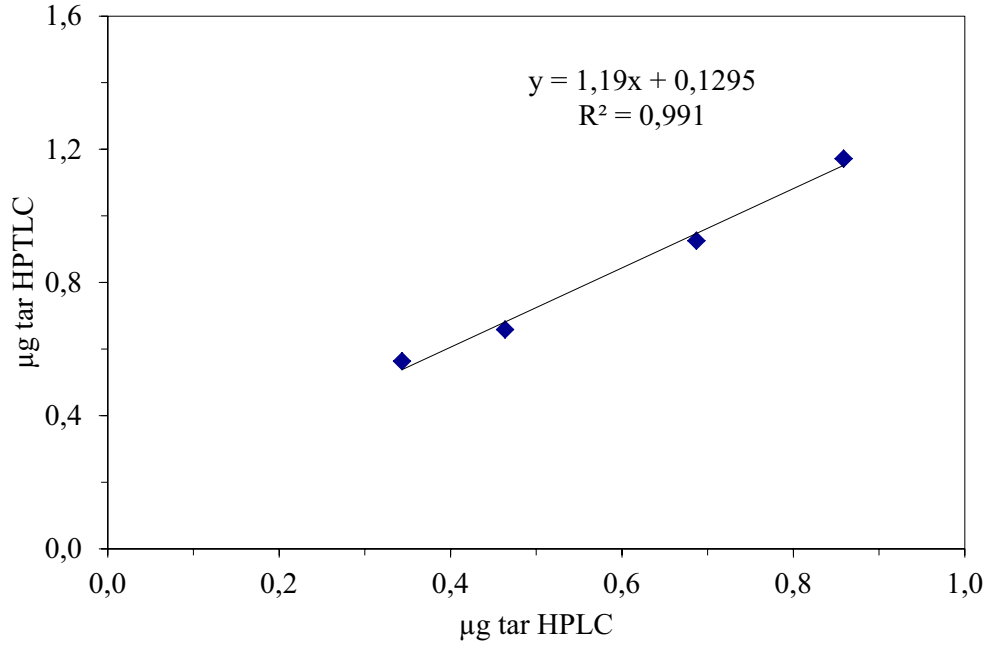

Figure 26: Study on the correlation for tar amount measured by HPLC/UV and tar amount quantified by means of HPTLC/UV and standard addition method.

4. Conclusions

The new analytical developments proposed in this work have shown promising potentialities.

From one hand, the UV spectroscopy development can lead to an adaptable on-line tar detection and quantification as the majority compounds (aromatics containing less than 5 rings) are detected in the near UV region with absorbance proportional to tar amount. A sensor could be settled on the "tar protocol sampling line" following absorbance during gas sampling. Additionally, off-line spectroscopy data treatments enable fast tar quantification by convolution of standard spectra with results showing sufficient precision closed to those obtained with the reference method adopted in this work, HPLC.

On the other hand, planar chromatography, showing great potentialities with the growing variety of stationary phases coupled with material improvements, was chosen for it potentiality of complete sample analysis. It has led to the development of an original separation method for tar analysis: it is possible to follow the aromatic composition regarding to the level of aromatic content family. Low temperature chromatographic conditions gave good resolution for PAHs from 2 to 5 rings, with a difference of condensed or non-condensed structure.

These completely original results could also be furthermore investigated to quantify each family of aromatics. However it was also possible to quantify the total PAHs content using a standard addition method merging all the aromatic compounds under the same peak.

References

Abbott D.C., Egam H., Thomson J. (1964) Some observations on the thin-layer chromatography of organo-chlorine pesticides. Journal of Chromatography A, 16:481-487

Billo E.J. (2001) Excel® for Chemists: A Comprehensive Guide. John Wiley & Sons, Inc. ISBNs: 0-471-39462-9.

Gaganis V., Pasadakis N., Smaragdis P., Varotsis N. (2003) Deconvolution of Overlapping HPLC Aromatic Hydrocarbons Peaks Using Independent Component Analysis (ICA). Mitsubishi Electric Research Laboratories http://www.merl.com

Harvey R.G. (1991) Polycyclic aromatic hydrocarbons: Chemistry and carcinogenicity. Cambridge monograph on cancer research. Cambridge University Press

Issaq H.J., Mangino M.M., Singer G.M., Wilbur D.J., Risser N.H. (1979) Effect of Temperature on the Separation of Conformational Isomers of Cyclic Nitrosamines by Thin-Layer Chromatography. Analytical Chemistry, 51(13) 2157–2159

Lawton W.H. and Sylvestre E.A. (1971) Self modeling curve resolution. Technometrics, 13:617-633

Matt M., Galvez E.M., Cebolla V.L., Membrado L., Bacaud R., Pessayre S. (2003) Improved separation and quantitative determination of hydrocarbon types in gas oil by normal phase high-performance TLC with UV and fluorescence scanning densitometry. Journal of Separation Science, 26:1665-1674

Merck ChromBook 2008/09 http://www.scribd.com/doc/35399143/Chrome-Book-Merck

Monakhova Y., Astakhov S., Kraskov A., Mushtakova S. (2010) Independent components in spectroscopic analysis of complex mixtures. Chemometrics and Intelligent Laboratory Systems, 103:108–115

NIST chemistry webbook: http://webbook.nist.gov

Poole C.F. (2003) Thin-layer chromatography: challenges and opportunities.

Journal of Chromatography A, 1000:963–984

Reimers C., Zielonka B., Stegmann R., Steinhart H. (2001) Determination of PAH in soil samples by High-Performance Thin-Layer Chrmatography (HPTLC). Journal of Soils and Sediments, 1(3):159-163

Sherma J. (2010) Planar chromatography. Analytical Chemistry, 82:4895-4910

Touraud E., Crone M., Thomas O. (1998) Rapid diagnosis of polycyclic aromatic hydrocarbons (PAH) in contaminated soils with the use of ultraviolet detection. Field Analytical Chemistry and Technology, 2(4):221–229

Tsoumanis C., Giokas D., Vlessidis A. (2010) Monitoring and classification of wastewater quality using supervised pattern recognition techniques and deterministic resolution of molecular absorption spectra based on multiwavelength UV spectra deconvolution. Talanta, 82:575–581

GENERAL CONCLUSIONS

Biomass gasification

Miscanthus x giganteus pellets of 6 mm diameter and crushed and sieved almond shells have been used as biomass feedstock for catalytic fluidized bed gasification. Comparing the results obtained using the two biomasses at analogous operating conditions, no significant differences concerning the gas yield, gas composition and tar content could be observed. Nevertheless, a higher ammonia content was found in case of Miscanthus gasification due to its higher nitrogen content.

The ammonia concentration in the producer gas drastically decrease by a factor 5 when an efficient catalyst, such as Ni/olivine, is used as primary in-bed catalyst. Therefore, in addition to the undeniable agricultural advantages of this biomass, Miscanthus x giganteus pellets have shown they could be successfully employed in fluidized bed gasification process.

When Miscanthus x giganteus straw pellets were tested at temperature higher than 850°C, no bed defluidization was observed. However, it has a considerably higher content of ash and chlorine when compared to almond shells. Considering that the stability, in long-term operation, of fluidized bed reactors can be seriously compromised by particle agglomeration phenomena, during project execution it was preferred to work with crushed almond shells.

During the work, innovative catalytic hot gas filters for in-situ tar and particulate abatement, as well as two interesting Ni- and Fe- based catalyst have were tested in real gasification conditions.

The innovative concept of integrating a catalytic hot gas filter in the gasifier freeboard was investigated using two catalytically activated filter candles provided by PALL GmbH (Germany):

- Catalytic filter candle with “catalytic layer” design;
- Catalytic filter candle with “fixed bed” design.

The catalytic activity of the candles were investigated and compared. The second candle contains a fixed bed of nickel particles protected by a filter layer; thanks to an integrated higher and better accessible Ni catalyst amount for tar reforming, the “fixed bed” candle leads to an increase in the gas yield by 69% and in its

hydrogen concentration. While, the “catalytic layer” design allows, in the optimum conditions, a relatively limited improvement in gas yield by 33%.
After a total gasification time of 22 h, the catalytic performance of the filter element with “fixed bed” design remains stable, though with a slight reduction in methane and tar conversion. Anyway the long-term test demonstrates that this innovative in-situ secondary catalyst is able to assure a decrease by 69% of the tar yield.
The pressure drop thought the filter candle was measured, and its value increases almost linearly with time, with a gradient reflecting the growing thickness of the particle layer that deposits on the filter. Clearly, in industrial application it will be necessary the adoption of a backpulsing system, which provides the efficient removal of the material deposited on the candle.

3.9wt% Ni/olivine and 10wt % Fe/olivine catalyst provided from the ECPM-LMSPC, University of Strasbourg (France) were tested under full operating conditions.

- Ni/olivine catalyst demonstrates to be very effective in terms of tar reforming. Comparing the results obtained using plain olivine particles in analogous conditions, Ni/olivine at 800 °C leads to a decreased tar yield by 76 %; As a consequence an increased gas and hydrogen yields were measured by 70 % and 131 %, respectively.

  Nevertheless, during the catalytic gasification test performed at temperature higher that that utilized in industrial application (900°C), a slightly decrease of the catalyst activity was observed in terms of gas yield and water conversion (tar sample was not available for this test).
- Fe/olivine appears a very interesting in-bed primary catalyst, for economic and environmental reasons: iron does not affect the catalyst cost due to its lower price in comparison to nickel. Moreover, the fines particles separated from the product gas, can be easily disposal due to the absence of carcinogenic metals such as nickel compounds.

  When 10wt% Fe/olivine is adopted as bed inventory a tar reforming extent by 49% is obtained; methane is also partially converted (16%); as a result,

an increased on the gas yield is reached (about 39%) and also hydrogen concentration raises 53% in the dry gas (N_2 free basis).

Further improvements have been obtained by combining the synergic catalytic effect of 10wt % Fe/olivine and the catalytic filter candle, resulting in a efficient tar abatement (-92% in the producer gas, -86% in tar yield), and a consequently increase of gas yield by 72%.
Also, the use of catalytic filter allows efficient particle separation, so that the final result is a hot and clean fuel gas made available right at the exit of the gasifier reactor.
When applied to small to medium gasification plant, this innovative catalyst system would determine a remarkable power plant simplification minimizing investment and operating costs, combined with the potential of much higher conversion efficiency of biomass energy to electric power.

Tar characterization

The standard tar sampling method proposed by the UNI CEN/TS 15439:2008 was used in this work. Though HPLC/UV were the analytical tool chosen to follow the tar evolution in the gasification samples, according to the process adopted. The method developed leads to analysis of the tar concentration and its composition without any pretreatment step or additional measurements, such as gravimetric analysis.

This robust chromatographic technique was also used as reference method for the development of new analytical strategies able to provide qualitative and quantitative analysis of tar in a single step without separation, evaporation or other time consuming operation.

- An UV spectroscopy based method was developed: this enable fast quantification of tars in by convolution of standard spectra, and it also has the potential to be adapted as on-line method for tar quantification, capable to assure a punctual control of the process performances. The

results obtained from 3 different gasification plant, of different size and design over 33 samples show a good agreement with the data obtained with the HPLC/UV.

- With a small amounts of solvents, relatively fast and easy handling and without the need of expensive equipment, planar chromatography provides an interesting method for qualitative and quantitative tar analyses.
  An original separation method for tar analysis by HPTLC/UV/FL enables to give information about the tar composition and concentration. The experiments carried out using an optimized combination of mobile phase (ethyl acetate, hexane) and stationary phase (RP-18 with concentrating zone) at low temperature chromatographic conditions (-20 °C) demonstrated good resolution for PAHs from 2 to 5 rings, with a difference of condensed or non-condensed structure.
  In addition, it was possible to quantify the total tar content using a standard addition method merging all the aromatic compounds under the same peak. The results showed a good correlation with the reference method adopted in this work.

Further work

The Fe/olivine catalyst tested demonstrated to be very effective in terms of tar reforming activity; anyway the realization of a long-term test will be preferable in order to evaluate more intensively the stability of the catalyst in the time and its behavior regard the formation of fines;

The UV method developed presents the interesting prospective to be used as an on-line control method for gasification experiments, thanks to utilization of on-line UV intensity display module;

In order to validate the promising quantitative results obtained by HPTLC/UV additional extensively investigation will be necessary;

Furthermore, considering the impact of heavy tar on the tar dewpoint, the quantification of each family of aromatics with a special regard to the heaviest (3-rings, 4-rings, ≥ 5-rings) will be one of the most interesting research ideas from the analytical point of view;

ANNEXES

Annex I: Excel spreadsheet for UV convolution

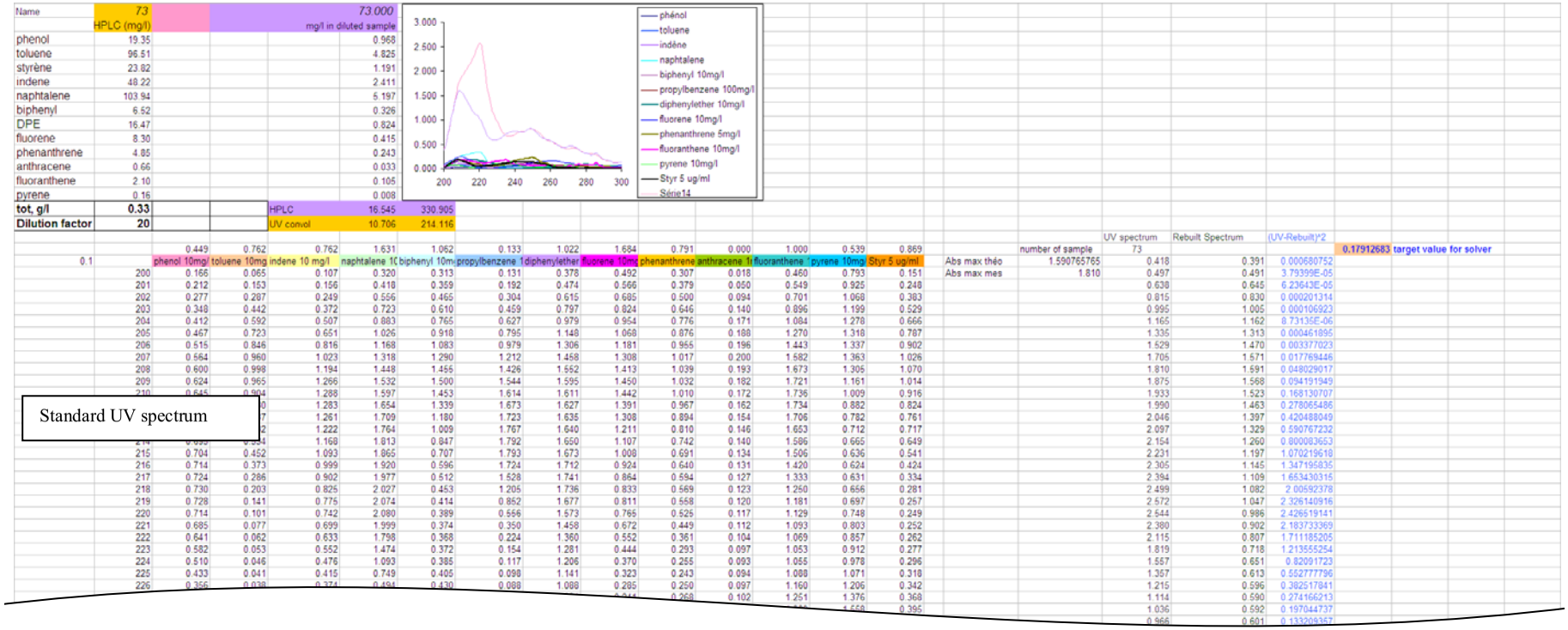

Name	73			73.000	
	HPLC (mg/l)			mg/l in diluted sample	
phenol	19.35			0.968	
toluene	96.51			4.825	
styrène	23.82			1.191	
indene	48.22			2.411	
naphtalene	103.94			5.197	
biphenyl	6.52			0.326	
DPE	16.47			0.824	
fluorene	8.30			0.415	
phenanthrene	4.85			0.243	
anthracene	0.66			0.033	
fluoranthene	2.10			0.105	
pyrene	0.16			0.008	
tot, g/l	**0.33**		HPLC	16.545	330.905
Dilution factor	**20**		UV convol	10.706	214.116

																UV spectrum	Rebuilt Spectrum	(UV-Rebuilt)^2	
		0.449	0.762	0.762	1.631	1.062	0.133	1.022	1.684	0.791	0.000	1.000	0.539	0.869		number of sample	73		0.17912683 target value for solver
0.1		phenol 10mg/	toluene 10mg	indene 10 mg/l	naphtalene 1(	biphenyl 10m	propylbenzene 1	diphenylether	fluorene 10mg	phenanthrene	anthracene 1	fluoranthene	pyrene 10mg/	Styr 5 ug/ml	Abs max théo	1.590765765	0.418	0.391	0.000680752
	200	0.166	0.065	0.107	0.320	0.313	0.131	0.378	0.492	0.307	0.018	0.460	0.793	0.151	Abs max mes	1.810	0.497	0.491	3.79399E-05
	201	0.212	0.153	0.156	0.418	0.359	0.192	0.474	0.566	0.379	0.050	0.549	0.925	0.248			0.638	0.645	6.23643E-05
	202	0.277	0.287	0.249	0.556	0.465	0.304	0.615	0.685	0.500	0.094	0.701	1.068	0.383			0.815	0.830	0.000201314
	203	0.348	0.442	0.372	0.723	0.610	0.459	0.797	0.824	0.646	0.140	0.896	1.199	0.529			0.995	1.005	0.000106923
	204	0.412	0.592	0.507	0.883	0.765	0.627	0.979	0.954	0.776	0.171	1.084	1.278	0.666			1.165	1.162	8.73135E-06
	205	0.467	0.723	0.651	1.026	0.918	0.795	1.148	1.068	0.876	0.188	1.270	1.318	0.787			1.335	1.313	0.000461895
	206	0.515	0.846	0.816	1.168	1.083	0.979	1.306	1.181	0.955	0.196	1.443	1.337	0.902			1.529	1.470	0.003377023
	207	0.564	0.960	1.023	1.318	1.290	1.212	1.458	1.308	1.017	0.200	1.582	1.363	1.026			1.705	1.571	0.017769446
	208	0.600	0.998	1.194	1.448	1.455	1.426	1.562	1.413	1.039	0.193	1.673	1.305	1.070			1.810	1.591	0.048029017
	209	0.624	0.965	1.266	1.532	1.500	1.544	1.595	1.450	1.032	0.182	1.721	1.161	1.014			1.875	1.568	0.094191949
	210	0.645	0.904	1.288	1.597	1.453	1.614	1.611	1.442	1.010	0.172	1.736	1.009	0.916			1.933	1.523	0.168130707
				1.283	1.654	1.339	1.673	1.627	1.391	0.967	0.162	1.734	0.882	0.824			1.990	1.463	0.278065486
				1.261	1.709	1.180	1.723	1.635	1.308	0.894	0.154	1.706	0.782	0.761			2.046	1.397	0.420488049
				1.222	1.764	1.009	1.767	1.640	1.211	0.810	0.146	1.653	0.712	0.717			2.097	1.329	0.590767232
	214	0.699	0.554	1.168	1.813	0.847	1.792	1.650	1.107	0.742	0.140	1.586	0.665	0.649			2.154	1.260	0.800083653
	215	0.704	0.452	1.093	1.865	0.707	1.793	1.673	1.008	0.691	0.134	1.506	0.636	0.541			2.231	1.197	1.070219618
	216	0.714	0.373	0.999	1.920	0.596	1.724	1.712	0.924	0.640	0.131	1.420	0.624	0.424			2.305	1.145	1.347195835
	217	0.724	0.286	0.902	1.977	0.512	1.528	1.741	0.864	0.594	0.127	1.333	0.631	0.334			2.394	1.109	1.653430315
	218	0.730	0.203	0.825	2.027	0.453	1.205	1.736	0.833	0.569	0.123	1.250	0.656	0.281			2.499	1.082	2.00592378
	219	0.728	0.141	0.776	2.074	0.414	0.852	1.677	0.811	0.558	0.120	1.181	0.697	0.257			2.572	1.047	2.326140916
	220	0.714	0.101	0.742	2.080	0.389	0.556	1.573	0.765	0.525	0.117	1.129	0.748	0.249			2.544	0.986	2.426519141
	221	0.685	0.077	0.699	1.999	0.374	0.350	1.458	0.672	0.449	0.112	1.093	0.803	0.252			2.380	0.902	2.183733369
	222	0.641	0.062	0.633	1.798	0.368	0.224	1.360	0.552	0.361	0.104	1.069	0.857	0.262			2.115	0.807	1.711185205
	223	0.582	0.053	0.552	1.474	0.372	0.154	1.281	0.444	0.293	0.097	1.053	0.912	0.277			1.819	0.718	1.213555254
	224	0.510	0.046	0.476	1.093	0.385	0.117	1.206	0.370	0.255	0.093	1.055	0.978	0.296			1.557	0.651	0.82091723
	225	0.433	0.041	0.415	0.749	0.405	0.098	1.141	0.323	0.243	0.094	1.088	1.071	0.318			1.357	0.613	0.552777796
	226	0.366	0.038	0.374	0.494	0.430	0.088	1.088	0.285	0.250	0.097	1.160	1.206	0.342			1.215	0.596	0.382517841
										0.268	0.102	1.251	1.376	0.368			1.114	0.590	0.274166213
													1.558	0.395			1.036	0.592	0.197044737
																	0.966	0.601	0.133208357

Standard UV spectrum

288	0.020	0.009	0.011	0.179	0.020	0.018											
289	0.017	0.009	0.010	0.127	0.018	0.018	0.542	0.287	0.194	0.008							
290	0.015	0.008	0.009	0.089	0.016	0.017	0.494	0.272	0.231	0.008	0.231	0.194	0.028				
291	0.013	0.008	0.008	0.062	0.014	0.016	0.449	0.258	0.278	0.008	0.163	0.207	0.024	0.163	0.170	5.50701E-05	
292	0.013	0.008	0.006	0.046	0.013	0.016	0.418	0.250	0.300	0.008	0.131	0.216	0.015	0.153	0.158	1.92453E-05	
293	0.012	0.008	0.004	0.035	0.012	0.015	0.408	0.242	0.264	0.008	0.114	0.221	0.009	0.143	0.142	2.09758E-06	
294	0.011	0.008	0.003	0.028	0.011	0.015	0.420	0.226	0.195	0.008	0.103	0.223	0.004	0.135	0.129	4.3271E-05	
295	0.011	0.008	0.002	0.024	0.010	0.015	0.434	0.212	0.130	0.008	0.096	0.223	0.002	0.130	0.121	8.51009E-05	
296	0.011	0.008	0.002	0.023	0.009	0.014	0.425	0.219	0.084	0.008	0.092	0.226	0.001	0.128	0.119	8.09471E-05	
297	0.011	0.007	0.002	0.022	0.009	0.014	0.382	0.261	0.056	0.007	0.091	0.232	0.001	0.127	0.121	3.54953E-05	
298	0.010	0.007	0.001	0.021	0.009	0.014	0.310	0.331	0.039	0.007	0.092	0.246	0.000	0.128	0.127	1.07908E-06	
299	0.010	0.007	0.001	0.020	0.008	0.014	0.247	0.402	0.030	0.007	0.095	0.265	0.000	0.128	0.129	1.70104E-06	
300	0.010	0.007	0.001	0.020	0.008	0.014	0.226	0.430	0.027	0.007	0.096	0.276	0.000	0.118	0.107	0.00013275	

	phénol	toluene	indène	naphtalene	biphenyl 10mg	propylbenzene 1	diphenylether	fluorene 10mg	phenanthrene	anthracene 1	fluoranthene	pyrene 10mg/	Styr 5 ug/ml
200	0.007	0.005	0.008	0.052	0.033	0.000	0.039	0.083	0.049	0.000	0.046	0.043	0.026
201	0.009	0.012	0.012	0.068	0.038	0.000	0.048	0.095	0.060	0.000	0.055	0.050	0.043
202	0.012	0.022	0.019	0.091	0.049	0.000	0.063	0.115	0.079	0.000	0.070	0.058	0.066
203	0.016	0.034	0.028	0.118	0.065	0.001	0.081	0.139	0.102	0.000	0.090	0.065	0.092
204	0.018	0.045	0.039	0.144	0.081	0.001	0.100	0.161	0.123	0.000	0.108	0.069	0.116
205	0.021	0.055	0.050	0.167	0.097	0.001	0.117	0.180	0.139	0.000	0.127	0.071	0.137
206	0.023	0.064	0.062	0.191	0.115	0.001	0.133	0.199	0.151	0.000	0.144	0.072	0.157
207	0.025	0.073	0.078	0.215	0.137	0.002	0.149	0.220	0.161	0.000	0.158	0.074	0.178
208	0.027	0.076	0.091	0.236	0.155	0.002	0.159	0.238	0.164	0.000	0.167	0.070	0.186
209	0.028	0.074	0.097	0.250	0.159	0.002	0.163	0.244	0.163	0.000	0.172	0.063	0.176
210	0.029	0.069	0.098	0.261	0.154	0.002	0.165	0.243	0.160	0.000	0.174	0.054	0.159
211	0.030	0.063	0.098	0.270	0.142	0.002	0.166	0.234	0.153	0.000	0.173	0.048	0.143
212	0.030	0.056	0.096	0.279	0.125	0.002	0.167	0.220	0.141	0.000	0.171	0.042	0.132
213	0.031	0.048	0.093	0.288	0.107	0.002	0.168	0.204	0.128	0.000	0.165	0.038	0.125
214	0.031	0.041	0.089	0.296	0.090	0.002	0.169	0.187	0.117	0.000	0.159	0.036	0.113
215	0.032	0.034	0.083	0.304	0.075	0.002	0.171	0.170	0.109	0.000	0.151	0.034	0.094
216	0.032	0.028	0.076	0.313	0.063	0.002	0.175	0.156	0.101	0.000	0.142	0.034	0.074
217	0.032	0.022	0.069	0.322	0.054	0.002	0.178	0.146	0.094	0.000	0.133	0.034	0.058
			0.063	0.331	0.048	0.002	0.177	0.140	0.090	0.000	0.125	0.035	0.049
			0.059	0.338	0.044	0.001	0.171	0.137	0.088	0.000	0.118	0.038	0.045
			0.057	0.339	0.041	0.001	0.161	0.129	0.083	0.000	0.113	0.040	0.043
			0.053	0.326	0.040	0.000	0.149	0.113	0.071	0.000	0.109	0.043	0.044
222	0.029	0.005	0.048	0.293	0.039	0.000	0.139	0.093	0.057	0.000	0.107	0.046	0.046
223	0.026	0.004	0.042	0.241	0.040	0.000	0.131	0.075	0.046	0.000	0.105	0.049	0.048
224	0.023	0.004	0.036	0.178	0.041	0.000	0.123	0.062	0.040	0.000	0.105	0.053	0.051
225	0.019	0.003	0.032	0.122	0.043	0.000	0.117	0.054	0.039	0.000	0.109	0.058	0.055
226	0.016	0.003	0.029	0.081	0.046	0.000	0.111	0.048	0.040	0.000	0.116	0.065	0.059
227	0.013	0.003	0.027	0.054	0.049	0.000	0.105	0.041	0.042	0.000	0.125	0.074	0.064
228	0.010	0.003	0.026	0.038	0.052	0.000	0.097	0.034	0.046	0.000	0.133	0.084	0.069
229	0.007	0.002	0.026	0.028	0.056	0.000	0.087	0.029	0.051	0.000	0.138	0.095	0.074
230	0.006	0.002	0.026	0.022	0.060	0.000	0.077	0.027	0.057	0.000	0.142	0.104	0.079
231	0.004	0.002	0.027	0.018	0.064	0.000	0.069	0.027	0.063	0.000	0.146	0.105	0.085
232	0.003	0.002	0.028	0.016	0.068	0.000	0.061	0.027	0.071	0.000	0.154	0.102	0.090
233	0.003	0.002	0.029	0.015	0.072	0.000	0.054	0.029	0.079	0.000	0.167	0.100	0.096
234	0.002	0.002	0.030	0.014	0.076	0.000	0.049	0.031	0.088	0.000	0.180	0.101	0.101
235	0.002	0.002	0.032	0.014	0.080	0.000	0.045	0.034	0.097	0.000	0.182	0.108	0.107
236	0.002	0.002	0.034	0.014	0.085	0.000	0.045	0.037	0.106	0.000	0.166	0.121	0.112
237	0.002	0.002	0.036	0.015	0.089	0.000	0.046	0.041	0.116	0.000	0.142	0.133	0.118
238	0.002	0.002	0.037	0.015	0.092	0.000	0.050	0.045	0.126	0.000	0.120	0.138	0.123
239	0.002	0.002	0.039	0.016	0.096	0.000	0.055	0.050	0.139	0.000	0.104	0.133	0.127
240	0.002	0.002	0.041	0.016	0.099	0.000	0.057	0.055	0.153	0.000	0.093	0.117	0.131
241	0.002	0.002	0.043	0.017	0.102	0.000	0.057	0.061	0.167	0.000	0.086	0.094	0.133
242	0.002	0.002	0.045	0.018	0.104	0.000	0.057	0.067	0.180	0.000	0.081	0.071	0.135
243	0.002	0.002	0.046	0.020	0.106	0.000	0.057	0.073	0.187	0.000	0.077	0.052	0.136
244	0.002	0.002	0.047	0.021	0.107	0.000	0.057	0.080	0.190	0.000	0.075	0.039	0.136

convoluted UV spectrum

Annex II: Characteristics of the HPTLC plates

HPTLC Nano-SIL 20 glass plates 10x10 cm (Macherey-Nagel GmbH & Co. KG, Düren Germany)

[http://www.mn-net.com/TLCStart/TLCphases/NanoSIL/tabid/5632/language/en-US/Default.aspx]:

- Unmodified Nano-silica layers for HPTLC;
- Features:
    - Nano silica 60, specific surface (BET) ~ 500 m^2/g, mean pore size 60 Å, specific pore volume 0.75 ml/g;
    - Particle size 2 – 10 µm;
    - Thickness of layer 0.20 mm
    - Binder: highly polymeric product, which is stable in almost all organic solvents and resistant towards aggressive visualisation reagents
    - Narrow fractionation of the silica particles allows sharper separations, shorter developing times, shorter migration distances, smaller samples and an increased detection sensitivity compared to TLC plates

HPTLC Silica gel 60 glass plates 20x10 cm (Merck KGaA, Darmstadt, Germany)

[http://www.merck-chemicals.com/hptlc-silica-gel-60/MDA_CHEM-105641/p_ABmb.s1LzOUAAAEWuOAfVhTl]:

- Unmodified Nano-silica layers for HPTLC;
- Features:
    - HPTLC plates deliver fast and quantitative analysis of complex samples for manual or automated use. HPTLC silica plates work three times faster than conventional TLC plates – and they are more sensitive;
    - Nano silica 60, mean pore size 60 Å;
    - The particle sizes range in HPTLC is between 4-8µm, which creates a smoother surface and a higher separation power than TLC plates.

HPTLC Silica gel 60 NH_2 glass plates 20x10 cm (Merck KGaA, Darmstadt, Germany)[http://www.merck-chemicals.com/hptlc-silica-gel-60-nh-2/MDA_CHEM-112572/p_Tzmb.s1LJOMAAAEWuuAfVhTl] and *HPTLC Silica gel 60 DIOL F_{254}s glass plates 10x10 cm (Merck KGaA, Darmstadt, Germany)* [http://www.merck-chemicals.com/hptlc-silica-gel-60-diol-f-2-5-4-s/MDA_CHEM-112668/p_Tzmb.s1LJOMAAAEWuuAfVhTl]:

- Modified Nano-silica layers for HPTLC;
- Features:
    - Nano silica 60, mean pore size 60 Å;
    - NH_2 and DIOL -modified silica sorbents are less polar then conventional silica phases, making them ideal for separating hydrophilic or charged substances;
    - The moderately polar diol-modified silica plates can be used for both normal phase and reversed phase systems;
    - Amino-modified NH_2 plates provide weak basic ion exchange characteristics with special selectivity for charged compounds.

Pre-coated glass plates RP-18, F_{254} for Nano TLC 10x10 cm (Macherey-Nagel GmbH & Co. KG, Düren Germany):

- Octadecyl-modified nano silica layers for HPTLC;

Those plates are no longer available.

HPTLC glass plates RP-18 W 20x10 cm (Merck KGaA, Darmstadt, Germany [http://www.merck-chemicals.com/hptlc-silica-gel-60-rp-18-w/MDA_CHEM-114296/p_9hOb.s1L87gAAAEWueAfVhTl]

- Nano-silica 60 (mean pore size 60 Å) partial octadecyl modified and wettable with water;
- Features:
    - RP modified plates serve two purposes: act as a pilot method for HPLC and allow to choose various solvent system for special separations. RP-modified silica layers are well suited for many separation challenges that unmodified silica cannot overcome. These layers use aqueous solvent systems to separate extremely non-polar

substances and analyze particular polar substances that can adapt to ion-pair chromatography. Also, RP-modified silica layers are less dependent on atmospheric humidity. Unlike unmodified silica, RP-phases do not exhibit catalytic activity. This makes them the plates of choice for unstable substance that tend to experience oxidative degradation.

Order of polarity: silica > DIOL > NH_2 > RP-18 W

HPTLC Silica gel 60 RP-18 with concentrating zone (20 x 2.5 cm) 20x10 glass plates (Merck KGaA, Darmstadt, Germany) [http://www.merck-chemicals.com/hptlc-silica-gel-60-rp-18-with-concentrating-zone-20-x-2-5-cm/MDA_CHEM-115037/p_lDKb.s1Ldl0AAAEWu.AfVhTl]:

- Nano-silica 60 (mean pore size 60 Å) partial octadecyl modified;
- Features:
    - These plates allow users to apply any kind of sample, even large volumes of diluted samples. They are based on different adsorption properties of two adsorbents. The first is a large pore concentrating adsorbent where the samples are applied; the second is a selective layer for separation. Regardless of the spots' shape, size, or position, the sample always concentrates as a narrow band where the two adsorbents overlap and where the separation starts. These plates allow users to quickly and easily apply any kind of sample, even large volumes of diluted samples.

RÉSUMÉ FRANÇAIS LONG

Production continue de gaz issus de la gazéification de la biomasse (miscanthus) dans un réacteur à lit fluidisé circulant. Caractérisation chimique des composés organiques lourds produits durant le procédé de gazéification

Introduction générale

Cette thèse a été réalisée dans le cadre d'une collaboration entre les Universités de Teramo

(Pr S. Rapagnà, Italie) et Paul Verlaine de Metz (M. Matt, R. Gruber, LCME), et financée par le ministère des affaires étrangères d'Italie .

Elle concerne une étude de la gazéification de la biomasse, à haute température et en présence de vapeur d'eau, dans des conditions catalytiques, l'objectif étant d'optimiser les conditions opératoires afin d'obtenir un gaz de synthèse (H_2+ CO) avec des rendements satisfaisants et le plus pur possible, en minimisant les goudrons produits.

Les expériences ont été réalisées sur un pilote de laboratoire correspondant à un réacteur en lit fluidisé mis au point et développé à Teramo par l'équipe du professeur S. Rapagnà

La méthodologie d'analyse des goudrons a été développée au LCME de Metz, sous la responsabilité de Dr M. Matt

Dans le procédé de gazéification, la biomasse solide est transformée à haute température, dans des conditions catalytiques, en présence d'air, d'oxygène ou de vapeur d'eau, en produits gazeux qui peuvent avoir différentes utilisations: la production d'hydrogène et de gaz de synthèse (Syngas), la production de chaleur

ou d'électricité, la synthèse de bioalcools et d'hydrocarbures liquides, etc. Ce procédé est cependant générateur de goudrons et de particules, de part la matière première d'origine végétale, préjudiciables pour une mise en application industrielle. Il est donc nécessaire de connaître et d'optimise les conditions de gazéification afin de minimiser la production de goudron.

Les études ont porté sur l'optimisation des conditions opératoires de gazéification dans un réacteur à lit fluidisé :

- 2 types de biomasse on été traités, les coques d'amandes et des granulés de Miscanthus x giganteus
- L'efficacité du lit a été évaluée en utilisant des systèmes catalytique tels que l'olivine, le Ni-Olivine , le Fe-Olivine également complétés par un système secondaire de bougies filtrantes à activité catalytiques qui présentent un intérêt en lit fluidisé pour la réduction des goudrons et particules .Les catalyseurs ont été préparés par l'équipe du Pr A.Kiennemann, de L'Université de Strasbourg (LMSPC)
- L'évaluation des performances générales du procédé en déterminant le rendement en gaz (Nm3dry/kg biomassedaf), la composition du Syngas (% volumetrique en H2, CO, CH4 et CO2), la teneur en goudrons (g/Nm3 gazsec), le bilan en masse et en carbone.
- Les goudrons produits variant selon le système de gazéification (lit fixe ou lit fluidisé) des conditions catalytiques, de l'échantillonnage (« Tar protocole » ou condensats) différents systèmes analytiques ont été évalués et validés.

Ainsi, dans un premier temps, (Chapitre I), un état de l'art est présenté sur la valorisation énergétique de la biomasse, sur les aspects suivants :

- Le contexte européen, et plus particulièrement en Italie et en France
- Les sources de biomasse en insistant sur le potentiel du Miscanthus X Giganteus (MXG)
- Les principes et le fonctionnement des procédés de gazéification
- La problématique des goudrons produits et les différentes approches analytiques pour leur détermination

Le chapitre II rappelle les objectifs du travail de thèse, et la répartition des tâches entre les deux sites de Teramo et de Metz

Le chapitre III concerne tous les aspects liés aux expériences de Gazéification des coques d'amande et du MXG réalisés à Teramo : configuration du réacteur, conditions expérimentales, résultats

Avant la conclusion générale, dans les chapitre IV et V sont développés tous les aspects liés à l'analyse des goudrons, par rapport à la démarche réalisée au sein du LCME :

- Caractérisation par une technique classique comme la HPLC couplée avec la spectroscopie UV, et validation de la méthode pour les goudrons de gazéification
- Analyse des mélanges par UV en utilisant des techniques de déconvolution des spectres
- Développement d'une méthode originale basée sur la chromatographie sur couche mince couplée à un détecteur basé sur l'UV et la fluorescence

Répartition des tâches et Objectifs

Expériences de gazéification catalytique réalisées à Teramo (UNITE)

Les expériences, listées ci-dessous, ont été menées avec différentes configurations de réacteur, en utilisant en particulier un filtre catalytique placé en haut du réacteur, développé à Teramo

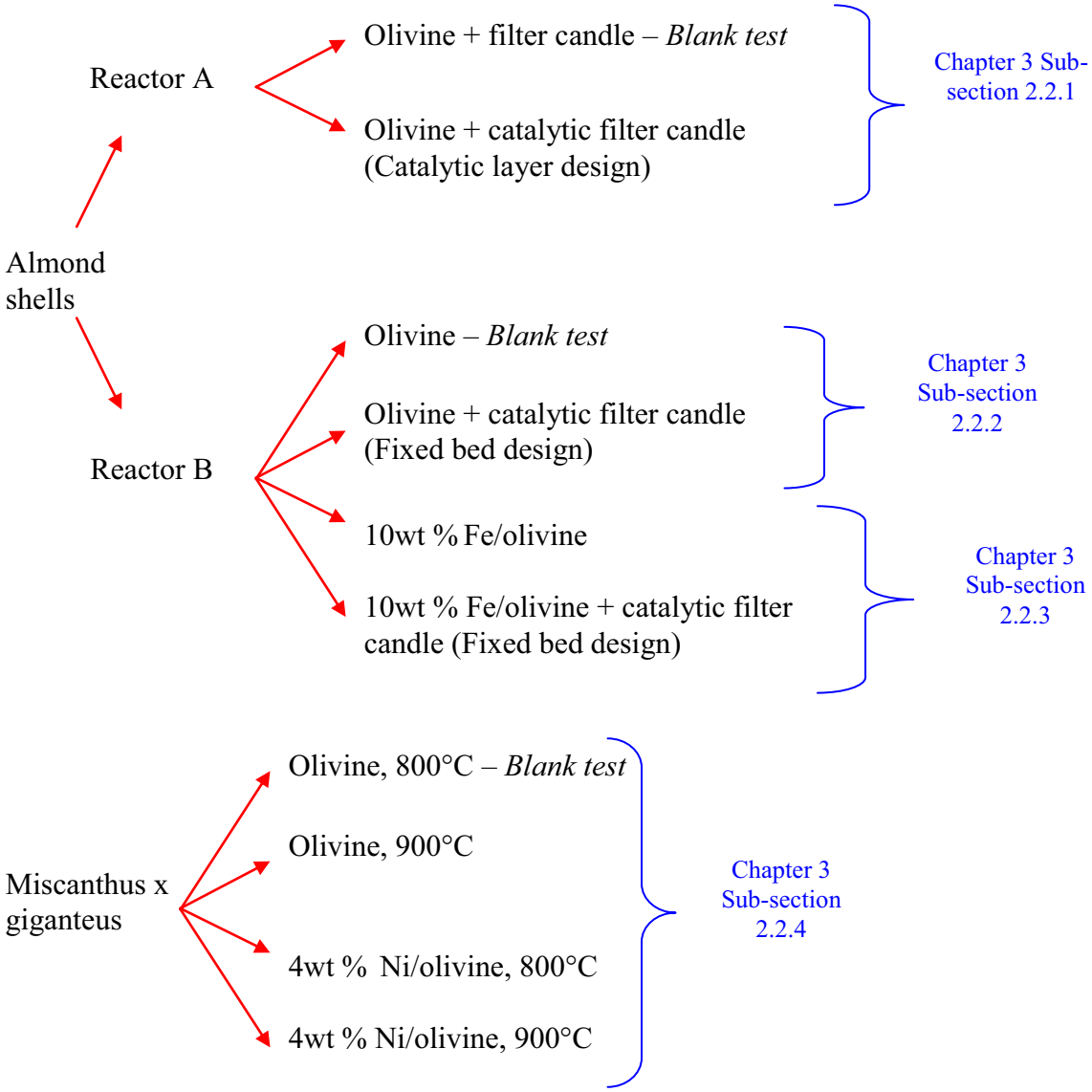

Figure 1: Set of experiments carried out in the University of Teramo

Développement d'un protocole d'analyse des goudrons réalisé à Metz (UPVM)

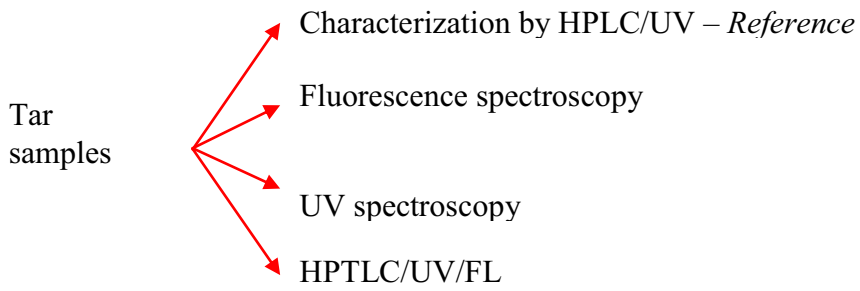

Figure 2: Développement analytique effectués au LCME de l'UPV Metz

Objectifs

- En termes de rendement et de pureté des gaz de synthèse obtenus à partir de coques d'amande et de MXG
- Evaluation de l'activité catalytique (catalyseurs primaires au cœur du réacteur et secondaires dans les filtres céramiques
- Influence des paramètres conditions opératoires sur les performances (rendements, bilans pondéraux, composition des gaz, taux de conversion)
- Caractérisation chimique des goudrons
- Mise au point d'un protocole original d'analyse des goudrons

I Analyse de la valorisation énergétique de la biomasse

I.1 Rappel sur les préconisations européennes

Il s'agit de la règle des trois vingt («20-20-20»), connue et acceptée par tout le monde, dont la dernière directive date de 2009:

- Diminution de 20 % des émissions de gaz par rapport au niveau de 1990
- 20 % des énergies doivent provenir d'une source renouvelable
- Diminution de 20 % de l'utilisation des énergies primaires par amélioration technologique

I.1.1 Place de la biomasse dans les objectifs 2020 : cas de l'Italie et de la France

Lorsqu'on regarde les réponses de la France et de l'Italie aux recommandations européennes, (tableau I), on peut noter que les objectifs sont ambitieux, et que par ailleurs la place de la biomasse dans les énergies alternatives est conséquente, le bois devant rester la ressource principale, mais sans écarter les autres origines (déchets, plantes…). Ainsi, à l'horizon 2020, les deux pays espèrent pouvoir produire respectivement 22 (France) et 17 (Italie) millions de Tonnes équivalent Pétrole (TEP) à partir de la biomasse.

TABLEAU I. Estimation de l'importance de la biomasse dans les énergies renouvelables selon les objectifs 2020 en France et en Italie

	FR	IT
2020 target (%)	23	17
Expected amount of Energy from RES, corresponding to the 2020 target (Mtoe)	35.6	22.6
Expected amount of energy from biomass (domestic supply) – NREAPs (Mtoe)	21.8	12.9
Energy from biomass (domestic supply) in total renewables (%)	61	57

I.2 Les sources de biomasse et leurs principales caractéristiques

La figure 3 rassemble les différentes sources de biomasse, différenciées des énergies fossiles du fait d'un bilan carbone théorique à zéro CO_2 lors de leur transformation énergétique, en particulier la combustion

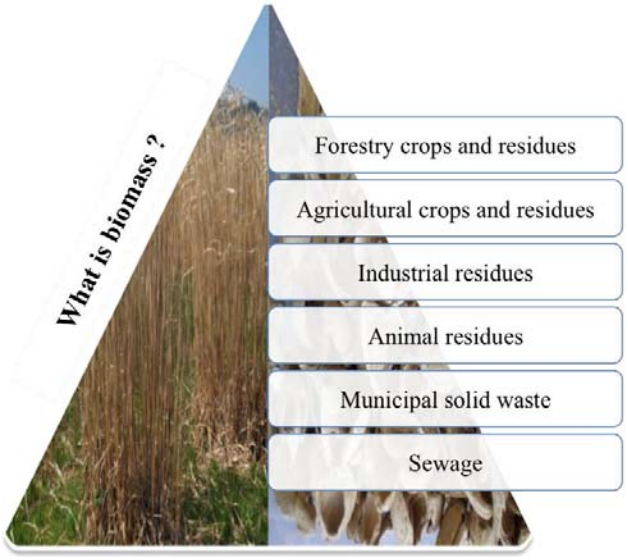

Figure 3: Différentes sources de biomasse

I.2.1 Les caractéristiques de la biomasse

Parmi les différentes catégories de biomasse utilisables dans le domaine des énergies renouvelables, les caractéristiques les plus déterminantes peuvent être résumées comme suit :

- Le pouvoir calorifique inférieur (PCI) ou supérieur (PCS), selon qu'on prenne en considération ou non la condensation de l'eau produite par combustion. Il représente certainement le paramètre le plus important en terme de valorisation énergétique, et dépendra évidemment de la composition élémentaire en C, H et O du composé. On peut estimer approximativement un incrément 0.39MJ/Kg par % supplémentaire de carbone pour le PCI d'une biomasse, une valeur de base pouvant être celle du bois, comme le peuplier par exemple, qui a une valeur de 18.5 MJ/Kg, comparée au charbon qui tourne autour de 30MJ/Kg

- L'humidité intrinsèque ou venant de l'environnement climatique, pouvant varier de 5 à 35% et qui va influencer sur les résultats en fonction aussi du procédé utilisé
- La teneur en matières volatiles et la valeur en Carbone fixe, qui sont des paramètres permettant de prévoir le comportement de la biomasse dans un traitement thermique
- Les matières minérales, qui se retrouvent sous forme de cendres. L'importance de la présence de certains éléments (Si, K, Ca, Cl…)peut avoir des répercussions plus ou moins néfastes dans certains procédés (corrosion, émanation de polluants, formation de mâchefer..)
- La densité, qui, lorsqu'elle est trop faible (la paille par exemple), génère des coûts importants de stockage et de transport, et nécessite par ailleurs des conditionnements adaptés en tant que matière première dans les procédés (granulés par exemple)

Par rapport à ces caractéristiques, il est important d'optimiser celles-ci, en termes de type d'énergie à produire (électricité, chaleur, biofuels) et d'adapter le type de biomasse au procédé envisagé. Par exemple, la biomasse peut-être un candidat intéressant pour envisager la gazéification à la vapeur d'eau, permettant de produire des gaz de synthèse ($CO+ H_2$)

I.3 Le Miscanthus X Giganteus, un candidat intéressant pour les énergies renouvelables

Le Miscanthus X Giganteus (MXG) est une herbe vivace à rhizome, appelé également herbe à éléphants d'origines tropicales et subtropicales, mais différentes espèces se retrouvent essentiellement en Asie de l'Est. Le Miscanthus a une remarquable capacité d'adaptation à différents environnements ce qui fait de cette nouvelle culture une plante appropriée pour les conditions climatiques de l'Europe et de l'Amérique du Nord.

Le MXG fait partie des plantes en C4 qui convertissent plus efficacement les nutriments, l'eau et les radiations solaires (+40% par rapport aux plantes C3) que les autres plantes par un mécanisme de photo respiration amélioré.

Composition du Miscanthus

En termes d'analyse élémentaire (Tableau II), le MXG est tout à fait classique de ce qu'on peut trouver dans la biomasse en général, le MXG se caractérisant également par une teneur en cellulose importante.

TABLEAU II: Composition du Miscanthus X Giganteus

Composition de la matière sèche (%)		Analyse élémentaire (%)		Composition des cendres (%)	
Cellulose	43	C	48,67	CO_3	4,53
Hémicellulose	27	H	5,45	SO_3	3,42
Lignine	24	O	42,5	Cl	3,39
Cendre	< 4	S	0,04	P_2O_6	3
		N	0,45	SiO_2	49,17
		Cl	0,23	Fe_2O_3	0,2
		Cendres	2,76	Al_2O_3	0,2
				CaO	4,57
				MgO	3,25
				Na_2O	0,21
				K_2O	23,74
				Autres	4,32

A côté de la silice, prédominante, les cendres contiennent de grandes quantités de potassium (K) et de calcium (Ca). C'est essentiellement ces éléments qui sont responsables du faible point de fusion de cendres du MXG (800-900°C). En outre, lors de la combustion du K peut être émis avec Cl sous la forme de gaz KCl. Ceci provoque la corrosion des surfaces de chauffage et la désactivation du catalyseur. Le pouvoir calorifique du miscanthus est de 16400 $kj.kg^{-1}$ soit environ 53% de celui de la houille (31000 $kJ.kg^{-1}$) .

II. Le point sur la gazéification de la biomasse

De manière générale, la gazéification .consiste en un procédé thermique permettant, via un agent chimique comme la vapeur d'eau, combinée ou non avec

de l'oxygène, d'obtenir à partir d'une matière première riche en carbone (charbon, résidus pétroliers, biomasse, méthane, déchets d'origines diverses) un gaz composé d'hydrogène et d'oxyde de carbone, pouvant être un excellent combustible ou servir , lorsqu'il est suffisamment propre, de matière première à la synthèse de nombreux produits chimiques de base

Les mécanismes chimiques intervenant dans le procédé sont complexes et peuvent être schématisés en quatre étapes principales et successives: une réduction importante de l'humidité, une première décomposition sous forme de pyrolyse produisant des matières volatiles et des goudrons (structures aromatiques plus ou moins condensées), une oxydation dont l'importance va dépendre de la quantité d'oxygène actif présent, et enfin en dernier lieu la gazéification elle-même sous forme de réduction des principaux composés intermédiaire par la vapeur d'eau principalement

De manière plus précise, les principales réactions qui interviennent dans le milieu sont les suivantes :

- La réaction principale et espérée concerne celle entre la vapeur d'eau et le carbone

  $C + H_2Ov \rightarrow H_2 + CO$ $\Delta H^0 = +131.4$ kJ/mol (1)

- La reaction de Boudouard qui consommé du carbone

  $CO_2 + C \rightarrow 2CO$ $\Delta H^0 = +172.6$ kJ/mol (2)

- La réaction du gaz à l'eau (Water-gas shift reaction WGS) qui permet d'augmenter les rendements en hydrogène

  $CO + H_2O_v \rightarrow CO_2 + H_2$ $\Delta H^0 = -42.0$ kJ/mol (3)

- Une réaction de méthanisation, indésirable dans le cas de la gazéification, peut se produire par réaction entre le carbone et l'hydrogène

  $C + 2H_2 \rightarrow CH_4$

Globalement on obtient un mélange gazeux qui contient du CO, H_2, CO_2, mais également des quantités plus ou moins importantes de composés indésirables : H_2S, HCl , NH_3, des goudrons et des particules.

En ce qui concerne les goudrons, qui font l'objet d'une partie importante de ce travail de thèse, on peut résumer l'évolution de leur structure sur le schéma suivant (Tableau III).

TABLEAU III: Evolution of de la composition des goudrons en function de la temperature [Milne et al, 1998]

Mixed oxigenates	→	Phenolic ethers	→	Alkyl phenolics	→	Heterocyclic ethers	→	PAHs	→	Larger PAHs
400°C		500°C		600°C		700°C		800°C		900°C

II.1 Technologies de purification des gaz

Dans notre étude, nous avons utilisé un réacteur à lit fluidisé qui sera décrit un peu plus loin.

Un problème essentiel est la purification des gaz formés, par différents procédés

En premier lieu, les particules produites ou entraînées dans le circuit sont éliminées au moyen d'un cyclone et de filtres

En ce qui concerne les goudrons, leur élimination est réalisée par cracking au moyen de catalyseurs appropriés souvent à base de dolomite ou d'olivine, en imprégnant le support d'un métal actif comme le Nikel ou le Fer.

II.2 Caractérisation des goudrons

Cette partie fait l'objet des chapitres IV et V

Il faut noter qu'il est essentiel, avant toute analyse, de s'affranchir du problème de l'échantillonnage des goudrons, qui doivent être récupérés, totalement ou en partie, en étant certain qu'ils soient représentatifs de l'ensemble des composés générés durant la réaction. C'est pourquoi nous avons adopté un protocole normalisé (*Technical specification UNI CEN/TS 15439:2008)*

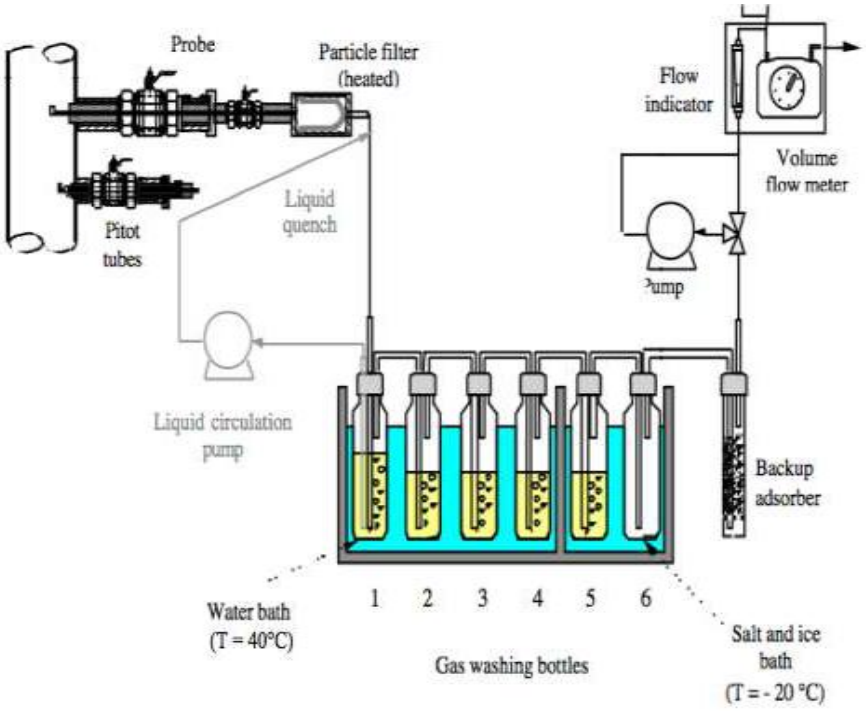

Figure 4 : Prélèvement des gaz

Le schéma de la figure 4 ci-dessus décrit la technique utilisée pour prélever les gaz, en effectuant un bullage dans l'isopropanol comme solvant.

III. La gazéification de la biomasse : Expériences et résultats

III.1. Partie expérimentale

Nous rappelons que les expériences de gazéification ont été réalisées sur le MXG, d'origine allemande (Trèves) sous forme de granulés de 8 puis de 6 mm, et d'autre part sur de la coque d'amande d'origine italienne, broyée et tamisée à 1mm. A partir du moment où nous avons adapté un filtre catalytique, le diamètre du tube d'alimentation ne permettait plus d'utiliser les granulés (bouchage de la canne d'alimentation provoquant des irrégularités au niveau des flux et des débits de gaz). De ce fait, toutes les expériences effectuées par la suite ont utilisé la coque d'amande.

Description de l'appareillage :

Le schéma ci-dessous (figure 5) décrit les principaux éléments constituants le montage du réacteur pilote développé à Teramo :

- Une alimentation en biomasse régulée par une vis d'Archimède, la biomasse étant chargée dans le réacteur via un tube de 0.1 m de diamètre interne. Le réacteur sera surmonté d'un système de support imprégné de catalyseur
- Un générateur de vapeur qui arrive par la partie inférieure, en mélange avec de l'azote
- Un cyclone et un filtre céramique pour éliminer les particules
- Des condenseurs pour piéger les goudrons, avec un système en dérivation utilisant de l'isopropanol, selon la norme CENT/TS 15439
- Des systèmes permettant d'analyser en continu les gaz formés, et de contrôler les débits gazeux

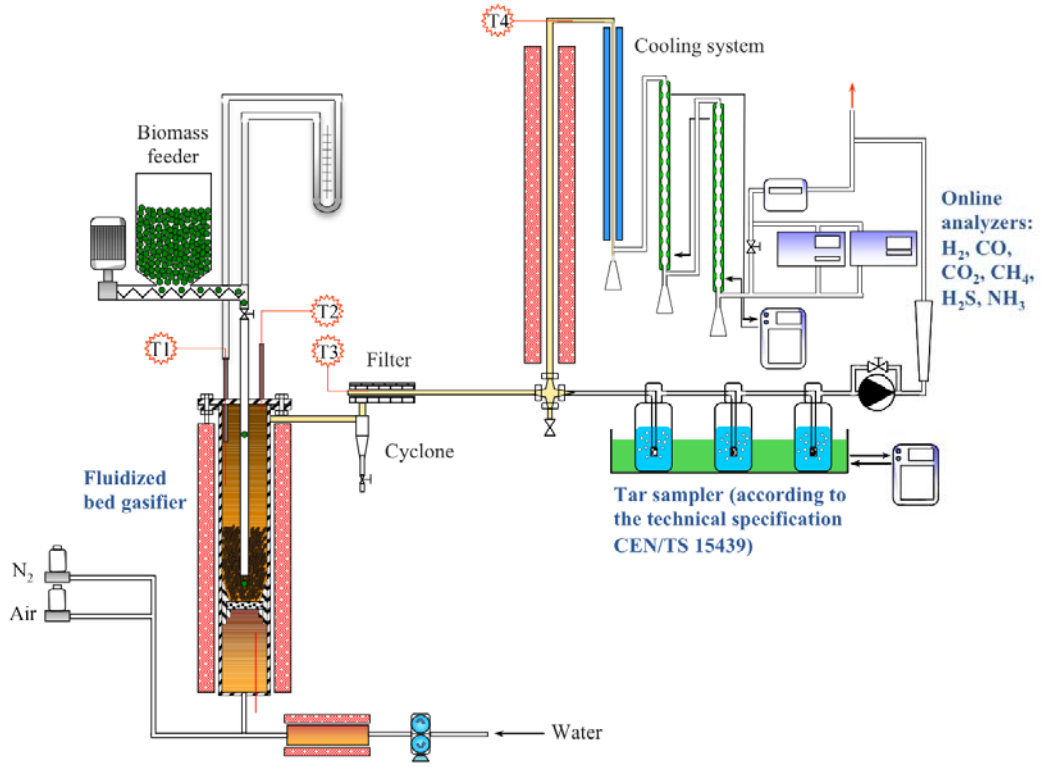

Figure 5 : Pilote de gazéification

En ce qui concerne l'aspect catalyse, très importante en gazéification pour minimiser la formation des goudrons et ainsi améliorer les rendements en gaz de synthèse propre, en plus de systèmes catalytique tels que l'olivine, le Ni-Olivine , le Fe-Olivine, introduits dans le cœur du réacteur, nous avons , dans un souci de meilleure efficacité, complété le montage par un système secondaire de bougies

filtrantes à activité catalytiques qui présentent un intérêt en lit fluidisé pour une meilleure élimination des goudrons.

Le schéma ci-dessous décrit le système de bougie céramique catalytique-non catalytique installé sur la partie supérieure du réacteur.

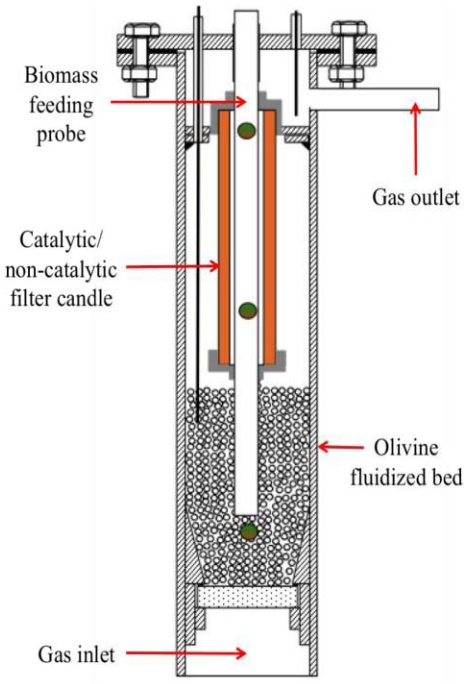

Figure 6 : Système de bougie céramique catalytique-non catalytique installé dans le reactor

Les tableaux suivants (IV, V, VI, VII), décrivent les conditions opératoires des différentes séries d'expérience (1 à 4) menées à Teramo

TABLE IV: Operating gasification conditions: OL = olivine; FC = Filter Candle; CFC = Catalytic Filter Candle (N250107001)

Gasification test	1-I	1-II	1-III	1-IV	1-V	1-VI
Duration, min	60	60	120	60	60	30
Bed temperature, °C	720-803	829	840	832	831	831
Biomass flow rate, g/min	8.0	8.0	8.0	8.0	8.0	10.0
N_2 flow rate, l/min	14.0	16.5	16.5	16.5	6.0	0
Steam feeding rate, g/min	6.6	6.6	6.7	7.2	7.8	13.3
Bed material	OL	OL	OL	OL	OL	OL
Filter candle	FC	FC	CFC	CFC	CFC	CFC

TABLE V: Operating gasification conditions. OL = Olivine; CFC = Catalytic Filter Candle (J041108.1)

Gasification test	2-I	2-II	2-III	2-IV	2-V	2-VI	2-VII	2-VIII	2-IX	2-X
Duration, min	60	90	56	120	120	160	120	180	240	230
Bed temperature, °C	808	815	808	814	813	814	813	813	811	808
Biomass flow rate, g/min	8.0	9.0	9.0	6.0	6.0	4.5	5.5	6.0	6.0	6.0
Nitrogen flow rate, l/min	11.2	12.0	12.0	11.2	12.0	9.0	6.0	5.0	5.0	5.4
Steam feeding rate, g/min	8.5	8.4	9.0	6.6	6.3	3.8	6.2	6.2	6.0	6.0
Bed material	OL	OL	OL	OL	OL	OL	OL	OL	OL	OL
Filter candle	-	CFC	CFC	CFC	CFC	CFC	CFC	CFC	CFC	CFC

TABLE VI : Operating gasification conditions. Fe/OL = 10wt %Fe/olivine; CFC = Catalytic Filter Candle (J041108.1)

Gasification test	3-I	3-II	3-III	3-IV	3-V
Duration, min	154	80	120	120	150
Bed temperature, °C	828	821	820	814	812
Biomass flow rate, g/min	5.0	5.0	5.7	5.0	5.6
Nitrogen flow rate, l/min	11.2	11.2	6.0	11.2	6.0
Steam feeding rate, g/min	6.0	6.0	6.0	6.0	5.0
Bed material	Fe/OL	Fe/OL	Fe/OL	Fe/OL	Fe/OL
Filter candle	-	-	-	CFC	CFC

TABLE VII : Operating gasification conditions. OL = OL = Ni-olivine

Gasification test	4-I	4-II	4-III	4-IV
Duration, min	60	60	120	60
Bed temperature, °C	798	899	799	901
Biomass flow rate, g/min	8.0	8.0	8.0	8.0
Nitrogen flow rate, l/min	17.0	17.0	17.2	17.0
Steam feeding rate, g/min	8.2	8.2	8.2	8.4
Bed material	OL	OL	Ni/OL	Ni/OL
Filter candle	-	-	-	-

III.2 Résultats et discussions

III.2.1 Coque d'amande avec un filtre commercial sans catalyseur (I-I et I-II) puis utlisant un support catalytique (I-III à I-VI, avec un précurseur MgO-Al_2O_3 imprégné de NiO)

Les résultats sont décrits tableau VIII. Ils sont principalement exprimés en termes de rendements et composition en gaz, conversion de la vapeur d'eau et du carbone)

On peut relever l'efficacité du filtre catalytique, qui se traduit par une augmentation significative du rendement en gaz de synthèse, en hydrogène et une réduction importante des goudrons. Par contre, dans cette configuration, le filtre s'est trouvé bloqué et a été endommagé par des problèmes de surpression menant à une cassure de la céramique

TABLE VIII : Results of almond shells steam gasification tests with a commercial filter candle (1-I and 1-II) and with a catalytic filter candle of "catalytic layer" design (1-III – 1-VI) housed in the gasifier freeboard.

	1-I	1-II	1-III	1-IV	1-V	1-VI
Duration of test (min)	60	60	120	60	60	30
Gasifier bed temperature (ºC)	720-803	829	840	832	831	831
Gasifier outlet temperature (°C)	675-715	750	791	780	801	801
Steam/biomass dry	0.89	0.89	0.91	0.97	1.06	1.44
Water conversion %	16	19	37	27	39	35
Gas yield (Nm^3 dry/kg daf)	0.9-1.1	1.30-1.40	1.60	1.60	1.55	1.80
Tar content (g/Nm^3 dry)	6.03	1.90	0.72	n.a.	0.70	0.92
Char residue (g/kg daf)	97	71	82	70	55*	
Carbon conversion %	79	85	89	85	88	
H_2 (vol% dry gas, N_2 free)	35-47	44	48	48	49	50
CO_2 (vol% dry gas, N_2 free)	22	21	20	21	22	23
CO (vol% dry gas, N_2 free)	32-26	26	26	25	23	21
CH_4 (vol% dry gas, N_2 free)	13-8	10	6	6	6	6
Filtration velocity (m/h)	85	106	145	110	77	64

*The total amount of char residue is relative to tests V and VI

III.2.2. Coque d'amande avec un filtre présentant un lit catalytique fixe (support SiC recouvert de MgO avec Ni), avec l'olivine comme catalyseur principal (série 2), puis avec de l'olivine imprégnée de Fer (série 3)

Les résultats sont présentés sur les tableaux IX et X. Un plus grand nombre de tests ont été réalisés avec ce montage (série 2), en faisant par exemple varier la durée des expériences, ou en recommençant certains essais avec le même filtre. De nouveau, les résultats confirment l'effet nettement positif du filtre catalytique sur les rendements et la qualité des gaz de synthèse obtenus.

Les meilleurs résultats ont été obtenus avec le Fer imprégné dans l'olivine (série 3).

On peut noter également que le filtre céramique a eu une meilleure tenue mécanique lors de sa récupération à la fin des manipulations, en particulier en minimisant le dépôt de particules sur les filtres, et en optimisant la vélocité des gaz à travers le filtre

TABLEAU IX: Results of steam gasification of almond shells with olivine bed inventory (2-I) and with a catalytic filter candle of "fixed bed" design (test 2-II – 2-X) housed in the gasifier freeboard.

	2-I	2-II	2-III	2-IV	2-V	2-VI	2-VII	2-VIII	2-IX	2-X
Duration of test (min)	*60*	90	56	120	120	160	120	180	240	230
Gasifier bed temperature (ºC)	*808*	815	808	814	813	814	813	813	811	808
Gasifier outlet temperature (°C)	*738*	816	816	825	815	818	822	812	809	819
Steam/biomass dry	*1.06*	0.94	1.00	1.10	1.06	0.85	1.13	1.03	1.00	0.99
Water conversion %	*16*	34	24	21	35	40	36	37	41	42
Gas yield (Nm^3 dry/kg daf)	*1.00*	1.65	1.54	1.49	1.62	1.60	1.68	1.77	1.77	1.79
Tar content (g/Nm^3 dry)	*3.67*	0.91	0.95	0.79	0.55	0.71	0.75	0.81	0.85	0.75
Char residue (g/kg daf)	*94*	68	107	70	68	78	66	48	36	41
Carbon conversion %	*80*	86	78	85	86	84	86	90	92	91
H_2 (vol% dry gas, N_2 free)	*39*	50	52	55	56	52	54	53	53	53
CO_2 (vol% dry gas, N_2 free)	*26*	23	23	22	21	19	22	20	20	20
CO (vol% dry gas, N_2 free)	*24*	21	22	20	20	23	19	22	22	22
CH_4 (vol% dry gas, N_2 free)	*10*	5	4	4	4	5	5	5	5	5
Filtration velocity (m/h)	-	102	95	81	79	63	61	62	61	62

TABLEAU X: Results of steam gasification of almond shells with 10wt% Fe/olivine bed inventory (3-I, 3-II and 3-III) and with 10wt% Fe/olivine + catalytic filter candle with "fixed bed" design (3-IV and 3-V)

	2-I	3-I	3-II	3-III	3-IV	3-V
Duration of test (min)	*60*	154	80	120	120	150
Gasifier bed temperature (ºC)	*808*	828	821	820	814	812
Gasifier outlet temperature (°C)	*738*	818	724	717	829	720
Steam/biomass dry	*1.06*	1.3	1.3	1.14	1.3	1.02
Water conversion %	*16*	20	19	25	29	37
Gas yield (Nm^3 dry/kg daf)	*1.00*	1.37	1.42	1.41	1.75	1.69
Tar content (g/Nm^3 dry)	*3.67*	1.18	1.67	n.a.	0.30	n.a.
Char residue (g/kg daf)	*94*	125	101	115	126	121
Carbon conversion %	*80*	74	79	77	74	75
H_2 (vol% dry gas, N_2 free)	*39*	53	53	52	56	54
CO_2 (vol% dry gas, N_2 free)	*26*	28	27	26	22	21
CO (vol% dry gas, N_2 free)	*24*	13	15	16	17	20
CH_4 (vol% dry gas, N_2 free)	*10*	6	6	6	4	5
Filtration velocity (m/h)	-	-	-	-	77	60

III.2.3 Gazéification du MXG , sans utilisation de filtre, en présence d'olivine et d'olivine imprégnée de Nickel (série 4, tableau XI)

Tableau XI: Results of MXG steam gasification tests with olivine bed inventory (test 4-I and 4-II) and Ni-olivine bed inventory (tests 4-III – 4-IV) at different operating temperatures

	4-I	4-II	4-III	4-IV
Duration of test (min)	60	60	120	60
Gasifier bed temperature (ºC)	798	899	799	901
Gasifier outlet temperature (°C)	752	841	786	897
Steam/biomass dry	1.10	1.10	1.10	1.10
Water conversion %	11	29	31	28
Gas yield (Nm3 dry/kg daf)	1.00	1.54	1.70	1.64
Tar content (g/Nm3 dry)	2.87	1.25	0.41	n.a.
Char residue (g/kg daf)	97	51	97	n.a.
Carbon conversion %	79	89	81	n.a.
H2 (vol% dry gas. N2 free)	37	45	50	50
CO2 (vol% dry gas. N2 free)	25	23	24	24
CO (vol% dry gas. N2 free)	24	22	19	19
CH4 (vol% dry gas. N2 free)	14	10	7	7

Dans ces expériences, ce sont essentiellement les paramètres température et la présence de Nickel qui on permis d'obtenir des résultats tout à fait corrects, avec un effet positif très net du Nickel, et une température optimale aux alentours de 850°C.

III.3 Conclusions

Les nombreuses expériences réalisées dans différentes conditions opératoires et avec des configurations originales mises au point à Teramo ont donné des résultats encourageants aussi bien au niveau des rendements en gaz de synthèse, comparables à ce qui a été trouvé sur d'autres types de biomasse, qu'au niveau du reformage des goudrons et que l'abattement de gaz indésirables comme CH_4, NH_3 et H_2S

L’adaptation d’un filtre catalytique à support fixe semble mieux adaptée, permettant une meilleure tenue mécanique du filtre et une meilleure accessibilité du Nickel en tant que catalyseur secondaire

En ce qui concerne le catalyseur primaire, logé au cœur du réacteur, le Fer sur Olivine a montré une excellente activité, et semble bien adapté pour des raisons économiques et environnementales.

IV. Caractérisation des goudrons issus de la gazéification de la biomasse par CLHP/UV

IV.1 Introduction

Pour évaluer l'efficacité du procédé Une analyse quantitative des goudrons dans le flux de syngas est fondamentale, ainsi que l'étape de conversion catalytique. Les problèmes pouvant résulter d'un encrassement du réacteur n'est pas lié à la quantité de goudrons mais à leur propriété et composition. La condensation de ces molécules est liée à l'ensemble du mélange composant le goudron présent dans le syngas.

Afin de pouvoir quantifier de façon représentative les composés organiques présents dans les goudrons, une méthode standardisée de prélèvement a été installée au niveau de l'équipement de gazéification en accord avec les spécifications de UNI CEN/TS 15439. Cette méthode est basée sur un prélèvement fractionnaire des goudrons dans le flux gazeux en régime stable (mode isocinétique) à la sortie du réacteur (chapitre II) : les goudrons volatils sont piégés par condensation lors du bullage des gaz dans de l'isopropanol. Le dosage est ensuite effectué après séparation en chromatographie liquide couplée à une détection par UV.

IV.2 Matériels et méthodes

Le dosage des goudrons est effectué après identification des composés aromatiques présents (obtenu par GC-MS, confirmé par les résultats décrits dans la littérature)

Des solutions mères des composés aromatiques à 1 mg/ml ont été préparées dans le dichlorométhane ou le méthanol pour préparer des solutions de mélange d'étalons dans l'isopropanol.

Les composés aromatiques quantifiés, ainsi que les conditions chromatographiques sont données page 103 et 104 de ce manuscrit.

IV.3 Résultats et discussions

IV.3.1 Validation de la méthode d'analyse

La quantification des 12 composés aromatiques majoritaires (confirmés par les données de la littérature Devi et al., 2005), présents dans les goudrons a été réalisée par étalonnage externe. Des courbes de calibration ont été obtenus en utilisant au moins 6 points de concentration, avec un nombre de répétition au moins de 3. Les paramètres de l'étalonnage sont regroupés dans le tableau XII.

Les concentrations des limites de détection et quantifications ont été déterminées respectivement pour 3 et 10 écarts types d'un échantillon à blanc et permettent de quantifier de faibles teneurs en composés aromatiques piégés dans le dispositif utilisé.

Les concentrations en goudrons ramenés au volume de gaz produits (mg/Nm^3) ont ainsi été déterminées en connaissant le volume de gaz bullant dans l'isopropanol, et les volumes de solvants utilisés.

La CLHP couplée à une détection UV a servi de méthode de référence pour les autres approches qui seront développées par la suite.

TABLEAU XII : Données de validation pour le dosage des composes aromatiques

	t_r (min)	C_{min} (mg/l)	C_{max} (mg/l)	n	Slope	y-intercept	R^2	LOD (mg/l)	LOQ (mg/l)
Ph-OH	5.5	5.33	1065.00	18	91.46	-154.12	0.996	3.14	6.55
Tol	18.1	14.00	2300.00	26	35.30	65.89	0.999	1.95	6.51
Styr	19.8	0.89	53.10	6	1622.93	-54.72	0.998	0.17	0.49
Ind	20.4	1.02	108.00	12	1114.22	1770.06	0.997	0.33	1.12
Nap	21.6	1.00	200.00	18	394.07	1575.17	0.991	0.06	0.22
Bph	22.3	0.21	41.20	16	2059.28	-535.52	0.990	0.28	0.32
DphE	27.9	1.36	150.00	13	337.4	1496.5	0.992	0.23	0.77
Fle	30.4	0.32	39.38	15	2903.10	-2431.60	0.998	0.86	0.93
Phe	31.9	0.11	16.50	16	4230.02	1431.75	0.995	0.03	0.10
Ant	33.5	0.05	5.50	18	8214.59	1174.03	0.992	0.01	0.03
Fla	36.2	0.42	39.75	13	1698.96	-823.01	0.999	0.53	0.77
Pyr	37.3	0.30	29.70	13	1318.98	-40.16	0.997	0.06	0.14

IV.3.2 Caractérisation des goudrons issus de la gazéification de la biomasse.

La biomasse, sous forme de granulats de coques d'amandes ou de miscanthus giganteus a été utilisée sous différentes conditions de gazéification avec un ensemble de système catalytique commerciaux ou produits par des partenaires industriels ou Universitaires .

La figure 7 représente la proportion de goudrons obtenus pour la gazéification des coques d'amande avec un catalyseur commercial (PALL GmbH). Les principaux composés sont constitués d'HAP légers (toluène, naphtalène indène et phénol). L'influence de la température est confirmée : l'augmentation de la température de 720 à 830°C permet de diminuer la teneur en goudron de de 9,7 à 7,3 g/Nm^3 de syngas.

A l'exception du styrène et du diphényl-éther, présentant une concentration qui a peu évoluée, ainsi que le naphtalène connu comme réfractaire au traitement thermique, la concentration des autres composés a significativement diminuée, pour obtenir une diminution de 40% pour les composés à 3 et 4 noyaux aromatiques.

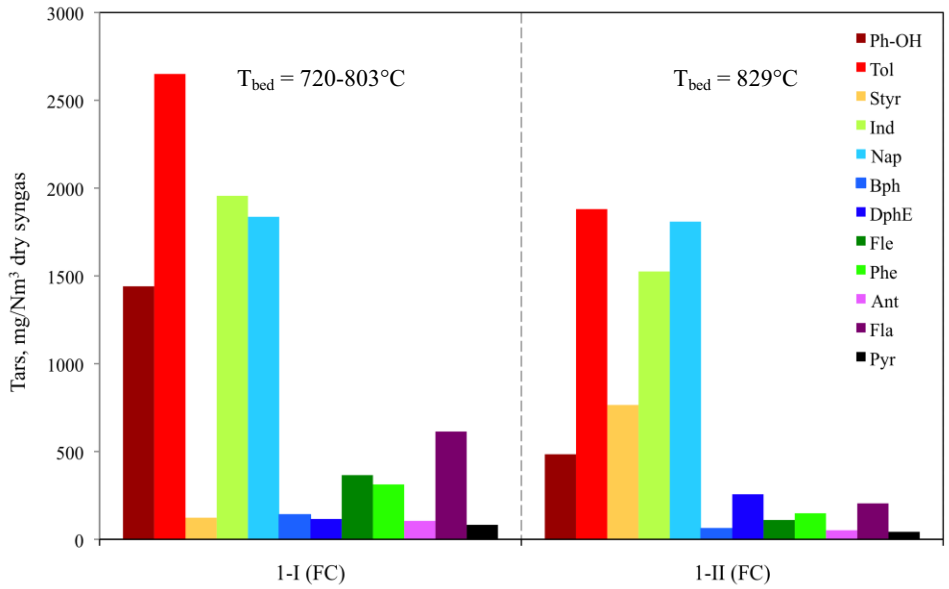

Figure 7: composition des goudrons issus de la gazéification de coques d'amandes sur bougie catalytique

L'activité de reformage des nouvelles bougies catalytiques en céramique a été évaluée en lit fixe avec les coques d'amande (figure 8) et ce, pendant 22h. Les

composés majoritaires formés dans les goudrons sont le toluène et le naphtalène. Cependant les teneurs sont bien moindres que dans le test de référence (sans bougie catalytique), montrant l'efficacité du reformage due au catalyseur à base de nickel. La même activité est montrée pour le reformage des HAP lourds, la plus grande activité ayant lieu durant les premières heures de fonctionnement. Cependant la quantité totale de goudron reste très basse : on observe en moyenne une concentration de 1,2 g/Nm^3 contre 8,6 g/Nm^3 pour le test de référence.

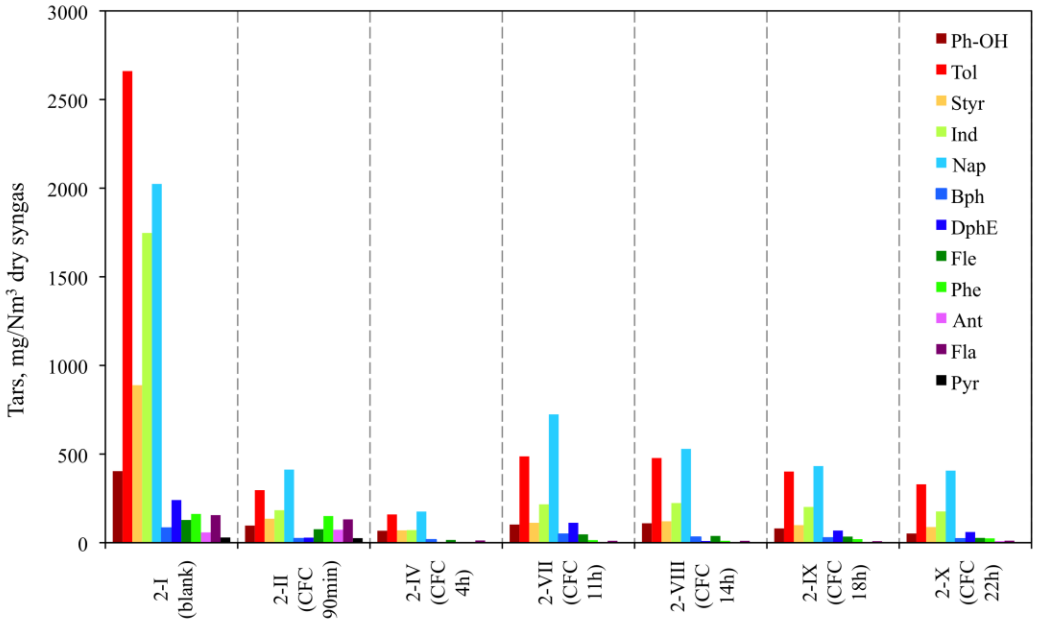

Figure 8: Evolution de la teneur en goudrons dans le syngas après gazéification de coques d'amandes sur bougie catalytique (CFC) en configuration lit fixe. Etude sur 22h ((2-II – 2-X) et test de référence (blank)

Des conditions similaires (bougies catalytiques, lit fixe) ont été utilisées en rajoutant de l'olivine (Fe/Olivine, 10% m/m) La composition des goudrons en présence et absence de bougie catalytique est montrée sur la figure 9.

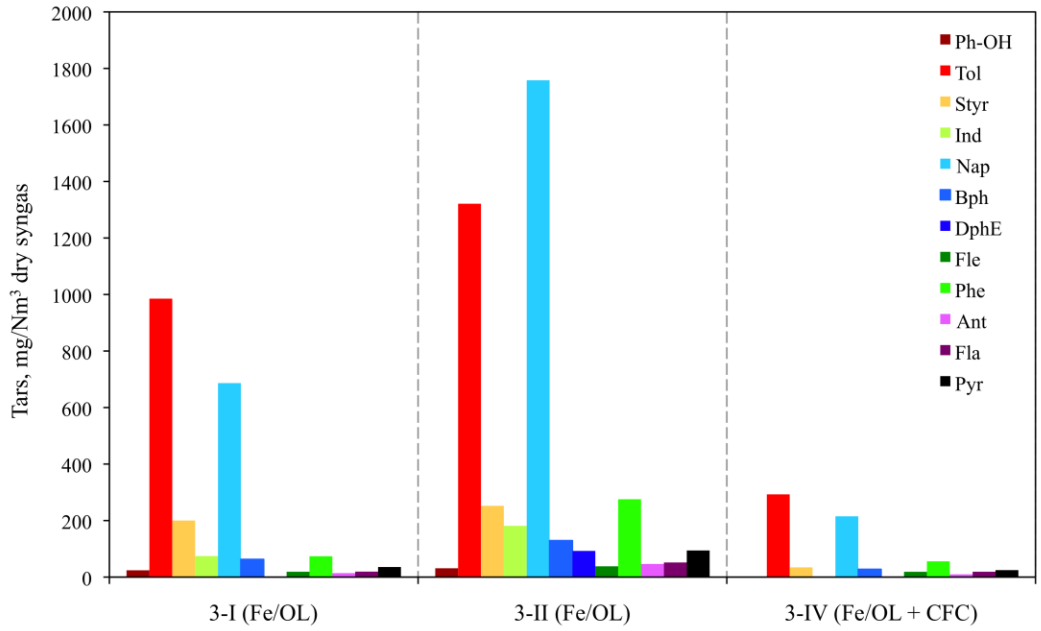

Figure 9: Composition des goudrons dans le syngas après gazéification en presence de Fe/Olivine (10wt % Fe/olivine 3-I and 3-II), ajout de la bougie catalytique (10wt % Fe/olivine plus CFC, 3-IV) sur lit fixe

En présence de Fer/Olivine, la concentration en goudron est réduite, grâce à l'activité de reformage du Fer. La teneur en goudron est réduite de plus de 70 % lorsque la Fer/olivine est utilisée par rapport à l'Olivine seule. La différence entre les tests 3-I et 3-II peut être expliquée par une différence de température dans le réacteur (818 et 724 °C respectivement), mais reflète également la difficulté du prélèvement d'échantillons selon la procédure normalisée, qui peut conduire à des différences dans l'échantillonnage. Lorsque le Fer/Olivine est associée au système de bougie catalytique (test 3-IV) une diminution importante des HAP légers et lourds est observée pour obtenir une concentration en goudron de 0,7 g/Nm^3 dans le gaz.

La gazéification de MXG a été menée en présence d'Olivine à 2 températures (800 et 900 C). L'influence du nickel sur l'olivine a également été évaluée (figure 10).

Les principales molécules sont composées d'aromatiques légers, l'augmentation de la température permettant une réduction significative de ces composés, excepté pour le naphtalène. L'utilisation de Nickel améliore les performances en terme de diminution des goudrons pour obtenir une concentration de 1,1 g/Nm^3 de gaz sec.

La production de goudron, ramenée au kg de biomasse est réduite de 80 %, comparé au test4-I.

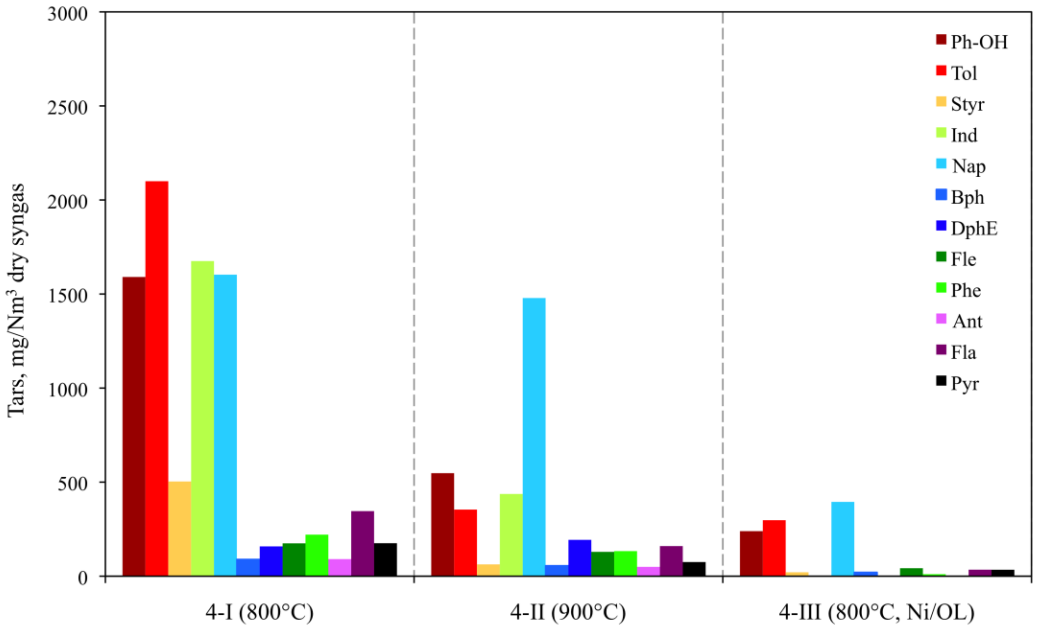

Figure 10: Distribution en goudrons pour la gazéification de MXG sur l'olivine à 800°C (4-I), 900°C (4-II) en présence de 4 % (m/m) Ni/olivine (4-III)

IV.3.3. Résumé des résultats les plus significatifs obtenus pour l'analyse des goudrons

L'ensemble des résultats obtenus sur les différentes campagnes de gazéifications sont regroupés dans la figure 11. Le tableau XIII montre l'évolution des teneurs en goudron dans le syngas en fonction des conditions opératoires. D'un point de vue qualitatif, il n'y a pas de différences significatives dans la composition des goudrons, quelle que soit la biomasse utilisée : les composés majoritaires sont constitués d'HAP de faible masse tels que le toluène, le styrène, l'indène et le naphtalène. La seule exception concerne la teneur en phénol, plus importante pour MXG. Cependant les 2 sources de biomasse montrent des résultats similaires, lorsque les conditions opératoires sont proches (test 2-I et test 4-I), la teneur en goudron relevée pour les coques d'amande est de 8,6 g/Nm^3 et de 8,7 g/Nm^3 pour MXG.

L'addition de Nickel au système catalytique permet de réduire les goudrons, grâce à son activité bien connue (4-III; 2-II,IV,VII-X).

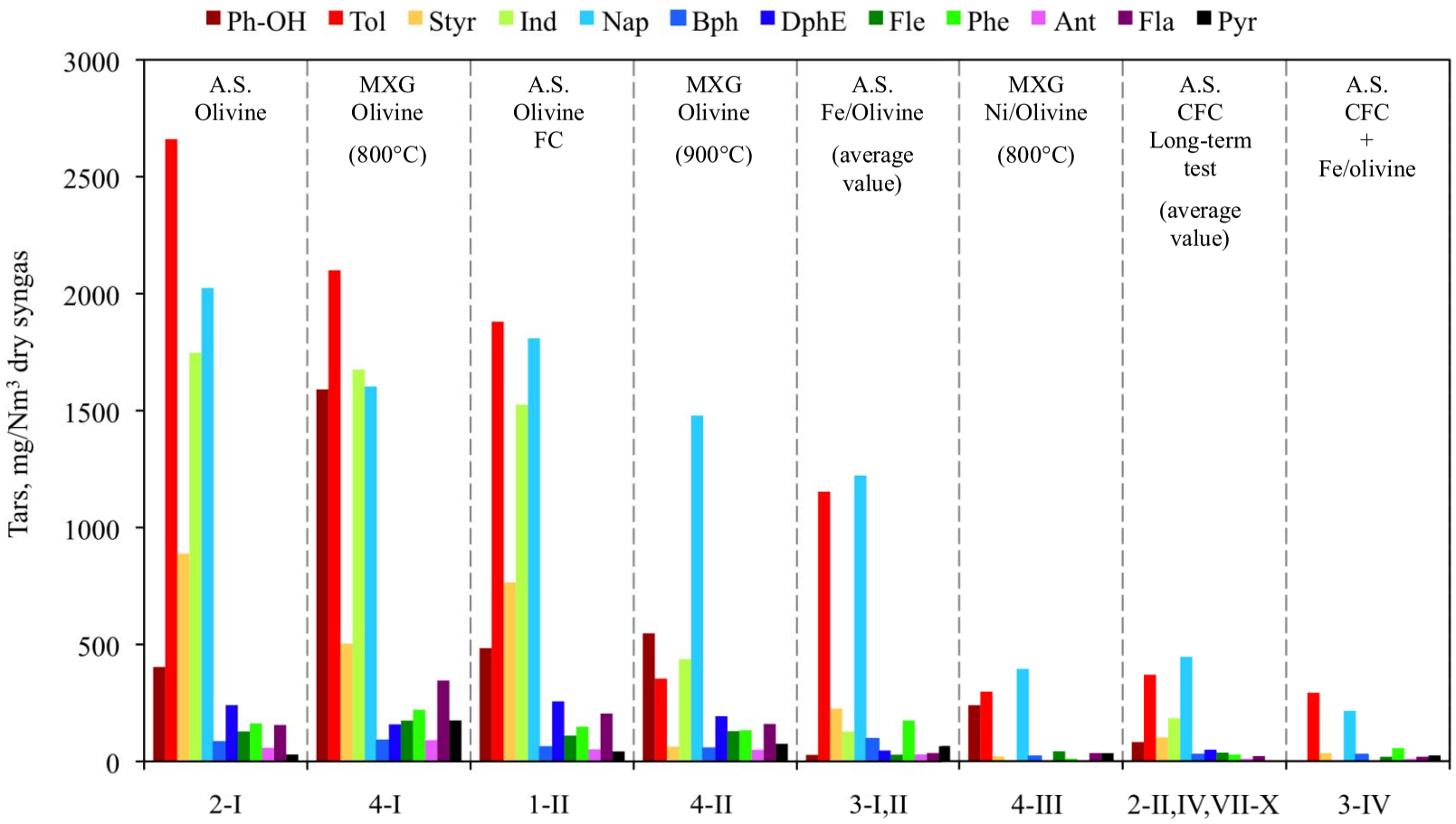

Figure 11: Distribution des goudrons issus de la gazéification (A.S. = coques d'amande)

Tableau XIII : Goudrons contenus dans les gaz obtenus lors des différentes campagnes, variation calculée par rapport au test 2-I (coque d'amandes sur lit d'olivine)

Gasification test	Tar content g/Nm^3 dry	Tar content in the producer gas, %	Tar content per kg biomass daf, %
2-I	***8.6***		
4-I	8.7	+2	+2
1-II	7.3	-14	15
4-II	3.7	-57	-36
3-I,II	3.2	-62	-48
4-III	1.1	-87	-78
2-II,IV,VII-X	1.4	-84	-73
3-IV	0.7	-92	-86

L'utilisation de Fer/Olivine conduit également au reformage de composés généralement réfractaires tels que le naphtalène. L'utilisation combinée de Fe/Olivine au système de bougie catalytique contenant du Nickel confirme l'effet synergique se traduisant par une diminution importante de goudrons.

IV.4. Conclusions

L'analyse des goudrons, échantillonnés selon le protocole normalisé UNI CEN/TS 15439 a été effectuée par chromatographie liquide couplée à une détection UV. Ces analyses ont montré le comportement similaire de la biomasse pour les mêmes conditions opératoires de gazéification : MXG peut être considéré comme une bonne source de biomasse pour la production de syngas.

Les performances des systèmes catalytiques ont pu être montrées, l'utilisation d'olivine imprégnée de fer est un système intéressant en tant que système de lit fluidisé. Le couplage à un deuxième système à base de Nickel porté par des bougies catalytiques améliore la conversion des goudrons, conduisant à des teneurs de 0,7 g/Nm^3 de goudrons.

V. Nouvelles méthodes pour l'analyse des goudrons

V.1 Analyse des goudrons en spectroscopie UV ou en chromatographie planaire

Les méthodes analytiques de référence demandent un temps d'analyse certain, et également un investissement en appareillage couteux. Le présent travail a visé à développer d'autres approches analytiques, pour proposer une technique facilement accessible dans tout laboratoire de chimie, la spectroscopie UV. Ainsi l'analyse sans séparation préalable est évaluée pour proposer un système adaptable pour un dosage en ligne.

Une autre approche repose sur le suivi par familles de composés aromatiques, une étude originale est proposée en chromatographie sur couches minces, couplée à une détection par UV ou par fluorescence.

V.2. Détermination des goudrons par spectroscopie UV

Une étude spectroscopique en UV a été effectuée sur l'ensemble des échantillons d'isopropanol obtenus après les tests de gazéification. Bien que le spectre représente une combinaison de l'absorption d'un grand nombre de composés aromatiques, il était intéressant de remarquer que l'intensité de l'absorption était le reflet de la concentration totale en HAP, malgré l'absence de bandes d'absorption caractéristiques d'un type de transition, qui n'est effectivement pas discernable dans le cadre de l'analyse de mélanges multicomposants.

Ainsi 2 approches ont été menées en parallèles, en s'appuyant au préalable sur le spectre d'absorption des solutions de goudrons condensés dans l'isopropanol :

- procéder par convolution de spectres étalons pour reconstituer le spectre du mélange de HAP
- mettre en évidence une relation entre l'absorption du mélange et la concentration en goudrons, et ce, indépendamment du pilote si il fonctionne sur le même procédé.

V.2.1 Dosages des goudrons par spectroscopie UV/Visible – Approche globale

Le dosage des composés organiques totaux est réalisable sur des analyseurs spécifiques après oxydations des composés organiques (TOC analyser), cependant elle ne peut être menée que sur des échantillons aqueux, limitant alors le mode de

prélèvement des goudrons. La nécessité de l'échantillonnage par le « Tar protocol » impose l'utilisation d'un solvant organique, l'isopropanol, limitant alors l'emploi de cette technique analytique. Ainsi l'adaptation d'une méthode de dosage rapide, semi-quantitative, permettrait le suivi du procédé en direct ne serait-ce que pour éviter la condensation des goudrons dans les tubulures.

Les composés aromatiques pouvant s'associer en solution vont influencer l'absorbance d'un mélange (suivant la nature et la concentration de la solution). Différentes dilutions (figure 12 A) (au $1/10^{ème}$ au $1/40^{ème}$) permettent de suivre l'évolution de l'absorbance des échantillons de goudron dans l'isopropanol, afin de déterminer le domaine de linéarité de l'absorbance. Le suivi du signal entre les longueurs d'onde de 220 à 300 nm présente un domaine de linéarité de la réponse en fonction du facteur de dilution (figure 12 B). L'absence de corrélation à 220 nm provient de la trop grande absorbance observée à cette longueur d'onde (> 1,5).

Les résultats de dosage après séparation (analyse par CLHP) ont servi de valeur étalon pour doser en UV les goudrons, en mesurant l'absorbance du mélange à une longueur d'onde donnée. Cette valeur étalon a servi à mettre en évidence une corrélation entre la concentration trouvée en CLHP et la concentration évaluée en UV sans séparation, et ce, à 5 longueurs d'onde différentes (254 nm, 260 nm, 271 nm, 280 nm and 285 nm)

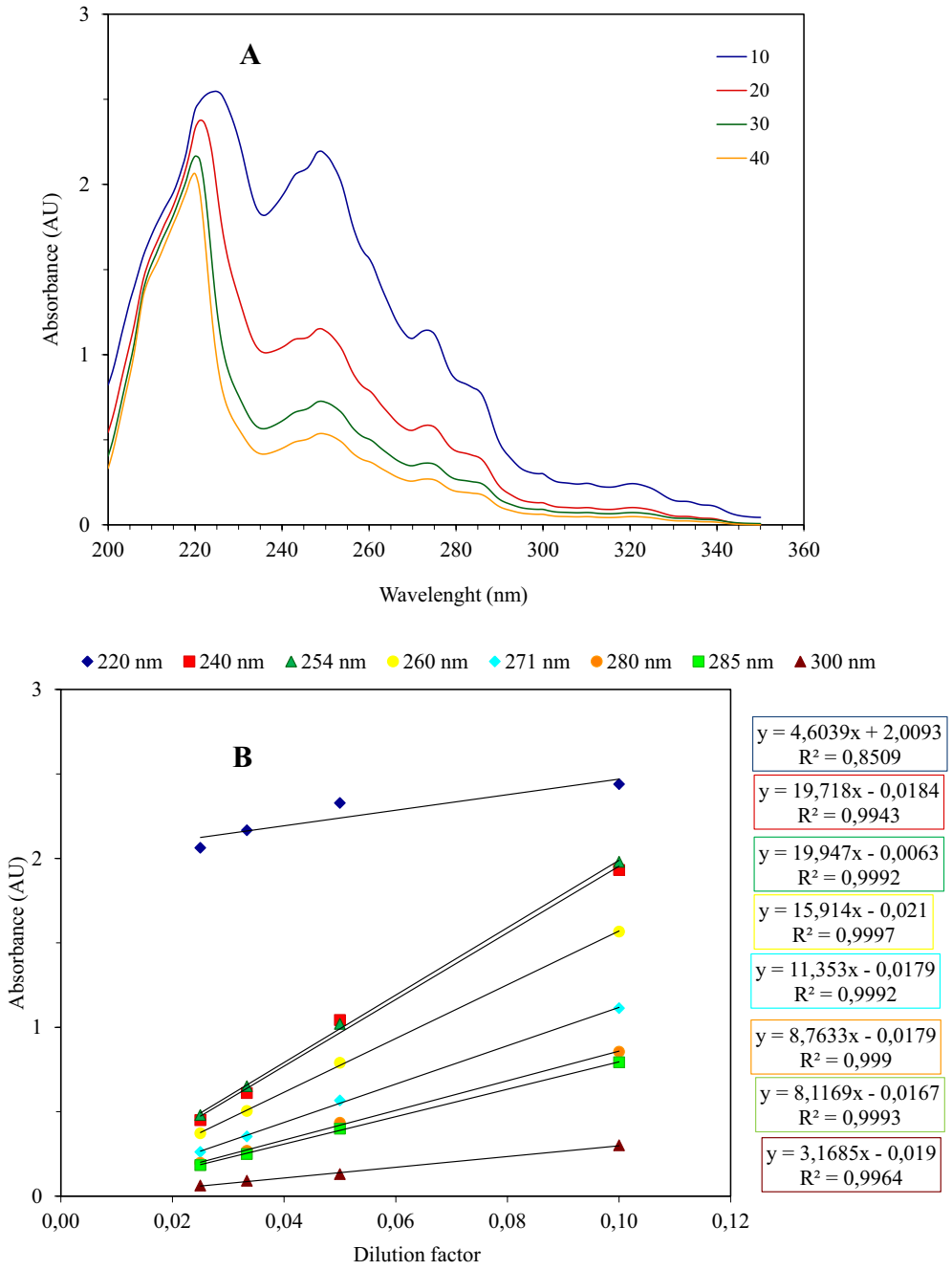

Figure 12: Spectre d'absorption de l'échantillon 3-III à différentes dilutions (1:10, 1:20, 1:30, 1:40) (A). Corrélation entre l'absorbance et la dilution à différentes longueurs d'onde (B)

Cependant la meilleure corrélation a été obtenue à 280 nm excepté pour 2 mesures (points en rouge) (figure 13). Les échantillons obtenus sur d'autres systèmes de gazéifications (CSIC en Espagne et ENEA en Italie) montrent également une bonne corrélation.

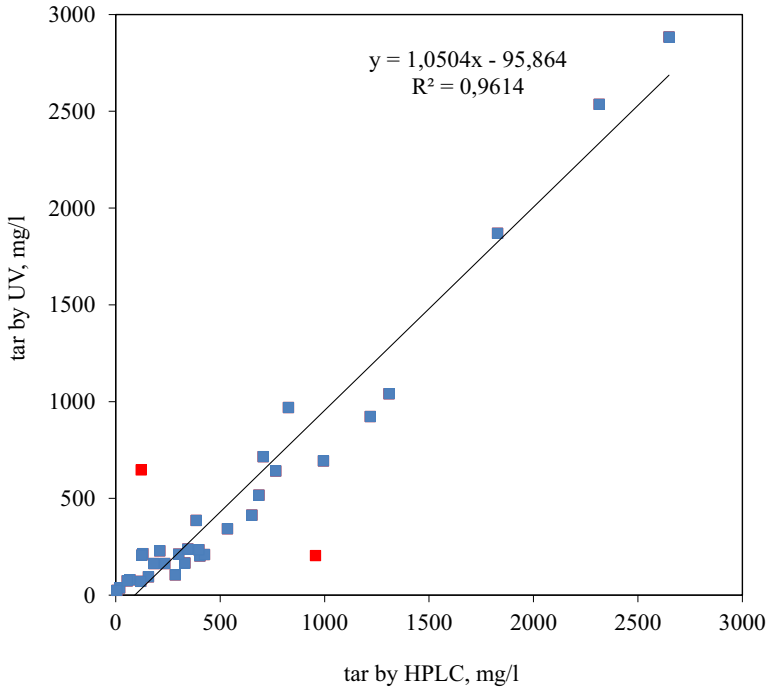

Figure 13: Corrélation des dosages CLHP-spectroscopie UV à A = 280 nm, pour 3 sites de gazéification – Teramo, CSIC, ENEA

V.2.1 Dosages des goudrons par spectroscopie UV/Visible – Approche par convolution

L'exploitation d'un spectre UV peut être également envisagé par une méthode de convolution mathématique correspondant à la somme de spectres de chaque composé présent dans le mélange. La loi de Beer Lambert étant une loi additive, une combinaison de spectres de composés étalons peuvent permettre de reconstituer le spectre du mélange. Après avoir identifié les composés aromatiques majoritaires par CG-SM le spectre UV de chacun des composés a été obtenu pour une concentration donnée pour des longueurs d'onde comprises entre 230 et 300 nm. La figure 14 donne le spectre de chacun des étalons utilisés pour reconstituer le spectre des mélanges de goudron (en pointillé orange).

Le solveur d'Excel a permis de recalculer la contribution de chaque composé aromatique en minimisant la différence obtenue entre le spectre réel et le spectre reconstruit.

Les meilleurs résultats obtenus couvraient le domaine 236-300 nm, à de plus faibles longueurs d'ondes, les transitions énergétiques sont peu spécifiques et

peuvent être influencées par la présence de benzène qui absorbe dans ce domaine (n'entre pas dans la détermination des goudrons). Un exemple de convolution est donné sur la figure 15.

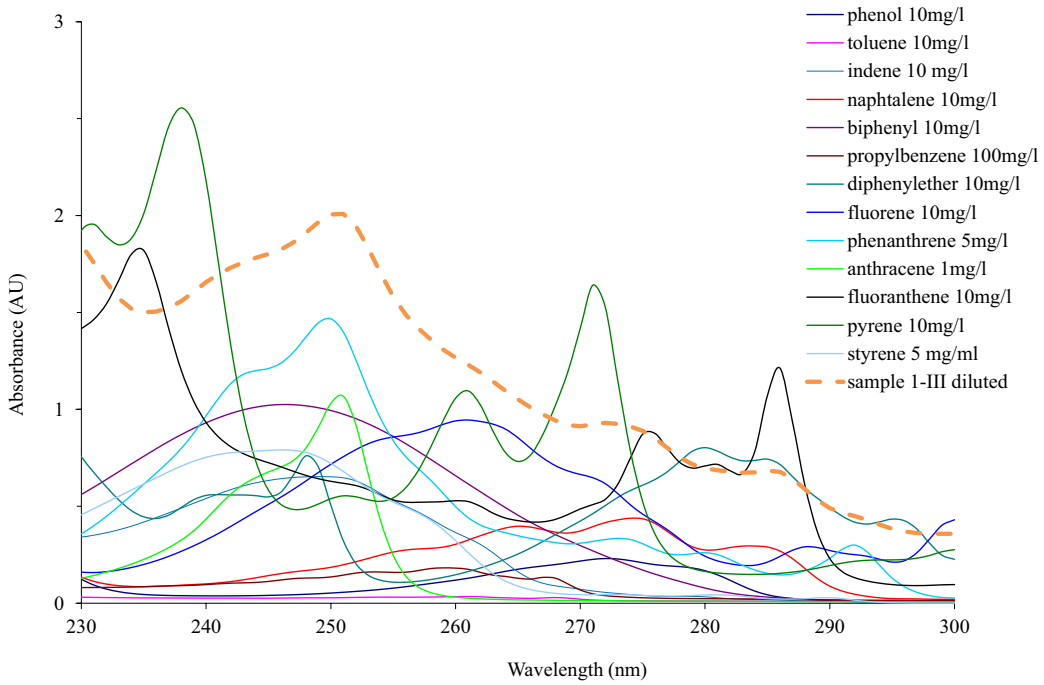

Figure 14: Spectre des étalons ayant servi à la reconstruction mathématique du spectre d'un mélange de HAP (pointillé)

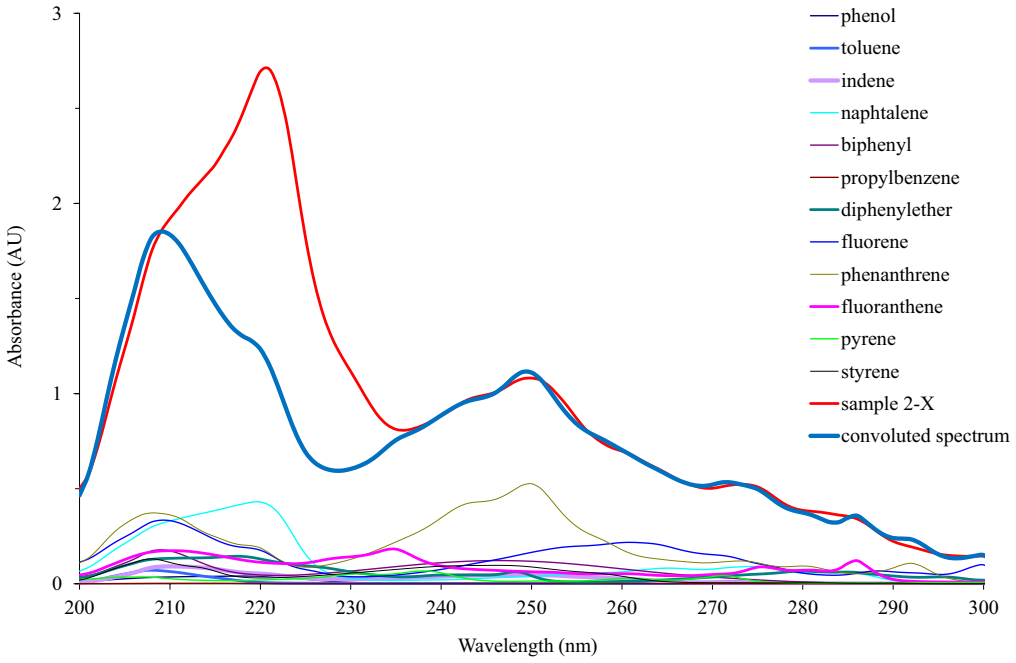

Figure 15 : Convolution de 12 composés aromatiques étalons pour la reconstitution d'un spectre UV d'un mélange

Le dosage quantitatif obtenu par cette méthode a été corrélé également avec les mesures faites après séparation (en CLHP) (figure 16 A et B), Une forte corrélation est mise en évidence, et ce, malgré l'origine des échantillons. Ainsi l'approche par convolution permet de quantifier les teneurs en goudron par le biais de l'enregistrement d'un spectre UV sans procéder par séparation de chaque composé.

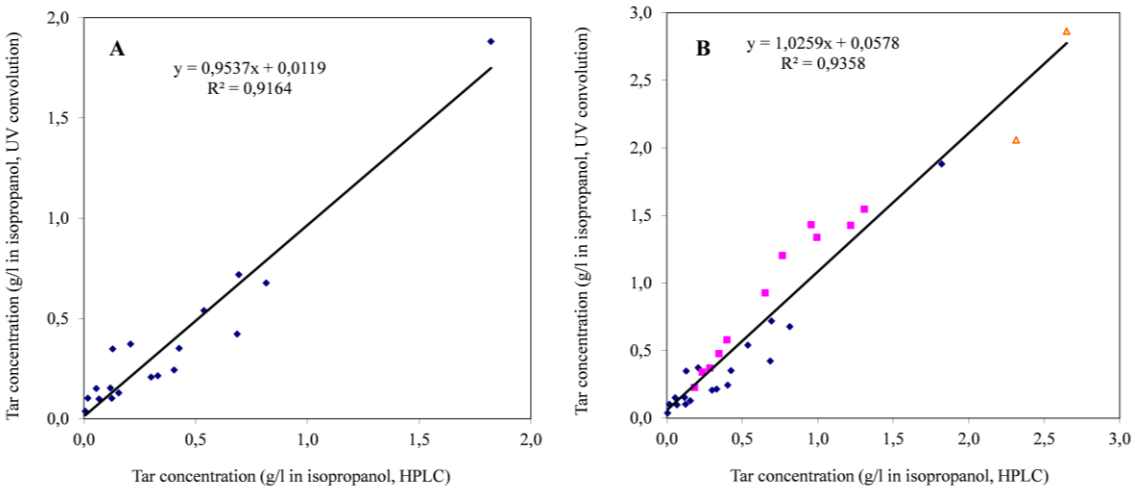

Figure 16: (**A**) Etude de la correlation sur le pilote de Téramo (**B**) correlation pour l'ensemble des échantillons sur les pilotes de Teramo◆, Zaragoza■, ENEA▲

V.3 Intérêt de la chromatographie planaire pour l'analyse des goudrons

V.3.1 Introduction

En complément de l'étude spectroscopique, il est apparu que l'analyse des goudrons pouvait être également proposée par une méthode séparative rapide telle que la chromatographie planaire. En effet, cette méthode permet l'analyse simultanée d'un grand nombre d'échantillons, les évolutions technologiques récentes offrent un contrôle des séparations, et une automatisation du traitement de l'échantillon, depuis son dépôt jusqu'à la détection. De plus, l'offre de phases stationnaires ayant augmentée, il est possible de travailler sur différents supports présentant des caractéristiques de séparation en phase normale, en phase inverse en adsorption, etc, tout comme les colonnes de CLHP.

V.3.2 Séparation des goudrons par famille de composés aromatiques

L'objectif principal de ce travail a consisté au développement d'une méthode pour caractériser les goudrons et ainsi de séparer les HAP en fonction du nombre de noyaux aromatiques qui les composent. En effet, les composés comportant 3 noyaux et plus posent problème dans le procédé car ils sont à l'origine de la diminution du point de condensation (dew point).

L'HPTLC présente l'intérêt de donner une information complète de la composition de l'échantillon, sans risque de perte d'information comme en chromatographie liquide ou gazeuse, où une adsorption irréversible est toujours possible en tête de colonne. La lecture de la plaque, du dépôt au front de solvant permet de renseigner rapidement sur la composition, le choix du mode de détection, UV ou fluorescence, offert par une détection avec le densimètre permet d'améliorer la sélectivité de la détection.

Une étude systématique des séparations a été menée sur les échantillons de goudron dans l'isopropanol en phase normale et en phase inverse (figure 17 A et B). Les meilleures séparations ont été obtenues sur des plaques greffées en C18 : il est possible de distinguer les différentes zones de migration des composés aromatiques, cependant la résolution reste faible.

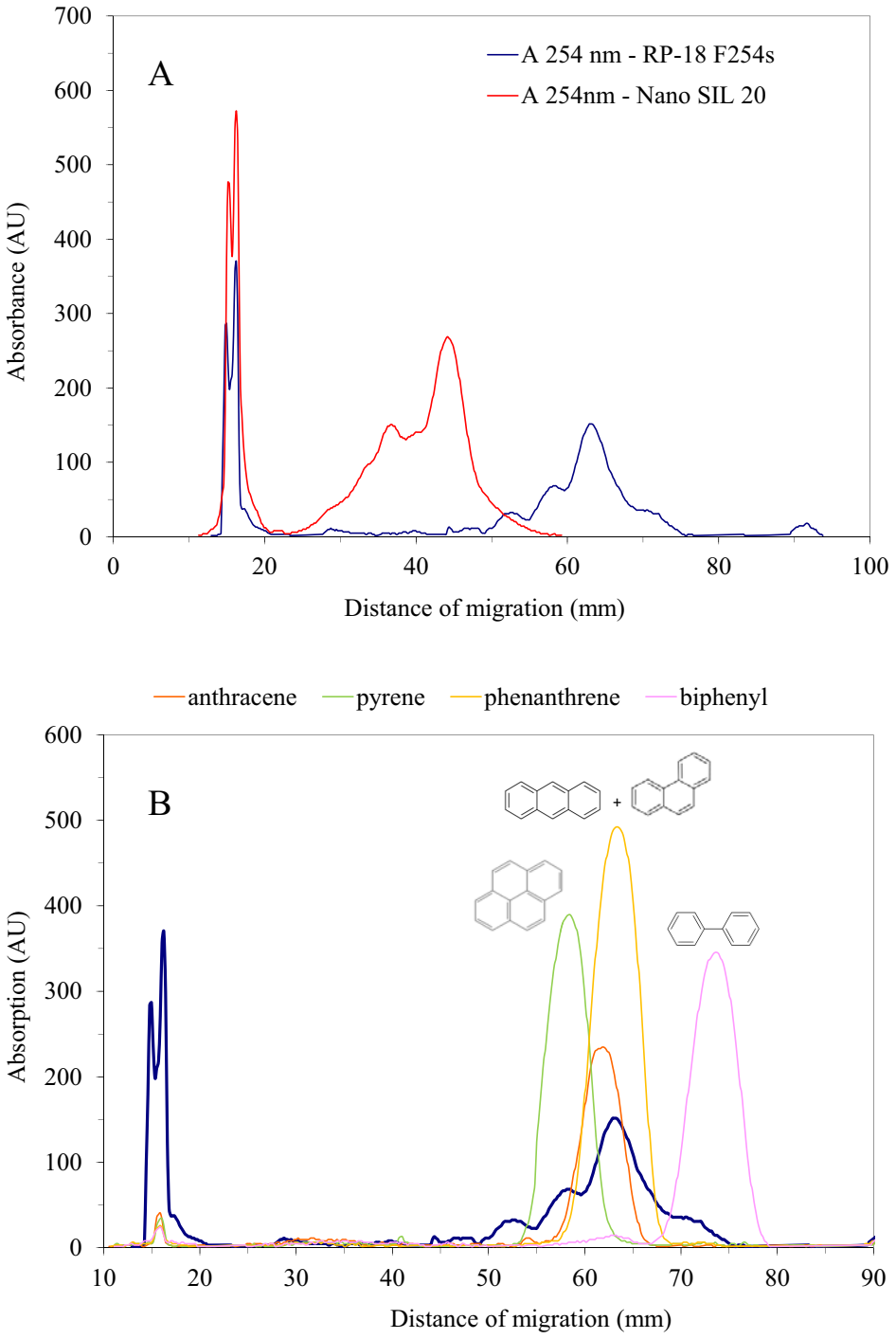

Figure 17: (**A**) Chromatogramme de l'échantillon 2-I (coque d'amandes sur lit d'olivine) par HPLTC Nano-SIL 20 et sur plaque RP-18 F_{254}. (**B**) Chromatogramme du même échantillon, migration d'étalons sur plaque RP-18 F_{254} ; migration avec du n-hexane sur 90 mm

Différentes combinaisons de solvants sur ces mêmes plaques n'ont pas permis d'améliorer la séparation, l'hexane étant le composé le moins polaire donnant la meilleure séparation sur ces types de plaques.

D'autres phases stationnaires ont alors été envisagées, et en particulier la séparation sur phase greffée en NH_2- (figure 18). Différentes applications dans le domaine pétrolier pour la séparation de composés aromatiques ont montré le rôle « donneur-accepteur » que pouvait jouer la fonction amine. Aucune étude n'a été menée à ce jour sur ce type d'échantillons.

La séparation sur plaque greffée en Diol n'a pas permis d'améliorer les résolutions (voir page 144)

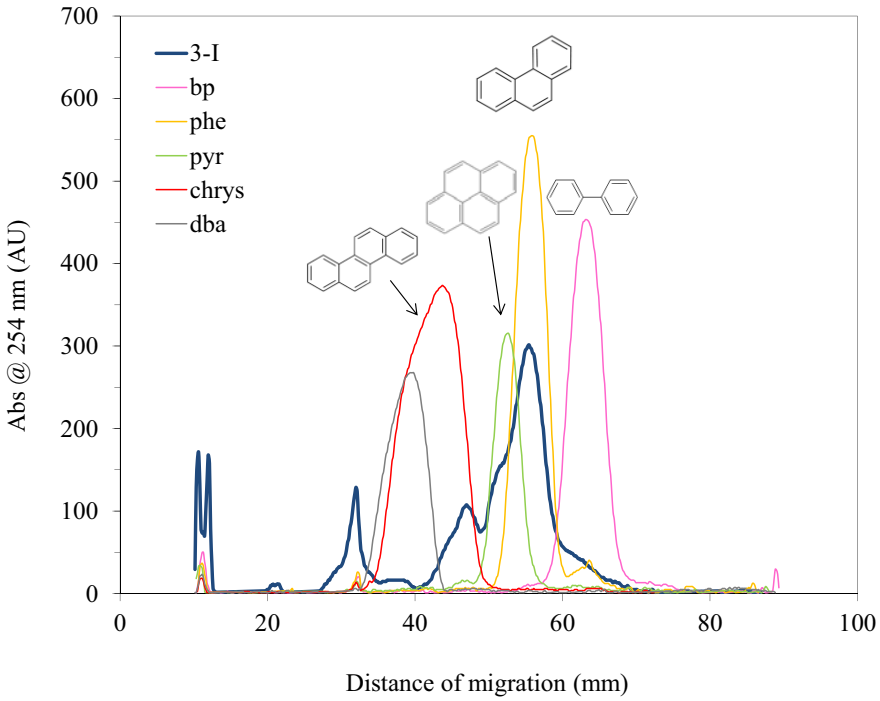

Figure 18: Chromatogramme de l'échantillon 3-I (Fe/olivine) et de 5 étalons sur plaque HPLTC Silica gel 60 NH_2 λ= 254 nm

Les meilleures séparations ont pu être obtenues en effectuant la migration des échantillons à basse température. Les informations relevées dans la littérature expliquent cette amélioration comme étant une limitation de la vitesse de migration, et de ce fait de la diffusion des molécules dans la phase stationnaire : les molécules restent concentrées dans leur zone de migration, améliorant la résolution. Une séparation intéressante par familles de HAP, incluant une

séparation faisant état du degré de condensation du composé aromatique a été observée en utilisant des plaques de phase inverse avec zone de concentration. La séparation a été menée avec 2 types de solvants successifs (Figure 19, Tableau XIV) et ce pour 2 températures de migration.

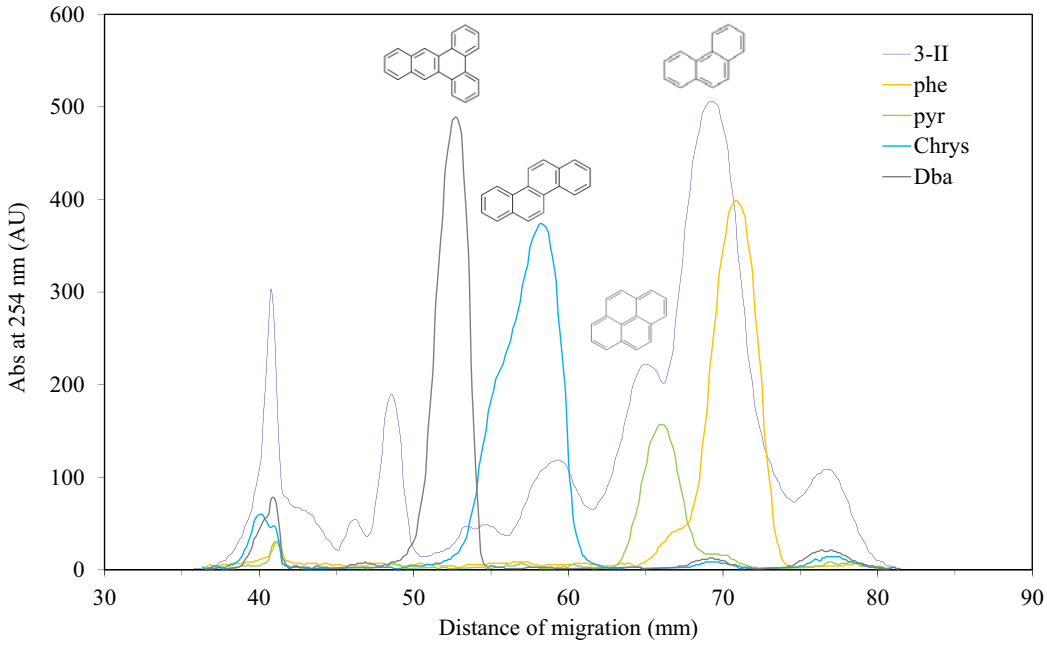

Figure 19: Chromatogramme de l'échantillon 3-II (Fe/olivine) et de 4 étalons sur plaque HPLTC Silica gel 60 RP-18 avec zone de concentration (migration à -23°C), λ= 254 nm

TABLEAU XIV: Facteurs de retention mesurés sur plaque HPTLC RP-18 Silica gel 60 après separation à 20°C et à -23 °C

	Rf at 20°C	**Rf at -23 °C**
Stationary phase	*HPTLC RP-18 Silica gel 60 with concentrating zone*	*HPTLC RP-18 Silica gel 60 with concentrating zone*
Mobile phase	*EtAc:n-Hex 50/50 v/v (35mm)* *n-Hex (90mm)*	*EtAc:n-Hex 50/50 v/v (35mm)* *n-Hex (90mm)*
Phe	0.79	0.79
Pyr	0.76	0.73
Chrys	0.69	0.64
DBA	0.62	0.58

V.3.3 Dosage des HAP totaux par HPTLC/UV

Une méthode de dosage par HPTLC est proposée en utilisant la méthode des ajouts dosés. Alors que la séparation sur colonne des composés aromatiques conduit à une quantification individuelle de chaque composé, il est également possible de procéder par regroupement des composés aromatiques sur une plaque de chromatographie planaire par un choix judicieux de solvant de migration.

Les échantillons de goudron ont été dilués pour obtenir une réponse linéaire lors de la détection des plaques. Un mélange de concentration connue de composés aromatiques étalons a permis d'effectuer des surcharges de chacune des dilutions. Ainsi les différentes courbes (figure 20) de dosage montrent qu'il est possible de quantifier les teneurs en goudron, une bonne corrélation a été obtenue en comparant les résultats obtenus par la méthode de référence, l'HPLC (figure 21).

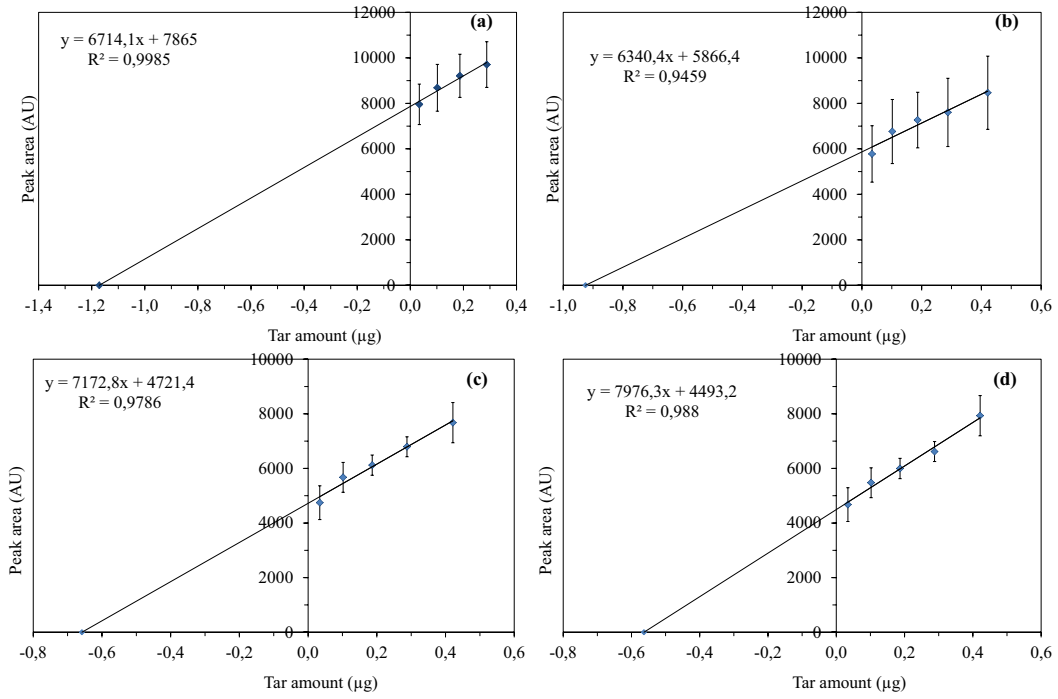

Figure 20 : Courbes de calibration obtenues par la méthode des ajouts dosés sur différentes dilutions de l'échantillon 3-II (Fe/olivine). Dilutions 1/8 v/v (**a**), 1/10 v/v (**b**), 1/15 v/v (**c**) and 1/20 v/v (**d**) avec addition de goudron "synthétique".

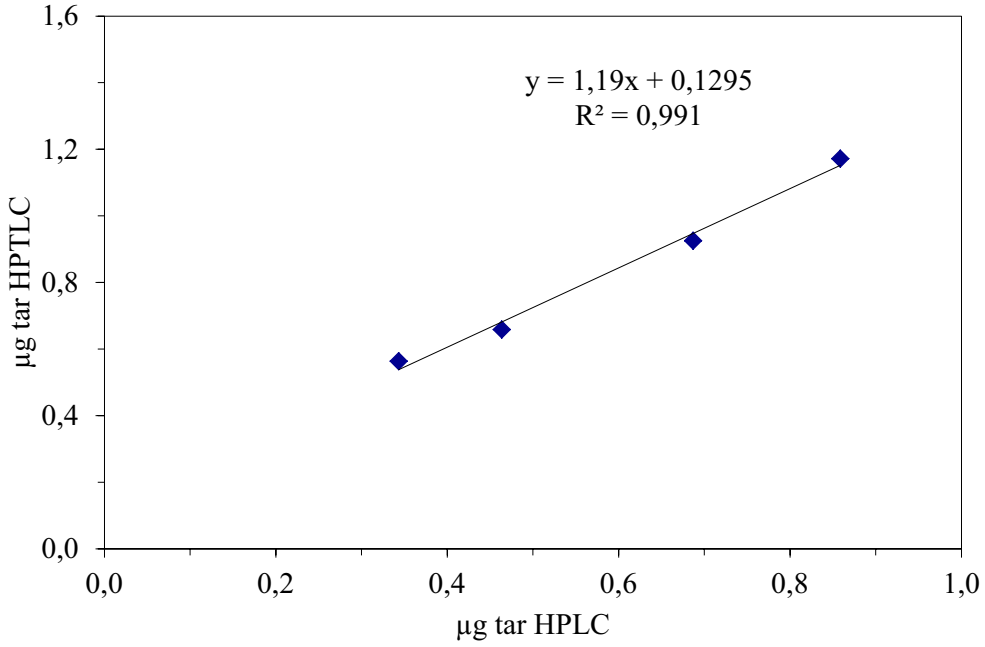

Figure 21: Corrélation du dosage des goudrons par HPLC/UV et par HPTLC par ajout dosé

V.4. Conclusions

Les nouvelles approches analytiques proposées dans ce travail ont montré un intérêt certain dans l'arsenal des méthodes analytiques classiques. La spectroscopie UV ouvre le champ de l'instrumentation en ligne pour le suivi direct de la production de goudrons, en équipant la ligne de prélèvement d'une cellule UV de mesure et en suivant l'évolution de l'absorbance de la solution d'isopropanol. Cette approche quantitative permet d'obtenir une bonne corrélation entre absorbance et concentration, et ce pour des mesures effectuées au-delà de 230 nm.

Une autre approche, utilisant la chromatographie planaire a également montré un intérêt de part la diversité des phases stationnaires et la rapidité de développement. Une séparation à basse température permet de suivre l'évolution des différentes familles de composés aromatiques pour un suivi rapide sur le terrain de l'efficacité du système de gazéification. Il est également possible de proposer un dosage des HAP totaux par méthode des ajouts dosés.

VI. Conclusions générales

Gazéification de la biomasse

Dans le procédé de gazéification, la biomasse solide est transformée à haute température, dans des conditions catalytiques, en présence d'air, d'oxygène ou de vapeur d'eau, en produits gazeux qui peuvent avoir différentes utilisations: la production d'hydrogène et de gaz de synthèse (Syngas), la production de chaleur ou d'électricité, la synthèse de bioalcools et d'hydrocarbures liquides, etc. Ce procédé est cependant générateur de goudrons et de particules, de part la matière première d'origine végétale, préjudiciables pour une mise en application industrielle. Il est donc nécessaire de connaître et d'optimise les conditions de gazéification afin de minimiser la production de goudron.

Les études ont porté sur l'optimisation des conditions opératoires de gazéification dans un réacteur à lit fluidisé :

- 2 types de biomasse on été traités, les coques d'amandes et des granulés de Miscanthus x giganteus
- L'efficacité du lit a été évaluée en utilisant des systèmes catalytique tels que l'olivine, le Ni-Olivine , le Fe-Olivine également complétés par un système secondaire de bougies filtrantes à activité catalytiques qui présentent un intérêt en luit fluidisé pour la réduction des goudrons et particules
- L'évaluation des performances générales du procédé en déterminant le rendement en gaz (Nm^3_{dry}/kg $biomasse_{daf}$), la composition du Syngas (% volumétrique en H_2, CO, CH_4 et CO_2), la teneur en goudrons (g/Nm^3 gaz_{sec}), le bilan en masse et en carbone.
- Les goudrons produits variant selon le système de gazéification (lit fixe ou lit fluidisé) des conditions catalytiques, de l'échantillonnage (« Tar protocole » ou condensats) différents systèmes analytiques ont été évalués et validés

L'analyse systématique des paramètres de gazéification a montré que la qualité de Syngas est améliorée lors de l'utilisation de systèmes de filtration des particules sur un lit à activité catalytique. L'augmentation du rapport H_2O_{gaz}/biomasse

entrant dans le réacteur est un paramètre favorable à la réduction des goudrons et l'amélioration de la conversion. Le réacteur a cependant subi une évolution de conception afin d'intégrer un système de bougies catalytiques. L'association d'un lit d'olivine et de bougies catalytiques permet d'augmenter le rendement de production d'hydrogène (de 39% à 55% V_{gaz} selon les conditions), dans un même temps les goudrons sont réduits de plus de 70% (de 3,7 à 0,8 $g/Nm^3_{\ gaz\ sec}$). L'association d'un lit catalytique (Fe Olivine) et de bougies catalytiques permet encore d'améliorer la conversion de la biomasse (i.e. diminution des goudrons à 0,3 $g/Nm^3_{\ gaz\ sec}$). Les sous produits (tels que NH_3 et H_2S) obtenus en faible concentration dans le procédé à lit fluidisé sont également largement réduits.

Caractérisation des goudrons

Concernant le travail développé en analyse des goudrons, différentes approches ont été menées en parallèle. Habituellement les goudrons sont déterminés par un dosage des composés organiques totaux sur les condensats en sortie de réacteur. Cependant cette technique ne permet pas de suivre l'efficacité de la conversion des composés aromatiques et les grandes imprécisions du prélèvement ont fait l'objet de nombreuses critiques relevées par le « Tar protocole ». Suite à la modification du système d'échantillonnages sur le pilote, la composition des goudrons a été suivie par CLHP couplée à une détection UV. En parallèle, d'autres approches ont été validées : elles permettront d'effectuer un suivi direct de la formation des goudrons lors de la gazéification par spectroscopie UV « en ligne ».

L'intérêt de la par chromatographie sur couche mince à haute performance a permis un dosage des composés aromatiques totaux par ajouts dosés. Une analyse semi-quantitative est également possible après séparation par famille de composés aromatiques en fonction du nombre de noyaux et du degré de condensation, ces développements sont totalement originaux pour le suivi des goudrons issus de la biomasse.

COVER PAGE

TITRE DE LA THESE EN FRANCAIS

PRODUCTION CONTINUE DE GAZ ISSUS DE LA GAZÉIFICATION DE LA BIOMASSE (MISCANTHUS) DANS UN RÉACTEUR À LIT FLUIDISÉ CIRCULANT. CARACTÉRISATION CHIMIQUE DES COMPOSÉS ORGANIQUES LOURDS PRODUITS DURANT LE PROCÉDÉ DE GAZÉIFICATION

RESUME DE LA THESE EN FRANCAIS

Dans le procédé de gazéification, la biomasse est transformée à haute température, dans des conditions catalytiques, en produits gazeux qui peuvent avoir différentes utilisations: la production gaz de synthèse (Syngas), la production de chaleur ou d'électricité, la synthèse de biocarburants, etc. Ce procédé est cependant générateur de goudrons et de particules, de part la matière première d'origine végétale. Il est donc nécessaire de connaître et d'optimiser les conditions de gazéification afin de minimiser la production de goudron.

Les études ont porté sur l'optimisation des conditions opératoires dans un réacteur à lit fluidisé sur des coques d'amandes et des granulés de Miscanthus x giganteus. L'efficacité du lit a été évaluée en utilisant des systèmes catalytique tels Olivine, Ni-Olivine , Fe-Olivine complétés par un système secondaire de bougies filtrantes à activité catalytiques. Au final, l'association d'un lit catalytique (Fe Olivine) et bougies catalytiques permet d'améliorer la conversion de la biomasse.

Afin de suivre l'efficacité de la conversion des composés aromatiques, chaque composant des goudrons a été dosé par CLHP. En parallèle, d'autres approches ont été validées : elles permettent d'effectuer un suivi en ligne de la formation des goudrons lors de la gazéification L'intérêt de la chromatographie sur couche mince a permis un dosage des composés aromatiques totaux par ajouts dosés. Une analyse semi-quantitative est également possible après séparation par famille de composés aromatiques en fonction du nombre de noyaux et du degré de condensation, ces développements sont totalement originaux pour le suivi des goudrons issus de la biomasse.

TITRE DE LA THESE EN ANGLAIS

SYNTHESIS GAS PRODUCTION BY CONTINUOUS BIOMASS GASIFICATION IN FLUIDIZED BED REACTOR. CHEMICAL CHARACTERIZATION OF THE HEAVY ORGANIC COMPOUNDS PRODUCED DURING THE GASIFICATION PROCESS

RESUME DE LA THESE EN ANGLAIS

Gasification could be defined as a group of processes that converts solid or liquid fuels into a combustible gas. Therefore, biomass gasification can be employed to meet different market needs. Among the different gasification technologies available, fluidized bed gasifiers are very attractive, because they take the advantage of the excellent mixing characteristics and high reaction rates of gas-solid mixtures.

Miscanthus x giganteus (MXG) pellets and crushed and sieved almond shells have been used as biomass feedstocks.

Comparing the results obtained using the two biomasses at analogous operating conditions, no significant differences concerning the gas yield, gas composition and tar content could be observed.

During the work, innovative catalytic hot gas filters for in-situ tar and particulate abatement, as well as two interesting Ni- and Fe- based catalyst have were tested in real gasification conditions.

Further improvements have been obtained by combining the synergic catalytic effect of Fe/olivine and the catalytic filter candle, resulting in a efficient tar abatement (-92% in the producer gas), and a consequently increase of gas yield by 72%. Also, the use of catalytic filter allows efficient particle separation, so that the final result is a hot and clean fuel gas made available right at the exit of the gasifier reactor.

The composition of tar was followed by HPLC as reference method. Other methods like HPTLC allow the separation of aromatic compounds according their number of aromatic rings. Quantification without separation was validated in order to control on line the production of tar during the gasification process.

MOTS-CLES : GAZEIFICATION, BIOMASSE, GOUDRONS, CLHP, HPTLC